

**UNCLASSIFIED**

---

---

**AD 267 700**

*Reproduced  
by the*


**ARMED SERVICES TECHNICAL INFORMATION AGENCY  
ARLINGTON HALL STATION  
ARLINGTON 12, VIRGINIA**



---

---

**UNCLASSIFIED**



NOTICE: When government or other drawings, specifications or other data are used for any purpose other than in connection with a definitely related government procurement operation, the U. S. Government thereby incurs no responsibility, nor any obligation whatsoever; and the fact that the Government may have formulated, furnished, or in any way supplied the said drawings, specifications, or other data is not to be regarded by implication or otherwise as in any manner licensing the holder or any other person or corporation, or conveying any rights or permission to manufacture, use or sell any patented invention that may in any way be related thereto.

**Best  
Available  
Copy**

267700

N-602-1-4

MCL - 905/1+2

**TECHNICAL DOCUMENTS LIAISON OFFICE  
UNEDITED ROUGH DRAFT TRANSLATION**

---

STEROMETRIC METALLURGY

BY: S. A. Saltykov

English Pages: 604

PAGES 1 - 309, PART I OF II PARTS

THIS TRANSLATION HAS BEEN PREPARED IN THIS MANNER TO PROVIDE THE REQUESTER/USER WITH INFORMATION IN THE SHORTEST POSSIBLE TIME. FURTHER EDITING WILL NOT BE ACCOMPLISHED BY THE PREPARING AGENCY UNLESS FULLY JUSTIFIED IN WRITING TO THE CHIEF, TECHNICAL DOCUMENTS LIAISON OFFICE, MCLTD, WP-AFB, OHIO

PREPARED BY:

TECHNICAL DOCUMENTS LIAISON OFFICE  
MCLTD  
WP-AFB, OHIO

MCL - 905/1+2

Date 6 Oct. 1961

S. A. SALT'YKOV

STEREOMETRICHESKAYA METALLOGRAFIYA

[Second Revised and Supplemented Edition]

Gosudarstvennoye Nauchno-Tekhnicheskoye Izdatel'stvo  
Literatury Po Chernoy i Tsvetnoy Metallurgii  
Moskva, 1958

444 Pages

MCL-905/1+2

ANNOTATION

The book presents the basic tenets of stereometric metallography, i.e. the combination of methods of quantitative evaluation of spatial microscopic structure of metals and alloys. Methods are described in detail for estimating the most important parameters of spatial microstructure.

It is demonstrated that the basic properties of metals and alloys and their behavior in the processes of hot and cold working are directly connected ~~quantitatively~~ quantitatively with parameters of stereometric structure.

The book is of interest for engineering-technical workers and ~~engineers~~ <sup>instructors</sup> at higher educational institutions, engaged in the field of investigating, processing and inspecting the quality of metals, as well as for students of the pertinent specialties.

Devoted to the memory of  
Academician Nikolay Timofeyevich Gudtsov

## PREFACE

The purpose of the book is to give a systematized and, as far as possible, complete portrayal of present-day methods of quantitative evaluation of spatial microscopic structure of metals and alloys. Such an evaluation, being the most effective and feasible from the physical viewpoint, has received wide recognition and is being used more and more by Soviet and foreign metallurgists. At the same time, ~~XX~~ descriptions of methods of stereometric evaluation are dispersed among numerous journal articles, often hard to obtain, which complicates the use of these methods. In comparison with the first ~~XXXXXXXX~~ edition, the present book has been revised and supplemented. Included is a description of new methods published in <sup>the</sup> Soviet and foreign press from the time of ~~XX~~ appearance of the first publication, as well as methods developed by the author in the metallurgical laboratory of the Yerevan Polytechnic Institute imeni ~~XX~~ Karl Marx. Considerable attention has been diverted to an analysis of foreign researches, which confirms that both in respect to priority, as well as in general state of the art, the stereometric ~~XXXXXXXXXX~~ metallography in the Soviet Union is ahead of that in foreign countries. The methods of quantitative evaluation of a plane structure are presented only to the extent necessary for obtaining the initial data being used for computing the parameters of spatial microstructure.

The author hopes that the book will promote the further popularization of methods of stereometric evaluation and, in <sup>particular, will</sup> ~~XXXXXXXXXXXX~~ stimulate the transition from semiquantitative methods of rough approximation to more precise and objective characterization of the structure with the aid of parameters of actual spatial structure.

CHAPTER I

MICROSCOPIC STRUCTURE OF ALLOYS AND METHODS OF THEIR  
CHARACTERISTICS

Section 1. Qualitative and ~~QUANT~~ Quantitative Appraisal of Microscopic Structure  
of Alloys

The dependence of the quality of steel upon its structure was first established by P.P.Anosov, who had used that successive combination of methods which now is called the microscopic method and comprises the basis of metallography (N.S.Kurnakov) (Bibl.2).

P.P.Anosov first introduced the semiquantitative scale for ~~XXXX~~ evaluating the quality of steel based on its macrostructure (Bibl.3).

Later D.K.Chernov developed this tendency and established the quantitative dependence of properties of steel (viscosity) on the actual parameter of its structure (size of grain) (Bibl.4).

In modern machine construction, the conditions of the work of metal in parts, tools and construction, and also the technology of its processing, compels the posing of ~~XXXX~~ especially rigid and numerous requirements for the quality of ~~XXXX~~ metal. Often these requirements relate directly to the structure of metal, and the conformity of the quality of metal to the requirements should never be checked by any methods other than metallographic ones. Even if it is sometimes possible, such a checking is not very graphic, reliable, or advantageous. Some ~~XXXX~~ examples are the determination of purity of steel with respect to content of nonmetallic inclusions, degree of heterogeneity of distribution of carbides, sizes of grain, depths of decarbonization and carbonization, presence of structurally free

cementite in soft steel and the nature of its arrangement, etc. The wide distribution of the network of factory laboratories in our time permits a realization of an analysis of metal structure everywhere. In many cases, metallographic analysis is conducted as a mandatory inspection method for testing metals, semifinished products and finished products, along with chemical analysis and mechanical testing. The inspection functions of metallographic analysis also required a new approach to an evaluation of the structure and to a portrayal of the results of analysis. In the standards, technological charts, and technical specifications, it is necessary to include quite definite and concise quantitative and dimensional requirements for structure, clearly and accurately defining the characteristics of the metal.

Examining the structure of metal and the products from it at various stages of the technological process and in finished production, the plant laboratories over a period of time accumulate extensive experimental material. In order that the accumulated valuable data can be advantageously used for controlling and improving the technological processes and raising the quality of the production by the plant, it is necessary to process these data systematically, to link the individual factors of the technological process with a structure, and the structure with the quality of production. In this case, the use of statistical methods of processing experimental data often permits one to find important and sometimes unexpected dependences and leads to conclusions which are valuable in practice. Using only a qualitative evaluation of structure, we cannot link it ~~with~~<sup>by</sup> any quantitative dependence with the values ~~typifying~~ typifying the technological process. A statistical processing of results of micro analysis is also unrealizable under these conditions. Only with a quantitative

or dimensional numerical evaluation of microstructure can one effectively use the experimental material being accumulated by the plant laboratories.

No less important is a quantitative appraisal of the structure in the researches, especially in those connected with a study of such processes, in which the structural elements change under the effect of mechanical, thermal and chemical factors only quantitatively or dimensionally. Some examples are the growth of ~~XXX~~ grain during heating, degree of ~~XXXXXX~~ coagulation of cementite during isothermic annealing, increase of ~~XXXX~~ quantity of <sup>6</sup>perlite during cementation etc. In such cases, the only effective means will be a quantitative or dimensional evaluation of structural elements (sizes of grain, numbers of carbide particles, quantity of <sup>6</sup>perlite).

For instance, a study of the recrystallization process many years ago compelled the development and introduction into metallographic procedures of a method (being used until the present) for estimating the sizes of grain based on its average area on a slide.

In the investigation of the kinetics of decomposition of <sup>austenite,</sup> ~~estonite~~, there is determined the content of various phases at various stages of the process. Indirect methods (magnetic, resistometric, ~~XXXXXXXXXX~~ dilatometric) are less convincing and not as reliable as the method of micro investigation, since the properties can change not entirely proportional to the change in the phase composition (Bibl.5).

Advances in the techniques of large magnifications permitted a solution of problems of the formation of a number of structures and permitted one to establish that the structures which were considered earlier to be qualitatively different in actuality have mainly a single type structure and the difference in them one from another reduces only to a quantitative difference <sup>in</sup> ~~XX~~ fixed parameters of structure.

Such for example are <sup>a</sup>perlite, sorbite, troostite having a flaky structure and differing in degree of ~~XXXXXXXXXX~~ dispersion of flakes of cementite and ferrite. It is evident that the concrete expression of the characteristics of such structures requires quantitative estimation.

In many cases, even a purely qualitative estimate of the structure proves to not supported be ~~XXXX~~ very well grounded and is discussed in various ways if it is not ~~XXXXXXXXXX~~ by quantitative characteristics. For instance, a case of a diametrically opposite definition of the concept "point <sup>a</sup>perlite" is noted by A.N.Chervyakov and A.N.Podvoyskiy (Bibl.6). ~~XXXXXXXXXXXX~~ Whereas N.A.Minkevich ~~XXXXXXXXXX~~ identifies point <sup>a</sup>perlite with granular <sup>a</sup>perlite, according to A.L.Baboshin "granular <sup>a</sup>perlite has nothing in common with point <sup>a</sup>perlite" (Bibl.7, 8). This contradiction is caused by a qualitative evaluation of the structure of <sup>a</sup>perlite of this type and obviously it can be avoided if we introduce the quantitative characteristics of grains of cementite into <sup>a</sup>perlite, speaking of "point", "fine", "average" or "large" grains.

Becoming familiar with any object, physical phenomena or process, we first of all obtain a qualitative concept concerning it. During a more profound study of the same object, we transfer from an initial qualitative cognition to a quantitative definition. In this connection, cases are possible when the quantitative study refutes the initial qualitative concept. Therefore qualitative-descriptive microscopic metallography is only the first, beginning stage of development of the science ~~XXXXXX~~ studying the microscopic structure of metals and alloys. The transition to ~~XXXXXXXXXXXXXXXXXXXX~~ dimensional-quantitative characteristics of microscopic structure is a natural and unavoidable path of further development of metallography. Based on a number of conditions, mainly enumerated above, it is quite

necessary to develop those methods of evaluating the structure and its elements, in which they would be characterized not by words but by numbers, especially since the majority of metallurgists agree with this approach. ~~XXXXXXXXXX~~

The quantitative methods of evaluating the structure, originating simultaneously with the advent of microscopic metallography, received especially wide acceptance and intensive development in the last 25 - 30 yrs. However, the vast majority of evaluation methods being applied, including the standard ones, are far from the best examples of quantitative evaluation of structure.

## Section 2. Methods of Numerical Rating of Microstructure

The number of methods published until now for rating the structure by conventional points, numbers, marks etc., continues to grow incessantly. Several dozens of such methods and scales are standardized and included in the pertinent state standards (GOST). All these scales and methods can be divided into two main categories, based on the method of constructing the scales.

To the first, most numerous category of scales, there belongs the series of <sup>photomicrographs</sup> ~~microphotographs~~ of single type structures (usually in a number ranging from 2 to 10, most often 4 - 5), chosen and renumbered in a series of gradual ~~XXX~~ change of element of structure, typifying the given scale. The degree of this change from one point to the following one is chosen arbitrarily, being ~~XXX~~ appraised subjectively by eye, and not connected by any fixed dependence with the index number of the structure in the scale (with the ~~XXXXX~~ point). In this case, an appraisal of the structure being analyzed can be conducted only visually by way of comparing it with a set of microphotographs of the scale.

Examples of such scales are as follows: scale of carbide heterogeneity of ~~XXXX~~ <sup>high-</sup> speed cutting steel based on GOST 5952 - 51, scales ~~XXXXXX~~ <sup>typifying</sup> the degree of rectilinearity,

nature of distribution and orientation of graphite of gray iron based on GOST 3443 - 46, scales for appraising the structurally free cementite and striated thin-layered ~~XXXXXX~~ high-quality steel based on GOST 5640 - 51, scales of nonmetallic inclusions ~~XXX~~ based on GOST 1778 - 42 and GOST 801 -47 and others.

are

The scales of the second category/based on a fixed dependence between the index number of the structure in the scale and the value of the geometric parameter ~~XXXXXX~~ microstructure of the ~~XXXXXXXXXX~~ (or of its elements), being measured and being characterized by the given scale. In certain cases, this dependence is expressed by a formula, linking the number (point) with the value of the parameter, but more often the values of parameter for any given number are established arbitrarily. The estimate of the structure can be conducted both approximately by visual comparison with ~~XXXXXX~~ microphotographs of a standard scale as well as more objectively and accurately by way of direct measurement of the pertinent parameter of the structure under a microscope or on a microphotograph. However the structure is evaluated not by an actual figure derived, but by a conventional number or point connecting the fixed limits of values of the parameter being measured.

In this category of scales, there belong the scales for evaluating the value of grain of steel based on GOST 5639 - 51 and the standard E 19 ASTM, a ~~XXXX~~ series of scales GOST 3443 - 46 for estimating the various elements of structure of gray iron (quantities and dispersions of <sup>a</sup>perlite, quantity of graphite, lengths of deposits), method of ~~XXXXXXXXXX~~ determining the index of <sup>contamination</sup> ~~XXXXXX~~ of steel by nonmetallic inclusions based on GOST 1778 -42 and others.

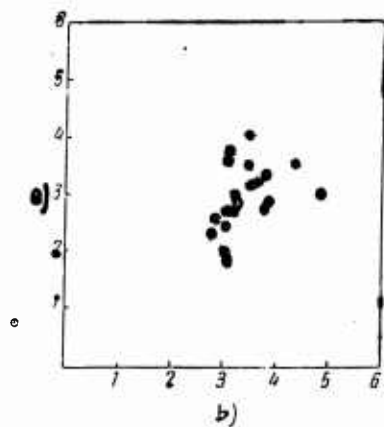
The main disadvantage of using these scales is the planar estimation of microstructure and of its separate elements, upon which we will dwell separately (see Section 5). Here we will examine only the secondary but very substantial



for samples of ball ~~XXX~~ bearing steel SHKH15.

A second important disadvantage of the principle of constructing scales of this type is their gradated nature and the system of evaluation by conventional points and not by ~~XXXXXX~~ actual values of geometric parameters of structure. In this connection, we cannot extend, in case of necessity, the scale in any direction or differentiate ~~more~~ more finely in a sector of interest to us. The gradated structure of the scale predetermines the standards of requirements for any given parameter of the structure or for the structure as a whole, whereas the establishment of these standards is the matter of the pertinent technical specifications or qualitative standards. Applying the gradated appraisal ~~XXX~~ by points or by numbers, we move beyond the limits of visibility of the method of analysis. We will ~~XXXXXX~~ clarify this proposition by an example.

Let us suppose that the mechanical or physical properties required of the given items made of gray iron are guaranteed by the amount of free carbon (graphite) in the iron within the limits from 2.4 to 3.0% (by weight), or from 7.7 to 9.5% of the volume of iron, ~~XXXXXX~~ occupied by graphite. According to



Steel  
Fig.1 - Comparison of Appraisals of Fouling of ~~XXX~~ by Nonmetallic Inclusions, Using the Mean Arithmetic Point ~~MX~~ Based on GOST 801 - 47 and Based on the Method of P.I.Melikhov. Based on Data of P.A.Dvoryanov (Bibl.11)  
a) Appraisal according to Melikhov; b) Mean arithmetic point GOST 801 - 47

GOST 3443 - 46, we have the following ~~XXXX~~ gradations by series of graphite:

- G 08 . . . . . 6 - 8% (volumetric)
- G 11 . . . . . 9 - 11%

Adhering to the standard classification, we cannot select a suitable type of structure based on quantity of graphite, since the limits of graphite content established for them do not coincide with the limits needed by us. We are compelled either to depart from the standard classification or else to introduce into the technical specifications both categories of graphite: both G 08 as well as G 11, known beforehand to be used for the omission of a considerable fraction of ~~standards~~ <sup>substandards.</sup> Obviously in the given case one should not use the graduated scale of standard classification and should reject the product based on actual quantity of graphite and the established concrete standards of its content.

The ~~XX~~ scales of structures predetermined the gradation of variations in elements of structures over the entire range of the scale, which often decreases the accuracy of estimate. In the same GOST 3443 - 46, for instance, provision is made for the following classes of structure of gray iron according to content of <sup>a</sup>perlite:

- P 15 . . . . . less than 25% of <sup>a</sup>perlite
- P 40 . . . . . 25 - 54% of <sup>a</sup>perlite
- P 65 . . . . . 55 - 74% of <sup>a</sup>perlite

Even in a simple visual appraisal, the actual content of <sup>a</sup>perlite in the ~~XXXXXX~~ structure can be established much more accurately.

In the research studies, one often uses fractional numbers in order to differentiate more finely the structure in a fixed interval and to determine the connection between the structure and properties or composition of the alloy. However, this can be done only in case the dependence of the point upon the parameter of the

structure is expressed by a definite formula.

Thus in investigating the effect of copper upon properties of gun iron, V.A.Davidenkov estimates the values of graphite deposits in fractional points (by numbers) of the scale ASTM (Bibl.12). The data obtained by V.A.Davidenkov (Bibl.13) are presented in Table 1.

Table 1

a)	b)	c)	
		d)	e)
5	none	6,00	5,00
6	0,27	6,50	6,50
7	0,40	6,75	—
8	0,62	7,00	6,50
9	0,82	7,00	7,00
10	1,02	7,25	7,00
11	1,20	7,50	7,00
12	1,53	7,50	7,50

a) No. of smelting; b) Copper, %; c) Amount of ~~graphite~~ deposits of graphite based on the ASTM scale; d) First ~~smelting~~ melt; e) Second ~~smelting~~ melt

An evaluation using decimals permitted us to clearly establish here the gradual fragmentation of flakes of graphite with an increase in copper content in the iron. Using in the given case only the whole numbers of the ASTM scale, it was impossible to obtain such a definite and clear dependence, using the estimate of graphite based on OST 26049, in which the graphite based on sizes of flakes has only four gradations, it was necessary to estimate all samples by the same point G 4 and we did not succeed in revealing any kind of general dependence.

A similar evaluation using decimals (with an accuracy up to tenths of a number) is used by N.A.Minkevich for the characteristics of the (size of grain) in high-speed ~~cast~~ steel based on the ASTM ~~(ASTM)~~ scale (Bibl.14).

The use of fractional numbers, to which researchers are forced to resort, deprives the point evaluation of one of its advantages, namely to express the result of analysis by a simple unequivocal number, and to reduce the data of the analysis to a simple code.

In many cases, the method of point rating of structure leads to explicitly observed results. The size of grain of steel based on the standard EI9 - 33 of the ASTM ~~XXX~~ is determined as a function of the number of grains located in one square inch of the area of the slide at magnification by 100 times (Bibl.16). For various numbers of grains, the standard establishes the following limits of number of grains (in calculation per 1 mm<sup>2</sup> of area of the slide):

No.8 . . . 1488 and more	No.6 . . . 372 = 744
No.7 . . . 744 = 1488	No.5 . . . 186 = 372

etc. At such a construction of the scale, it turns out that if we have three samples of steel in which the numbers of grains per 1 mm<sup>2</sup> of microsection, as a ~~XX~~ result of direct calculation, are found to equal 740, 750, and 1480, we are compelled to designate the first sample with the number 6 and the second and third ones with the number 7. ~~XXXXXXXXXX~~ Hence the practically identical first two samples obtained a different code number, while the second and third samples in which the numbers of grains differ by almost twice, are designated by the very same number. In any other type of analysis or tests (chemical, mechanical) such a graded method of evaluation would prove to be ~~absurd~~ ~~observed~~ absurd. Unfortunately, it is permanently accepted in microscopic ~~XXXXXXXXXX~~ metallography and the scale GOST 5639 - 51 is similar to the one examined above.

From what has been said above, it follows that the main disadvantage of the method of standard scales is the appraisal using conventional points ~~for~~ or numbers and

the stepwise, ~~XXXXX~~ erratic nature of the scales, caused by this. To the extent that the method of visual estimate of structure is distinguished by great simplicity and ~~XX~~ requires a minimum of time and effort, it can be used effectively in all cases when the approximate evaluation results obtained prove to be acceptable in practice. However, for the reasons presented above, one should ~~give up~~<sup>abandon</sup> the evaluation of structures of standard scales and results of analysis by conventional points, numbers XXX etc. It is necessary to replace them by geometric parameters of structure or of its elements whenever this is technically realizable.

To obtain more accurate and reliable results, the same parameters can be rated not visually but directly measured or computed under a microscope or in microphotography.

### Section 3. ~~XXXX~~ Standard Methods of Rating the Microstructure

All the methods of quantitative estimation of microstructure comprising both the Soviet GOST as well as the foreign standards, proceed from the principle of a point rating. Therefore the typical disadvantages considered in the previous paragraph are inherent to them. Along with them, there exist numerous inaccuracies and technical shortcomings in almost all standard scales and methods of estimation and in the means of their practical accomplishment. Let us consider here several of the most important standard methods having the most widespread use in metallographic practice.

One of the oldest methods of such a type is an estimation of grain size of steel, which was first standardized in the USA in 1933 (standard of the ~~XXXX~~ ASTM E 19 - 33). This scale was used even before its standardization over a number of years in factories of the USA, and later received wide use in many countries, including the USSR. It turns out that both the scale itself and the methods of its use should be greatly revised.

At the same time, the scales being introduced both in American standards as well as in GOST 5639 - 51 are unsatisfactory. The series of microphotographs of hypereutectoid steel consisting of eight numbers, and the scales (identical to it) in the standards E 19 - 33 and GOST 5639 - 51, provide an incorrect concept of the grain size, corresponding to the given number on the scale. As was shown by us, the structures for grain sizes No.2 and No.3 of the scale actually belong to No.3 and No.4 respectively, i.e. higher by one number than that indicated (Bibl.17). Similar ~~XXXXXXXXXX~~ divergences are also observed in a varying degree for structures corresponding to other numbers of a standard scale. The scale of sketched structures and also the limits established by standards for sizes of grains of each number are also unsuccessful. In the sketched scale of the standard of the ASTM E 19 - 38 T and GOST 5639 - 51, the grains are quite uniform in sizes and the limits of fluctuations of these sizes within the confines of an individual number of grain are considerably less than is usually observed in actual structures. As ~~XXX~~ W.Johnson correctly notes, at the most favorable circumstances not more than half of the grains visible on a microsection of commercial metal fall within the limits set by a single number of the scale of the standard (Bibl.18).

In GOST 5639 - 51, geometric parameters of grains of various numbers are presented. In three columns of the same table of the ~~XX~~ standard, it is indicated, for example, that grain No.8 characterized by an average area of  $500 \text{ microns}^2$ , by a number of grains from  $1 \text{ mm}^2$  of area of the microsection, equals 2048, while the number of grains visible under a microscope at a magnification of 100 for an area of  $10 \text{ cm}^2$  equals 192. A simple comparison of these figures indicates that ~~XXXX~~ they contradict one another. If the average area of one grain equals  $500 \text{ microns}^2$ ,

obviously the number of grains for an area of  $1 \text{ mm}^2$  should equal 2000 and not 2048. At the same time, since the area of  $10 \text{ cm}^2$  at magnification of 100 corresponds to the natural area of the microsection equaling  $0.1 \text{ mm}^2$ , the number of grains in this area should equal 200 and not 192. The parameters of grain of all the remaining numbers of the scale are characterized by just such contradictory data.

The techniques of calculating the grains are not generally accepted. In certain cases it is ~~recommended~~ recommended, in calculating the number of grains on the slide, not to take into consideration the "random fine grains, representing sections through angles of actually large grains" ~~(Bibl.19, 20, 21)~~ (Bibl.19, 20, 21). Therefore, the researcher quite arbitrarily rates the structure to the ~~XXX~~ extent that by actual inspection he must solve ~~XXX~~ an unsolvable problem, namely which of the fine grains visible on the slide are sections of really small grains and which of them represent "sections through angles" of actually large grains. In other cases, it is recommended not to determine the average size of grains but their maximum size (Bibl.22). Understandably, such a diverse approach to calculating the grains makes their appraisal arbitrary and decreases the accuracy of results.

It is also inefficient to estimate such a practically important element of steel structure as nonmetallic inclusions. Indicative in this respect is the conclusion reached in 1939 by the subcommittee on a method of estimating nonmetallic inclusions of the British committee on the heterogeneity of a ~~XXXX~~ <sup>steel</sup> ingot, which examined many different methods proposed for characterizing the ~~XXX~~ fouling of steel by nonmetallic inclusions (Bibl.23): "A. All attempts of quantitative and qualitative determination of nonmetallic inclusions failed to lead to the development of methods permitting the control of the steel production process; B. None of these methods provide the possibility of obtaining sufficiently constant ~~XXXXXX~~ <sup>numbers</sup> and cannot

serve as a reliable method for estimating the quality of steel during its delivery acceptance; and ~~accept~~; C. Further studies are necessary for finding a satisfactory method for defining a nonmetallic ~~XXXXXX~~ inclusion".

In spite of the great number of studies in this area, ~~XX~~ the methods (standardized later) of estimating the nonmetallic inclusions in steel (GOST 1778 - 42, GOST 801 - 47) received no better responses than that presented above.

We will restrict ourselves to data of the investigation of N.K.Sokolov and ~~XXXXXXXXXX~~ M.I.Vinograd in which there was used extensive test material of the current inspection of the smeltings of ball bearing steel type ~~XX~~ ShKh15 for several years, and also of a number of experimental smeltings (Bibl.24). The research indicated that, using the method of rating according to the GOST 801 - 47 (rating according to maximum point), suitable metal is often rejected in practice and steels with considerably fouled nonmetallic inclusions are passed (accepted).

At a properly constructed method of rating, the increase in the quantity of samples from smelting should lead, generally speaking, to an increase in accuracy of analysis and reliability of the result obtained. According to the actual standard method, the increase in number of samples always leads to an increase in probability of rejection, independently of the degree of fouling of the given smelting. This is explained in that the reading of the smelting is conducted on the basis of the maximum point, while the samples being characterized by a fixed point according to oxides, <sup>are</sup> found in any smelting, but with a frequency typical for it. The more samples that are ~~XXXXXXXXXX~~ investigated from the smelting, the higher the probability of finding a field of ~~V<sub>max</sub>~~ with a rating point higher than that permitted, which also leads to a rejection of the smelting. Thence it follows that a rating based on 3 - 5 samples, as is provided for by the standard, often yields random results.

The authors of the investigation arrive at the conclusion that the standard method is unsuitable as a result of the insufficient reliability of inspection, that is, the results of rating depend to a considerable degree not upon the quality of the smelting but upon the quality of the control samples. Figure 1 presented above also confirms the fortuitous nature of the estimation being obtained during the use of the standard methodology.

In our opinion the most important disadvantage of existing rating scales for the impure state of steel with nonmetallic inclusions is the attempt to combine in one scale the rating of two indexes which generally speaking are independent of each other. These indexes, mainly determining the effect of inclusions of the given type upon the quality of steel, are: a) The general state of impurity of the steel, characterized by the part of the volume of steel occupied by the inclusions, and b) The dispersed state of inclusions which can be estimated by their quantity or sizes.

The overall impurity of steel by inclusions of the given type deteriorates the quality of steel. However the inclusions occurring in the same part of the volume of metal may have a different dispersed state, which in its turn reflects upon the quality of the steel. As P.A.Dvorysnov demonstrated, the sizes of the inclusions extending to the surface of contact, exercise a decisive ~~influence~~ influence upon the fatigue chipping of the hardened bearing steel. The less the area of contact of the bodies of turning, the less the maximum permissible sizes of inclusions (Bibl.172). At a low overall ~~impurity of steel~~ fouling of steel by inclusions of the given type, quite large inclusions are permissible and vice versa. Thence it is apparent that it is necessary ~~to~~ to have a separate evaluation of the total impurity of steel and dispersed

state of the inclusions. Moreover, the existing scales are so constructed that this factor is not taken into account in them at all. The division of scales into two groups (being used in certain cases) according to criterion of dispersed state of inclusions is insufficient.

In gray irons, an important element of the structure, mainly determining the ~~XXXXXXXX~~ properties of ~~XXXXX~~ iron, is graphite. Based on GOST 3443 - 46, provision is made for a quite detailed appraisal of the graphite deposits. Graphite in gray iron is classified according to quantity (6 categories), according to nature of distribution (5 types), according to length of graphite deposits (8 groups), according to ratio of their length to thickness (6 subgroups), according to degree of rectilinearity (3 kinds), according to nature of distribution (4 forms) and (3 variants). ~~XXXXX~~ However according to orientation ~~(XXXXXXXXXXXX)(XXXXXXXXXX)~~ in practice even this diversified characteristic of the structure of graphite often proves unsatisfactory and compels one to resort to scales other than the standard ones. At the same time, certain ~~XXXXX~~ types of standard evaluation are superfluous and usually are not applied.

The ~~XX~~ quantity of graphite is characterized by an average percent of the area occupied by a graphite in the field of ~~vision~~ <sup>view</sup> of the microscope. This value, as we shall see later, coincides with the volumetric content of graphite in iron. In Table 2, along with the norms of the ~~XXXXXX~~ <sup>quantity</sup> of graphite, according to ~~XXXXXX~~ <sup>standard</sup> we also present exemplary numbers of the corresponding weight content of graphite which were computed by us. Carbon content in castings made of construction gray iron of various types (from SCh00 ~~XX~~ to SCh38-60) usually falls within the limits from 2.5 to 4.0% by weight (Bibl.25). Insofar as the quantity of bonded carbon usually comprises around 0.5 - 0.7%, the weight content of free carbon (graphite) proves to fall within the limits from 1.8 to 3.3%. A comparison of these figures with the

Table 2

a)	b)	c)
G 02	below 3	below 0,9
G 05	3— 5	0,9—1,5
G 08	6— 8	1,8—2,4
G 11	9—11	2,7—3,4
G 14	12—15	3,7—4,7
G 17	above 15	above 4,7

a) Categories; b) Quantity of graphite, % of area; c) Content of graphite, % (by weight)

data in Table 2 indicates that, although the standard provides for six gradations according to quantity of graphite, ~~XXXXXX~~ practically all types of castings are included by only two categories, that is G08 and G11. The remaining four categories, comprising two thirds of the scale, remain unused and the quantitative evaluation ~~XXXX~~ actually is converted to a qualitative one.

Depending upon the principal length of graphite deposits, the structure of gray iron is subdivided in GOST 3443 - 46 into eight types. A similar scale which was proposed by Macon and Hamilton ~~(XXXXXX)~~ (Bibl.12), or standardized in the USA in 1941 (standard A247 - 41T ASTM). The norms of our standard are presented in Table 3. In the same place the norms of the ASTM scale are also presented.

According to data of ~~XXXXXXXXXXXX~~ N.G.Girshovich, in practice the most frequently encountered range of sizes of graphite deposits comprises from 20 to 700 microns (Bibl.25). The data of Norber and Bolton, who investigated the sizes of graphite deposits in six groups of castings with a structure of graphite ranging from extremely fine to ~~XXXX~~ very coarse, coincide with these data. According to these data, the average length of deposits do not exceed 150 microns, and the maximum did not exceed 700 microns (Bibl.26). ~~XXXXXXXXXXXX~~ G.N.Troitskiy considers

Table 3

a)	b)	c)		
		d)	e)	f)
Gg1	above 1000	960	1280	—
Gg2	500—1000	480	640	960
Gg3	250—490	240	320	480
Gg4	120—240	120	160	240
Gg5	60—110	60	80	120
Gg6	30—50	30	40	60
Gg7	15—25	15	20	30
Gg8	below 15	—	10	15

a) Group; b) Principal length of graphite deposits based on GOST 3443 - 46, microns;  
 c) ~~XX~~ Length of graphite deposits based on the ~~ASTM~~ ASTM scale, microns; d) Minimum;  
 e) Average; f) Maximum

that the practically most important range of sizes of graphite deposits have a length from 50 to 500 microns, while the actual range amounts to from 1 to 100 microns (Bibl.27). In Table 4, we present data of measurements of graphite deposits found in six groups of ~~XXXXXXXX~~ castings, obtained by Norber~~█~~ and Bolton.

The data presented indicate that only four or five groups from the eight groups of the standard, characterizing relatively fine deposits (ranging from Gg4 to Gg8 based on GOST 3443 - 46 or from No.4 to No.8 based on the ASTM scale) can have practical interest and wide use. Understandably, this quantity of gradations is insufficient for a differentiated appraisal of the dimensions of graphite deposits of ~~XXX~~ diverse machine construction castings. It represents only half of the number of iron types of construction gray ~~XXXX~~ established by GOST 1412 - 48. Hence, not only samples of various smeltings of the same type of gray iron, but also samples of castings of related types are usually rated by the same group based on the measurement of graphite deposits. This sharply limits the possibility of metallographic control of the iron casting and, in particular, makes impossible the introduction of statistical

control for the length of graphite deposits. Therefore, in many cases, the

Table 4

a)		
b)	c)	d)
1	4	20
2	10	30
5	25	100
10	100	200
15	125	250
40	150	700

a) Actual length of graphite deposits, microns; b) Minimum; c) Average;  
d) Maximum

factories use their own scales, differentiating more finely the graphite deposits according to length and consisting, e.g. of 16 numbers. Above we have already presented another example of a more precise appraisal, with the use of decimals of the ASTM scale (see Table 1).

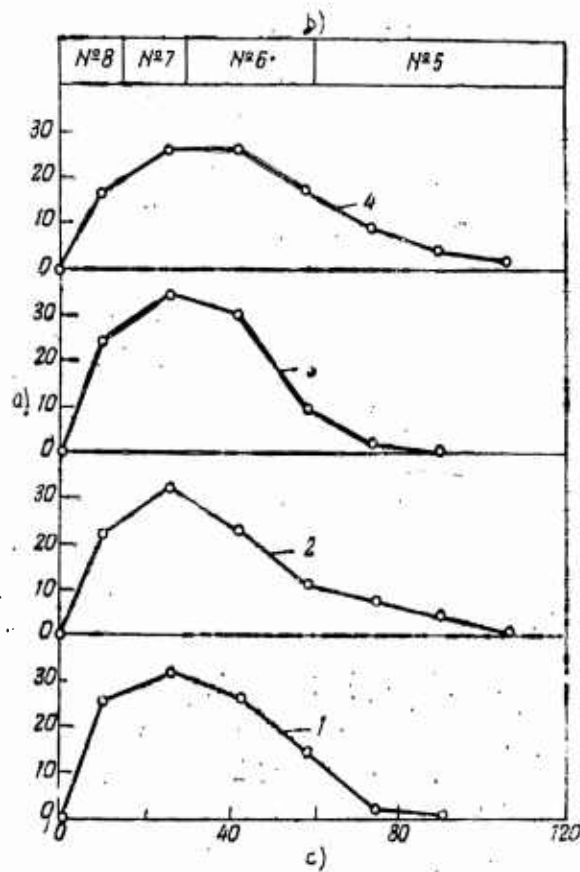
S.M.Skorodziyevskiy measured a large number of graphite deposits in the castings of tractor bushings, type ~~CHTZ~~ ChTZ (approximately based on 2000 measurements for each sample) (Bibl.28). Based on these data, we have constructed curves of the distribution of deposits based on their length, shown in Fig.2 for four samples. The mean length of deposits for each of them is expressed by the following numbers:

No. of sample . . . . .	1	2	3	4
Average length, microns	32	36	31	42

These figures indicate that the examined samples correspond in average length of graphite deposits to the numbers 6 and 6.5 in the ASTM scale (see Table 3). At the same time, the distribution curves indicate that deviations in length of deposits go beyond the artificial and unfounded limits of the ASTM scale, which does not refer

to the GOST 3443 - 46 scale, inasmuch as in it there are established the standards of the "principal" length of deposits, and not the minimum and maximum as in the ASTM scale.

We will limit ourselves to the above-considered standard scales, assuming that they show quite clearly the disadvantages of the most widely used methods of rating the structure with the aid of ~~XXX~~ scales. All of the methods of rating considered in the present section are relatively the best, inasmuch as an estimation based on these scales is connected with ~~XXXXXXXXXX~~ definite geometric parameters of the visible structure of the metal. Nevertheless, the use of these methods quite often creates only the semblance of a quantitative estimation of the structure.



Four Castings of  
 Fig.2 - Distribution of Lengths of Graphite Deposits in ~~XXXXXXXXXX~~ of ~~XX~~  
 Tractor Bushings. Based on data of ~~XXXXXXXXXX~~ S.M.Skorodziyevskiy (Bibl.28)  
 a) Frequency, %; b) Limits based on the ASTM scale; c) Microns

Additional errors are caused by the planar estimation of the structure, instead of its spatial characteristics. In a number of cases, this to a considerable degree devalues the standard methods of analysis.

#### Section 4. Spatial Structure of an Alloy and Methods of Studying It

From the point of view of its spatial structure, any metal or alloy can be regarded as a conglomerate, consisting of a multitude of microscopic bodies, filling the investigated sector of ~~XXX~~ space, and permanently interconnected by surfaces ~~the~~ contact with each other. Depending upon geometric outlines or process of formation, these bodies are usually called crystals, crystallites, deposits, inclusions, grains, globules, spheroids, nests, flakes, plates, small leaves, needles etc. A most common term for these microscopic bodies can be the concept "crystallite", if they all have a crystalline inner structure. However, taking into account that among them are found the formations of amorphous structure (for instance, vitreous nonmetallic inclusions), ~~XXXXXXXXXX~~ we propose a ~~more~~ more rational term "microscopic particle" or ~~XXXXXXXX~~ "micro-particle", which we will use in the subsequent discussion.

Each micro-particle (metallic or nonmetallic) is a structural individual of microscopic structure of the given metal alloy, in the same way that the elementary cell is such for the crystal structure of a body. Micro-particles represent micro-volumes of crystal lattices, of one or another phase of alloy (elements, ~~XXX~~ solid solutions, chemical compounds, etc.) if they have a crystal structure.

In pure metals and alloys having a single-phase structure, all micro-particles are usually characterized statistically by a single type geometric form, for instance by the form of a regular but on the average of equi-axial polyhedrons. In other cases, there is possible the presence of two or more groups of micro-particles belonging to

the same phase of alloy ~~XXX~~ and having a uniform crystal lattice, but differing in geometric form. For instance, in soft steel we note two groups of micro-particles of ferrite; the particles of one of them, entering the composition of <sup>a</sup>perlite are characterized by a thin-lamellar form, whereas particles of the second group have the form of polyhedrons ("of a grain" of ferrite).

The inner structure of the vast majority of micro particles is characterized by a crystal lattice, determining the pattern of spatial arrangement of atoms, comprising the micro particle. However the actual micro particles constitute, as is known, complex formations consisting of blocks of a mosaic structure. Also of complex structure are the transitional boundary zones between adjacent micro-particles ~~XXXXXXXX~~ and blocks; these zones are not simple geometric ~~XXXXXXXX~~ interfaces, but have a fixed actual thickness. The composition and, hence the inner structure of ~~XXXXXXXXXXXX~~ micro-particles, are heterogeneous within the volume of a separate micro-particle etc. We shall dwell in more detail on these problems later on.

The actual, three-dimensional microscopic structure of metal is not accessible to direct observation, since metal is not transparent. We can see only the structure, obtained in the intersection of metal by the plane of a metallographic microsection, i.e. the two-dimensional structure of a cut or section of metal. Nevertheless, such a structure gives us a direct ~~XXX~~ and graphic ~~XXX~~ <sup>idea</sup> of the microscopic structure of the metal. The visible two-dimensional ~~XXXXXXXXXXXX~~ <sup>microstructure</sup> should serve as initial material for recreating according to it the patterns of actual three-dimensional microscopic metal structure. In metallography ~~XXXXXXXXXXXX~~ <sup>and microphotography,</sup> or when observing in a microscope, the planar structure is considered, with very rare exceptions, as the final goal of the analysis being conducted, in spite of the fact

that with appropriate processing, they could yield a more complete data concerning the spatial microscopic structure of the metal. As we noted above, the object of all standardized methods of metallographic analysis is also comprised by planar microstructure.

An important advantage of metallographic analysis is the clarity of the pattern being observed; however this clear pattern is rarely used for a more precise spatial estimation of the geometric parameters of the structure; this is the source of the disadvantages. The metallographer often overlooks the fact that the visible structure of a microsection is only a portrayal on the surface of a spatial microscopic structure of the alloy.

The plane elements of the visible microstructure exist only on the slide, comprising random sections of microparticles of various phases of the alloy. All those geometric parameters of two-dimensional structure which we can measure or compute on a microsection, do not exist in an actual three-dimensional structure of an alloy, although they are connected with it and are determined unequivocally by it.

A knowledge of the form of dependence of geometric parameters of a plane structure upon the spatial structure of an alloy is quite mandatory in developing any method of quantitative appraisal of the microstructure. The disregarding of this condition often leads to the obtainment of distorted, and sometimes of quite erroneous concepts concerning the actual structure of the alloy.

A study of the ~~XXXXXXXX~~ structure of alloys in connection with the processes of thermal, mechanical and other types of action upon it can give us a correct concept of the physical nature of the transpiring processes of conversions or changes, in an alloy only when we quantitatively link the factors of outer effect and indexes

of properties of the alloy with the geometric parameters of its actual spatial structure. To seek a quantitative dependence among these factors, indexes of properties of alloys, and parameters of plane microstructure of it is just as unfeasible as establishing a dependence between the properties and behavior of a ~~mono~~<sup>single</sup> crystal and its x-ray photograph, not having determined in advance according to it the parameters of true structure of the crystal lattice.

If we limit ourselves to a quantitative characteristic of only the plane microstructure of the alloy, in the optimum case we succeed in establishing only the empirical, ~~XXXXXXXXXX~~<sup>semiquantitative</sup> dependences among its parameters on the one hand, and on the other between the composition, properties and machining of the alloy. One can establish the physical nature of these dependences, find or verify the laws determining them, generalize and extend them to other cases only when one proceeds from the true three-dimensional structure during the evaluation.

#### Section 5. Inadequacy of a Plane Evaluation of Microstructure

In metallographic terminology, there is much confusion in the definitions of the geometric form of various elements of structure; this confusion is caused by the fact that in the ~~XXXXXXXXXX~~ selection of a definition, sometimes one proceeds from a plane picture, being observed on the ~~XXXXXXXXXX~~ microsection, and sometimes uses the actual spatial structure of the alloy as a basis. Therefore one can find in metallographic practice such definitions as "twinning plane" and "twinning line", "plate of ferrite" and "strip of ferrite" (in pearlite), "boundary surfaces" and "lines of boundaries", "cementite shell" and "cementite grid", etc. Therein, almost never are indications made as to what exactly is intended - a plane structure of a spatial structure. For instance, in GOST 3443 - 46, one speaks of the "thickness" of graphite deposits of gray iron, whereas actually what is meant is the width of sections of graphite plates visible on the microsection. As a result of the vagueness



the chance of coincidence of plane ~~XXXX~~ of a plate with the plane of a microsection is quite trivial. Nevertheless, A.P.Gulyayev and Ye.V.Petunina managed to detect

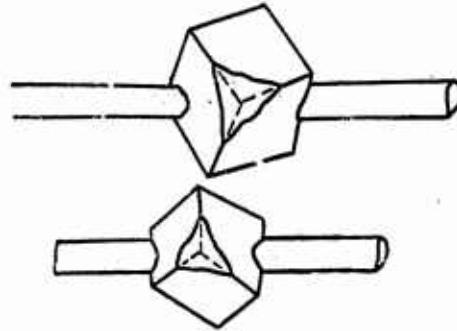


Fig.3 - Needle-Shaped Micro Particles of  $Cu_6Sn_5$  and SnSb Micro Particles of Cubic Form Taken from Babbitt by the Method of Hot Filtration. The diagram is based on a photograph of by M.P.Slavinskiy and N.L.Kleyman (Bibl.29)

and photograph several martensite plates which coincided with the plane of the microsection. One of them is shown in Fig.4 which also constitutes ~~XX~~ an additional confirmation of the platelike structure of martensite. Hence, in this case the ~~XXXX~~ concept "needle" ~~XXXX~~ already refers not to a three-dimensional structure but to a two-dimensional section of micro particles being observed on the microsection.

A similar duality of approach to evaluation of the form of micro particles in itself leads sometimes to serious results. For instance, the author of one paper suggested three formulas for computing the volume of the transformed phase as a function of the time of isothermic delay, at differing uniform state of growth of nuclei: ~~monodimensional~~ <sup>one</sup>dimensional ("of a needle"), two-dimensional ("plate") and three-dimensional ("spherulite"). An experimental checking of the formula for monodimensional growth was conducted for the isothermic transformation of supercooled ~~XXXXXX~~ austenite in ~~XXXXXX~~ "needlelike" troostite, where ~~there~~ there was obtained a good coincidence of calculation with experiment (Bibl.32). However since in reality the "needlelike" troostite as well as the "needlelike" martensite have a lamellar form, experimental checking actually refuted the formula of the author and did not confirm its validity.

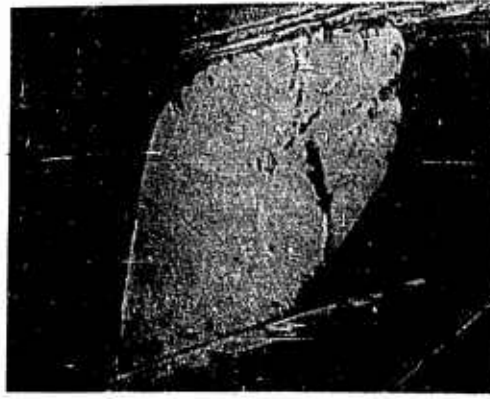


Fig.4 - Martensite Formation (White Component), not Having a Needlelike Form, - ~~the~~ Plane of Microsection Coincided with Plane of Martensite Plate [after A.P.Gulyayev and Ye.V.Petunina (Bibl.31)]

Obviously, it is necessary to stick to a single approach in the choice of terms typifying the geometric form of structural elements, which should be chosen based on the actual three-~~XX~~ dimensional structure of <sup>microparticles.</sup> ~~XXXXXX~~ In those cases when one is discussing the parameters of two-dimensional structure, the use of the appropriate terms should be specifically spelled out.

In a quantitative evaluation of the microscopic structure of metal, it is quite necessary to link the parameters of plane structure with the parameters of spatial structure. The lack of such a linkage may comprise a source of grave errors and of incorrect conclusions. For instance, ~~IX~~ I.L.Mirkin, having investigated the processes of secondary crystallization of steel, remarks: "A simple counting of the grains (this means the two-dimensional grains in the plane of a microsection - S.S.) or a measurement of their size leads to a quite untrue conclusion concerning the linear rate of crystallization and rate of nucleation. Analysis and experience indicate that a large number of grains in the microsection sometimes can be detected during a ~~XXX~~ low value of rate of nucleation and, contrariwise, a small

number of grains are detected in case of a high rate of nucleation. Such an externally paradoxical phenomenon ensues from the inequality of sizes of grains and the need of referring them to the volume of steel, whereas the counting is conducted on the plane (surface) of the microsection. This same circumstance needs to be taken into account in a determination of the quantity and size of slag inclusions, carbides, oxides and other deposits usually being determined under a microscope; based on the latter condition, the existing methods of their microanalysis required a reexamination, and our concepts regarding ~~the~~ <sup>the</sup> number of them present in steel are basically erroneous" (Bibl.33).

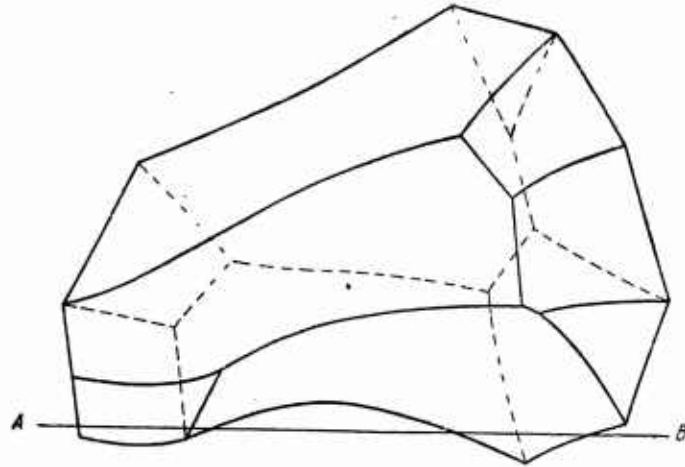


Fig.5 • Individual Grain Taken from a Piece of Coarse-Grained Steel.

Drawing by D.K.Chernov (Bibl.4)

We will show how, using the standard method of ~~XX~~ determining the size of grain of steel, one can obtain <sup>(a)</sup> ~~the~~ concept opposite to that of the actual average size of three-dimensional grains. In Fig.5 is shown an individual grain removed from a piece of coarse-grained steel by D.K.Chernov, based on his actual drawing (Bibl.4). We can easily see that if the plane of the microsection passes along the line AB, perpendicularly to the <sup>plane of the paper,</sup> ~~surface of the drawing,~~ we will see in the microsection two

sections of this grain, not connected one with the other in the plane of the microsection. Therefore we will naturally take them for two independent grains in the counting of the number of plane grains and in a determination of the average area. The more complex the shape of the three-dimensional grains, at one and the same average volume of them, the ~~greater~~ more the two-dimensional grains that will be observed per unit ~~of~~ area of microsection, the greater will be the lack of correspondence between the actual and apparent size of the grain.

In case of especially complex forms of spatial grains, on the microsection there may even be observed ~~the~~ so-called "isolated grains", described first by V.N.Sveshnikov (Bibl.34) and later noted by V.M.Zamoruyev in ~~XXXXX~~ <sup>specimens</sup> samples of cuprous soft ~~XX~~ steel (Bibl.35). Such a grain would be more correctly termed "a grain within a grain", since the boundaries of the "isolated" grain on the microsection represent a closed curve, not contacting the network of lines of boundaries of other grains. In Fig.6 we show the microstructure of ~~XXXXXX~~ austenite steel, containing 18% Cr and 8% Ni (Bibl.36), in which one can see three such "isolated" grains, indicated by arrows. Judging by the orientation of lines of boundaries on the microsection, two of them located farther to the right belong to one and the same spatial grain/<sup>to</sup> which ~~XXXXXX~~ there evidently belongs the elongated flat grain located somewhat lower.

Isolated (~~XXXXXX~~) grains occur relatively rarely. However, very often in microslides one finds grains located close together, revealing a uniform color in case of deep pickling or a uniform orientation of <sup>slip</sup> lines, ~~of slippage~~, which serves as a confirmation of their belonging to one and the same volumetric grain.



Fig.6 - Isolated Grains in Austenite Steel (18% Cr and 8% Ni)  
(Sibl.36)

The ~~the~~ regular shape of grains approaching a spherical shape also does not protect us from mistakes, if the judgment of the average size of a three-dimensional grain is based on measurement of the average area of two-dimensional grains or on a counting of the number of grains in a fixed area of a cut ~~XXX~~ (microsection). At single-phase structure and ~~equiaxial~~ <sup>equiaxial</sup> ~~expected~~ shape of grains, the dependence between the quantity of ~~XXX~~ three-dimensional grains per unit ~~of~~ volume of metal and the number of their sections per unit ~~of~~ <sup>the</sup> area of microsection may be expressed by the following equation

$$N = kn^{3/2}, \quad (5.1)$$

where N is the number of three-dimensional grains per 1 mm<sup>3</sup> of metal;

n is the number of their two-dimensional sections per 1 mm<sup>2</sup> of cut.

The value of <sup>the</sup> coefficient k depends upon <sup>the</sup> fluctuation in sizes of three-dimensional grains. For the usually observed structures, the values of this coefficient change within limits ranging roughly from 0.75 to 1.0. Thus, even at an ideally regular form of grains and at one and the same number of two-dimensional grains occurring in the cut, the quantity of three-dimensional grains per unit ~~of~~ volume of metal and the average volume of grain may differ within the limits of around 25%, owing only

to the fluctuation of their sizes. Thence it is clear that the value of only the number  $n$  is not enough for judging the actual dimensions of average three-dimensional grain. Therefore the standard method of determining the grain size based on GOST 5639 - 51 cannot furnish a correct concept of the true grain size, even if it is ideally uniform in shape\*. The presence of grains with concave surface increases the error.

The same takes place in a determination of the quantity and sizes of nonmetallic inclusions. We present the following example (according to I.L.Mirkin): if, per unit volume of one type of steel there are 1000 inclusions 20 microns in diameter, while in another type of steel there are 2000 inclusions with a diameter of 10 microns, in a microanalysis of the ~~XXXXX~~ samples of both steels, we will observe approximately the same quantity of them per unit ~~XX~~ area of the microsection (Bibl.37). In any steel, the inclusions are heterogeneous in sizes. Thence it follows that, based on the quantity of inclusions in a cut, one can by no means obtain a proper concept of the fraction of large and small inclusions, concerning the total quantity of inclusions or the degree of contamination of the steel.

The parameters typifying the kinetics of the process of crystallization are determined according to the change in quantity of micro<sup>o</sup>particles of the newly forming phase and their sizes <sup>as a</sup> ~~is~~ function of time of the isothermic soaking. For round micro<sup>o</sup>particles, the following mathematically precise relationship between the

---

\* Here it is appropriate to note that the term "actual grain", being used in GOST 5639 - 51 for signifying the actual size of plane grains of steel, is quite unsuccessful. By "actual" grain it is natural to ~~XXXXX~~ understand the true three-dimensional grains of steel, in contradiction to the visible size of two ~~XX~~ dimensional-grains <sup>in</sup> ~~XX~~ the microsection, which could lead to ~~XX~~ misunderstandings.

microparticles  
quantity of ~~XXXXXXXXXX~~ per unit ~~of~~ volume of metal N and number of their

sections per unit ~~of~~ area of cut, n is valid:

$$n = N\bar{D}, \quad (5.2)$$

where  $\bar{D}$  ~~is~~ the ~~average~~ arithmetic <sup>mean</sup> value of diameter of microparticles.

The number n may increase owing to an increase in average diameter of ~~the~~ microparticles, ~~XXXXXXXXXX~~ in case of their unchanged quantity per unit ~~of~~ volume of metal N, or even owing to an increase of this number at unchanged average diameter of ~~the~~ micro particles  $\bar{D}$ . It is also possible that ~~it~~ <sup>the number</sup> will grow owing to a simultaneous increase in N and  $\bar{D}$ . Thence it follows ~~XXXX~~ quite obviously that neither the rate of nucleation of crystallization nor the linear rate of growth can be determined, proceeding only from one number n and the kinetics of its change <sup>as</sup> ~~is~~ a function of time of isothermic soaking.

Meanwhile, G.Tamman proposed a formula for calculating the linear rate of displacement of boundaries of grain at isothermic recrystallization, based on the kinetics of change in the quantity of two-dimensional grains (Bibl.38):

$$a = \frac{1}{z \sqrt{n}}, \quad (5.3)$$

where a is the linear rate of displacement of ~~grain~~ <sup>the</sup> boundaries;

z is the duration of annealing.

In ~~XXXX~~ the light of what has been stated above, it is clear that the G.Tamman formula is inaccurate. Moreover, the very concept of rate of displacement of boundaries lacks physical meaning in application to single-phase polycrystalline aggregates in case of collective recrystallization, and is unsuccessful.

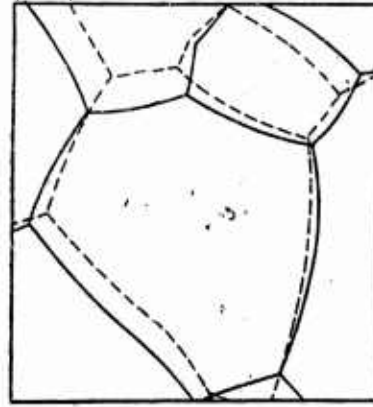


Fig.7 - Displacement of ~~Lines~~ ~~Boundaries~~ of Aluminum Grains on a Cut at 600°. Solid lines equal after two minutes of soaking, broken lines equal after an additional 30 sec soaking. The diagram is taken from a ~~microphotograph~~ (Bibl.39)

In Fig.7, based on photomicrography (Bibl.39), there is shown the displacement of ~~lines of grain boundaries~~ grain boundary lines on a cut of aluminum: the solid lines show the position of boundaries after two minutes of soaking at 600°, while the broken lines show the same after an extra 30 sec soaking at the same temperature. The displacement of any sector of the ~~line of boundary~~ line of boundary between two adjacent grains may be characterized by a fixed linear velocity, but if this rate is positive with reference to one grain (growth), then it is negative in relation to the second. If we examine the polycrystal as a whole, the average rate of displacement will obviously equal zero. One could have taken into consideration the displacement of boundaries only of growing grains, but from the drawing it is apparent that the boundaries of the same grain may ~~displace~~ shift at a positive rate at one place, and ~~with~~ at a negative rate at another place. Hence, "linear rate of displacement of boundaries" in the given case ~~is~~ proves a very indefinite and conditional concept.

In spite of the fact that, more than 20 yrs ago, I. I. L. Mirkin proved the

impossibility of a correct calculation of ~~parameters of crystallization~~ without taking into account the connection of plane structure with spatial structure (Bibl.33), up to recent times attempts of such a kind have been continuing. For instance, one can point to the criticism <sup>by</sup> S.R.Lilly and ~~of~~ I.K.Stanley of the method of studying the rate of crystallization on a plane, which S.F.Rejter used in investigating the kinetics of recrystallization of low-carbon steel (Bibl.40).

At the same time, if the forms are known of the connection of geometric parameters of spatial structure and of plane structure, one cannot only calculate correctly the parameters of crystallization but also compute in advance the geometric parameters of plane structure, proceeding from the propositions at the basis of the theory of the crystallization process. Then it is easy to compare these computational parameters with test data for checking the validity of the theoretical assumptions.

For instance, to the process of graphitization of white <sup>cast</sup> iron, there is usually attributed a normal crystallization kinetics, typified by the nucleation of ~~graphitization~~ graphitization and by the growth of graphite ~~deposits~~ deposits. If the rate of nucleation of graphitization is constant during the process of isothermic soaking or even gradually decreases, the total quantity of graphite deposits per unit of volume of iron should continuously increase. The quantity of sections of graphite deposits visible per unit ~~of~~ area of cut should increase still more intensively, as follows from formula (5.2), inasmuch as the dimensions of deposits increase during the process of graphitization. The computational curve of the change in number of deposits of graphite per unit ~~of~~ cut area is shown in Fig.8 (curve 1). Curves 2, 3, and 4 in the same figure are drawn for the first stage of graphitization of samples of three smeltings of white iron based on test data of B.F.Sobolev (Bibl.42).

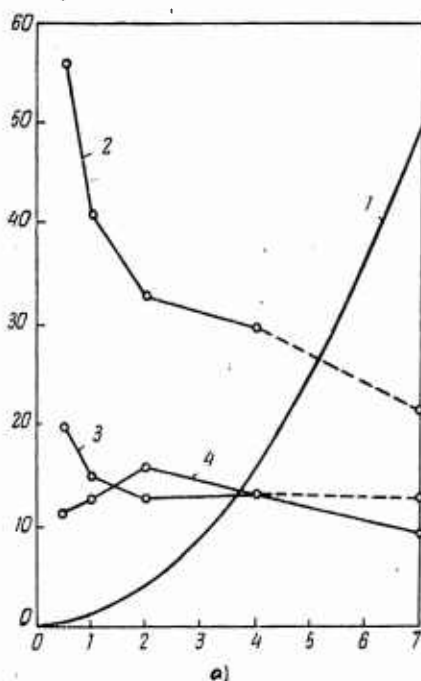
They show how the quantity of deposits on a ~~XXXX~~ microsection actually changes depending upon the duration of ~~XXXXXX~~ annealing at 970°C.

Comparing the computational and test ~~XXXX~~ curves, it is easy to see that between them there exists neither a quantitative or even a qualitative correspondence:

~~XXXXXX~~ in place  
~~XXXXXX~~/of the expected growth of the number of clusters, ~~XX~~ the number decreases.

It is obvious that the process of graphitization transpires at prepared centers (nuclei), while the quantity of deposits continually decreases in the process of isothermic annealing owing to their coagulation. The actual term "nucleation" under these conditions ~~loses~~ *loses* meaning and our concept of the kinetics of ~~the~~ *the* graphitization process should be reexamined.

The example presented ~~g~~ shows that a



study of the spatial structure of alloy proves quite effective in checking by experiment the correctness of any hypotheses and theories ~~XX~~ connected with transformations in alloys. According to the successful expression of S.S. Smith and L. Guttman, the thinking of scientists is usually limited by the same ~~dimensionality~~ *dimensionality* ~~XXXXXX~~

which is possessed ~~XXXX~~ by the structures studied by them (Bibl.43). Therefore only from a change ~~XX~~ a study of plane structure to a study of three-dimensional structure can give a ~~correct~~ *correct* ~~proper~~ *proper* concept of the

Fig.8 - Kinetics of Change in Quantity n of Graphite Deposits per 1 mm<sup>2</sup> of Cut in the Process of First Stage of Graphitization of Three Smeltings of White Iron (Curves 2, 3 and 4). Based on data of B.F. Sobolev (Bibl.42)

a) Time (hrs)  
~~nature and physical nature of phenomena being observed in alloys~~

nature and physical essence of phenomena being observed in alloys.

What has been stated shows convincingly enough the helplessness and inadequacies of the quantitative evaluation of a plane structure, if it is not tied in with the spatial structure of the alloy. The rational and most effective way of developing metallographic analysis requires the use, not of the quantitative characteristic of structure in general, but such an evaluation which would be based on the spatial structure of the alloy. Both the parameters of spatial structure as well as the parameters of plane structure, on the basis of which they may be computed, should be evaluated as natural geometric ~~values~~ <sup>quantities</sup> without any ~~kind~~ <sup>kind</sup> of coding or designating them with conventional point symbols or numbers.

#### Section 6. Basic Parameters of Spatial Structure

The form of particles making up a metallic aggregate is rarely geometrically uniform. The microparticles can be convex geometric bodies, but can also be bounded by concave surfaces. Quite often the microparticles have dimensions which are about uniform in all directions (~~equiaxed~~ <sup>equiaxed</sup> microparticles - grains, globules, spheroids). However, microparticles can also occur in which the dimensions in two directions predominate considerably over the dimension in a third direction (plates, ~~small leaves~~ <sup>lamellae</sup>), or actual particles having a predominating dimension only in one direction (needles, threads, rods). In certain cases, the microparticles are relatively massive formations with closed internal cavities, filled with microparticles of other phases or structural components (ferrite with ~~granular ferrite~~ <sup>pearlite,</sup> cementite in ledeburite, etc.).

The sizes of microparticles also change within wide limits in a given small volume of alloy, which is the object of microanalysis.

The mutual arrangement of microparticles of one or of several phases is random



microscopic structure of the object being analyzed, as a whole.

The selection of parameters of <sup>the</sup> spatial~~ly~~ microscopic structure of an alloy, which can feasibly be measured during metallographic analysis, is determined by the role of <sup>the</sup> (elements ~~and~~ microstructure), ~~typified~~, typified by these parameters, in the processes of transformations and alloys and their effect ~~upon~~ upon the properties of the alloy. At the same time, these parameters should be determined by the application of technically accessible but <sup>not</sup> too unwieldy and sufficiently precise methods of metallographic analysis.

From this viewpoint, the most important characteristic of <sup>the</sup> microscopic structure of an alloy is its quantitative volumetric structural or phase composition, by which we mean the fraction of each structural component or phase in the volume of the alloy, usually being expressed in volumetric percentages. In a study of the kinetics of structural transformation in alloys, the change of structural and phase composition, <sup>as a</sup> ~~in the~~ function of time, is a necessary and sufficient index of the course of the process.

Knowing the fraction of the volume of alloy being taken up by each structural component or phase, and having access to the values of their specific weights, we can easily proceed from volumetric structural composition to weight composition. It is just as easy to proceed from weight structural composition to chemical composition of the alloy, if we know the chemical composition of each phase or structural component.

EX Using the simple rule ~~of~~ mixture, on the basis of quantitative volumetric structural composition of the alloy, we can also compute its specific weight.

In a number of cases, using simple formulas, one can calculate in first approximation the indexes of mechanical properties of an alloy (hardness, ultimate

strength ~~XXX~~ etc.). For this, in addition to volumetric ~~XXXXX~~ <sup>the</sup> structural composition of alloy, it is necessary to have available the corresponding indexes of mechanical properties of each structural component.

Hence, a knowledge of the volumetric structural or phase composition of the alloy permits one to connect ~~XX~~ quantitatively its structure with the chemical composition, physical and mechanical properties of the alloy, which serves as a valuable means of reciprocal ~~XX~~ checking and correcting of various types of investigation of the metal.

An equally important parameter of microscopic structure is the value of total surface of <sup>the</sup> grains of metal for microparticles of various phases and structural components of <sup>am</sup> alloy, referred to ~~unit~~ ~~of~~ ~~the~~ volume. This value, (specific area) called by us the specific surface/ of grains or microparticles plays an exclusively important part both in the processes of ~~XXXXXX~~ transformations in alloys as well as in a determination of their diverse properties.

Based on a differing orientation of spatial lattices in each pair of contacting microparticles of pure metal, on the boundary of their contact there exists a layer of atoms in which they are arranged irregularly. The same takes place also (interface) crystal at the boundary of contact/ of various ~~XXXXXX~~ lattices of each pair of microparticles of different phases.

In the boundary layer, the position of atoms is fixed by forces acting from the side of both adjacent lattices, and constitutes a compromise position between those being determined by each of them separately. The layer of irregularly arranged atoms has a certain thickness, although it is trivial in comparison with the extent of the boundary layer. Therefore the boundaries of grains and of microparticles are not geometric ~~surfaces~~ but are <sup>areas</sup> ~~areas~~ <sup>regions</sup> possessing a fixed volume. These <sup>regions</sup> ~~areas~~ are called

intercrystalline interstratifications (Bibl.45) or, more correctly, intercrystallite zones (Bibl.46).

At the boundary of various contacting ~~XXXXXXXXXXXX~~ crystal lattices or of uniform but variously oriented lattices, there occurs a ~~XXXXXXXXXXXX~~ "thickening" of energy. The energy level here is higher than within the volume of the crystal lattices, the atoms are connected less stably than those found within the regular lattice, the transitional layer is less stable thermodynamically, and its atoms are more mobile and inclined toward rearrangement and migration.

causes the exclusive activity  
This ~~XXXXXXXXXXXX~~ of atoms of intercrystallite zones and explains why they possess the leading part in the processes of interphase transformations, growth of grain, creep of metals, diffusion, nucleation of crystallization of a new phase, etc., which has been noted many times in the past by the practice of metallography.

As is known, the mechanical properties of an alloy are ~~the~~<sup>a</sup> function not only of the structural composition but also of the dispersed state. At one and the ~~XX~~ same volumetric phase composition of <sup>an</sup> alloy, the value of specific surface of microparticles serves as a reliable standard of the degree of dispersed state of ~~the~~ microscopic ~~XXXXXXXX~~ structure of the alloy. Therefore, knowing the value of specific surface of various phases and structural components, we can in second approximation refine the indexes of mechanical properties computed on the basis of structural composition. In many cases, the mechanical properties of an alloy prove to be connected with the value of the specific surface by simple linear dependences. The same can be said concerning a series of physical properties of alloy, specifically the magnetic properties and specific weight.

The plastic deformation of ~~XXX~~ a metal is accompanied by the appearance of a

fixed orientation of intercrystallite surfaces relative to the direction of the forces ~~XX~~ acting in the metal. Therefore a study not only ~~of~~ the value, but also of the spatial orientation of surfaces of microparticles proves quite valuable in ~~XXXXXXXXXX~~ researching the processes of plastic deformation of metal.

The intercrystallite boundary zones of ~~XXXXXXXX~~ microparticles are not the only areas ~~XXXX~~ of metal having increased energy and therefore actively taking part in the processes of transformations and of changes in structure. At formation of polycrystalline structure of pure metal or of single-phase alloy, a microparticle growing from the center of crystallization, encountering on the path of its growth the closest adjacent microparticle and coming into contact with it, forms a boundary, which is common to both microparticles. This interface continues to increase along with the further growth of the microparticles forming it ~~WX~~ until it encounters the surface of the nearest third microparticle. As a result of such a meeting, two more faces (~~faces~~) are formed between this third microparticle and the two first ones. All these ~~XXXX~~ faces are intersected along one line, i.e. a lattice edge, common for all three microparticles. The growth of this edge is limited by encounters with the surface of the nearest fourth microparticle, which will be accompanied by the formation of a <sup>vertex</sup> point ~~of~~ ~~XXXX~~, common ~~to~~ <sup>to</sup> ~~XXXX~~ the four microparticles, that is polyhedrons. Hence, each face in the polycrystalline aggregate belongs to two microparticles, and each edge belongs to three, while each <sup>vertex</sup> point of the ~~peak~~ belongs to four microparticles.

It is necessary to stipulate that in reality, the process of formation of a polycrystalline structure is considerably more complex, since simultaneously with the growth of microparticles there proceeds the process of collective recrystallization. However, this does not change the main character of the final microscopic structure

of the polycrystalline aggregate. Therefore in a polyhedral structure, there are observed intercrystallite zones of three types, namely two boundary (~~edges~~<sup>sides</sup> of polyhedrons), three boundary (edges of polyhedrons) and four boundary (~~peaks~~<sup>vertices</sup> of polyhedrons).

The degree of irregularity of arrangement of atoms in the zones of edges of polyhedrons is higher than in the zones of their ~~faces~~<sup>sides</sup>, since here the atoms are situated under the simultaneous effect of crystalline orders of three differently oriented lattices. Accordingly the level of energy and activity of atoms of three-boundary intercrystalline zones is higher than that of two-boundary zones, and the thermodynamic stability is lower. A still more irregular arrangement is possessed by atoms of the four-boundary intercrystallite zones, where their position is a compromise one between those being fixed by each of the four crystal orders, converging at the <sup>vertex</sup> ~~points of the vertices~~ of the polyhedrons of the spatial lattices.

It is known that in the ~~XXXXXX~~ submerging of any mineral in a supersaturated salt solution, the corners and edges of the crystals prove to be especially active (Bibl.47). In metal alloys in many cases the microstructure serves as a proof that the same position is also valid for them. Very often one can observe the formation of a new phase at the point of contact of three grains of the original polyhedral structure in a microsection. It is clear that this point is the track of a line of edge on the surface of the cut. For instance, in Fig.9 one can see the formation of ~~XXX~~ troostite with preference for the points of contacts of three grains in ~~high-speed~~<sup>high-speed</sup> steel of the ~~PAST~~ type (Bibl.48).

The line of the edges of grains is also of great practical interest because during the creep of metal, the start of the formation of cracks, leading subsequently to final disruption, as a rule is concentrated at the contact points of these

grains (Bibl.49).

The lines of contact points of three microparticles, i.e., the lines of

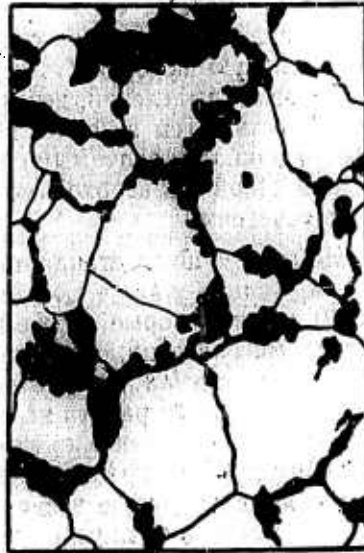


Fig.9 - Principal Formation of Troostite at the Points of Contact of Austenite Grains. After A.P.Gulyayev (Bibl.48)

their number of points of/vertexes per unit ~~of~~ volume of metal.

Of great interest is the quantity of microparticles occurring per unit ~~of~~ volume of alloy. A study of the kinetics of crystallization, recrystallization, determination of true parameters of these processes and of actual dimension (volume) of microparticles is not realizable, if we cannot determine this parameter of the microscopic structure of an alloy. It is necessary to note that the finding of the actual number of microparticles in a volume of alloy is one of the most complex problems of spatial metallographic analysis.

The enumerated parameters cannot give an exhaustive characteristic of the spatial microstructure of the alloy. Having the values of all these parameters at our disposal, one can by no means fully reproduce on their basis the "architecture"

edges of polyhedrons, form in the metal a continuous spatial network which may be estimated quantitatively as the total extent of the lines of edges per unit ~~of~~ volume of metal. The points of contacts of four grains, i.e., the vertexes of polyhedrons are estimated as their quantity. We have every basis for introducing into the list of most important parameters of microscopic structure of metal the length of lines of edges of polyhedrons, and also the

of microstructure of an alloy. For ~~XX~~ instance, knowing the volumetric content of graphite in gray iron, its specific surface and linear extent of edges of graphite deposits, it is impossible to judge the degree of their "vorticity". Nevertheless, the above listed parameters are the most significant and ~~XXXXXXXX~~ reflect the structure of the alloy to the degree which is necessary for judging the properties and behavior of the alloy.

Not counting the scales of standard structures in effect abroad, in the Soviet Union alone more than 30 scales have been standardized, which also do not take in all of the requirements of metallographic analysis. To foresee and to provide for all of the possible cases of <sup>o</sup>quantitative evaluation is obviously impossible, and the present report does not pretend to do this to any degree. To evaluate the special elements of microstructure, to the extent that this is required for practical or research purposes, would possibly require the ~~XXXXXXXX~~ introduction of a number of other parameters and the development of methods of their determination. However, in all cases it is necessary to proceed from the basic assumption: the evaluation of the structure should be conducted quantitatively, with values of geometric parameters of spatial microstructure of the alloy in every case when this is possible.

The system of methods of metallographic analysis permitting a determination of the geometric parameters of spatial microscopic structure of metals and alloys is called by us "stereometric metallography". Quite often, methods of such a type are connected by the concept "quantitative metallography", which is incorrect, since the same concept also includes the methods of quantitative analysis of a plane microstructure. In order to emphasize the basic features of the proposed system of methods, i.e. the volumetric state of the object of analysis (from Greek ~~stereo~~ ~~XXXXX~~

stereo - spatial) and the strictly quantitative nature of their evaluation (from the Greek metron - measure, dimension), we ~~we~~ advance the term proposed by us for this branch of science concerning metals, as the most acceptable term. Accordingly, in the future discussion, we will use the terms stereometric structure, stereometric evaluation, stereometric analysis etc.

#### Section 7. Development of Methods of Stereometric Micro Analysis

As we saw above, the quantitative estimation of the structure of steel, in comparison with its mechanical properties and conditions of heat treating was first used as early as 1868 by D.K.Chernov. However, the maximum development of the method of stereometric evaluation of ~~XXXXXXXXXX~~ microstructure occurred mainly in the last 20 - 25 yrs. The leading place in the development of this branch of knowledge was occupied and continues to be occupied by Russian and Soviet metallurgists and petrographers.

~~THE~~ The problem of <sup>a</sup> quantitative determination of volumetric phase composition was first posed and solved by petrography with reference to rocks. Since there is ~~no~~ no main difference between the determination of the mineralogical composition of rocks and the structural composition of alloys, the methods developed by petrography can be mechanically transferred to metallurgy.

In 1847 M.Deless first used the planimetric method of determining the mineralogical composition of rocks, while in 1898 A.Rozival proposed a more convenient linear method of analysis (Bibl.50).

The quantitative determination of structural composition of alloys in metallurgy was first conducted by Ye.P.Polushkin in 1924. For this purpose, he designed a "metallographic planimeter". The volumetric structural composition which was found was converted to weight composition (based on specific weights of structural

components) and the data derived showed good agreement in comparison with data of chemical analysis (Bibl.51). The most improved method of analysis, namely the point method was developed by A.A.Glagolev in 1931 with application to rocks ~~(Bibl.52)~~ (Bibl.52, 53) and was proposed by him also for application to the structural analysis of alloys in 1935 (Bibl.54). The point method permits the application, during analysis, of various devices, to a certain degree mechanizing the process of analysis and considerably facilitating the work of the observer, accelerating the process of analysis and expediting the obtainment of greater accuracy. A number of such devices (push ~~XXXXXX~~ integrators) were designed by the author of the method. The Glagolev method received widespread fame and dissemination both here in the Soviet Union as well as abroad, and ~~was~~ <sup>is</sup> used with equal success in the ~~the~~ analysis of rocks and of metal alloys.

The method of determining the value of specific surface, i.e. of interface of microparticles of two phases per unit ~~of~~ volume of metal, was first developed by N.T.Belyayev in 1922 for one special case, namely the structure of lamellar <sup>o</sup>perlite (Bibl.55, 56). The method is based on the specific structure of lamellar <sup>o</sup>perlite interlamellar spacing in it, and the constancy of the ~~interplate spacing~~ <sup>interplate spacing</sup> ~~XXXXXX~~ therefore it cannot be extended to any structure of another type. It has been used many times, right up to recent times, by a number of researchers who had studied the <sup>o</sup>perlite transformation of austenite. Specifically, N.T.Belyayev first used the expression "stereometric" in application to the volumetric geometric structure of metal ("stereometry of a <sup>o</sup>perlite grain").

In 1937, J.J.Rutherford, R.H.Aborn, and E.Bain tried to determine the specific surface of microparticles of a polyhedral structure (Bibl.57). The method developed by them is based on an idealized form of microparticles which are assumed to be

geometrically uniform polyhedrons (~~XXXXXXXXXXXXXXXX~~ (cubo-octahedrons) and also on a number of other assumptions. Since the actual shape of microparticles is far from ideal, the method is not a strict one and is not of interest ~~XXX~~ at present.

A universal method of determining the value of specific surface, equally suitable for any shape of microparticles of nondeformed (isometric) structures, is called the method of random secants, developed in 1945 by S.A.Saltykov (Bibl.58, 59).

The method is mathematically strict and in practice is exceedingly simple, permitting the use of ~~XXXXXXXX~~ devices speeding up the measurement under a microscope or in photomicrography. Later on, ~~XXXX~~ the method of random secants was also extended to deformed (oriented) structures. In 1952, S.A.Saltykov proposed a method of ~~XXXXXXXXXXXX~~ approximate ~~XXXXXXXXXX~~ evaluation of specific surface of structures, having a linear ~~of~~ plane statistical symmetry (Bibl.60). In 1954, A.G.Spektor proposed a mathematically precise method, applicable to deformed structures only with a linear (axial) statistical symmetry (Bibl.61). The method of random secants received complete recognition and is used in research activities, constituting the basic method of determining the specific surface of microparticles.

~~XXXX~~ The method of quantitative evaluation of the second type of intercrystallite zones is that of total extent of lines of edges of microparticles per unit ~~of~~ volume of metal, developed in 1950 by S.A.Saltykov (Bibl.17\*. The method is also mathematically rigorous and is quite simple methodologically.

---

L.Guttman

\* It is noteworthy that considerably later, in 1953, S.S.Smith and ~~XXXXXXXX~~ described a method of determining the value of specific surface of microparticles and the linear extent of their edges, under the name of the method ~~XXXXXX~~ "random sections" (Bibl.43). Their method and formulas are quite identical with the methods and formulas published respectively in 1945 - 46 (Bibl.58, 59) and in 1950 by S.A.Saltykov (Bibl.17), but S.S.Smith and L.Guttman make no references whatsoever to these studies.

As was mentioned above, the maximum experimental difficulties are encountered in the determination of the quantity of microparticles in the ~~EX~~ volume of alloy. The approximate formulas, not having <sup>serious</sup> ~~XXXXXXXXXX~~ bases, have been proposed many times for this purpose, however ~~XXX~~ <sup>(a)</sup> rigorous method was developed only for microparticles of spherical form and forms close to it. A precise formula, connecting the diameter of volumetric microparticles, the quantity of them per unit ~~of~~ volume of alloy and the number of sections of particles on a plane was given in 1935 by I.L.Mirkin for a system of isodispersed microparticles (Bibl.33). Later, this formula was extended by S.A.Saltykov to the polydispersed systems of spherical particles. These formulas are insufficient for determining the quantity of microparticles in a volume of alloy, however they have great significance in the development of methods of such a determination.

A very valuable method of computing the quantity of round microparticles was developed by E.Scheil in 1931, and later this was somewhat improved by him (Bibl.62, 63, 64). The Scheil method permits one to determine both the total quantity of microparticles in a volume of alloy, as well as the distribution of microparticles according to their sizes (diameter). A disadvantage of the method is its <sup>unwieldiness,</sup> ~~XXXXXXXXXX~~ which aroused many to work in the direction of its improvement.

Simplified methods based on the Scheil method were developed by ~~XXXXXXXXXXXXXXXXXXXX~~ H.A.Schwartz (Bibl.65), W.Johnson (Bibl.18), S.A.Saltykov (Bibl.66), A.G.Spektor (Bibl.67). Nevertheless, even the best of the existing methods of computing the distribution of microparticles remain unwieldy and complicated.

The Scheil method was used many times in a study of the kinetics of crystallization for determining the crystallization parameters. Up to the appearance of the method of random secants, the Scheil method was also used for computing the specific surface

of round microparticles.

In the above mentioned method of J.Rutherford and others (Bibl.57), the quantity of microparticles in a volume is computed, based on the number of their sections per unit ~~of~~ area of cut. However, since these two parameters are not connected by a well-defined relationship, the values obtained can be ~~XXX~~ regarded only as very approximate. A precise method of determining the quantity of spherical microparticles (without their distribution by sizes) was proposed by S.A.Saltykov in 1947 under the name "method of diverse diameters" (Bibl.63). The method is sufficiently simple experimentally.

The most poorly represented at the present time ~~XX~~ are the methods of determining the characteristics of the form of microparticles. In individual cases, the spatial form of microparticles can be established by the method of successive grindings with ~~the~~ construction of a volumetric model of individual microparticles. The above mentioned method of perpendicular sections of A.P.Gulyayev and Ye.V.Petunina also permits one to determine the form and dimensions only of individual microparticles. Therefore one of the most pressing problems of stereometric (solid geometry) metallography is the development of statistical characteristics of the form of microparticles of the given type.

The ~~XXXXXXXXXX~~ principle first applied by D.K.Chernov of establishing a quantitative interrelationship between the properties of metal, its machining and the parameters of microstructure receive development in the activities of Soviet metallurgists. The use of methods of quantitative evaluation of spatial structure in the reports of M.S.Aronovich, M.Ye.Blanter, S.Z.Bokshteyn, S.M.Vinarov, M.I.Vinograd, A.I.Gardin, A.P.Gulyayev, B.B.Gulyayev, N.K.Lebedeva, I.L.Mirkin, L.S.Moroz, P.O.Pashkov, G.I.Pogodin-Alekseyev, A.I.Skakov, S.M.Skorodziyevskiy, A.G.Spektor,

A.N.Chervyakov, and of others ~~XXXX~~ served for recognition and propagation of the methods of stereometric metallography. Of the number of foreign metallurgists, from the same standpoint one should make mention of E.Scheil, R.Meil, W.Johnson, M.Gensamer, ~~XXXXXXXXXX~~ S.Smith, ~~XXXX~~ L.Beck, G.Kostron, R.Howard and others.

Besides the above mentioned methods of determining the parameters of microstructure, there is required a development of quantitative evaluation of the uniformity and homogeneity of the spatial microstructure. The most important and urgent problem is the translation of standard methods characterizing microstructure into the language of stereometric evaluation. For instance, now it is already possible to note that the evaluation of the granular structure of steel ~~XXXX~~ based on the value of specific surface of microstructures is methodologically more correct and experimentally considerably more improved and more simple, than the standard method being used for determining the size of a grain of steel. Therefore we need an ~~XXX~~ insistent and active struggle for the replacement of obsolete methods of evaluating plane microstructure by already developed, more efficient methods of stereometric evaluation.

#### Section 8. Technical Means and Features of Stereometric Micro<sup>o</sup>Analysis

The most important advantage of stereometric micro<sup>o</sup>analysis is the fact that its use does not require any major new technical resources for any kind of basic changes in the process of preparing the microsection. Therefore the methods described in the present book are accessible for any laboratory, equipped with ~~the~~ simple metallographic apparatus. In this paragraph, we shall examine the general conditions and requirements, equally in effect for all methods of stereometric evaluation. Later, in a description of individual types of stereometric microanalysis, <sup>accomplishment.</sup> we will give special instructions on the techniques of their ~~XXX~~ practical ~~XXXXXXXXXX~~

For a ~~XXXX~~ determination of the actual values of parameters of spatial microstructure based on the nontransparency of the items being analysed, we will ~~XXXXXX~~ proceed only from a plane microstructure. As a result of the intersection by the plane of a cut of individual microparticle, we can observe its random section, which cannot give us a concept either of the actual sizes of the microparticle or of its geometric form. However, while the section of a separate microparticle represents a figure of random form and size, the statistical association of sections ~~IX~~ of a practically infinitely large number of microparticles can already be regarded as an accurate reflection of microscopic structure of the alloy. Taking this into account, one can determine the geometric parameters of the spatial microstructure of an alloy ~~XXXXXX~~ based on its plane microstructure with any accuracy, which may be required. In most cases, ~~XXXXXX~~ one microsection is enough for this, while in case of oriented structures (during transcrystallization, plastic deformation), the number of required microsections may increase to two.

In cast or rolled metal the structure as a rule is irregular in cross section to a greater or lesser degree. For instance, in Fig.10 is shown the distribution of a quantity of deposits of carbon of annealing based on section of samples of forged iron 25 mm in diameter based on data of the author (Bibl.69); a similar distribution pattern is noted for forged iron by I.I.Khoroshev (Bibl.41).

M.M.Shteynberg, I.N.Bogachev, G.A.Zykov and R.Sh.Shklyar found that the size of a grain of transformer steel and the degree of its uniformity change from the surface of the sheet to its core, as is illustrated by the data in Table 5 (Bibl.70).

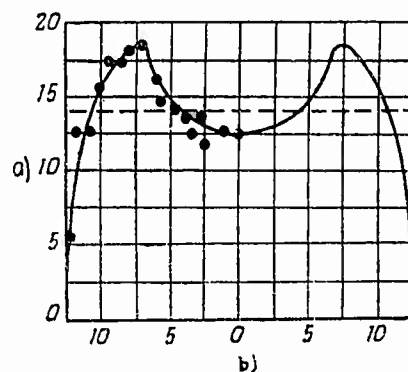


Fig.10 - Distribution of Graphite Deposits according to Section (Diameter) of Round Sample of Malleable Cast Iron. Decrease in quantity of deposits at surface as result of surface decarbonizing during annealing

a) Number of centers per  $\text{mm}^2$ ; b) Distance from center, mm

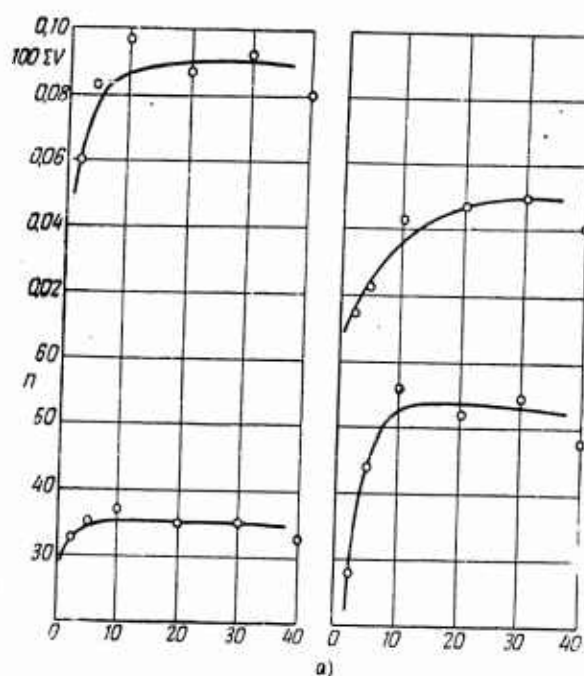


Fig.11 - Typical Distribution of Nonmetallic Inclusions in Section of Steel Castings Weighing 10 kg, Cast from One Smelting in a Ceramic (on left) and Iron (on right) Form.  $100 \Sigma V$  - volumetric % of inclusions,  $n$  - number of inclusions per  $1 \text{ mm}^2$  of area of cut [B.B.Gulyayev (Bibl.71)]

a) Distance from surface, mm

Table 5

a)	b)		
	c)	d)	e)
750	0,03	0,034	0,04
900	0,05	0,06	0,068
1200	0,075	0,26	0,46

a) Annealing temperature, °C; b) Size of grain, mm<sup>2</sup>; c) On the surface of sample; d) At a depth of 0.04 mm; e) At a depth of 0.06 mm

In Fig.11 is shown the distribution of a number of nonmetallic inclusions and their volumetric percent according to section of steel castings 10 kg in weight, which were hardened in ceramic and iron forms, after data of B.B.Gulyayev (Bibl.71). On the basis of the data presented and a number of other data, one can notice a general regularity, that is, from the surface to the center of the section, the dispersed state of the structure decreases.

Inasmuch as the structure in most cases remains qualitatively uniform in cross section, the choice of location of <sup>the</sup> plane of cut during conventional <sup>5</sup> qualitative determinations does not play a substantial part. It is another matter in quantitative microanalysis; here the place and direction of <sup>the</sup> plane of cut needs to be chosen very carefully, taking into account the possible irregularity of structure along the section.

Let us examine  $\bar{X}$  how the choice of section of cut is reflected upon the results of quantitative microanalysis if the structure is irregular. For simplicity, we will limit ourselves to a case when the ground sample can be divided into two zones according to uniformity of structure. Let us assume, that in zone 1, the parameter of structure interesting to us is characterized by the value  $G_1$ , while in

zone 2, by value  $C_2$ . Let us also assume that the diameter of zone 2 equals half the diameter of the sample (Fig.12).

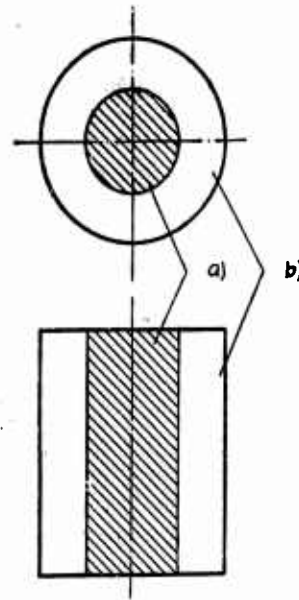


Fig.12 - Effect of Location of Plane of Cut upon Result of Quantitative Microanalysis at Irregularity of Structure Having an Axial Symmetry  
a) Zone 2; b) Zone 1

In a transverse cut, the area of zone 1 comprises 0.75 of the area of the cut, while in zone 2 it comprises 0.25. Therefore, in a determination of the value of parameter  $C$  for the sample as a whole according to transverse cut, we get the value:

$$C_{\perp} = 0,75 C_1 + 0,25 C_2.$$

In a longitudinal cut, passing along the axis of the sample, the areas of both zones will be uniform and will equal 0,50 of the area of cut. Therefore in evaluating the structure of the sample as a whole based on longitudinal cut, the value of parameter  $C$  will differ

considerably from the value found in the transverse cut:

$$C_{\parallel} = 0,50 C_1 + 0,50 C_2.$$

It is easy to see that the volume occupied by zone 2 constitutes  $\frac{1}{4}$  of the volume of the sample, i.e. coincides with the part being occupied by this zone in the transverse cut. Therefore the quantitative result of the analysis, obtained in the transverse cut, will correspond to the actual average parameter of spatial structure, whereas in the longitudinal cut, we get an incorrect result. If the plane of the longitudinal cut will not coincide with the axis of the sample, the error of the evaluation will be all the greater, the farther this is separated from the axis. In the plane, located at a distance of half the radius from the center,

zone 2 will not be represented at all.

The situation does not change if the parameter of the structure changes regularly from the surface to the center, as this is shown in Figs.10 and 11. Here we can divide the samples into a number of concentric zones and the pattern of deliberations, just as in the final result, will remain the same as in the above considered schematic example. At a given ~~XXXX~~ increase, any field of <sup>view</sup> vision on the transverse cut represents the same volume of metal, while on the longitudinal cut the volume of metal being represented by the given field of <sup>view</sup> ~~vision-XXXX~~ constitutes a function of the distance of this field from the axis of rolling or casting. The given field of <sup>view</sup> ~~vision~~ represents a lesser volume of metal, the closer it is located to the axis of the sample. If in a determination of any parameter, the fields of vision are located uniformly along the entire cut, the result of micro-analysis of transverse cut will then provide a correct representation of the average value for this parameter ~~XX~~ in the volume of metal. In case of a longitudinal cut and in presence of irregularity in structure along the section, the result will prove erroneous.

The longitudinal microsections are widely used in an estimation of the contamination of steel by nonmetallic inclusions. Since usually the central zone of section of rolling is more contaminated, in the evaluation along the longitudinal cut the average degree of contamination will always prove higher than it is in actuality. If the longitudinal cut however is not axial, the result of micro-analysis then depends upon the ~~XXXX~~ distance between the plane of the microsection and the axis of rolling, and also upon the degree of heterogeneity along the section.

Based on what has been presented, the plane of the cut should be so chosen that in any other plane parallel to that selected, the structure would be statistically

identical not only qualitatively but also quantitatively. In certain cases, there proved to be ~~unavoidable~~ unavoidable the use of longitudinal cuts. However in this connection, it is mandatory to take into account the importance ("weight") of the parameter, measured in each field of ~~vision~~<sup>view</sup>, determining the distance from the center of field of vision to the axis of rolling, with subsequent calculation of the average suspended value of the given parameter according to all fields of vision, <sup>was</sup> in which it ~~is~~ measured.

Since the visible two-dimensional structure is a geometrically flat section of <sup>3</sup> spatial conglomerate of ~~micro~~ microparticles, it is necessary that the surface of the microsection be as close as possible to an ideal plane and have a minimum micro relief, unavoidable in the process of preparing the slide.

A study of micro relief of metallographic ~~sections~~ sections (cuts) was conducted by N.M.Zarubin with the aid of the interferometer of V.P.Linnik (Bibl.72). He established that the micro relief is mainly developed as early as in the process of polishing, that is the polished surfaces of microsections are always obtained as relief sections and not as plane sections. The ~~value~~<sup>degree</sup> of relief depends upon the method of preparing the section and upon the structure of the sample. The obtainment of a greater relief is promoted by ~~a~~ prolonged polishing (and repolishing), by a coarse-grained structure, and considerable difference in the hardness of the components of structure. Etching (pickling) does not exert a noticeable effect upon the ~~value~~<sup>extent</sup> of micro relief, being obtained during polishing.

In high-strength iron, having an almost purely ferrite base, the value of micro irregularities (difference in levels) between the grains of ferrite after polishing and pickling amounts to 0.17 microns. After ~~an~~ additional polishing, this value reached 0.8 - 0.9 microns. The depth of hollows of graphite correspondingly

increased from 0.70 microns to such an extent that it could not be measured (more than 20 microns). On the microsection of another sample of high-strength iron, the amount of micro irregularity<sup>ies</sup> between the ferrite and ~~per~~<sup>a</sup>lite amounted to 0.15 microns.

In coarsely grained chromium alloy, the value of micro irregularity between carbides of chromium and ~~per~~<sup>a</sup>lite reach 1.2 microns on a pickled microsection; the micro hardness of carbides reaches 1200 and of ~~per~~<sup>a</sup>lite 625. In a finely grained chromium alloy, the value of micro irregularity constituted a total of 0.13 microns before pickling and increased very little during pickling.

Inasmuch as the depth of relief (embossing) is mainly determined by the duration of polishing (and the use of repolishing), to obtain minimum relief, of great importance is a good preliminary preparation of the surface, ~~leading~~<sup>keeping</sup> to a minimum the time needed for polishing. For ferrous metals, N.M.Zarubin recommends the following types of processing the microsection, assuring the obtainment of micro irregularity<sup>ies</sup> within the limits up to 0.5 micron:

a) Grinding the microsection with carborundum stone, files and emery cloths.

Polishing with water suspension of aluminum oxide;

b) The same preliminary processing as in the previous case, polishing with passivating suspension (10 - 20 gms of sodium nitrate, ~~XXX~~ 3 gms of calcinated soda, up to 10 gms of aluminum oxide per liter of water).

The maximum relief state occurs at electric polishing of ferrous metals and at polishing of nonferrous metals by "strong pickling (etching)". In all these cases, the micro irregularity<sup>ies</sup> reaching 4 microns.

The ~~value~~<sup>amount</sup> of micro irregularity<sup>ies</sup> which can be permitted during quantitative micro analysis depends upon the type of structure being analyzed and the type of



scale. The limits of movement of the microscope stand should assure an inspection of the entire surface of the microsection being analyzed, from one set up, without changing its position on the stand. In order that any point of the cut will be accessible for observation, it is desirable that the microsection does not rest by a part of its surface against the fastening plate of the microscope stand. Hence, one should give preference to a low position of ~~XXX~~ the microsection, as this takes place in vertical microscopes.

In an analysis of the oriented structures, it is necessary to turn the microsection relative to <sup>the</sup> direction of movement of <sup>the</sup> stand with an accuracy up to  $1^\circ$ . The polarization microscopes of the type MP-2 and MP-3 are ~~equipped~~ equipped with rotating stands. One can use rotating cover plates equipped with a degree scale, as for instance in the MM-7 microscope. The preparation of such inserts for any microscope does not present any technical difficulty. The insert should have one or two clamps for fastening the sample, in order to avoid the possibility of its displacement during the rotation of the insert.

In certain cases, it is feasible to make the measurement of <sup>structural</sup> elements of ~~the ground~~ <sup>the ground</sup> ~~structure on the~~ <sup>camera.</sup> glass of the microscope ~~compartment~~. For this it is necessary that the microscope have a sufficiently powerful source of ~~XX~~ illumination.

Among the existing designs of microscopes, the most handy for our purposes is the microhardness meter PMT-3 under the condition that <sup>its microscopic</sup> ~~XXXXXXXXXX~~ stand is equipped with a rotating insert having a degree scale. Also convenient are the <sup>polarization</sup> ~~potentiometric~~ microscopes having an opaque-illuminator, rotating stand and with a two-coordinate preparation guiding device, mounted on the stand. It is quite desirable that in the development of new designs of metallographic microscopes, one take into account the requirements of quantitative metallographic analysis.

In addition to the standard set of objectives and eyepieces, attached to each microscope, it is necessary to have a set of eyepieces for quantitative measurements during visual observations. The main items in this set are:

a) An eyepiece-micrometer having a ruler divided into 100 parts, prepared with magnifications of 7 and 15. It is desirable that the scale of this eyepiece, shown in Fig.13, does not exceed in length 0.75 - 0.8 of the diameter of the field of <sup>view</sup> vision. Quite necessary is the presence of a longitudinal diametral line which not is/available in all eyepieces of a similar type;

b) Square grid-reticulated eyepiece. The scale of the eyepiece, containing 256 squares, similar to that shown in Fig.14, is used for eyepieces 23 mm in diameter. For eyepieces of larger diameter (30 mm) grids containing 400 squares can be used. ~~Such grids are used in polarization microscopes~~ Polarization microscopes have such eyepieces;

c) A <sup>screw type</sup> ~~XXXXXX~~ eyepiece-micrometer <sup>cross hair</sup> ~~XXXXXX~~ equipped with a ~~XXXXXX~~ shown in Fig.15, type AM 9-2. ~~XXXX~~ The point of the crossing of the threads has a displacement of 8 mm, being measured with an accuracy of 0.01 mm. In case of the lack of such an eyepiece, one can use an eyepiece having a stationary cross hair.

With the aid of the object-micrometer, one determines the value of division of ruler of the eyepiece micrometer for each of the objectives of the optical set of the microscope. The same is done for measuring the cells of the square-grid eyepiece and for moving the cross hair <sup>o</sup> of the screw type eyepiece-micrometer. ~~XX~~ It is advantageous to measure the diameter of the field of vision for all combinations of lenses and eyepieces and to compute the visible areas of the fields of vision.

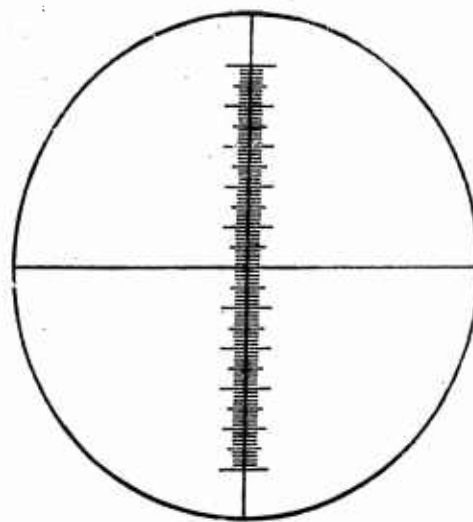


Fig.13 - Eyepiece-Micrometer

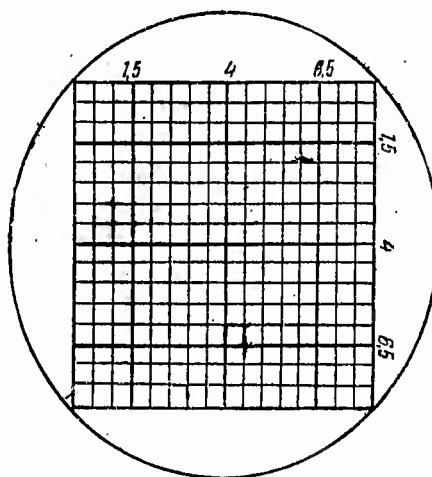


Fig.14 - Square-Reticulated Eyepiece

In quantitative micro-analysis, it is often necessary to calculate a considerable number of certain values (number of grains in field of vision, number of points etc.). The calculation is considerably speeded up and is made more reliable if instead of oral counting there is used a counter adding up the number of ~~push-downs.~~ ~~push-downs.~~ The simplest counter of such a type, made by the factory "Schetmash", is shown in Fig.16.

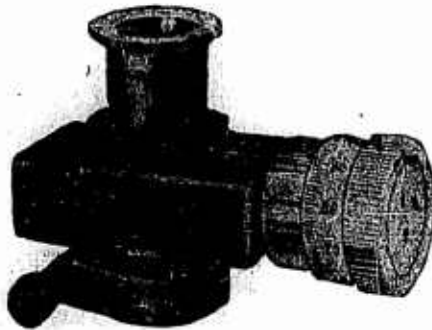


Fig.15 - Screwtype Eyepiece-Micrometer

eliminate the possibility of the effect of individual traits<sup>(personal factor)</sup> of the observer on the results obtained. In this respect, an example is the equipping of devices with

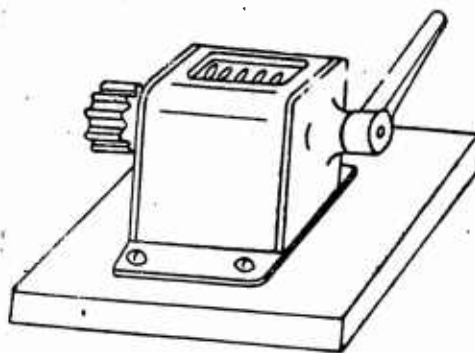


Fig.16 - Manual Counter "Schetmash"

observed<sup>6</sup> with the structure of standard scales, which had received wide distribution

It is noteworthy that the ~~XX~~ development and introduction into metallographic practice of specialized devices for the quantitative microanalysis would greatly simplify and accelerate its conduct, would ~~XXXXX~~ make more accurate and reliable the data obtained, if one could (personal factor) eliminate the possibility of the effect of individual traits<sup>^</sup> of the observer on the results obtained. In this respect, an example is the equipping of devices with quantitative methods of geometric microanalysis of rocks. Many of the devices being used in petrography can also ~~XXX~~ be used in metallographic quantitative analysis. The use of stereometric evaluation of the structure of alloy does not exclude the use of the method of visual ~~XXXXXXXXXX~~ evaluation by way of comparing the structure<sup>6</sup> being

in metallographic practice. The visual evaluation is distinguished by unique speed and simplicity, therefore ~~XXXX~~ its use is desirable in large-scale inspection tests under conditions of plant laboratories. However one should in no way forget that these qualities of visual evaluation are achieved owing to the accuracy of determination. It is subjective and therefore is inferior to the results of direct measurements or calculations of the parameters of interest to us.

The scales of standard structures being used in stereometric metallography, are basically different from the scales being used for most standard semiquantitative analyses. Each standard structure should be evaluated as a precise value of that parameter, for the visual evaluation of which it is intended, but not in any case by conventional index points or numbers. Gradations between adjacent standard structures in the scale are selected in conformity with that accuracy which is required by us from the given control test and which one can attain in practice during visual evaluation.

~~XXXX~~ For instance if we conduct large-scale control tests of steel, evaluating its structure on the basis of two criteria, namely the quantity of <sup>a</sup>perlite and its structure (disperse state), we should have two series of standard ~~XXXX~~ ~~XXXX~~ ~~XXXX~~ photomicrographs. One of them, under magnification<sup>a</sup>, let us say, ~~equal~~<sup>ab)</sup> 100, corresponding to the working magnification during control inspection, should contain a number of photos(or sketched structures) with an increasing content of <sup>a</sup>perlite.

If the accuracy of identification of <sup>a</sup>perlite during visual evaluation is assumed to equal 5% of the absolute content of <sup>a</sup>perlite, the standard ~~XX~~ photomicrographs should be prepared with the appropriate gradations (0, 5, 10, 15, 20 ... % of <sup>a</sup>perlite according to area). The character of the structure as a whole (ferrite in the form of a network, <sup>a</sup>perlite and ferrite in the form of separate grains etc.) in the

control samples of steel and in the standard photomicrographs should be identical, since this promotes a greater accuracy of identification during visual evaluation. In calibrating the ~~XXX~~ actual standard structure, the content (area of  $\overset{a}{\perp}$ perlite) should be determined directly in the actual photomicrograph, and not on the ~~XXXXXXXXXXXX~~ microsection from which the photos are made.

Just as for an estimation of the dispersed state of  $\overset{a}{\perp}$ perlite, which we assume is conducted at <sup>a</sup>magnification of 1000, we prepare a set of standard photomicrographs at this magnification. In each ~~XXXXXXXXXX~~ photomicrograph there is indicated precisely the measured <sup>parameter</sup> $\overset{a}{\perp}$  (specifically on ~~XXX~~ it) and then, ~~XXX~~ in a similar manner, the computed <sup>spatial</sup> parameter of ~~XXXXXXXX~~ structure of  $\overset{a}{\perp}$ perlite, characterizing its dispersed state, namely the value of interlamellar distance or the actual value of specific surface of cementite.

In an evaluation of the quantity of  $\overset{a}{\perp}$ perlite and its dispersed state, one does not use any kind of conventional symbols or codes. The estimation is conducted by natural values of geometric parameters of spatial structure, namely the volumetric percent of  $\overset{a}{\perp}$ perlite, interlamellar distance in microns, specific surface of cementite in  $\text{mm}^2/\text{mm}^3$ . In the described method of construction of scale, we always have the possibility of prolonging <sup>it</sup> or dividing <sup>it</sup> more finely in any individual sector.

The sets of standard photomicrographs should be of a nature ~~XXXXXX~~ inherent to the structures being inspected in the given production. For instance, one should never use the same scale of quantity of  $\overset{a}{\perp}$ perlite for cast steel, for rolling with the absence or presence of striation. Any standardization of sets of standard structures inevitably decreases the accuracy of the evaluations obtained.

If great accuracy is required and the tests are not large-scale, the measurement of parameters then should be conducted by the methods described in the following chapters.

It needs to be emphasized that all these methods are statistical and therefore the accuracy of estimation is all the higher the more the readings or measurements that are conducted for obtaining the average value of the parameter being measured. Therein, in determining any average value, it is necessary to choose the items being measured at random, without any preference in relation to any given category of values being measured and without rejecting those ~~of them~~ which are even quite substantially different from the vast majority of measurements. In the history of statistical analysis, the following quite indicative case is known.

In the past Century, measurements were conducted in England for determining geographic longitudes. In the first processing of the data obtained, not all the data were used but only those ~~of them~~ which agreed best of all with each other. The results proved so inaccurate that the measurements were completely rejected. However, the data of measurements were retained and when subsequently they were reprocessed, wherein in the calculation all data were accepted, even those which appeared contradictory, the results proved excellent (Bibl.73). Therefore, also in the ~~XXXXXXXXXX~~ determination, e.g. of the value of average grain it is necessary to take into account all grains without exception in a fixed area, without disregarding even the smallest of them.

In the further discussion it is convenient to adopt a system of symbols of geometric parameters of spatial and plane structures, which were used in previous studies. Various geometric parameters of individual microparticles are ~~signified~~ <sup>designated</sup> with by letters of the Latin alphabet, which it is conventional to denote the corresponding parameters of geometric bodies and figures: volume  $V$ , surface  $S$ , area  $F$ , linear dimensions  $L$  and  $D$  etc. The corresponding average values are signified by the same

letters with a vinculum drawn over them. The total values, referred to a unit volume of metal or to a unit area of microsection, we ~~designate~~ designate with the sum ~~Σ~~ sign ~~Σ~~ Σ, placed before the symbol of the appropriate parameter. The phase of any component of the structure, to which the given parameter is referred, is written on the right in the form of ~~an index~~ a subscript.

Table 6

Title of Parameter	Symbol	Dimensional <del>index</del>
Volume of individual microparticle . . . . .	V	mm <sup>3</sup>
Surface of individual microparticle . . . . .	S	mm <sup>2</sup>
Diameter of spherical microparticle . . . . .	D	mm
Length of linear element of spatial microstructure	L	mm
Number of microparticles per unit volume of alloy	N	mm <sup>-3</sup>
Total volume of <del>of</del> microparticles per unit volume of alloy . . . . .	ΣV	mm <sup>3</sup> /mm <sup>3</sup>
Total surface of microparticles per unit <del>of</del> volume of alloy . . . . .	ΣS	mm <sup>2</sup> /mm <sup>3</sup>
Total length of linear elements of spatial microstructure per unit volume of alloy . . . .	ΣL	mm/mm <sup>3</sup>
Area of individual section of microparticle in microsection . . . . .	F	mm <sup>2</sup>
Perimeter of individual section of microparticle on the cut . . . . .	P	mm
Diameter of section of round microparticle on cut	d	mm
Length of linear element of plane microstructure	l	mm
Number of sections of microparticles per unit area of cut . . . . .	n	mm <sup>-2</sup>
Total area of sections of microparticles per unit area of cut . . . . .	ΣF	mm <sup>2</sup> /mm <sup>2</sup>
Total length of perimeters of sections of microparticles per unit area of cut . . . . .	ΣP	mm/mm <sup>2</sup>

For instance, the total surface of graphite deposits per unit volume of iron is denoted by  $\Sigma S_{gr}$ , the average volume of carbide particle by  $V_k$ , etc. The system

of notations and the corresponding units of measurements of parameters are presented in Table 6.

CHAPTER II  
QUANTITATIVE PHASE AND STRUCTURAL VOLUMETRIC COMPOSITION  
OF AN ALLOY

Section 9. Phase and Structural Composition of Alloy

Regarding <sup>an</sup> alloy as a conglomerate of microparticles, one can refer these microparticles to one or the other phase or structural component. The total volume of microparticles of any phase, occurring in a unit volume of alloy, ~~XXXX~~ determine the part ~~being~~ occupied by this phase of the volume of alloy, which ~~XX~~ can also be expressed in volume percentages. In metallography, the phase and structural composition of an alloy is often determined, using the "rule of segments", permitting one to determine (based on relative quantity of phase or structural component) the composition of <sup>the</sup> alloy and vice versa. A classic example of such a type is the determination of the content of carbon in steel, based on the amount of <sup>the</sup> perlite in its structure.

no a/

Originally, the methods of quantitative analysis of phase composition of complex aggregates were developed by ~~XXXX~~ geologists and petrographers with reference to rocks more than 100 yrs ago, for finding their mineralogical composition. At present, these methods have received a high state of improvement both in ~~XXXX~~ rapidity of carrying out the analysis, as well as in accuracy, agreeing successfully with chemical analysis and supplementing it. A great contribution to the development of improved methods and the ~~XXXXXXXXXX~~ development of appropriate devices was made by A.A.Glagolev, whose valuable monograph (Bibl.50) is quite useful not only for petrographers but also for each metallurgist interested in quantitative microanalysis.

inadmissibly

In this respect, metallography has ~~XXXXXXXXXXXXXXXXXXXX~~ lagged. As V.Yum-Rozeri and others (Bibl.277) testify, many metallurgists have an erroneous concept even of the relationship between the quantities of phases on an area of a cut and in the volume of the alloy, assuming that the ratio of areas of phases on the cut should be raised to the power  $3/2$ , in order to obtain the ratio of volumes of phases in the alloy. Up to the present, ~~XXXX~~ the most primitive methods are being used for determining the areas of phases and structural components on a microsection, and in the textbooks for metallography and metallurgy, it is almost a rule that no other methods of determining the phase and structural composition, other than an estimation of areas "by sight", are mentioned ~~(XXXX)~~ (Bibl.74, 75). At the same time, a knowledge of the phase and structural composition of the alloy is quite important for the metallurgist. The structural composition of an alloy provides us with such data about it, which cannot be obtained by the methods of chemical analysis, as for instance the content in steel of structures of varying degree of decay of austenite (~~per~~<sup>2</sup>lite, sorbite, troostite etc.).

Evidently the reason for the lagging of metallography in this field is the lack of familiarity of metallurgists with the potentialities of qualitative determination of structural composition and ~~XXXXXXXX~~ the widespread incorrect concept of it as a very inaccurate type of analysis, which ~~XXXXXXXXXX~~ can yield only approximate figures, considerably inferior to the chemical analysis data. We will show in a number of examples taken from the practice of petrography and metallography that this is far from the case.

In a description of the Ahumada palasite, given by O.Farrington, a photograph

was presented of the polished surface of palasite, and its specific weight was given. N.P.Chirvinskiy conducted measurements of quantities of components (well visible on a photograph) of components of rock (nickel iron and olivine), and using theoretical specific weights of the components, computed the specific ~~weight~~ weight of palasite, which proved higher than the figure presented by O.Farrington.

N.P.Chirvinskiy writes ~~XXXX~~ "I asked him to conduct a checking determination of the specific weight of palasite, and it turned out that I was correct, which was testified to not only by a letter in my name, but also in one of the later reports" (Bibl.76). Hence, the quantitative microanalysis proved more reliable and more accurate than such a methodologically simple determination as that of specific weight.

As early as 1924, Ye.P.Polushkin, having made a "metallographic planimeter" of the most primitive design, conducted a determination of structural composition of a number of samples of steels, irons and ~~XXXXXX~~ phosphoritic bronze. Based on specific weights of structural elements of alloy and of the alloy itself, on the basis of planimetric measurements of areas ~~being~~ occupied by these elements on the cut, he computed the ~~XXXXXX~~ chemical composition of the alloy and compared it with the chemical analysis data. The data obtained are presented in Table 7 and indicate the good convergence (correlation) of figures obtained by way of microscopic and chemical analyses (Bibl.51). The same kind of deviation (sic) is also often observed during repeated chemical analyses.

In recent times, the use of more improved methods and special devices increased even more the accuracy and reliability of determining the phase composition of alloys and permitted its use in the area of metallurgy, requiring an especially accurate and

reliable method, namely in the construction of equilibrium diagrams.

Recently, L.Beck and S.Smith, using the method of quantitative microanalysis, successfully conducted an investigation to refine the position of the lines of the equilibrium diagram of copper and zinc alloys, delimiting the areas of existence of  $\alpha, \alpha + \beta, \beta, \beta + \gamma$  and  $\gamma$ -phases (Bibl.77). By way of quantitative

Table 7

a)	b)	c)	
		d)	e)
Rolled steel . . . . .	f)	0,20	0,24
Cast crucible steel, annealed at 1000°C . . . . .	»	0,46	0,50
The same . . . . .	»	0,74	0,78
The same . . . . .	»	1,24	1,32
The same . . . . .	»	3,93	3,80
White iron with traces of graphite . . . . .	g)	1,43	1,40
Gray iron (3.04% C and 2.89% Si) . . . . .	»	10,38	10,33
Phosphoric copper . . . . .			

a) Characteristic of alloy; b) Element; c) Weight content, %, determined; d) Planimetrically; e) By chemical analysis; f) Carbon; g) Phosphorus

microanalysis, there was determined the phase composition of each two-phase alloy.

In Fig.17 are shown types of derived ~~dependencies~~ dependences of quantity of  $\beta$ -phase in the structure as a function of the content of copper in the alloy at various temperatures of phase equilibrium. The group of lines in Fig.17, a ~~was~~ <sup>was</sup> ~~like~~ <sup>like</sup>

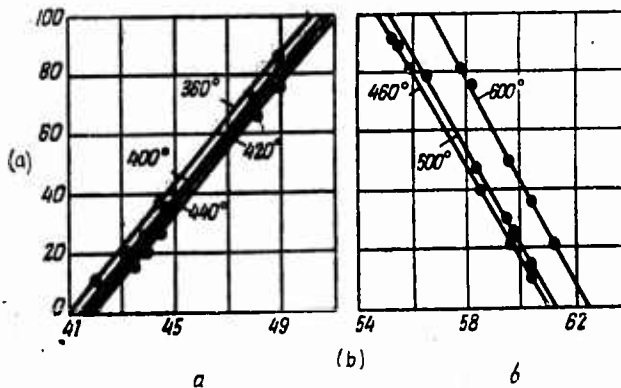


Fig.17 - Metall graphic Determination of Content of  $\beta$ -Phase in Alloys of Copper with Zinc, in State of Equilibrium with  $\gamma$ -Phase (a) and with  $\alpha$ -Phase (b) at Various Temperatures [L.Beck and S.Smith (Bibl.77)]

a) Weight content of  $\beta$ -phase; b) Weight content of copper, %

obtained for equilibrium of  $\beta$ -phase with the  $\gamma$ -phase, while in Fig.17,b for equilibrium of  $\beta$ -phase with the  $\alpha$ -phase. There was established, as we shall see, a very distinct linear relationship, which permits one, by way of slight extrapolation, to find concentrations of copper ~~XXXX~~ corresponding to the 0 and 100% content of  $\beta$ -phase at various temperature. These concentrations also fix the position of ~~XX~~ lines of an equilibrium diagram at given temperatures. Measurement of parameters of the lattice agrees well with the data obtained by way of quantitative microanalysis.

However, along with the successful use of this method, it is noteworthy that in the practice of metallurgy there also takes place such cases when the results of metallographic analysis prove unsatisfactory. For instance, J.R.Lane and N.J.Grant, using methods of quantitative microanalysis (Bibl.78), were unable to reveal the kinetics of change in content of ~~XXXXXXXXXXXXXXXXXX~~ carbides of chromium, niobium and tantalum during the aging of heat-resistant steels. This only confirms the need for familiarizing metallurgists with the actual potentialities of individual methods of determining the phase composition with the purpose of their more correct application.

Cavalieri  
~~XXXXXX~~

Section 10. Principle of Cavalieri and Its Application to Quantitative Metallographic Analysis

Existing methods of quantitative phase and structural analysis both of rocks and of metal alloys are based on the so-called principle of ~~XXXXXXXXXX~~ Cavalieri.

A student ~~XXXXXX~~ of Galileo, the Italian geometrician Bonaventura Cavalieri (1598 - 1647) proposed methods of measuring and comparing the areas of plane figures and also the volumes of bodies with the aid of a unique type of infinitely small values, namely "indivisible ~~as the~~ continuous" (79). Cavalieri regards plane figures as consisting of a infinitely large number of mutually parallel lines, and bodies as

consisting of <sup>an</sup> infinitely large number of mutually parallel planes.

Therefore for comparison of areas of two figures, straight lines are used which are parallel to a certain given ~~straight~~ <sup>right</sup> line (called the regulus). An infinite number of parallel straight lines ~~XXX~~ is located between the two straight lines tangent to these figures from opposite sides. These two lines are called "paired tangents" and one of them is usually taken as the regulus. If the lengths of the segments, cutting off the outlines of the figures at each of the straight lines, equal each other by pairs ~~or~~ are located in a fixed position constant for all pairs of segments, then the areas of the figures under consideration will also equal each other or will be located in the same ~~XXXXX~~ relationships as the segment.

Let FEHG and ABCD (Fig.18) be compared with one another, wherein both figures are enclosed between the parallel lines IK and LM bounding them; we can take either of the parallel lines for the regulus. Let us intersect them with a number of straight lines parallel to the regulus, and we will compare segments RS with NO, FH with BD, and TV with PQ. If all these pairs of segments equal each other (as occurs in Fig.18), and also any other straight line parallel to the regulus, ~~XXXXXXXX~~ intersecting the figure, yields ~~6~~ segments, which are equal to each other by pairs, then the actual figures FEHG and ABCD will be of equal area. However if all pairs of segments were situated in a fixed position with relation to each other, the areas of figures would occur in the very same relationship.

Similarly to what has been said ~~XXXXX~~ above, the principle of Cavalieri ~~XXXXXXXX~~ ~~XXXXXXXXXXXXX~~ is used to compare the volumes of two bodies, the only difference being that the straight lines are replaced by plane figures, and the segments by sections.

Let us consider two bodies, formed by rotation ~~XXXXX~~ ~~XXXXX~~ about the axis OC' of the

~~XXX~~

semicircle AO'B, ~~XXXX~~ written into the rectangle ABDC and the triangle COD (Fig.19).

The semicircle forms a "cup", the axial section of which is hachured in the drawing, while the ~~XXX~~ triangle forms a cone. It may be shown that in any horizontal section surface of revolution, the ~~area of rotation~~, formed by the segment within the "cup" ab, equals the ~~area of~~ surface of revolution formed by the segment within the cone cd. To the extent that this is so, according to the principle of Cavalieri, the volumes of the "cup" in the cone also equal each ~~XXXX~~ other, which takes place in reality.

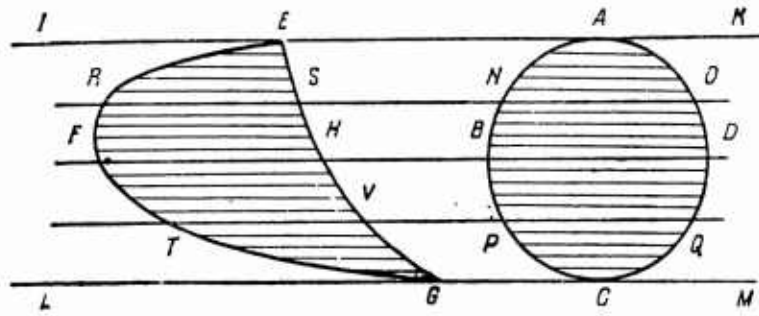


Fig.18 - Comparison of Areas of Two Figures according to Lengths of Paired Segments (according to Cavalieri)

As we see, using the Cavalieri principle, we can replace the measurement of areas of two figures, being compared, by a measurement of segments of straight lines, and the measurement ~~XX~~ of volumes of two bodies (being compared) can be replaced by a measurement of areas. Otherwise expressed, we get the chance to decrease the degree of dimensionality of the elements being measured in comparison with the dimensionality of the objects themselves. This permits a determination of the volume of microparticles based on their plane sections on a microsection or based on segments of lines passing within the microparticles.

The Cavilieri principle was generalized in 1929 with application to quantitative microscopic analysis by A.Aker in the following form: if several groups of contours

on a plane, located between parallel straight lines, have intersections (segments), whose lengths are in constant proportion with any line, parallel to the two given lines, the areas of these groups of contours will then occur in the same proportion or ratio themselves.

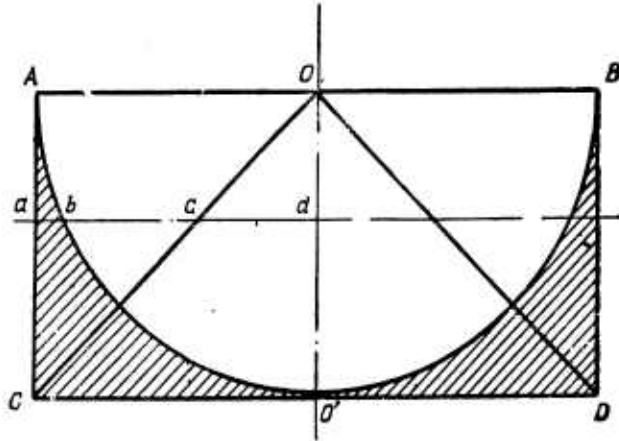


Fig.19 - Comparison of Volumes of Two Bodies (of a <sup>"cup"</sup> ~~cup~~ and Paired of a cone) Based on Areas of Paired Sections

In exactly the same way, if several groups of bodies located between two parallel planes have sections, whose areas are at a constant ratio in any plane, parallel to the two given ones, the volumes of these groups of bodies will then be at the same ratio occur in the same relationship (will have the same ratio) (Bibl.50).

In the volume of a two-phase alloy, distinguished by a uniform distribution of microparticles of phases  $\alpha$  and  $\beta$ , let us set off the cube (1), shown in Fig.20, and we will compare it with cube (2) of the same size. The plane of the bases of both cubes A we will accept as the regulus and draw a series of planes, parallel to it and intersecting both cubes. On the upper face of cube (2) we set off the area abde, equaling the area occupied by the  $\alpha$ -phase on the upper face of cube (1). If the phase composition of the alloy is ideally uniform, then in any plane, parallel to the regulus, the area occupied by the  $\alpha$ -phase will

have one and the same value. Therefore the relationship of ~~XXXX~~ volumes of phases  $\alpha$  and  $\beta$  in the alloy, in conformity with the proposition of Cavalieri-Aker, will equal the relationship of volumes of hachured and nonhachured ~~XXXXXX~~ sectors of cube (2) or, which is the same, will equal the ~~relationship~~ <sup>ratio</sup> of rectangles  $abde$  ~~and~~  $bcef$ .

Moreover, if we accept the ~~XXXXXX~~ line  $ik$  for the regulus, then ~~in~~ <sup>on</sup> any line, parallel to it, drawn on the upper ~~face~~ <sup>face</sup> of the cube (or on any parallel section), the total length of the segments passing within the  $\alpha$ -phase will be constant and will equal the value  $ab$ . Therefore the relationship of volumes of phases in the alloy will also equal the relationship of lengths of segments  $ab$  and  $bc$ .

Consequently from the proposition of Cavalieri-Aker, one can form the following quantities, namely the volume occupied conclusion: the three ~~values, namely volume, area, being occupied~~ <sup>quantities</sup> by any phase  $\alpha$  in the interior of the alloy; the area occupied ~~interior of alloy, area, being occupied~~ <sup>interior of an</sup> by the same phase per unit ~~area of cut;~~ <sup>area of an</sup> and the total length of segments of a straight line passing within this phase, referred to the length of a straight line intersecting the alloy (or cut), are numerically equal to one another. Otherwise expressed, the percent content of a given phase in the ~~volume of an alloy,~~ <sup>interior of an</sup> on the area of the cut, or on the length of the straight line is expressed by the same ~~value~~ <sup>quantity</sup>.

In actual alloys with which we must deal, the phase composition is not ideally uniform in volume, and the samples being studied under the microscope have finite dimensions. Therefore in the diagram shown in Fig. 21 there will occur a fluctuation of area being occupied by the  $\alpha$ -phase, ~~in~~ <sup>in</sup> differing sections, parallel to the regulus  $A$ , and also a fluctuation of lengths of segments passing within the  $\alpha$ -phase, on various lines parallel to regulus  $ik$  (as is illustrated by the wavy lines

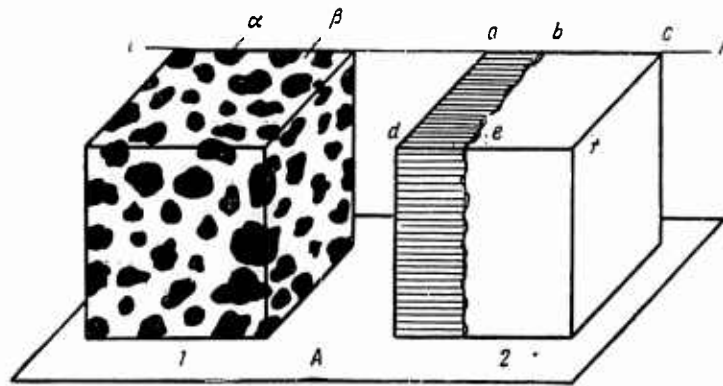


Fig.20 - Application of Cavalieri-Aker Principle at Uniform Structure of Alloy

in Fig.20). Hence, these values can be regarded as statistically constant and, strictly speaking, the content of <sup>&</sup><sub>A</sub> given phase in the microsection coincides mathematically exactly with the volumetric content of this phase in an infinitely thin layer directly contiguous to the plane of the microsection. The matching of data, obtained in a random microsection, to the volumetric phase composition depends upon the chemical and structural uniformity of the alloy and also upon the correctness of choice of position of the ~~XXXXXXXXXX~~ microsection's plane.

M.S.Aronovich and I.M.Lyubarskiy made measurements of an area of microsection occupied by nonmetallic inclusions, in a number of samples of rolled steel, wherein for each sample a pair of transverse cuts was prepared. The curve shown in Fig.21 drawn on the basis of their data (Bibl.80), confirms the practical constancy of the total areas of nonmetallic inclusions in <sup>A</sup> paired microsections of each sample.

It is quite obvious that the variation in readings for various cuts, being caused by fluctuation in chemical and structural composition in the volume of the ingot, casting, or rolled piece, should in no way be confused with the accuracy of the method of determining the phase composition in the volume based on relationship of areas in the cut or, what is more <sup>important,</sup> should not raise doubt as ~~XXX~~ to the correctness

of its mathematical basis. The method, permitting the exposure and estimation of the degree of heterogeneity of phase composition is more sensitive and therefore

more valuable than the method incapable of revealing it.

Therefore the fluctuation in readings of individual cuts is fully regular. At the same time, it is necessary to note a number of factors, upon which there significantly depend the maximum conformity

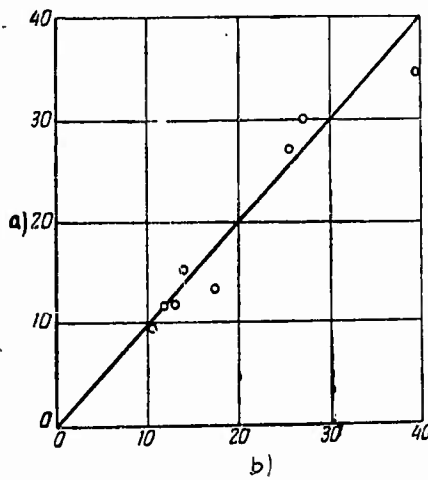


Fig.21 - Total Areas of Nonmetallic Inclusions in Paired Sections of Rods of Rolled Metal [after M.S.Aronovich and I.M.Lyubarskiy (Bibl.80)]  
a) Second section; b) First section

of the phase and structural composition, determined on the basis of ~~relationship~~ <sup>the ratio of</sup> ~~of~~ <sup>relationship</sup> areas in the microsection to the actual volumetric composition of the alloy.

Section 11. Spatial Symmetry of Microstructure and Selection of Microsection Surface

As a rule, in alloys there ~~takes place~~ <sup>occurs</sup> a zonal heterogeneity of microscopic structure in general and ~~of~~ phase composition, specifically caused by the process of formation of the ingot and its subsequent ~~mechanical~~ working.

In most cases, the curve of change in phase composition in the direction from ~~the~~ center to ~~the~~ <sup>an</sup> surface of ingot, rolled, or cast piece, runs evenly and ~~is~~ is symmetrical relative to the axis or to the surface of symmetry of the item. The Cavalieri-Aker principle will unconditionally remain in force in these cases also, but great significance is acquired by the proper choice of a section, intended for microscopic investigation.

Let us examine two main types of nonuniformity of phase composition, found most frequently:

Nonuniformity

a) Irregularity with axial symmetry, typical for articles which have a predominant dimension in one direction, namely rolled or cast pieces of approximately equiaxed transverse section, wire, axles, shafts, etc;

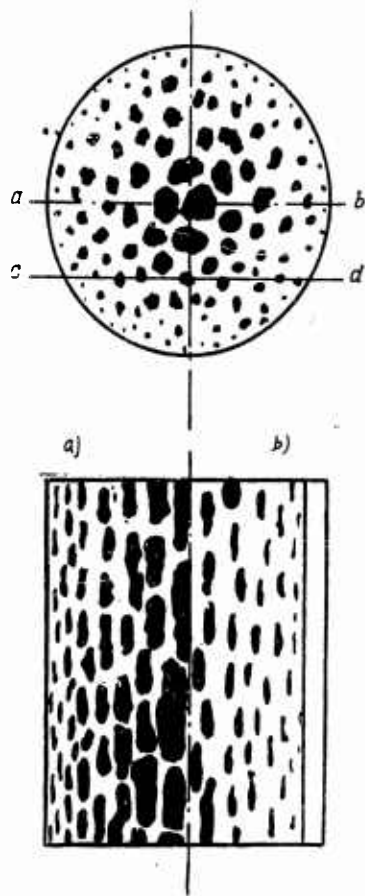


Fig.22 - Irregularity of Structure with Axial Symmetry and Its Effect upon the Surface Structure, as a Function of the Position of the Plane of the Microsection  
a) Along ab; b) Along cd

Depending upon the Position of the Plane of the Microsection this value, determined in a number of cross sections, reflects the disproportion in the chemical and structural composition along the length of the rod, and its statistically average value coincides exactly with the content of given phase in the volume of alloy. Limiting ourselves to a single cross section for judging the volumetric phase composition, we risk the making of an error in the value which is relatively small, being determined by deviation in composition along the length of rod.

b) Nonuniformity with surface symmetry, typical for articles in which the spread in directions exceeds two markedly over the dimension in the third measurement, namely rolled sheets, plate-type castings, etc.

In Fig.22, we show schematically the disproportion in the composition in a rolled piece of round profile, having axial symmetry. It is clear that the structure in all cross sections proves similar and the content of the given phase in all such sections will be a statistically constant quantity. Deviation in

In a series of longitudinal microsections, the surfaces of which coincide with

the axis of the rod, the content of given phase will also be a statistical constant. However the statistically average figure for this value, even though determined for a very high number of samples, will not coincide with the content of <sup>av</sup> given phase in the volume of the alloy, as ~~was~~ was shown in ~~XXXXXX~~ Section 8. Moreover, in the longitudinal cuts there is reflected not only the change in composition ~~according~~ along the length of rod, but also the distribution of disproportion ~~according to section~~ along the cross section, if its symmetry deviates from axial (for instance, in the presence of a segregation in rolled stock of square ~~in a rolled piece of~~ round profile).

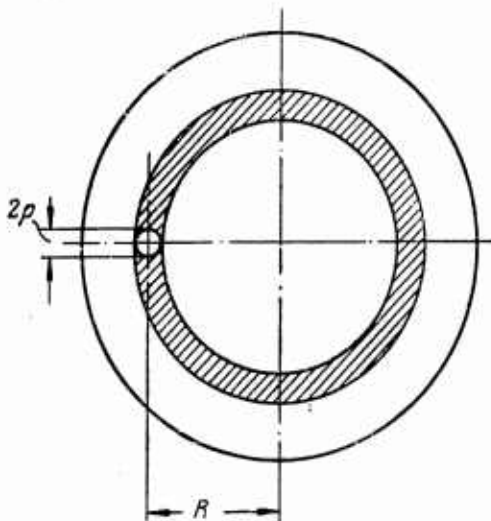


Fig.23 - Diagram ~~XX~~ for Conclusion of Eq.(11.3)

Therefore, in the case of axial symmetry of heterogeneity of phase composition, it ~~is~~ is most feasible to use cross ~~sections~~ cuts. This proposition was reflected in a number of methods ~~of~~ for determining the contamination of steel by nonmetallic inclusions (the method of the Ukrainian ~~XX~~ Institute of the Metals

etc.), although basically for this purpose ~~the~~ longitudinal axial cuts are used. Using the latter, we can estimate the inclusions ~~XXXXXX~~ according to the types, having a differing effect upon the properties of steel, with a division of them into brittle, plastic and solid inclusions, determining them quantitatively. Therefore, let us consider the conditions under which an estimate based on a longitudinal cut will agree with the content of the given phase in ~~a volume of~~ the interior of metal.

In Fig.23, there is shown a cross section of round rolled iron, the structure of

which, as we assume, has ~~an~~ axial symmetry. If the radius of the field of ~~vision~~ <sup>view</sup> of the microscope equals  $\rho$ , while the center of the field is located at the distance  $R$  from the center of the section (i.e. from the axis of symmetry), this field then represents the structure of the hachured annular zone in the cut, the area of which equals:

$$F = \pi [(R + \rho)^2 - (R - \rho)^2] = 4\pi R \rho. \quad (11.1)$$

Let us assume that we determined the relative area of the given phase in a number of fields of ~~view~~ <sup>view</sup> ~~characterizing~~ ~~the~~ ~~various~~ ~~annular~~ ~~zones~~ characterizing the various annular zones of cross section of the rolled iron. If in the fields of ~~view~~ <sup>view</sup>, the centers of which are located at the distances  $R_1, R_2, R_3 \dots$  from the axis of symmetry, there are obtained respectively the values of content of the unknown phase, equaling  $a_1, a_2, a_3 \dots$ , then the average suspended content, typifying the entire area of the section as a whole, will equal:

$$\bar{a} = \frac{a_1 F_1 + a_2 F_2 + a_3 F_3 + \dots}{F_1 + F_2 + F_3 + \dots} \quad (11.2)$$

or, having substituted the corresponding values of annular areas from ~~eq.~~ eq.(11.1), we get:

$$\bar{a} = \frac{a_1 R_1 + a_2 R_2 + a_3 R_3 + \dots}{R_1 + R_2 + R_3 + \dots} \quad (11.3)$$

The last formula is a mathematically precise expression of <sup>the</sup> average content of phase both in the area of the cut, as well as in the volume of the alloy. Moreover, this formula is suitable for computing the average suspended value of any other structural parameter, variable in cross section, ~~parameter of the structure, changing in section,~~ ~~and also of other indexes of~~ <sup>cross</sup> properties of the alloy, the value of which is not constant in section. For instance, based on eq.(11.3), one can compute the mean value of hardness, typifying as a whole <sup>a</sup> the entire volume of hardened steel cylindrical ~~specimen,~~ <sup>specimen,</sup> incompletely annealed.

weighed

~~THE~~ The need for computing the average ~~value~~ and not merely the average  
 arithmetical view,  
~~XXXXXXXXXX~~ value based on data obtained in a number of fields of ~~view~~ ~~XXXXXX~~, was  
 noted at an earlier data. To estimate the content of nonmetallic inclusions in  
 a volume of steel, there are known, e.g., the methods of Gerti for cast steel  
 (Bibl.82) and Fert-Brown for rolling (Bibl.23), taking into account the importance  
 of evaluating each field of ~~view~~ ~~XXXXXX~~. Nevertheless, in most cases, there is adopted  
 the simple arithmetic mean without taking into account ~~XXXXXX~~ the distance of the  
 field of ~~view~~ ~~XXXXXX~~ from the center of the ~~specimen~~ ~~XXXXXX~~. Depending upon the degree of  
 dissimilarity of phase composition, this may lead to the obtainment of high readings  
 (estimates).

Based on data of B.B.Gulyeva, presented in Fig.12, the volumetric percentage  
 of nonmetallic inclusions ~~changes along~~ ~~XXXXXX~~ varies along  
 the radius of a steel casting approximately  
 as follows:

Distance from Center, mm	Volumetric Percent of Inclusions
10	0,041
20	0,051
30	0,048
40	0,043
45	0,023
47,5	0,014

The ~~XXXXXX~~ arithmetic mean comprises 0.0367% by volume, whereas based on eq.(11.3),  
 we get 0.0327%. Hence, for the case of relatively slight dissimilarity owing only  
~~XXXX~~ to incorrectness of the mathematical calculation, the error in determination  
 comprises more than 12% of the actual average content of inclusions in the volume of  
 steel.

~~XXX~~ Equation (11.3) is valid both for transverse as well as for longitudinal cuts,  
 but ~~XX~~ its use presupposes a mandatory linear uniform arrangement of the fields of  
 view  
~~XXXXXX~~ along the radius or diameter of the section of the article (in a transverse

fields of ~~view~~<sup>view</sup> or longitudinal cut). If the ~~XXXXXXXXXX~~ take in the entire area of the transverse cut or are distributed statistically ~~XXXXXX~~ evenly along it, one should compute the overall estimate as the arithmetic mean, since the areas of annular zones and hence the number of fields of ~~view~~<sup>view</sup> occurring in them are proportional to the radii of the corresponding zones. In a lengthwise cut, even at uniform distribution of fields of ~~view~~<sup>view</sup> along the cut, the use of eq.(11.3) is quite mandatory, since here the area of sections of all annular zones are the same and do not depend upon their radius.

~~It~~<sup>This</sup> is a simpler matter in the presence of plane symmetry of ~~XXXXXXXXXX~~<sup>the</sup> heterogeneity of phase composition. In Fig.24 we show schematically a part of the volume of a rolled sheet, having the form of a ~~XXXXXXXXXX~~ parallelepiped (1), which we will compare with the same parallelepiped (2). In the upper face of the latter we set off the area abde, equaling ~~XX~~ the area occupied by the  $\alpha$ -phase in the same ~~XXXXXX~~ side of parallelepiped (1). Having assumed the plane of base A for the regulus, we draw a number of sections, parallel to it and intersecting both parallelepipeds. Since in each section the area, occupied by the  $\alpha$ -phase, is statistically constant, according to the Cavalieri-Aker principle, the ratio of ~~the~~ volumes of the  $\alpha$ - and  $\beta$ -phases in the alloy will equal the ratio of volumes of the ~~XXXXXX~~<sup>XXXXXX</sup> hatched and ~~non-hatched~~<sup>non-hatched</sup> sectors of the parallelepiped (2) or ~~to~~ the ratio of areas of the rectangles abde and bcef. Moreover, if we take the line ik for the regulus, then on any line parallel to it and intersecting both parallelepipeds, the total length of segments passing within the  $\alpha$ -phase will be constant and equal to the segment ab. Therefore the ratio of volumes of phases in the alloy will also equal the ratio of lengths of the segments ab and bc.

From the diagram in Fig.24 it is clear that it is quite irrational to locate the planes of the cuts parallel to the surface of the sheet. In a number of such cuts, there will occur abrupt changes in the phase ~~XXX~~ composition, the ~~average~~ <sup>mean-square</sup> ~~average~~ <sup>average</sup> ~~average~~ deviation of content of each phase will prove quite considerable with relation to the average contents of phases and a large number of cuts will be needed for obtaining more or less reliable values, reflecting the actual phase composition in the volume of alloy.

Thence it follows that a mandatory condition which must be observed during quantitative microanalysis of alloys with plane symmetry of heterogeneity, is the perpendicularity of the plane of the cut or of the intersecting lines to the plane of symmetry <sup>the</sup> of heterogeneity, or which is the same, to the surface of the sheet (or to the plane of the ~~XXX~~ side of the casting, ingot, surface of plate etc.). Only under this condition does the ratio of the phases in the area of cut and in the intersecting line coincide with the actual <sup>phase ratio</sup> ~~ratio (relationship) of phases~~ in the volume of the alloy.

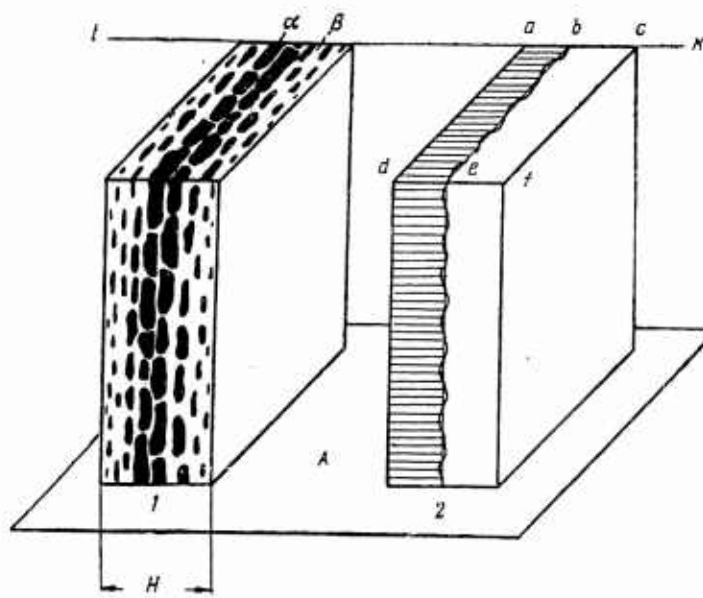


Fig.24 - Use of the Cavalari-Aker Principle in Case of Structure with Plane Symmetry: H - Thickness of Sheet

Here we examined only two types of symmetry of <sup>the</sup> heterogeneity; however they take in the vast majority of objects of microanalysis. ~~XX~~ We restrict ~~XXXXXXXXXX~~ ourselves to the above presented examples, because they are sufficient for ~~the~~ metallurgists to be able to approach knowingly the selection of a plane of cut and ~~the~~ the use of the primary data obtained during ~~XXXXXXXXXX~~ microanalysis and ~~XX~~ in more complex cases, which here we shall in no way foresee or describe.

#### Section 12. Effect of Nature of Structure

The ~~XXXXXXXXXX~~ proposition of Cavalieri-Aker proceeds from the assumption that a cut of a multicomponent aggregate represents a geometric plane. Moreover, from data adduced in Section 8 it follows that the surface of ~~XX~~ metallographic cuts is not ideally flat, but has a microrelief with <sup>a</sup> depth of the order of 0.1 - 0.5 micron, which can even prove to be considerably greater in case of improper preparation of ~~the~~ cut.

If the sizes of microparticles considerably surpass the depth of microrelief upon the of the cut, its influence ~~XXXX~~ result of ~~XXX~~ quantitative determination of phase composition can then be disregarded. However, the error becomes quite noticeable when the depth of microrelief is comparable with the sizes of the particles. Thence it follows that ~~the~~ difficulties should arise in an analysis of highly dispersed phases, especially during investigation under an electron microscope. Among the phases of such a type, ~~XX~~ of great interest are above all the carbide phases and the nonmetallic ~~XXXXXXXXXX~~ inclusions in steel.

In the electron-microscopic analysis of dispersed ferrite-carbide mixtures, there occurs as a rule an increased content of carbide phase as compared with theoretical calculation. An electron-microscopic investigation of the structure of troostite and of annealed martensite, conducted by N.N. Buynov and R.M. Lerinman,

showed that the area being occupied by carbides considerably ~~surpasses~~<sup>exceeds</sup> the area ~~being~~ determined by the ratio of ferrite and carbide in these structures. A similar observation was made earlier by ~~RYMAYANIKH~~ R. Heidreich and V. Pek (Bibl.83). M.N. Lyulicheva obtained the following dependence of ~~the~~ content of carbide phase, ~~being~~ photomicrographs, observed in electron ~~RYMAYANIKH~~ upon the temperature of 10-hr annealing of type U7 steel (the content of carbon was 0.69%, the volume of carbide phase by calculation was ~~RYMAYANIKH~~ 10.6%):

Annealing Temperature, °C	Volume of Carbide Phase, %
450	45
550	38
650	29
700	15

Only a prolonged annealing at a temperature of 680 - 700° assured a sufficient enlarging of the microparticles of carbides and the coincidence of data of microanalysis with the theoretical calculation (Bibl.84). It is noteworthy that the observed increase in content of carbides along with the increase of their degree of dispersion, ~~dispersed state~~, possibly is by no means fully attributable to the shortcomings of the techniques of microanalysis, since there is no assurance of the constancy of the composition of carbides, obtained under various conditions and having a differing degree of dispersion. ~~dispersed state~~. For example, based on B.A. Apayev's data, obtained on the basis of magnetic analysis of ~~RYMAYANIKH~~ U12 steel, the content of carbide phase can constitute 27 - 45% (Bibl.85). At the same time, N.M. Popova ~~is~~ found that the composition of carbides, deposited by an electrolytic solution of carbon steels, ~~RYMAYANIKH~~<sup>tempered and</sup> annealed at temperatures ranging from 200 - 400°C, is constant and corresponds to the formula for cementite (Bibl.86). In any case, the apparent increase in content of carbide phase follows logically from the fact of abrupt differing corrodibility of carbides and of ferrite base, and the surface of cut being obtained owing to this

relief.

In the case of a granular form of carbides, the ideal plane a - a (Fig.25,A) intersects a number of grains, wherein the ~~XXXXXXXXXX~~ occurrence of a body of intersected grains on one or ~~XXXX~~ the other side of the surface is equally probable. At polishing and pickling, ~~XX~~ <sup>the</sup> carbides hardly change at all, whereas the ferrite base is easily pickled and its average level is determined by the plane b - b (Fig.25,B).

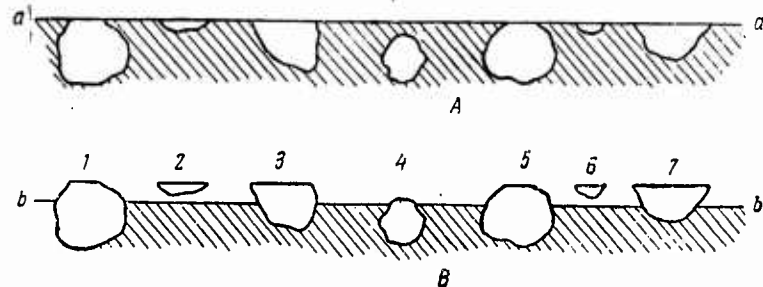


Fig.25 - Effect of Microrelief of Cut upon the Visible <sup>Quantity</sup> ~~XXXXXXXXXX~~ of Carbide Phase at Granular Form of Carbides

Owing to this, there will occur:

- a) An increase in the visible dimension of the part of grains, intersected by the original plane a - a, the body of which is located within the volume of the cut (grains 1 and 5 in Fig.25);
- b) The appearance of new grains in the field of <sup>(view)</sup> vision, occurring earlier below the level of cut, i.e. below the plane a - a (grain 4);
- c) The disappearance from the field of <sup>(view)</sup> vision of those grains, ~~the body of~~ <sup>whose body</sup> ~~which occurred~~ <sup>lies</sup> outside of the volume of cut, while the height of the marked-off plane a - a of the segment is less than the depth of relief (grains 2 and 6).
- d) Preservation almost without change of the original visible size of grains, the body of which ~~occurs~~ <sup>lies</sup> outside of the volume of cut, but the height of the marked-off plane a - a of segment is greater than the depth of relief (grains 3 and 7).

As the result of such a complex change in the ~~XXX~~ pattern of the surface of

the cut, there also occurs an apparent increase in the content of carbide phase. To this one should add that the grains of carbides, especially their sharp edges, also are partly dissolved during pickling, and the level of the ferrite base is evidently irregular, increasing in places of contact with the grains of carbides.

Ⓢ If the carbides are lamellar in form, the pattern obtained during pickling, schematically shown in Fig.26, explains the cause of the apparent increase in content of carbide phase in this case. The correct relationship of the carbide and ferrite phases can be obtained by measuring the thicknesses of ferrite and cementite plates in those grains of perlite in which these plates form a ~~XXXXXX~~ <sup>right angle</sup> with the plane of the cut.

The quantitative electron-microscopic analysis of dispersed carbide phases is of great interest. Specifically, in the presence of an accurate method of determining the phase composition of the structure, it is possible to solve in a well-defined manner the problem of the constancy of composition of cementite and the existence of intermediate carbide phases, at the present time constituting a debatable problem. Recently A.I.Gardin stated the concept that if we had at our disposal a pickling agent, possessing the capability of selective dissolving of cementite, the possibility would appear for revealing the inner ~~XXXXXX~~ structure of a cementite crystal (Bibl.87).

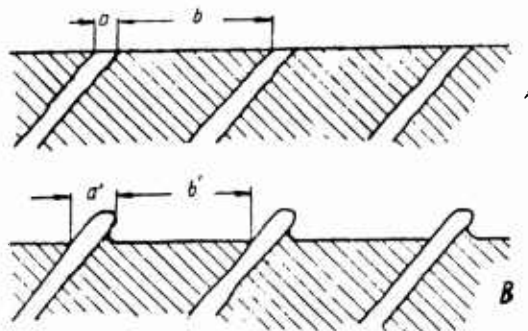


Fig.26 - Effect of Microrelief of Cut upon Visible Amount of Carbide Phase at Lamellar Form of Carbides

In working with optical microscopes, if we use cuts with a minimum microrelief, in this case it is then easy to get quite satisfactory results of determining the phase composition. S.Z.Bokshteyn (Bibl.88) investigated in carbon and alloyed steels the average diameter of sections of carbide particles visible <sup>in the</sup> cut, which usually fell within the limits from 0.3 to 0.7 microns. The diameter of grains was measured in photomicrographs, taken at magnification of 2000 with a subsequent ~~enlargement~~ <sup>enlargement</sup> to 10,000. In samples of hardened steel, containing by chemical analysis 0.40% C, annealed at 630° with varying soaking (from 10 min up to 25 hrs), the carbon content figured on the basis of microanalysis data constituted:

Mean Diameter of Grains, microns	Carbon Content, %
0,34	0,37
0,42	0,36
0,44	0,40
0,50	0,38
0,56	0,39

Taking into ~~the~~ account the high dispersed state of the structure, the accuracy obtained can be considered quite satisfactory. Hence, the determination of the phase ~~composition~~ <sup>composition</sup> of less dispersed structures should have an even greater accuracy.

In structures pickled with picric or nitric acids, the shiny "small islands" of carbides as a rule are surrounded by dark rings of greater or less width. Based on the observations of S.Z.Bokshteyn, the best coincidence of the data of chemical and of microscopic analyses are obtained if the size of carbides is determined on the basis of the average result among the measurements based on the outer and inner contours. The pickling with sodium picrate removes the need for measurements on the basis of two contours and promotes the obtainment of more accurate data.

Somewhat different phenomena, accordingly leading to other results, occur during

the determination of content of nonmetallic ~~XXXX~~ inclusions in steel. In this case, the specific features of microanalysis are: the use of mostly lengthwise cuts and an examination of the inclusions in the unpickled cut.

As is known, the results of estimations of lamellar (platelike) inclusions (sulfide, silicate) based on standard scales, at the use of lengthwise cuts, greatly depend upon the degree of pressure during rolling. Table 8 shows the change in average index point based on the IK scale and the width of sulfide ~~XX~~ impurities as a function of the diameter of section, being obtained from the initial ingot with a section of 325 × 325 mm (Bibl.89).

Table 8

a)	b)	c)
87	3,28	4
51	3,42	3
28	2,21	1
15	1,05	1
9	0,82	<1
6,5	0,71	<1

- a) Diameter of section, mm; b) Average index point according to IK scale;  
c) Average width of impurities, microns

As we see, there occurs a simultaneous decrease both of the total length of inclusions (expressed as an ~~XXXX~~ index point), as well of their width. Hence, with an increase in pressure during rolling, the area of inclusions ~~is~~ visible ~~and~~ on the cut constantly decreases, which understandably does not point to ~~the~~ <sup>an</sup> actual decrease in content of inclusions in the steel but to ~~the~~ technical shortcomings of the method of microanalysis being used. This is confirmed by the fact that, in the use of transverse cuts, the deviations in estimation of area practically are independent of the degree of pressure, and ~~XXXXXX~~ the variations in estimations

do not go beyond the limits of usual random errors. In Table 9, we present data on the weight content of impurities (computed according to microanalysis data) in sheets of 5 mm thickness in comparison with their content in rods of various cross section, from which these sheets were obtained (Bibl.81).

Table 9

a)	b)	
	c)	d)
30×30	0,0186	0,0163
35×35	0,0397	0,0379
36×36	0,0663	0,0654
45×45	0,0443	0,0489
70×70	0,0945	0,0875
diam 45	0,0641	0,0761
» 45	0,0773	0,0750
» 50	0,1104	0,1107
» 65	0,0584	0,0536
» 65	0,0599	0,0581

a) Size of rods, mm; b) Content of impurities, % (by weight) (based on microanalysis); c) In rods; d) In sheets

M.I.Vinograd, having investigated the effect of deformation upon different types of estimation of nonmetallic inclusions, arrived at the following conclusions:

a) The index point of estimation of lamellar ~~XX~~ inclusions in lengthwise cuts based on standard scales decreases with an increase in the degree of deformation;

b) The content of oxides in volume percentages, being determined in a transverse cut, ~~XX~~ does not depend upon the degree of deformation; the content of sulfides decreases somewhat at greater degrees of deformation, since therein a part of the sulfide impurities go beyond the limits of visibility (Bibl.81).

An estimation based on standard scales is connected with the ~~XXX~~ mandatory use of standard magnification, usually taken to equal 100. Therefore, with an increase in the degree of pressure, a fixed part of the lamellar inclusions become invisible.

At individual measurement of inclusions in a transverse cut, the observer is not connected with magnification and therefore the systematic error is many times less than in comparison with standard scales.

Moreover, in the preparation of the cut, a part of the inclusions "are smeared" by the metal. Since the cut is ~~XXXXXXXX~~ <sup>studied</sup> without pickling, this part of inclusions is not considered during microanalysis. The phenomenon of "smearing" is promoted by a decrease in diameter of ~~the~~ inclusions and such an arrangement of the surface of the cut at which it does not intersect the extended inclusions crosswise, as this is shown in Fig.27,a, but passes almost as a tangent plane with reference to the round surface of the ~~XX~~ inclusion (Fig.27,b). The fact of "smearing" of

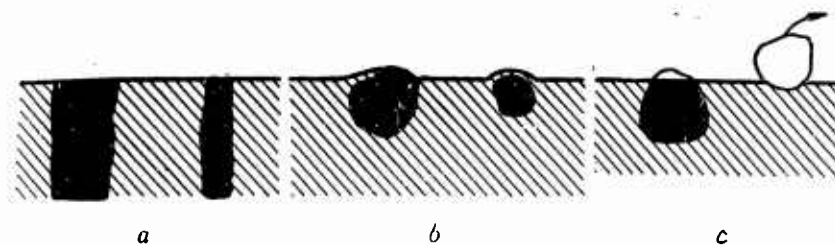


Fig.27 - Diagram of "Smearing" and Crumbling of Nonmetallic ~~XX~~ Inclusions at Lengthwise Arrangement of Plane of Cut

(a - Transverse cut; b and c - Lengthwise cuts)

inclusions is confirmed by the experimental data of ~~XXXX~~ B.B.Gulyayev, who counted the number of sulfide ~~inclusions~~ <sup>inclusions on</sup> ~~in a slide and, XXXXXXXX~~ <sup>with this,</sup> ~~parallel~~ <sup>on</sup> sulfuric impressions taken from this same cut (microsection). Results of calculations according to section of steel casting with a diameter of 100 mm, cast in a sand ~~XXXXX~~ mold, are shown in Fig.28 (Bibl.71).

While a sulfuric impression gives a correct picture of ~~XXXX~~ the increase of the degree of dispersion of inclusions ~~in dispersed state of XXXXXXXX~~ <sup>the</sup> in proportion to ~~increase in~~ <sup>the</sup> rate of hardening,

inclusions,  
microanalysis reveals a lesser fraction of ~~impurities~~, the more they are dispersed.

larger ~~in~~ deposits,  
The fact of "smearing" and of considerably ~~more~~ for instance,  
deposits of graphite in gray iron, is <sup>well</sup> known in metallographic practice.

There can also occur a crushing of the inclusions, the body of which is located beyond the volume of the cut and a very small part of it is cut off by the surface ~~(Fig.27,c)~~ (Fig.27,c).

In the transverse cut, we observe and are able to measure the actual diameter of ~~inclusions~~, whereas in the lengthwise cut, the visible width of ~~in~~ inclusions depends upon the distance between the plane of the cut and the axis of ~~the~~ <sup>the</sup> inclusion, and therefore is always less than the diameter of the ~~inclusion~~, <sup>inclusion,</sup> coinciding with it only in isolated cases, when the axis of ~~the~~ <sup>the</sup> inclusion matches the plane of the cut. On the average, the visible width of ~~in~~ inclusions comprises around three-fourths of their actual diameter.

Finally, in the lengthwise ~~cut~~ cut, we have the chance to see and to measure ~~plastic~~ <sup>plastic</sup> considerably less ~~inclusions~~ inclusions than in a transverse cut. If we represent the inclusions in the form of threads (fibers) with a diameter  $D$  and <sup>a</sup> length  $L$ , and their amount is denoted by ~~quantity~~ <sup>quantity</sup> per unit ~~of~~ volume of steel ~~is denoted~~ <sup>is denoted</sup> by  $N$ , then, as we shall show below, the quantity of inclusions visible per unit ~~of~~ area of lengthwise cut, will be proportional to the diameter of inclusions and is ~~determined~~ <sup>determined</sup> by the equation

$$n_1 = DN,$$

while the quantity of inclusions, ~~is~~ <sup>per unit area</sup> visible ~~in a unit of area~~ of cross cut, is proportional to the length of ~~inclusions~~ <sup>inclusions</sup> and equals:

$$n_2 = LN.$$

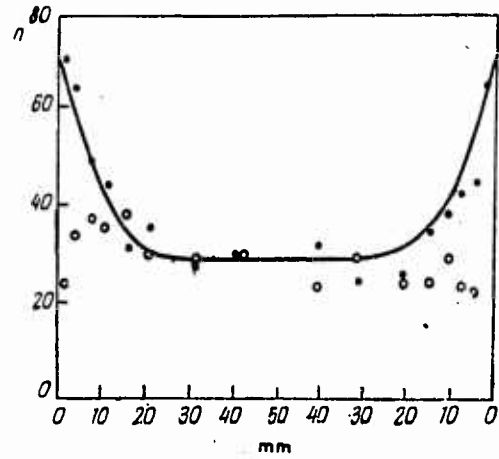


Fig.28 - Distribution of Sulfide ~~Inclusions~~ <sup>Inclusions</sup> along ~~Section of a~~ <sup>Cross</sup> Steel Casting 100 mm in Diameter, Based on ~~the~~ Data of Computations in a Cut (Circles) and in a Sulfuric Imprint (Dots). [After B.B.Gulyayev (Bibl.71)].

From the equations presented, it follows that the ratio of quantities of inclusions ~~per unit of~~ <sup>inclusions</sup> area of transverse and lengthwise cuts is equal to the ratio of the length of ~~inclusions~~ <sup>inclusions</sup> to their diameter. Since the length of plastic inclusions exceeds their diameter by dozens and hundreds of times, the ~~inclusions~~ <sup>inclusions</sup> in the cross section are greater by just as many times as in comparison with the lengthwise cut.

In microanalysis of lengthwise cuts, there is lost a considerably greater part of ~~inclusions~~ <sup>inclusions</sup> than in cross cuts, which decreases the accuracy of determinations. Moreover, in the use of lengthwise cuts, it is necessary to compute additionally the average weight index of ~~the~~ estimation based on ~~eq.~~ <sup>eq.</sup> (11.3).

The distribution of inclusions in steel by sizes is subjected to the asymmetric curve of distribution with a maximum. The impurities which are smallest in size are also present in steel in the least quantity. Therefore the loss even of a considerable part of fine ~~inclusions~~ <sup>inclusions</sup> does not lower significantly the total area of ~~the~~ inclusions,

being determined on the basis of a cut of XX cast steel or rolled steel (if the cut is located perpendicular~~ly~~ to the axis of rolling). A comparison of microanalysis data and of chemical data shows a good convergence. In Fig.29,

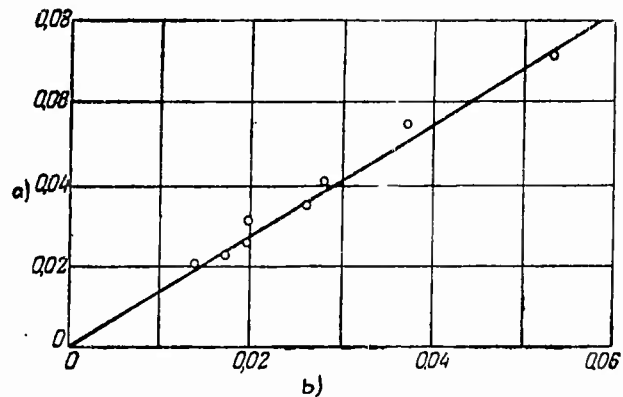


Fig.29 - Dependence between Results of Determining the Content of Nonmetallic Inclusions by Microscopic and Chemical Methods of Analysis. After data of M.S.Aronovich and I.M.Lyubarskiy (Bibl.80)  
 a) Microscopic method; b) Weight, % of inclusions

we show the dependence between results of chemical and microscopic analysis, obtained for rail steel by M.S.Aronovich and I.M.Lyubarskiy (Bibl.80). A similar verification, conducted by P.Ya.Kravtsov, also showed the conformity of the data of both types of analysis (Bibl.90).

Summing up the data and concepts presented in the present paragraph, we can state that fully satisfactory results of determining the phase composition can also be obtained ~~XXXXXXXXXX~~ under the most unfavorable cases, caused by a highly dispersed state and low content of the phase being analyzed. Decisive significance is possessed by the proper choice of <sup>the</sup> plane of cut, a careful preparation of <sup>the</sup> cut and minimum relief of its surface, the use of sufficiently large magnifications, as well as the use of optical microscopes.

Section 13. Planimetric Method of Determining the Phase and Structural Volumetric Composition of Alloy

The planimetric method of analysis of rocks was proposed and first applied by M. Deless in 1847.

The outlines of grains of individual minerals, composing the rock, visible on the polished surface of a sample, were transferred by Deless to transparent paper, coloring the grains of each of the minerals with a designated color. Then he glued the transparent paper to a metal sheet, for greater accuracy of weighing, cut the grains with shears, sorted according to conventional colors (by minerals), and then detached and weighed the foil separately for each of the minerals. The weight values obtained for each of the ~~XXXXXXXXXXXX~~ minerals composing the rock were proportional to the area of the corresponding minerals in the microsection and hence to the volume being occupied in the rock.

At present, in an ~~XX~~ analysis of the microstructure of alloys and rocks, the following basic methods are used for measuring the areas of components:

- a) ~~The~~ Determination of area, occupied by a given phase, at visual observation with the aid of a square-reticulated eyepiece, namely the cellular method;
- b) Individual measuring off of the sections of microparticles at visual observation with ~~the~~ <sup>the</sup> aid of an eyepiece-micrometer, with ~~the~~ subsequent calculation or other type of estimation of the area of each section and with their summation;
- c) Measurement of area of sections of microparticles by various methods, being conducted in photomicrography or in a drawing, ~~conducted~~ <sup>made</sup> with the aid of the Abbe drawing equipment;
- d) Determination of relative area of given phase at visual observation by way of comparing the visible structure with a standard scale.

It is feasible to use the planimetric method at low content of <sup>a</sup> given phase in the structure (not more than 5 - 10%), since in these cases it is more effective than the linear or point methods. We will explain this in ~~XXXXXXXXXX~~ the following ~~XXXXXXXXXX~~ example.

In the point method, the relative area of <sup>a</sup> given phase is determined by the fraction of ~~nodal~~ nodal ~~points~~ <sup>the</sup> points of square-grid eyepiece, occurring in a grain of the phase being analyzed. If, for instance, the content of nonmetallic inclusions in steel equals 0.01% by volume, then the probability of ~~the~~ occurrence in them of a separate point equals 0.0001, and of one of the 441 nodal points of <sup>the</sup> square-grid eyepiece (containing 400 cells), correspondingly 0.0441. ~~XXXXXXXXXX~~ Otherwise expressed, on the average the occurrence of one single nodal point of the eyepiece in an inclusion (impurity) will take place only once during the inspection of 23 fields of <sup>view</sup> ~~vision~~, and for the obtainment of more or less reliable data, the number of fields should be many times greater. Moreover, using the planimetric method, we can estimate the area of all inclusions, visible in a field of <sup>view</sup> ~~vision~~, and obtain reliable data in a small number of fields of ~~vision~~ view.

The measurement of area of a given phase in ~~XXXXXXXXXX~~ photomicrographs or drawings can be conducted more accurately than in visual observation directly under a microscope; however, the preparation of ~~microphotographs~~ <sup>photomicrographs</sup> or drawings limits the number of fields of view in which the measurements are conducted.

Therefore a more accurate estimation of single fields of view can be obtained by measurements in photomicrographs and drawings, and the more accurate estimation of the sample as a whole can be obtained at direct measurements under a microscope. The method of planimetry in ~~microphotographs~~ <sup>photomicrographs</sup> and drawings, intended for standard scales is of quantitative estimation, ~~XXX~~ mandatory, independently of the content of the given

phase. Moreover, it is often used in an ~~XRAY~~ analysis of highly dispersed structure, containing a great number of grains on the microsection even at use of large magnifications, which complicates the measurement during visual observation.

In addition to the planimetric method, there is also the cellular method of determining the phase composition. However, this method has a number of major disadvantages, which greatly restrict its use in metallurgy; therefore there are no bases for considering it here.

In metallographic practice, the relatively most widespread use is made of methods of individual measurement of linear dimensions of sections of microparticles in a cut with the aid of an eyepiece-micrometer (see Fig.13) with subsequent estimation of the part of the area of the cut occupied by microparticles of the given phase. This method found application mainly for estimating the content of nonmetallic inclusions in steel and graphite in iron. Usually transverse cuts are used in determining the content of nonmetallic inclusions in rolled steel.

The sections of microparticles are measured in two mutually perpendicular directions, if they are not equal <sup>in</sup> ~~axial~~. Therein, the sections visible in the field of view usually do not match the ruler of the eyepiece-micrometer, but their length and width are estimated in divisions of the scale by eye. Then one determines the area of each section taking into account its shape, the total area of all sections in each field of view and in all fields of view and, finally, the relative area occupied by the given phase in the cut and hence in the volume of the alloy.

For making the calculations easier, the sections of microparticles having approximately equal areas are grouped and estimated by a fixed index point based

on special scales. The number of inclusions of each group are then ~~XXXI~~ multiplied by the appropriate factor ("magnitude"), taking into account the average area of sections of the given group, the products are added together and yield the "index", proportional to the fraction of area being occupied by the given phase in the cut. For estimating the nonmetallic inclusions in steel and the graphite in forged iron, there was proposed a large number of various scales which were similar in ~~their~~ construction. As an example, we consider the method developed by M.S.Aronovich, I.M.Lyubarskiy, and Ye.K.Yefanova, also known as the method of the Ukrainian Institute of Metals (UIM) (Bibl.80, 91).

Using the UIM method, one can determine the content of nonmetallic inclusions in cast metal, in sheet, strip and bar rolled ~~metal~~ <sup>stock</sup> (in transverse cuts). In a number of fields of view, at magnification of 200 - 250, there is measured the the inclusions, length and width of ~~impurities~~, whereupon their area is estimated in square divisions of the ruler of the eyepiece-micrometer. Therein it is assumed that the cross sections of the inclusions ~~sections of impurities~~ in the cut can have the form of circles, ellipses and ~~extended~~ <sup>elongated</sup> rectangles (threadlike inclusions). The area of ~~extended impurities~~ <sup>elongated inclusions</sup> is determined by the product of the length of ~~impurity~~ <sup>the</sup> inclusion times its width, and the area of ~~the~~ <sup>inclusions</sup> elliptical ~~ones~~ as 0.8 of this product. Depending upon the area obtained, all inclusions of the given field of view are classified by groups, according to the standards presented in Table 10. Then the number of inclusions in each group is ("weighed") multiplied by the corresponding index (~~weight~~) <sup>"weight"</sup> equaling the average area of inclusions of the given group in square divisions of the scale of the eyepiece-micrometer. Totaling the obtained products by all groups, one obtains the complete area of impurities in ~~XXXX~~ the given field of view. The ratio of the obtained total to the area of the field of view, measured in the same square units of the scale of the

eyepiece, provides the unknown value of relative area (or volume), occupied by the inclusions in the given field of vision.

Table 10

a)	b)	c)	d)	e)
1	0,10--0,25	0,3--0,5	$\frac{1}{4}$	0,18
2	0,25--0,50	0,5--0,8	$\frac{1}{2}$	0,38
3	0,50--1,50	0,8--1,4	1	1
4	1,50--2,50	1,4--1,8	2	2
5	2,50--5,50	1,8--2,5	4	4
6	5,50--10,50	2,5--4,5	8	8
7	10,50--21,50	4,5--5,2	16	16
8	21,50--42,50	5,2--7,4	32	32

a) Group; b) Limits of area of impurities in square divisions of scale of eyepiece; c) Limits of diameter in divisions of scale; d) Weight (index); e) Average area in the group

Calculation in a number of fields of view demonstrated that the accumulated average value quickly becomes stabilized, as this is apparent from the curve ~~plotted~~ on the basis of test data (Fig.30). Therefore it is sufficient to measure all the inclusions in 10 fields of view. However, this conclusion can in no way be considered universal, because the obtained accuracy is determined by the number of measured impurities, and hence, ~~is~~ <sup>being</sup> limited by the standard number of fields of view, we set the accuracy of analysis as a function of the purity of the steel. One can agree in no way with the method proposed by the authors for computing the obtained volumetric content of inclusions in the ~~weight content~~ <sup>weight content</sup>. Such a calculation can ~~XXXX~~ scarcely be justified because the choice of specific weight of inclusions is arbitrary, and the feasibility of such a type of calculation is lacking. It is quite obvious that specifically the total volume of inclusions (and also their form and dispersed state), disrupting the continuity of the metal, exerts an effect upon the strength of the steel, which depends in no way upon the specific weight of the

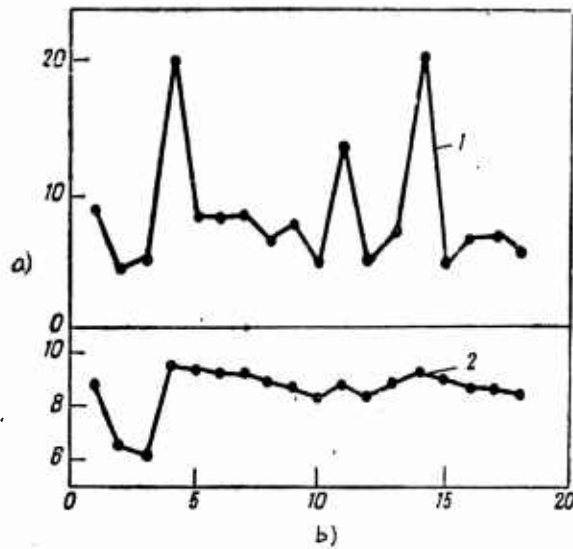


Fig.30 - Index of Contamination of Steel by Nometallic Inclusions in Individual Fields of View (1) and Stabilizations of Accumulated Average Value (2). After data of M.S.Aronovich and I.M.Lyubarskiy (Bibl.80)

a) Index; b) Number of field of vision

inclusions; therefore ~~XXXX~~ their weight content is not indicative.

The data presented indicate that the method described yields sufficiently reliable results and good agreement with the data of chemical analysis (see

Fig.29). The methods of estimating the content of nonmetallic inclusions, not ~~having~~ <sup>showing</sup> essentially important differences from the above-described method, were

also proposed by P.M.Dontsov (Bibl.92), P.I.Melikhov (Bibl.10), ~~XXXXXX~~ <sup>Ye.Ye.Malyshevoy</sup>

(Bibl.93), S.G.Voinov, and V.A.Boyarshinov (Bibl.94). A similar method for

estimating the graphite of ~~XXXX~~ <sup>malleable</sup> iron was proposed by V.M.Shpeyzman and

Ye.V.Yelenevskaya (Bibl.95).

The scales of all these methods of evaluation were constructed in such a way that the diameters of inclusions ~~XXXX~~ increase from group to group in an arithmetic or, in most cases, a geometric progression, and the rate of growth of average area of inclusions in a group is correspondingly ever higher. Such a

construction of scales is unfeasible and decreases the accuracy of the method, since the total area of inclusions is determined basically by the inclusions of large size~~ed~~ and these inclusions are specifically estimated as the most approximate, in a rough manner, since the interval of change in area of inclusions in the group increases from group to group. Since the purpose of analysis is the determination of total area of ~~XX~~ inclusions of various sizes, the scale should be constructed, proceeding from a uniform increase of the specific area of inclusions from one group to the other, i.e. based on arithmetic progression of average area and not of diameter of impurities.

A somewhat different method of determining the total area of inclusions and graphite in gray iron, differing from ~~XXXX~~<sup>the above</sup> listed ~~XXXX~~ calculation based on scales, was described by S.M.Skorodziyevskiy (Bibl.28, 96). According to this method, in a number of fields of view three statistically average values, namely the quantity of impurities in the field of view, the length and width of inclusions (or of graphite deposits) are determined by way of calculating and measuring the sizes. The average area of impurities is found as the product of their average length times average width, and the total area of inclusions in the field of view is found as the product of average area of inclusions times their average quantity in one field of view. It is desirable that all three values be measured or calculated in the same fields of view. The obtainment of total area of inclusions (or of graphite) by the method described somewhat complicates the determination, since it requires a separate determination of three average values.

The determination of average area of sections of microparticles and, specifically, of nonmetallic impurities may be considerably simplified and accelerated, and

accuracy increased correspondingly, in the ~~XXX~~ use of special eyepiece inserts, similar to that shown in Fig.31. In estimating the inclusions of rounded form in cast steel or in the cross cut of rolled steel, they are compared with a number of dark circles, for which the value of area, changing in the sequence of a simple arithmetic series of numbers, is indicated on the insert, wherein for a unit there is adopted the area of the smallest circle. The entire area of the square, measured in the same units, equals 4800. ~~XX~~ The ~~XXX~~ determination of relative area of inclusions is conducted as follows.

The magnification of <sup>the</sup> microscope should be so chosen that the largest inclusions found on the cut are close in area to the largest circles of the insert. In calculating, all inclusions falling within the square are taken into account, as well as those from the inclusions intersected by the perimeter of the square, the greater half of which proved to fall within the square. All these impurities are

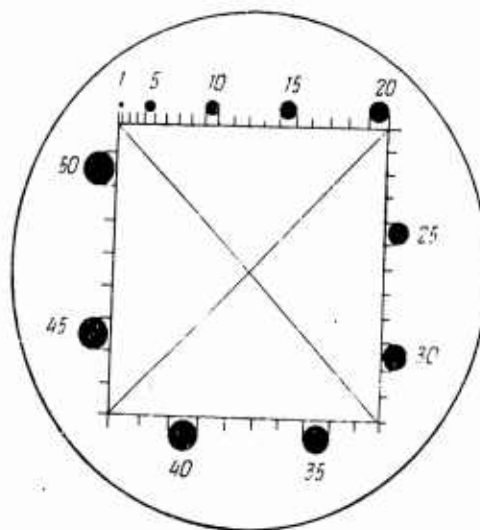


Fig.31 - Ocular Insert for Estimating the Area of Inclusions of Rounded Form

compared with the circles, and the area of each inclusion is estimated. These

numbers are totaled for all impurities of a given field of vision or by way of oral counting, or even with the aid of two hand counters (see Fig.16), of which one counts the units, and the second counts the groups of ten. The inclusions smaller than circle (1) of the smallest size on the insert, are mentally combined into groups. The ~~XXXXX~~ square of the insert is divided <sup>into</sup> ~~XX~~ four equal sectors for facilitating the calculation in the presence of a large number of inclusions.

The total of the figures for all <sup>inclusions</sup> ~~XXXXXX~~ of the given field of view, divided by 48, directly express<sup>es</sup> the percent of area, occupied by inclusions on the cut, or in the volume of steel. The calculation is repeated in several fields of view and there is derived an average estimation for ~~XXXX~~ <sup>the entire</sup> cut. Since the area of the cut, on which the calculation of area of <sup>inclusions</sup> ~~XXXXXX~~ is conducted, and also the area of the actual inclusions, are measured by one and the same units, the result obtained is independent of the ~~XXX~~ magnification being used and does not require any further conversions.

In the use of special ocular insert, the need is done away with of recording the number of inclusions by groups, as well as the subsequent multiplication of these numbers by index and adding, which greatly facilitates the process of analysis, the duration of which is much less than for example in computation based on the method of M.S.Aronovich and I.M.Lyubarskiy.

The method described is <sup>the</sup> most simple, rapid and accurate ~~and~~ <sup>of</sup> all ~~XX~~ of the methods of estimating the content of nonmetallic inclusions in steel.

The method of measuring the area of sections of microparticles in microphotographs and drawings has limited use. The area of its use is mainly as <sup>an</sup> estimation of structures of standard scales, for obtaining their precise characteristics.

The accuracy of all <sup>three</sup> ~~XXXXX~~ variations, examined in the present paragraph, of the

planimetric method of estimating the phase and structural composition of an alloy is determined ~~XXX~~ by the quantity of individual grains which were measured by one or another method in the process of analysis. From the rich experience of petrographic structural analysis, it follows that ~~the~~ error <sup>can</sup> not exceeding 1% of the value ~~XXX~~ being determined <sup>is</sup> assured at a number of measured grains equaling 1000 (Bibl.50). Since the error is inversely proportional to the square root of the number of measurements, one can determine the value of possible error as a function of the number of grains being measured during analysis, by the following numbers.

Number of Grains Measured	Error, %	Number of Grains Measured	Error, %
50	4,47	600	1,29
100	3,16	700	1,20
200	2,24	800	1,12
300	1,83	900	1,05
400	1,58	1000	1,00
500	1,41	2000	0,71

The figures adduced may be used for determining the error of identification of content of phases or components of ~~XXXXXXXX~~ structure by the methods of individual measuring of sections of various phases in a microscope or in ~~XX~~ photomicrographs and drawings of structure.

A fourth type of planimetric method is the determination of relative area of phase or structural component by way of visual comparison of <sup>the</sup> structure with standard scales; this is least accurate, since it introduces the element of subjectivity into the evaluation. However the simplicity of this type of estimation and the possibility of a ~~XX~~ rapid examination and evaluation of large areas in a short time make this method quite effective, if a great accuracy of analysis is not required.

Scales for estimation of phase or structural composition are numerous. Among the great number of standard scales serving for characteristics of the most diverse elements of structure of steel and iron, one can note two scales of such a type listed in GOST 3443 - 46. These scales are intended for determining the content of ~~per~~ <sup>by</sup> perlite and graphite in gray iron, but are not distinguished either by accuracy or by technical improvement of reproduction of standard structures.

A number of scales intended for evaluation based on structure of steel of ~~weight content~~ <sup>by</sup> inclusions of nonmetallic ~~impurities~~ of various type, were developed by R.B.Malashenko (Bibl.98). In supplement to the index point estimation, S.G.Voinov and ~~XXXX~~ V.A.Boyarshinov introduced values of areas occupied by oxides and sulfides in standard photomicrographs of known scales of nonmetallic inclusions GOST 801 - 47 [based on data of the metallographic laboratory, TsNIICM (Bibl.99)]. These data show the complete lack of regular dependence between the value of the area ~~XX~~ occupied by the inclusions and the index point.

The value of area being occupied by nonmetallic ~~impurities~~ <sup>inclusions</sup> is set at the basis of the new scale shown in Fig.32, developed by N.K.Lebedev, ~~XXXX~~ M.I.Vinograd, and S.A.Kiseleva (Bibl.37). Here, the area of inclusions increases in geometric progression with the denominator (2). The construction of this drawn scale may be considered exemplary, if the number of index points were proportional to the area of impurities, i.e. also were determined by a geometric series with a denominator (2). In the opposite case, the average ~~XXXXX~~ index point determined on the basis of a number of fields of view, will not correspond to the average area of inclusions in these fields.

A poor polygraphic reproduction of scales sharply decreases the accuracy of

determination, and sometimes makes it impossible.

More convenient and accurate are the scales placed directly in the eyepiece of the microscope, which permits the conduct of evaluation without moving away from the eyepiece and makes it possible to make a better comparison of the analyzed structure with the standard structure. Therefore worthy of attention is the design of an eyepiece with revolving inserted scales, manufactured by the *Bausch* ~~Best~~ and Lomb Firm (USA) for determining the value of a grain of steel according to ASTM.

A very significant disadvantage of all types of planimetric determination of phase and structural composition is the ~~XXXXXXXXXX~~ impossibility of its mechanization or automation by way of using various counting devices, which would facilitate the work of the observer. In calculating the squares, or in ~~XXXXXX~~ individual measurement of sizes of sections under a microscope, it is easy to go astray; one can count the same ~~XXXXXX~~ grains twice or not count others at all, etc. Therefore the new methods of analysis (linear and point) have practically crowded out the planimetric method in the petrographic analysis of rocks.

Nevertheless, the specifics of metallographic analysis fully justify the use of certain types of the planimetric method in a number of cases. Here first of all ~~one~~ one can include cases of determining the phase composition by the method of individual measurement of sections of microparticles at very low content of phase being determined and its high dispersed state (nonmetallic inclusions in cast steel and in the cross cuts of rolled steel of ~~equiaxial~~ <sup>*equiaxed*</sup> section, carbide phase at granular form of carbides, graphite at rounded form of deposits, etc.). The measurement of area of sections of microparticles of the given phase in photomicrographs of sketched structures, intended for standard scales, serving for estimating the area

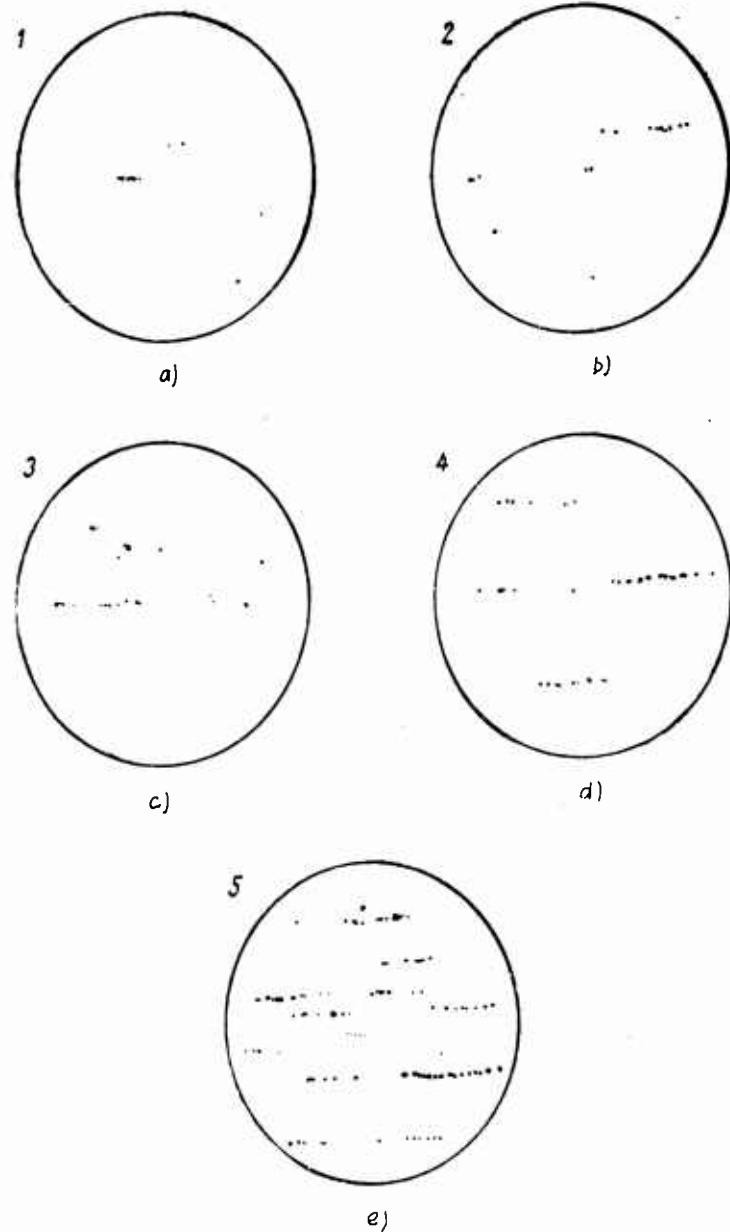


Fig.32 - Scale of Comparison for Estimating the Contamination of Steel by Nonmetallic Inclusions (TsNIIChM) (Bibl.87)

Brittle Inclusions - Oxides

- a) Area of inclusions  $0.27 \times 10^{-3} \text{ mm}^2$ ; b) Area of inclusions  $0.55 \times 10^{-3} \text{ mm}^2$ ;  
 c) Area of inclusions  $1.10 \times 10^{-3} \text{ mm}^2$ ; d) Area of inclusions  $2.20 \times 10^{-3} \text{ mm}^2$ ;  
 e) Area of inclusions  $4.40 \times 10^{-3} \text{ mm}^2$

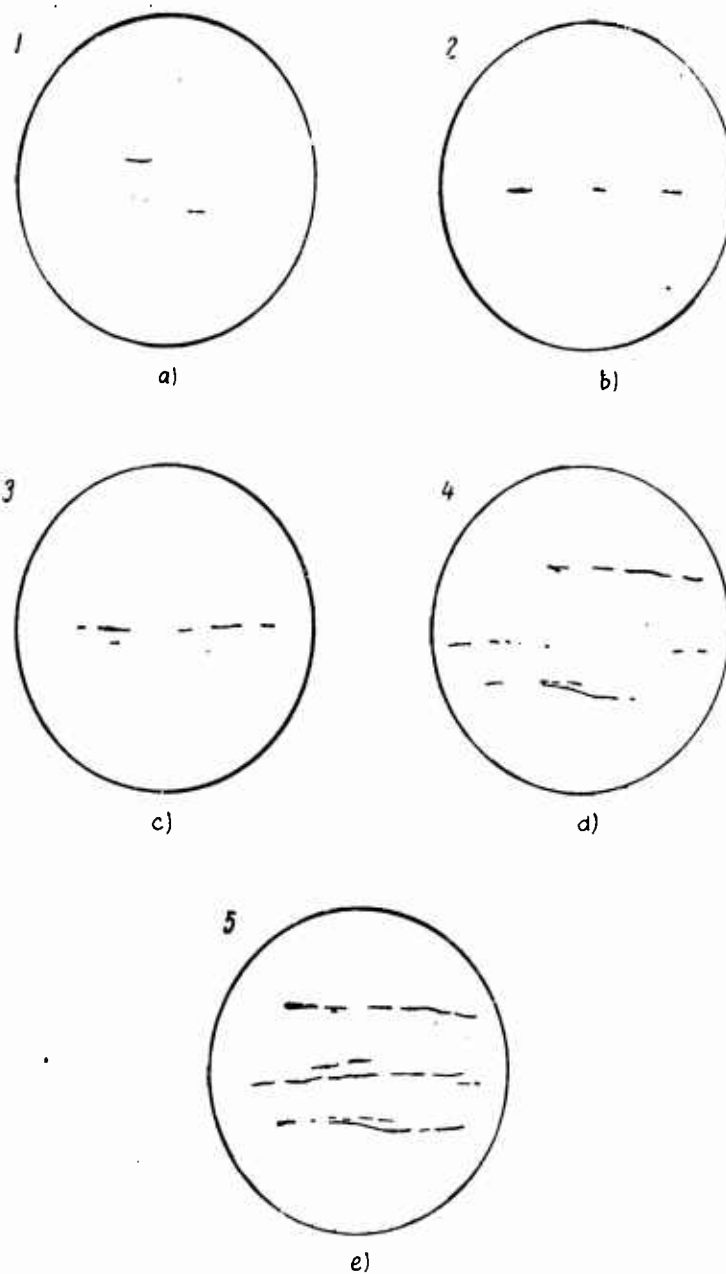


Fig.32 (Continuation)

Plastic Inclusions - Sulfides

- a) Area of inclusions  $0.50 \times 10^{-3} \text{ mm}^2$ ; b) Area of inclusions  $1.00 \times 10^{-3} \text{ mm}^2$ ;  
 c) Area of inclusions  $2.00 \times 10^{-3} \text{ mm}^2$ ; d) Area of inclusions  $4.00 \times 10^{-3} \text{ mm}^2$  ;  
 e) Area of inclusions  $8.00 \times 10^{-3} \text{ mm}^2$

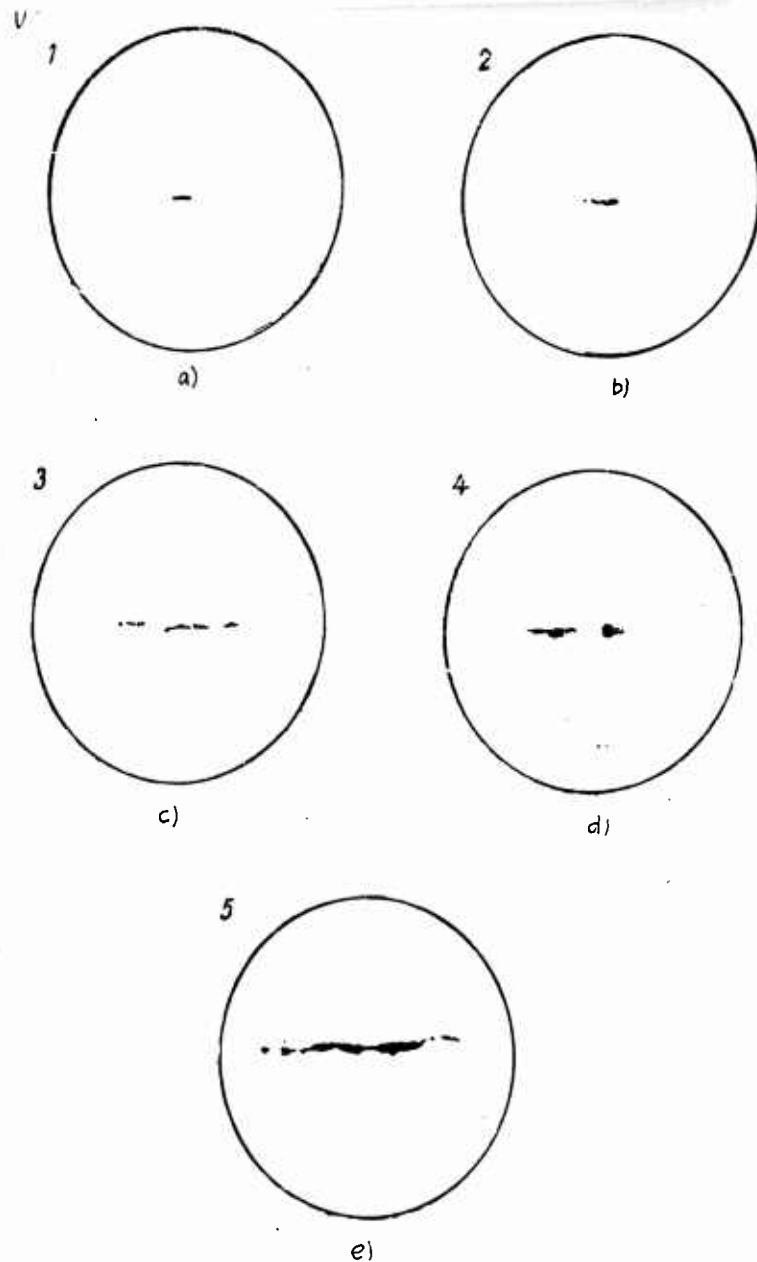


Fig.32 - (Continuation)

Brittle Inclusions - Silicates

- a) Area of inclusions  $0.37 \times 10^{-3} \text{ mm}^2$ ; b) Area of inclusions  $0.75 \times 10^{-3} \text{ mm}^2$ ;  
 c) Area of inclusions  $1.50 \times 10^{-3} \text{ mm}^2$ ; d) Area of inclusions IX  $3.00 \times 10^{-3} \text{ mm}^2$ ;  
 e) Area of inclusions  $6.00 \times 10^{-3} \text{ mm}^2$

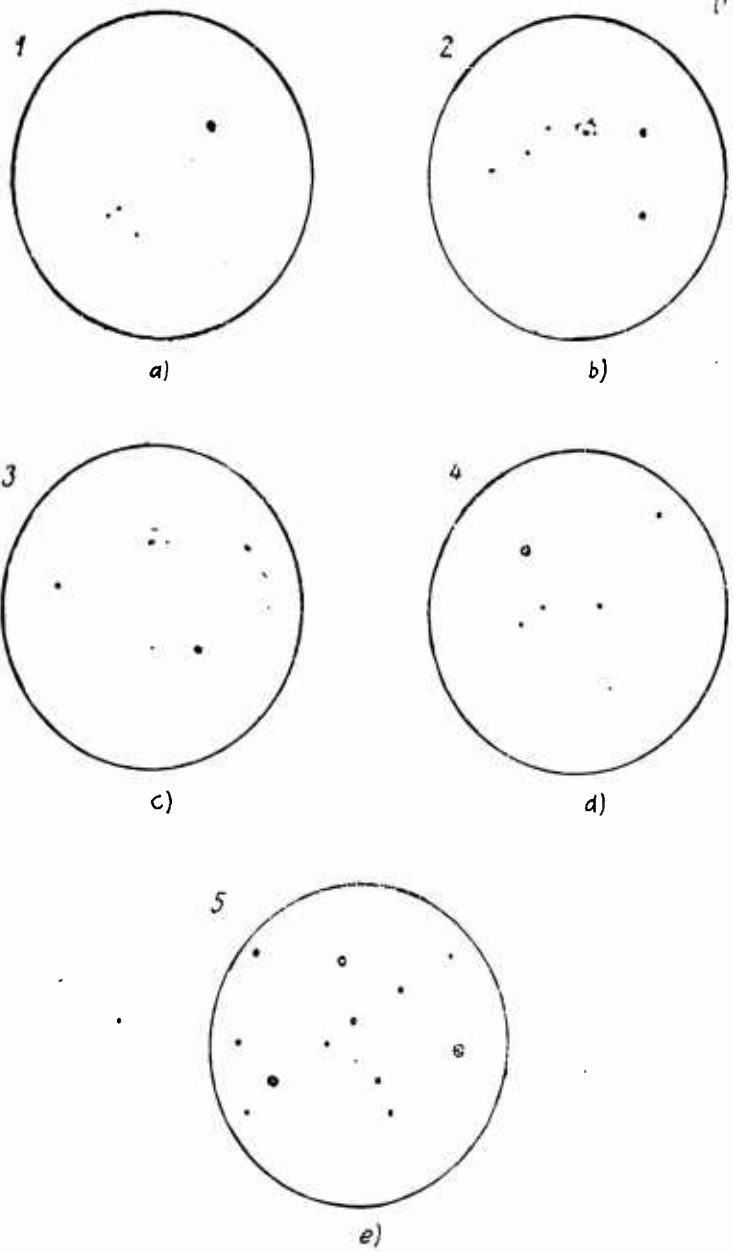


Fig.32 - (Continuation)

Nondeforming Glubular Inclusions ( $\text{SiO}_2$ , ~~silicates~~ Silicates)

- a) Area of inclusions  $0.27 \times 10^{-3} \text{ mm}^2$ ; b) Area of inclusions  $0.55 \times 10^{-3} \text{ mm}^2$ ;  
 c) Area of inclusions  $1.10 \times 10^{-3} \text{ mm}^2$ ; d) Area of inclusions  $2.20 \times 10^{-3} \text{ mm}^2$ ;  
 e) Area of inclusions  $4.40 \times 10^{-3} \text{ mm}^2$

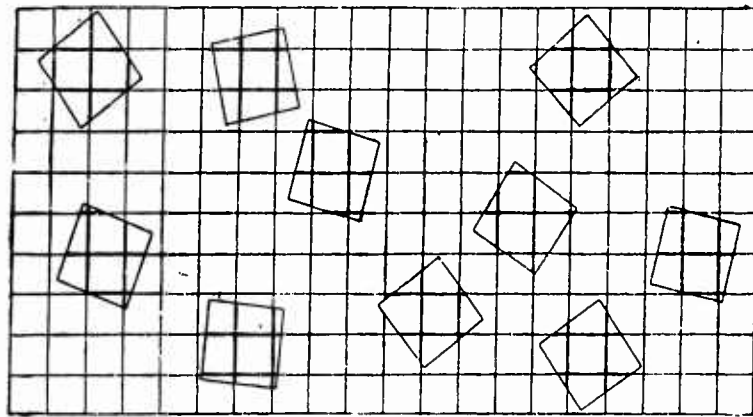
is  
or volumetric content of this phase, ~~XXX~~ most feasibly conducted with the aid of  
the Amsler planimeter, independently of the content of <sup>a</sup> given phase.

Very promising is the use of specialized inserted ocular scales, especially  
the removable ones, intended for individual estimation of area of separate  
sections of microparticles, and also for <sup>an</sup> overall evaluation of relative area of  
a given phase in the field of view as a whole (of nonmetallic inclusions and  
<sup>a</sup> perlite in steel, graphite, ferrite and phosphide eutectics in iron, etc.).

#### Section 14. Linear Method of Determining Phase and Structural Volumetric Composition of an Alloy and Its Application

The linear method first proposed in ~~XX~~ 1898 by A. Rozival for determining the  
mineralogical composition of rocks <sup>under</sup> ~~in~~ a microscope is based on the Cavalieri-Aker  
principle, according to which the measurements of ~~XX~~ bodies can be replaced not  
only by measurement of areas but also of lengths of segments. The advantage of  
the linear method over the planimetric one consists firstly in greater simplicity  
and accuracy of measurement of lengths of segments as compared with measurement  
of areas and secondly in the possibility of automating the process of totaling the  
lengths of segments, falling in each of the phases of the structure being analyzed.

In Fig. 33, a diagram is presented illustrating the use of the Cavalieri-Aker  
principle in the linear method of microanalysis (Bibl. 50). In an area, consisting  
of 200 squares, 10 squares are scattered irregularly, the area of ~~XXXXX~~ each of which  
equals ~~XXXXXX~~ 4 squares and hence the part of area of the drawing taken up by the  
squares amounts to 0.2 or 20%. If we measure the lengths of segments of horizontal  
and vertical lines, passing through the area of squares and set off in ~~XXXX~~ the  
drawing by thick lines, add them up, and divide the total obtained by the entire  
length of lines intersecting the drawing, the value obtained will be all the closer  
to 0.2 the more lines we draw or hence, the ~~XXXXXX~~ more ~~XX~~ segments we measure.



Principle  
 Fig.33 - Application of the ~~XXXXXXXXXX~~ Cavalieri-Aker ~~XXXXXXXXXX~~ in the  
 Linear Method of Microanalysis (after A.Rozival)

The essence of the linear method consists in that the structure, visible ~~under~~ <sup>under</sup> a microscope or in a ~~XX~~ photomicrograph, consisting of any quantity of phases or structural components, is intersected by a straight line or a number of lines. The contours of sections of ~~XXXXXXXXXXXXXX~~ microparticles of individual phases on the cut ~~cut~~ <sup>separate</sup> ~~XXXXXXXXXX~~ these lines into individual segments. If we add up separately the lengths of the segments falling on each of the phases of structure, and divide the total by the total length of intersecting lines, the quotients obtained, according to the Cavalieri-Aker principle, will equal the parts of area of the cut or the volume of alloy which each of these phases occupies. The correspondence will be all the more accurate, the longer the intersecting lines, drawn on the cut or on the photomicrograph.

As A.Rozival demonstrated, these lines should not necessarily be straight, but can also be curves, which does not affect the final result. The lines can be drawn arbitrarily, and not necessarily in the form of a grid of parallel and equidistant lines. It is only important that the lines take in the entire area

being analyzed and that they are equally distributed over the area. In practice, there are accomplished two types of use of the linear method in analysis <sup>under</sup> a microscope, which can be called the methods of stationary and mobile microsection.

In working by the first method (method of stationary microsection), we use the usual eyepiece-micrometer equipped with a ruler, divided into 100 equal parts (see Fig.13). For instance, in the examination of the ~~XXXXXX~~ structure of pre-eutectoid annealed steel, of the 100 divisions of the diametral line on the scale of the eyepiece, a part of the divisions ~~XXXX~~ fall to ferrite, and the remaining ones, to ~~XXXXXX~~ (if we disregard the content of nonmetallic ~~XXXXXXXXXX~~ inclusions), as this is shown in Fig.34. At the given position of the ruler, 82 divisions fall to



Fig.34 - Determination of Structural Composition of Steel by the Ruler Method at Stationary Cut. For the ~~XXXXXX~~ component, 18 divisions of the ruler out of 100 were taken up

ferrite, and 18 to ~~XXXXXX~~ <sup>pearlite</sup>. Therefore the content of ferrite and ~~XXXXXX~~ <sup>pearlite</sup> on the lines of the scale is determined by the figures 82% and 18%, respectively. ~~XXXXXX~~ Understandably, in an adjacent field of view, or even in the same one, upon turning or a slight displacement of the ruler, the number of divisions falling to ferrite and ~~XXXXXX~~ <sup>pearlite</sup> will prove to be different. However, the statistically average value of number of divisions falling to the given structural component, in conformity with the Cavalieri-Aker principle, will equal the content of this structure in the area of the cut and in the volume of the alloy. To obtain a reliable average value,

the measurement needs to be repeated in a number of fields of view, equally distributed about the area of the cut and all the area surrounding it. It is feasible to compute the divisions, falling to all structural components, in addition to that one which is present in the maximum amount, and the number of divisions falling to it can be determined by the difference.

lengths  
The ~~XXXX~~ of segments of the ruler of the eyepiece, falling to the individual range ~~XXXX~~ of phases being analyzed or structural components, are usually estimated as whole numbers of divisions of the ruler. Since the actual length of these segments, generally speaking, does not equal <sup>a</sup> whole number of divisions, the error of determination will be all the greater, the shorter the segments, i.e. the more dispersed the structure and the less the magnification. Therefore, it is desirable ~~XXX~~ to use ~~these~~ magnifications at which the length of one segment, on the average, equals at least 5 - 10 divisions of the eyepiece scale. The segments, the lengths of which are less than one division, are mentally combined into groups and are estimated as whole numbers of divisions.

The larger the fields of ~~vision that are~~ <sup>view</sup> chosen for calculation at <sup>a</sup> given magnification, the more accurate will be the result of analysis. However, at the same time its unwieldiness also increases; therefore, the problem of the minimum number of fields of ~~vision~~ <sup>view</sup> which should be examined in order to assure obtaining a given accuracy of analysis, is quite considerable and will be considered separately.

In distinction from that examined above, the analysis in case of a movable cut <sup>is</sup> conducted at continual displacement of the cut in one direction, at simultaneous observation of ~~the~~ <sup>the</sup> structure in the eyepiece with ~~the~~ cross-hair. Therein, we add up the lengths of the path of cut during passage through the point of the eyepiece cross hair for each of the structural components separately. Figure 35

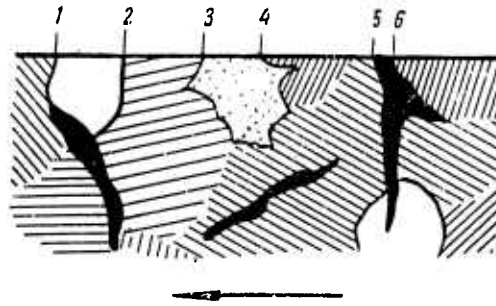


Fig.35 - Determination of Structural Composition of Iron  
by Linear Method at Movement of Cut

explains the method of linear analysis in case of movable microsection. A straight line, intersecting the structure of gray iron, is the path of the point of cross hair of the eyepiece in the microsection during its displacement. Usually the microsection is moved from one edge to the other, then in opposite direction along a line parallel to the first and standing off from it at a certain distance, etc. If the movement of <sup>the</sup> cut is realized by a micrometer screw, the length of <sup>the</sup> path is totaled automatically. Since we need to measure the lengths of paths of the microsection during passage through the point of cross-hair for each of the structural components separately, the passage through a sector of each of them should be conducted by different micrometer screws, each of which ~~XXXXXX~~ and independently of ~~XXXXXX~~ the others, move the cut in the same direction, and also register the length of this movement. Thence it follows that the number of micrometer screws, moving the cut independently one from the other and in the same direction should be not less than the number of the structural components, the content of which is subjected to determination.

In the case of a structure shown in Fig.35, <sup>shifting of the</sup> ~~the movement of~~ cut is accomplished by the first micrometer screw, until a sector of ferrite has advanced along the line 1 - 2 through the point of eyepiece cross-hair in the direction indicated

by the arrow. When the point of cross-hair reaches the boundary ~~KN~~ of the  
ferrite and ~~XXXXXXXX~~ <sup>pearlite</sup> sector at point 2, the movement of the cut begins to be  
accomplished by the second micrometer screw along the line 2 - 3. The advance  
through the sector of phosphoritic eutectics 3 - 4 is ~~XXXXXXXX~~ accomplished by  
a third micrometer screw, while for movement through the ~~XXXXXXXX~~ <sup>pearlite</sup> sector 4 - 5, one  
again returns to the second micrometer ~~XXXX~~ screw, etc. After the cut has been  
examined along a number of parallel lines, the micrometer screws determine the  
total lengths of path of cross-hair point of eyepiece through the ferrite, ~~XXXXXXXX~~ <sup>pearlite,</sup>  
phosphoritic eutectics, graphite and nonmetallic ~~XXXXXXXX~~ inclusions. The ratios  
of each of these values to their total determine the portions occupied by each of  
the enumerated components of the structure on the ~~IX~~ lines conducted, areas of  
cut and in the volume of the alloy. ~~IX~~ The lines of displacement of the cut  
can be run in different directions and cannot be mutually parallel. These lines  
can also be curves, for instance a spiral. The sole requirement is the uniform  
encircling by the ~~IX~~ lines of the entire surface of the cut.

In this method, no kind of calculations or recordings are necessary.

Since the microscope ~~stands~~ <sup>stages</sup> and the two coordinate preparation guides have  
only one micrometer screw for ~~movement of~~ <sup>shifting the</sup> cut in a given direction, for using this  
method of analysis, special ~~stands~~ <sup>stages</sup> ~~IX~~ equipped with several micrometer screws,  
moving (independently of one another) the microsection in the same direction, are  
then necessary. ~~Basic stands~~ <sup>Stages</sup> of various types exist, ~~IX~~ equipped for setting up  
with standard ~~benches~~ <sup>benches</sup> of polarization microscopes. Since these ~~stands~~ <sup>stages</sup> automatically  
add up the lengths of segments, they are called integrational.

Any of the ~~stands~~ <sup>stages</sup> intended for determining ~~IX~~ the phase or structural  
composition by the linear method, should assure the accomplishment of two operations:

a) ~~The~~ sequential movement of the microsection and

b) ~~The~~ recording of ~~XXX~~ values of displacement separately for each phase

or component of the structure.

In earlier type bench <sup>stage</sup> stands, the conduct of both operations was combined in one device, and in more improved later designs, these operations are carried out separately by separate devices.

The first device of such a type, a diagram of which is shown in Fig.36, was proposed in 1916 by S.Shend. The device of S.Shend consists of a stationary frame (1), fastened on ~~a bench stand~~ <sup>the stage</sup> of a microscope, and of two movable frames (2) and (3), the displacement of which is realized by the independent micrometer ~~XXX~~ screws (4) and (5). Microsection (6) is mounted in the internal movable frame (3). Shend's device permits one to analyze an alloy, the structure of which

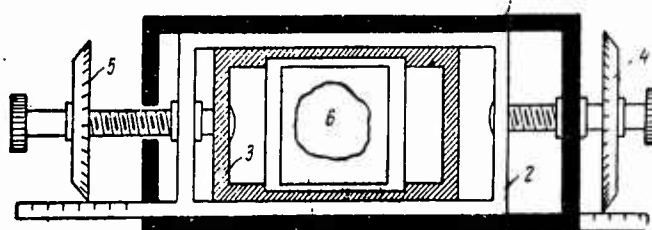


Fig.36 - Diagram of S.Shend's Device (Bibl.50)

~~XXX~~ consists of two components. One can also determine the content of one of the components of the structure, if their number is greater than 2. In this case, the movement through the point of the cross-hair by the component being analyzed is accomplished by one micrometer screw, and the movement of all remaining components of alloy structure is accomplished by a second screw.

A shortcoming of the Shend device is the small number of components of structure being determined simultaneously and the possibility of moving the cut

only in one direction; after having finished inspection along one line, it is necessary to move by hand the cut, in order to carry on inspection along a second line. The second of these disadvantages was removed in the device of K. Sheumann, which has a third micrometer screw, located at right angles to the two first screws.

Wentworth <sup>ing stage</sup> integrational bench stand (1923) permits a simultaneous  
The ~~XX~~

~~XXXXXX~~ determination of five structural components. In this ~~stand~~ <sup>stage,</sup> five micrometer ~~XXXX~~ screws are set on one axis and movement of the cut is accomplished by way of turning one of the five heads (drums), on which the reading is conducted. ~~XXXX~~ Displacements in transverse direction cannot be realized on the ~~Wentworth~~ <sup>Wentworth</sup> device.

This device was improved by Ye. K. Smirnov, who introduced cross movement of the microsection, having mounted on the ~~stand of the device~~ <sup>stage of the instrument</sup> a common two-coordinate preparation guide. Of such a type, the improved ~~integrational bench stand~~ <sup>integrating stage</sup> of the type ISA, intended for determining the content of six structural components, is made by the Test Optical-Mechanical Plant of the Trust ~~(XXXXXXXX)~~ "Russkiye Samotsvety".

As is evident from Fig. 37, the ~~stand~~ <sup>stage</sup> ISA has six heads (drums), the division scale of which corresponds to movement of the cut by 0.01 mm. Three heads can move the cut by 25 mm each, while the three remaining ones can move it by 15 mm each. The maximum total movement equals 90 mm. The two-coordinate preparation guides mounted on the test stand (not shown in Fig. 37) permits the displacement of the cut in transverse direction, and also permits one to determine the content of the seventh structural component, if this is necessary.

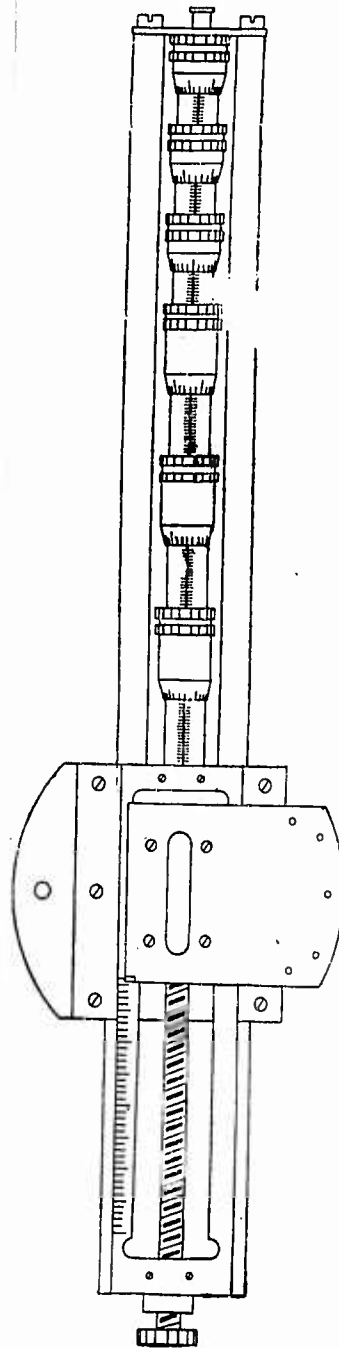
~~integrational test stand~~ <sup>integrating stages</sup> of K. ~~Sheumann-Leitz~~ <sup>Scheumann-Leitz</sup> (1929), A. Dollar (1937) and

also many others/permit one to conduct simultaneous determination of six structural components. In the above cited study of L. Beck and S. Smith, the determination of

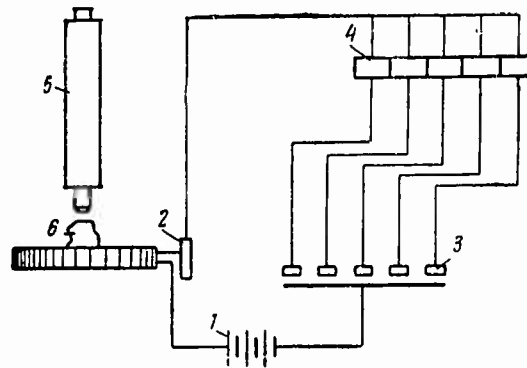
phase composition of brass was determined with the aid of a integrating stage hydraulic ~~integration test stand~~ <sup>(stage)</sup>

permitting one to determine the content of three components (Bibl.77).

The listed designs of ~~test stands~~ <sup>stages</sup>, especially for determining several phases, are unwieldy and ~~inconvenient~~ inconvenient in operation. Therefore, the new approach, ~~proposed~~ <sup>proposed</sup> in 1931 by A.A.Glagolev, to a design of such devices is very valuable and boils down to a division ~~of the device~~ of the device into two or three independent mechanisms. On the ~~stage~~ <sup>stage</sup> of the microscope are mounted only runners ~~(sleds)~~ <sup>(sleds)</sup> for movement of the microsection, while the counting device (recorder), measuring and totaling the segments, is mounted separately. The connection between ~~sled~~ <sup>sled</sup> the ~~slides~~ <sup>slides</sup> and the recorder can either be electric or mechanical. A.A.Glagolev developed a number of designs of devices



Integrating Stage  
 Fig.37 - ~~Integrating Test Stand~~, Type ISA,  
 for Simultaneous Determination of Content  
 of Six Structural Components by Linear  
 Method



Integrator:  
 Fig.38 - Diagram of A.A.Glagolev's Electric ~~XXXXXXXXXX~~

1 - Small battery; 2 - Current breaker; 3 - Switch; 4 - Electromagnetic counters; 5 - Microscope; 6 - Cut being analyzed (Bibl.50)

of such a type, namely, integrators, with both types of connection, being accomplished by a flexible electric cord (electric integrator) or flexible shaft (rotor-integrator) (Bibl.50).

Let us examine the diagram of the electric integrator of Glagolev, shown in Fig.38. Direct current with an intensity of 6 - 8 volts from the ~~XXXX~~ small battery I enters the current breaker (2), connected with the ~~slide~~ <sup>sled</sup> of the microscope, serving for moving the microsection. The breaker is arranged in such a way that at movement of the ~~slide~~ <sup>sleds</sup> with the microsection mounted on them, the number of interruptions of current is ~~XXXX~~ proportional to the length of movement of the ~~XXXX~~ cut in the field of view. Then current enters switch (3), which consists of a number of buttons or keys. Pressing on one key or another, the observer directs the current to one of the five electromagnetic counters of ~~XXXX~~ the <sup>current</sup> recorder (4), which totals the number of interruptions ~~of current~~, proportional to displacement of the cut. Each of the counters of the recorder has been designated in advance for taking into account a definite structural component of the alloy being analyzed.

An observer, working with the Glagolev electric integrator, turns with his right hand the head of the micrometer screw of the microscope <sup>slid,</sup> ~~slides,~~ moving the cut and at the same time bringing into action the current breaker connected with the head. At the same time, he presses with one of the fingers of his left hand that switch key which is ~~XXXXXXXX~~ <sup>intended</sup> for ~~XXXXXX~~ taking into account the structural component located at the given moment in the point of the eyepiece cross-hair, in transition from the sector of one sector of the structural component to the section of another, the observer releases one key and at the same time presses on another.

<sup>observer</sup>  
The ~~XXXXXXXX~~ can carry out the entire operation without moving his eye from the microscope eyepiece. After finishing the inspection of a series of lines, which uniformly take in the entire surface of the ~~XXXXXXXX~~ microsection, the figures shown by the electromagnetic counters are proportional to the content of the corresponding structural components in the alloy. The calculation of structural composition reduces to a determination of ratios of readings of each counter to the sum of readings and to a multiplication of the obtained quotients by 100 for finding the composition in volumetric percentages.

Using the ideas of Glagolev, a number of foreign firms manufactured integrators, comprising variants of the Glagolev electric and rotor integrators. Such for instance, are the "sigma" device made by the <sup>Fuss Co,</sup> ~~Fyuss Firm,~~ the ~~XXXX~~ C.Hurlbut electric counter (Bibl.100) and others.

The integrators facilitate and accelerate the laborious work and raise the accuracy of determinations. For instance, the electric integrator and rotor-integrator permit a determination of the structural composition of five or six component alloys in 30 min with an error not exceeding 1%.

All the devices described above are adapted for polarization microscopes, although several of them can also be mounted on the ~~stand~~<sup>stage</sup> of a metallographic microscope. It is much more convenient to use as a microscope the device for determining microhardness of type PMT-3 with a low-position ~~stand~~<sup>stage</sup> or even to use conventional polarization microscopes, ~~equipped~~ equipped with opaque-illuminators and a monocular insert for transferring the optical axis of the eyepiece from vertical to horizontal position, which facilitates the observation.

#### Section 15. Accuracy of Linear Method

Let us examine the determination of content of pearlite in steel, conducted by the method of stationary microsection in 30 fields of view. Taking the calculation of lengths of segments in each field of view as an independent analysis, we get 30 results. In the second column of Table 11, these 30 results, obtained experimentally, are presented. At an actual content of pearlite in steel, ~~equaling 19%~~ equaling 19% (by volume), in individual fields of view, the number of divisions of the ruler falling to pearlite will vary from 12 to 31. In the third column of Table 1 is presented the increasing total, while in the fourth graph are shown the accumulated average values of content of pearlite for the same 30 fields of view. In Fig.39, we show graphically the change in the ~~results~~ results obtained in separate fields of view (broken curve 1), and of the ~~accumulated~~<sup>cumulative</sup> average (curve 2).

As is obvious from the data in ~~Table 11~~ Table 11 and especially in the curve of Fig.39, the results of determination in individual fields of view will vary within wide limits, whereas the curve of ~~average~~<sup>cumulative</sup> average has a damping appearance. In the examination of more than 17 - 18 fields of view (in the given case), the cumulative average is so stabilized that the actual deviation in one direction or another from the actual content of pearlite (19%) does not exceed 0.5% of it. ~~With~~<sup>With</sup>

Table 11

a)	F	$\Sigma F$	$\frac{\Sigma F}{n}$	F <sup>2</sup>
1	23	23	23,0	529
2	20	43	21,5	400
3	19	62	20,7	361
4	12	74	18,5	144
5	16	90	18,0	256
6	27	117	19,5	729
7	31	148	21,1	961
8	18	166	20,8	324
9	28	194	21,6	784
10	16	210	21,0	256
11	15	225	20,5	225
12	17	242	20,2	289
13	19	261	20,1	361
14	16	277	19,8	256
15	14	291	19,4	196
16	15	306	19,1	225
17	12	318	18,7	144
18	18	336	18,7	324
19	21	357	18,8	441
20	16	373	18,7	256
21	17	390	18,6	289
22	21	411	18,7	441
23	26	437	19,0	676
24	25	462	19,3	625
25	15	477	19,1	225
26	20	497	19,1	400
27	14	511	18,9	196
28	19	530	18,9	361
29	15	545	18,8	225
30	23	568	18,9	529
Total	568	—	—	11428
Mean	18,93	—	—	380, 93

a) No. of field of view, n; b) Total; c) ~~Average~~

further increase in the number of fields of view, the limits of variations of cumulative average become narrower and narrower. Hence, continually increasing the number of fields of vision, we can get the required accuracy of analysis in working with the method of stationary microsection. Strictly speaking, the accuracy of linear analysis is determined not by the number of fields of ~~vision~~ <sup>view</sup> or by length of intersecting lines, but by the number of segments obtained and measured during the process of analysis.

In examining the cut under ~~the~~ a microscope, the number of intersected segments depends upon the optical magnification and upon the ~~dispersed~~ <sup>degree of dispersion</sup> state of the structural

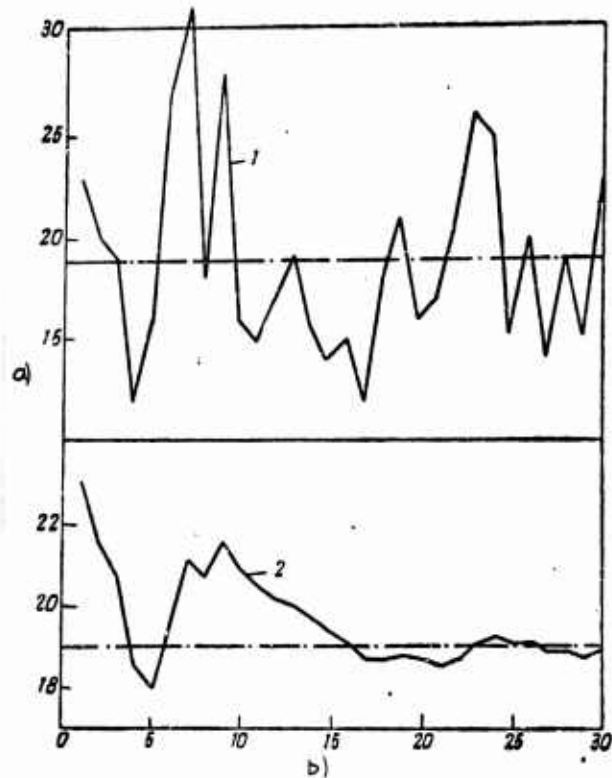


Fig.38 - Results of Determination of Content of Pearlite by Linear Method in Individual Fields of View (1) and Stabilization of Cumulative Average (2)

a) Content of pearlite, %; b) Number of field of view

component under analysis. It is disadvantageous to get a large number of segments by using smaller magnification, since the shorter the average length of the segment, the less the accuracy of measuring the segments. Therefore, it is feasible to use large magnifications; and to assure obtaining the necessary number of segments, it is better to examine a large number of fields of view.

S.Shend notes that conducting the examination of a cut on the basis of a number of parallel lines, it is necessary to <sup>space</sup> ~~set~~ them ~~one from another~~ by a distance which is greater than the average cross section of the grain of structure under analysis, in order not to intersect the same grain more than once. This is not mandatory: The same grain may be intersected any number of times under the

stipulation that the intersecting lines uniformly cover the entire surface of the cut.

Curve (2) in Fig. 39 gives only a qualitative picture of increase in accuracy of analysis along with increase in ~~XXXXXX~~ <sup>the</sup> number of measured segments. In order to obtain concrete values of <sup>the</sup> expected error, it is necessary to have a value of mean ~~quadratic~~ <sup>square</sup> deviation of results of repeated analyses, conducted under uniform conditions, from the ~~XXXXXX~~ actual content of given ~~XXXXXXXXXX~~ structural components in the alloy. Let us grant that we conducted a number of analyses of the same cut, preserving the constancy of conditions of analysis, namely measuring in each analysis the same number of ~~XX~~ segments, using a uniform magnification, etc. Conducting n independent analyses, we get, generally speaking, n different results, although many of them can coincide one with another. Let us ~~signify~~ <sup>denote</sup> these results, ~~being~~ expressed in percentages of volume of alloy, by  $F_1, F_2, F_3, \dots, F_n$ . Then the mean arithmetic value of content of <sup>a</sup> given ~~XXXXXXXXXX~~ <sup>structural</sup> component equals

$$\bar{F} = \frac{F_1 + F_2 + F_3 + \dots + F_n}{n} \quad (15.1)$$

The mean ~~quadratic~~ <sup>square</sup> deviation of results of analysis, which constitutes the initial value for computing the error of determination, is conveniently computed on the basis of the equation:

$$\sigma' \{F\} = \sqrt{\bar{F}^2 - (\bar{F})^2}, \quad (15.2)$$

where the ~~value~~ <sup>quantity</sup>  $\bar{F}^2$  constitutes the ~~mean arithmetic~~ <sup>mean square</sup> of results of individual analyses, i.e.

$$\bar{F}^2 = \frac{F_1^2 + F_2^2 + F_3^2 + \dots + F_n^2}{n} \quad (15.3)$$

The mean ~~quadratic~~ <sup>-square</sup> deviation computed according to eq. (15.2) depends upon the number of independent determinations conducted for obtaining the mean values of the

quantities for  
~~symbols~~ F and F<sup>2</sup>. In order to get a corrected value ~~(XX)~~ σ{F}, not depending  
 the number of  
 upon ~~quantity~~ of determinations, the result obtained from eq.(15.2) needs to  
 be multiplied by a coefficient.

$$\sqrt{\frac{n}{n-1}} \quad (15.4)$$

Let us examine now, as an example, the data of 30 independent determinations  
 adduced in Table 11. From these data, it follows that

$$\bar{F} = 18,93\% \text{ and } \bar{F}^2 = 380,93.$$

Therefore, computing according to eq.(15.2) the value of ~~mean quadratic~~ the mean-square  
 deviation, we get:

$$\sigma' \{F\} = \sqrt{380,93 - (18,93)^2} = 5,04\%.$$

In order to obtain the corrected value of ~~mean quadratic~~ the mean-square  
 deviation, we multiply  
 the obtained value ~~XXX~~ by the coefficient, computed on the basis of eq.(15.4), in  
 which n equals 30, i.e. according to the number of independent determinations:

$$\sigma \{F\} = 5,04 \sqrt{\frac{30}{30-1}} = 5,13\%.$$

The last value (5.13%) is final and sufficient for computing the possible error of  
 analysis, ~~being~~ conducted under the given actual conditions (structure, length of  
 intersecting lines).

According to the theory of probability, no more than half the results of  
~~XXX~~ independent analysis can ~~XX~~ deviated from the true value by a value greater than  
 0.6745 of the mean ~~quadratic~~ <sup>-square</sup> deviation, in one direction or another. In our case,  
 the lower limit will equal 18.93 - (0.6745 × 5.13) = 15.47%, while the upper limit  
 will be 18.93 + (0.6745 × 5.13) = 22.39% of pearlite. In actuality, from the data

of the second column in Table 2, it follows that out of 30 analyses, within the computed limits there fall the results of 15 analyses, and the remaining 15 go beyond these limits.

It is practically impossible ~~THEXXXXXXXXXXXXXXXXXXXXXX~~ to get results of analysis with the tripled mean-  
*square*  
quadratic deviation. In our case, this corresponds to the limits from  
 $18.93 - (3 \times 5.13) = 3.54\%$  up to ~~18.93~~  $18.93 + (3 \times 5.13) = 34.32\%$  of pearlite. In the second column of Table 12, there actually are no results going beyond the limits found.

In the first case, the reliability of results of analysis is characterized by a probability of 0.5 or 50%; this means that, of the large number of independent analyses, not less than 50% of their results fall within the computational limits. In the first case, reliability equals 1 or 100% (more precisely, 0.9973 or 99.73%); hence, the results of all analyses practically fall within the computational limits.

The theory of probability *correlates* connects the value of deviation of ~~result~~ *the* analysis *results* from the true value of the unknown (i.e. absolute error of analysis), the reliability of obtaining the error, not exceeding the caused error, and the value of mean-*square*  
~~quadratic~~ deviation:

$$\Delta = t \sigma \{F\}, \quad (15.5)$$

where  $\Delta$  is the absolute error of analysis in percents of area of cut or volume of alloy;

$t$  is the standardized deviation, clearly connected with the probability or reliability of expected error  $P$ ;

$\sigma\{F\}$  is the mean *square*  
~~quadratic~~ deviation.

In its turn, the value of standardized deviation  $t$  is connected with the

probability or reliability of result of determination P by the following

dependence:

$$P = \sqrt{\frac{2}{\pi}} \int_0^t e^{-\frac{t^2}{2}} \cdot dt. \quad (15.6)$$

Since the integral in (15.6) is not chosen, we adduce in Table 12 the values of probability P for various values of standardized deviation t and vice versa.

It follows from eq.(15.5) and Table 12 that, for the actual case, being examined by us, of determining the amount of pearlite, the absolute error of determination, at ~~its~~ reliability ~~being~~ fixed by the probability 0.5 or 50%, equals

$$\Delta = 0,6745 \cdot 5,13 = 3,46\%$$

of pearlite. This signifies that ~~from~~ <sup>of</sup> the results of a large number of independent analyses conducted under identical conditions, not less than 50% of all results will have an absolute error not exceeding 3.46% of area of cut or volume of alloy. Such an error, characterized by the reliability of 0.5 or 50%, is called the probable error and comprises the chief characteristic of accuracy of analysis.

Table 12

t	P	t	P	P	t
0,10	0,0796	1,40	0,8384	0,50	0,6745
0,20	0,1586	1,50	0,8664	0,60	0,8416
0,30	0,2358	1,60	0,8904	0,70	1,0364
0,40	0,3108	1,70	0,9108	0,80	1,2816
0,50	0,3830	1,80	0,9282	0,90	1,6449
0,60	0,4514	1,90	0,9426	0,95	1,9600
0,70	0,5160	2,00	0,9544	0,98	2,3263
0,80	0,5762	2,20	0,9722	0,99	2,5758
0,90	0,6318	2,40	0,9836	0,998	3,0902
1,00	0,6826	2,60	0,9906		
1,10	0,7286	2,80	0,9948		
1,20	0,7698	3,00	0,9973		
1,30	0,8064	4,00	0,999936		

If we, not changing the conditions of conducting the analysis of the given structure, pose more rigorous ~~requirements~~ requirements for the reliability of the results being obtained, assuming for instance a reliability P, not equaling 0.5 but 0.7, the absolute error of determination increases to

$$\Delta = 1,0364 \cdot 5,13 = 5,32\%$$

of pearlite. Hence, increasing the value P, it is necessary to change at the same time the allowable absolute error (at the assigned conditions of analysis).

Taking into account the requirements posed for results of analysis, ~~we~~ we should regulate its precision, being determined by the value of acceptable absolute error and by the reliability of assuring it. However, being affected at the same time by fixed standards of value for  $\Delta$  and P, we by the same token predetermine the necessity of obtaining a fully concrete value of mean quadratic deviation, as this follows from eq.(15.5). This last value depends upon the conditions of analysis, i.e. upon the ~~nature~~ nature of the structure being analyzed, upon the length and position of the ~~intersecting lines~~ secants. Therefore it appears ~~MX~~ necessary to establish a dependence between conditions of analysis and value of mean ~~quadratic~~ quadratic deviation being derived under these conditions; however the absence of geometric validity of contours of structure does not permit one to do this theoretically. Therefore we will strive to establish it empirically.

~~THESE ARE THE RESULTS OF THE ANALYSIS OF THE STRUCTURE OF THE~~ According to A.A.Clagolev, ~~THESE ARE THE RESULTS OF THE ANALYSIS OF THE STRUCTURE OF THE~~ the error of linear analysis, and hence also the value of mean ~~quadratic~~ <sup>-square</sup> quadratic deviation of results of a number of repeated analyses from the actual content of <sup>a)</sup> given structural component are determined in a well-defined manner by the number of individual segments measured in the process of analysis (Bibl.50). Data of a series of analyses of various structures indicated,

however, that the mean ~~quadratic~~<sup>-square</sup> deviation depends both upon the content of the component being analyzed in the alloy as well as upon the nature of the structure.

The value of mean ~~quadratic~~<sup>-square</sup> deviation is inversely proportional to the square root ~~from~~<sup>of</sup> a number of observations or measurements. As stated above, in our case a unit of measurement is a separate segment obtained at ~~the~~<sup>the</sup> intersection of a microparticle by ~~XXXXXXXXXXXXXXXXXXXX~~<sup>a secant</sup>. Therefore we verified the dependence between the number of segments measured during determination of content of ~~a~~<sup>a</sup> given structural component, and the value of mean ~~quadratic~~<sup>-square</sup> deviation. For each cut, by the stationary microsection method (with ~~use~~<sup>the</sup> of an ocular-micrometer), we conducted a series of identification of the same structural component. In each series, a different number of segments was obtained for each determination. This was achieved either by the use of various magnifications (by changing the lens), or by a calculation with the same magnification but ~~XXX~~<sup>at</sup> a different length~~s~~<sup>the</sup> of calibrated part of the eyepiece. Typical dependences between the number of measured ~~XXXXXXXXXX~~<sup>the</sup> segments and the value obtained for mean ~~quadratic~~<sup>-square</sup> deviation, shown in Fig.40, reliably confirm that for each given structure there exists a dependence of the type

$$\sigma \{F\} = \frac{A}{\sqrt{z}}, \quad (15.7)$$

where z is the quantity of individual segments measured in the process of each independent determination.

The number of segments is directly proportional to the length of ~~XXXXXXXXXX~~<sup>lines</sup> secants, ~~lines~~ on which the measurements were conducted. Therefore it is clear that the effect of the length of secant upon the value  $\sigma\{F\}$  is taken into account by the

denominator of eq.(15.7), while its numerator depends only upon the nature of structure and the location of the ~~XXXXXXXXXXXX~~ secants. The direction of the secants does not play a part unless the structure is ~~XXXX~~ isotropic, i.e., if its nature does not depend upon the direction, (even if only in the plane of the cut).

From the curves, similar to those shown in Fig.40, we obtain the following values for numerator A of eq.(15.7) for diverse structures and structural components:

$$A = \sqrt{z} \sigma \{F\}$$

Graphite of gray iron, lamellae slightly <del>XXXX</del> bent, distributed unevenly, isolated one from the other. Content of graphite equals 5.8% by volume (line 1 in Fig.40) . . . . .	14.5
Ferrite, forming a network about <del>XXXXXXXXXX</del> equiaxial grains of <del>XXX</del> pearlite. Content of ferrite, 16.1% . . . . .	22.1
$\beta$ -phase in transverse cut of rod of two-phase brass having an equiaxial <del>XXXXXXXXXX</del> structure. Content of $\beta$ -phase, 21.0% . . . . .	29.7
Pearlite component in transverse cut of rod of pre-eutectoid annealed steel having <del>XXXXXXXXXX</del> equiaxial structure . Pearlite content, <del>XXXX</del> 28.7% . . . . .	28.9
Ferrite, forming a broken network with traces of Widmanstaetten structure in cross cut of rod of pre-eutectoid steel. Ferrite content, <del>equals</del> 32.8% (line 2 in Fig.40) . . . . .	32.8
Pearlite component in cross cut of rod of pre-eutectoid steel having <del>XXXXXXXXXX</del> equiaxial structure. Pearlite content, 35.8% . . . . .	29.2
Martensite component in troostite-martensite structure of <del>XXXXXX</del> tempered steel. Content of martensite component, 40.5% . . . . .	31.9

Analyzing the results obtained, one can note that the product  $\sqrt{z} \cdot \sigma \{F\} = A$  depends upon the content of the structural component being analyzed in the alloy. With an increase in this content (within the limits investigated), the value of A increases rapidly at first and then slowly.

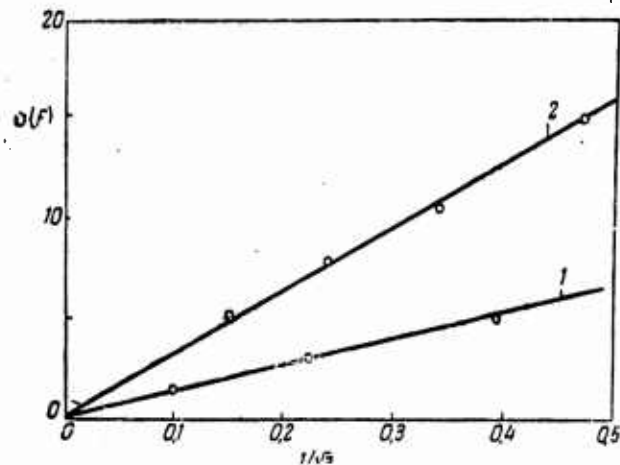


Fig.4.0 - Dependence of Value of Mean ~~Quadratic~~ <sup>- Square</sup> Deviation  $\sigma\{F\}$  upon Number Z of Segments Measured

In the two-phase structures, the number of segments of a secant falling on each of the structural components is evidently uniform. By ~~the~~ simple substitution of the value  $(100 - F)$  instead of F in equations (15.1), (15.3), and (15.2), it can be shown that such a substitution does not affect the result of computing the mean ~~quadratic~~ <sup>- square</sup> deviation. Thence it ~~XXX~~ follows that the values for A, found for two-phase structures, are actual for both structural components, in spite of their different content ~~in~~ <sup>the</sup> structure. For instance, the uniform value of the product  $\sqrt{Z} \cdot \sigma\{F\}$ , equaling 14.5, is obtained both for ~~the~~ <sup>a</sup> content of 5.8% (graphite) as well as for ~~the~~ <sup>a</sup> content supplementing this value by 100%, i.e. for 94.2% (metallic base of iron), etc.

Hence, the numerator A of eq.(15.7) should ~~XXXXXX~~ <sup>include</sup> a factor, depending upon the content of the component F being analyzed and ~~XXX~~ having identical values at ~~the~~ substitution in it both of the value F as well as  $(100 - F)$ . The appearance of this factor is as follows:

$$\sqrt{F(100 - F)}, \quad (15.8)$$

Transforming in the appropriate manner the earlier obtained dependence (15.7),

we get a formula permitting us to find the value of mean <sup>-square</sup> quadratic deviation by a calculational method:

$$\sigma(F) = K \frac{\sqrt{F(10 - F)}}{\sqrt{z}} \quad (15.9)$$

Substituting the data of seven different analyses into eq.(15.9), we can observe that K is constant. It turns out that this factor for the investigated structures changes within relatively narrow limits, namely from 0.60 to 0.73. The mean value of the coefficient for structures, the nature of which is independent ~~the~~ of direction of secants on the plane of the cut, is fixed by the value 0.65. In Fig.41, we show the dependence between the content of structural component being analyzed in alloy F, and value of the product  $\sqrt{z} \cdot \sigma(F)$ , constructed on basis of ~~the~~ experimental data presented above. The curve presented in Fig.41 corresponds to eq.(15.9), in which the factor of proportionality is assumed to equal 0.65. The dependence obtained confirms the adequate reliability of eq.(15.9), and the possibility of its use for computing the value of the expected mean <sup>-square</sup> quadratic deviation.

In those cases when the structure has a definite orientation, the direction of secants affects the value of factor K. By <sup>the</sup> linear method, we determined the pearlite content in soft steel, the structure of which on a lengthwise cut had a sharply striation. manifested ~~hand-drawn~~ In one series of determinations, the secants were located

~~perpendicular to direction of bands~~ <sup>the</sup> perpendicular to direction of <sup>the striation</sup> bands, and in the second, parallel to it.

It turned out that in both cases, there was derived a distinct dependence between the number of segments, at single determination, and value of mean <sup>the -square</sup> quadratic deviation, similar to that shown in Fig.40. However, ~~in~~ <sup>in</sup> the first case the product  $\sqrt{z} \cdot \sigma(F)$

proved to equal 13.2, while in the second it was considerably greater, namely 32.9. The pearlite content in the structure was found to equal 17.8% and 18.3% respectively. The substitution of the obtained values into eq.(15.9) permits

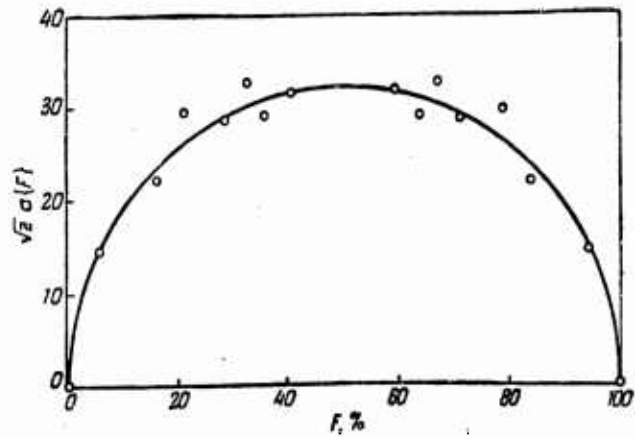


Fig.41 - Dependence between Content F of Component Being Analyzed and Value of the Product

$$\sqrt{z \cdot \sigma(F)}$$

in the case of striation, one to establish that ~~the~~ secants, parallel to the ~~direction of striation~~, the factor K it is equals 0.85, while at perpendicular ones, 0.34 in all.

Hence, in a determination of the content of structural component by linear method in striated structures, the ~~secants~~ secants need to be arranged perpendicularly to the direction of striation. Therein, measuring an even number of segments, we get a considerably smaller error than at random orientation of secants, and much less than at their arrangement parallel to the direction of lamination.

It is noteworthy that in addition to the examined factors, ~~the~~ the value of factor K of eq.(15.9), ~~is affected by~~ <sup>is affected by</sup> the uniformity of distribution of component being analyzed according to field of microsection. The method of objective ~~quantitative~~ quantitative estimation of uniformity of structure has not yet been proposed, therefore we are deprived of the chance to take this factor into consideration in eq.(15.9).

However, it is worth mentioning that in the most unfavorable case, the maximum value of <sup>the</sup> factor K does not exceed 1. In an analysis of any structure, the network of secants should evenly cover the entire surface of the cut. If the ~~structure~~ <sup>structure</sup> is irregular, the fulfillment of this requirement is especially important. It is quite evident that it is not difficult to measure the necessary number of segments for a small part of the area of the cut, especially if the structure is dispersed. However the result achieved thereby will not typify the cut as a whole, but only that part of it on which the secants were located.

Combining eqs.(15.5) and (15.9), we get a final equation for computing the value of absolute error of the linear method of analysis:

$$\Delta = Kt \sqrt{\frac{F(100 - F)}{z}} \quad (15.10)$$

The necessary number of segments are computed on the basis of the equation:

$$z = K^2 \left( \frac{t}{\Delta} \right)^2 F(100 - F) \quad (15.11)$$

Now we determine the error of analysis, being fulfilled by <sup>the</sup> linear method. Here two cases are possible, which we shall examine below: a) determination of error of analysis already conducted a posteriori and b) determination of number of segments which need to be measured for assuring the given accuracy of analysis.

We assume that in the process of an analysis already conducted, there was <sup>while</sup> measured a total of 500 segments, ~~at~~ the content of structural components was found to equal 32%. Substituting these values z and F into eq.(15.10) and setting the factor K equal to 1, we get:

$$\Delta = 2,08 t.$$

For computing the probable error of determination (P = 0.50 or 50%), we find in

Table 12 the corresponding value <sup>of</sup> ~~at~~ standard deviation t and we determine the

probable absolute error of analysis:

$$\Delta = 2,08 \cdot 0,6745 = 1,4\%$$

Hence the real content of <sup>the</sup> component being analyzed may differ from the value found by us (32%) by not more than 1.4%, with a reliability equaling 50%.

For a preliminary calculation of <sup>the</sup> required number of segments, it is first necessary to set a value of allowable absolute error  $\Delta$  and with <sup>a</sup> reliability of assurance  $P$ . Let us set up a probable error of determination ( $P = 0.50$  or 50%), not exceeding 1% of the area of the cut or the volume of the alloy. From Table 12, we find the corresponding value of ~~XXXXXXXXXX~~ standard deviation 0.6745. In addition, we need to know, even if only approximately, the unknown content of the structural component  $F$  being analyzed. Let us assume that this content, appraised visually, equals 20%. Substituting the listed values into eq.(15.11), and setting the factor  $K$  equal to 1, we get:

$$z = \left( \frac{0,6745}{1} \right)^2 \cdot 20 (100 - 20) = 728.$$

Having examined the cut in such fields of view or on secants of such total length <sup>b</sup> that the total number of segments amounts to 728, we get a result of analysis differing from the true content of <sup>a</sup> given structural component by not more than 1% in 50 cases out of 100. Let us now examine the remaining 50% of cases of analyses in which the error can ~~XXXX~~ surpass the computed value, namely 1%. Under <sup>the</sup> conditions of analysis selected by us, the value of mean <sup>-square</sup> quadratic deviation being determined by eq.(15.9) will equal (at  $K = 1$ ):

$$\sigma(F) = \sqrt{\frac{20(100 - 20)}{728}} = 1,48\%$$

Substituting this value in eq.(15.5), we get:

$$\Delta = 1,48t.$$

According to this dependence, one can compute the probability of obtaining errors exceeding 1%. Let us ~~XXXXXXXXXX~~ substitute instead of  $\Delta$ , in sequence, the numbers 1.5; 2.0; 3.0; 4.0 etc., and based on the obtained values of standard deviation  $t$ , we find from Table 12 the pertinent probabilities of such errors. It turns out that, if in 50 cases out of 100<sup>0</sup> the error does not exceed 1%, then in 68% of the cases it will be less than 1.5%, in 82% of the cases less than 2%, in 96% of the cases less than 3%, in 99% of the cases less than 4%, while ~~XXX~~ <sup>an</sup> error exceeding 4% is fairly improbable.

The example presented shows that although ~~XXX~~ at relatively high reliability of analysis, typified by the probability of 0.50, a large percentage<sup>n</sup> of tests can deviate from <sup>the</sup> computed value of absolute error, nevertheless the absolute value of error at these deviations will not ~~XX~~ reach inadmissibly great values. The probability of getting an error greater than that computed, quickly decreases with an increase in absolute value of <sup>the</sup> error. Therefore one ~~XXXX~~ should not attain an exceedingly high reliability of analysis. Subsequently in the majority of cases, we will evaluate the accuracy of analysis with the value of probable error.

To avoid calculations based on eq.(15.10) for obtaining <sup>the</sup> value of absolute error or <sup>that</sup> based on ~~XXXX~~ eq.(15.11) for determining the needed number of segments, we have compiled the reference <sup>T</sup>ables 13 - 16. The data of Tables 13 and 15 are intended for the reliability of the result of analysis, being determined with a probability of 0.50 or 50% (standard deviation 0.6745), while Tables 14 and 16 are for a considerably higher reliability, ~~XXXXXX~~ typified by the probability of 0.9544 or 95.44% (standard deviation 2.00). In the compilation of all <sup>T</sup>ables, we proceeded from the most unfavorable conditions of analysis, assuming the factor  $K$

TABLE XXXI  
Table 13

Probable Absolute Error of Determination at Linear and  
Point Analysis

a)	b)													
	1 99	2 98	3 97	4 96	5 95	10 90	15 85	20 80	25 75	30 70	35 65	40 60	45 55	50
10	2,10	2,96	3,60	4,14	4,60	6,33	7,53	8,44	9,13	9,65	10,05	10,31	10,48	10,52
20	1,48	2,08	2,54	2,92	3,25	4,47	5,32	5,96	6,46	6,83	7,11	7,30	7,41	7,45
50	0,94	1,32	1,61	1,85	2,06	2,83	3,36	3,77	4,08	4,32	4,49	4,61	4,69	4,71
100	0,65	0,93	1,14	1,31	1,45	2,00	2,38	2,67	2,89	3,06	3,18	3,27	3,32	3,33
200	0,47	0,66	0,80	0,92	1,03	1,41	1,68	1,88	2,04	2,16	2,25	2,31	2,34	2,36
300	0,38	0,54	0,66	0,75	0,84	1,15	1,37	1,54	1,67	1,76	1,83	1,88	1,91	1,92
400	0,33	0,47	0,57	0,65	0,73	1,00	1,19	1,33	1,44	1,53	1,59	1,63	1,66	1,67
500	0,30	0,42	0,51	0,58	0,65	0,89	1,06	1,19	1,29	1,36	1,42	1,46	1,48	1,49
600	0,27	0,38	0,46	0,53	0,59	0,82	0,97	1,09	1,18	1,25	1,30	1,33	1,35	1,36
700	0,25	0,35	0,43	0,49	0,55	0,76	0,90	1,01	1,09	1,15	1,20	1,23	1,25	1,26
800	0,23	0,33	0,40	0,46	0,51	0,71	0,84	0,94	1,02	1,08	1,12	1,15	1,17	1,18
900	0,22	0,31	0,38	0,44	0,48	0,67	0,79	0,89	0,96	1,02	1,06	1,09	1,11	1,11
1000	0,21	0,30	0,36	0,41	0,46	0,63	0,75	0,81	0,91	0,97	1,00	1,03	1,05	1,05
2000	0,15	0,21	0,25	0,29	0,32	0,45	0,53	0,60	0,65	0,68	0,71	0,73	0,74	0,74
3000	0,12	0,17	0,21	0,24	0,27	0,37	0,43	0,49	0,53	0,56	0,58	0,60	0,61	0,61
4000	0,10	0,15	0,18	0,21	0,23	0,32	0,38	0,42	0,46	0,48	0,50	0,52	0,52	0,53
5000	0,09	0,13	0,16	0,18	0,21	0,28	0,34	0,38	0,41	0,43	0,45	0,46	0,47	0,47
10000	0,07	0,09	0,11	0,13	0,15	0,20	0,24	0,27	0,29	0,31	0,32	0,33	0,33	0,33
15000	0,05	0,08	0,09	0,11	0,12	0,16	0,19	0,22	0,24	0,25	0,26	0,27	0,27	0,27
20000	0,05	0,07	0,08	0,09	0,10	0,14	0,17	0,19	0,20	0,22	0,22	0,23	0,23	0,24
25000	0,04	0,06	0,07	0,08	0,09	0,13	0,15	0,17	0,18	0,19	0,20	0,21	0,21	0,21
30000	0,04	0,05	0,07	0,08	0,08	0,12	0,14	0,15	0,17	0,18	0,18	0,19	0,19	0,19
40000	0,03	0,05	0,06	0,07	0,07	0,10	0,12	0,13	0,14	0,15	0,16	0,16	0,17	0,17
50000	0,03	0,04	0,05	0,06	0,06	0,09	0,11	0,12	0,13	0,14	0,14	0,15	0,15	0,15
100000	0,02	0,03	0,04	0,04	0,05	0,06	0,08	0,08	0,09	0,10	0,10	0,10	0,10	0,11

a) Number of points (of segments); b) Content of phase F, %

of eqs.(15.10) and (15.11) as equal to 1. However even in this case, a uniform distribution of secants over the entire area of the cut was mandatory.

If the analysis has already been conducted and it is required to establish its error a posteriori, we use Tables 13 and 14. According to the content, determined by analysis, of the examined structural component F and according to the number of segments measured in the process of analysis, we find from Table 13 the probable absolute error of determination. According to the same initial data, we find from Table 14 the value of absolute error which ~~was~~ not exceeded in ~~95~~ 95 cases of analysis out of 100.

If it is required that we conduct an analysis, the probable absolute error

Table 14

Absolute Error of Determination during Linear and Point

Analysis with  $\Delta$  Probability of 0.9544

a)	b)														
	0 100	1 99	2 98	3 97	4 96	5 95	10 90	15 85	20 80	25 75	30 70	35 65	40 60	45 55	50
50	—	—	—	—	—	—	—	—	—	—	—	—	13,83	14,07	14,13
100	—	—	—	—	—	—	—	7,14	8,00	8,67	9,18	9,54	9,81	9,96	10,00
200	—	—	—	—	—	—	4,23	5,04	5,64	6,12	6,48	6,75	6,93	7,02	7,08
300	—	—	—	—	—	2,52	3,45	4,11	4,62	5,00	5,28	5,49	5,64	5,73	5,76
400	—	—	—	—	1,95	2,19	3,00	3,57	4,00	4,32	4,59	4,77	4,89	4,98	5,00
500	—	—	—	1,53	1,74	1,95	2,67	3,18	3,57	3,87	4,08	4,26	4,38	4,44	4,47
600	—	—	1,14	1,38	1,59	1,77	2,46	2,91	3,27	3,54	3,75	3,90	4,00	4,05	4,08
700	—	—	1,05	1,29	1,47	1,65	2,28	2,70	3,03	3,27	3,45	3,60	3,69	3,75	3,78
800	—	—	1,00	1,20	1,38	1,53	2,13	2,52	2,82	3,06	3,24	3,36	3,45	3,51	3,54
900	—	—	0,93	1,14	1,32	1,44	2,00	2,37	2,67	2,88	3,06	3,18	3,27	3,33	3,33
1000	—	—	0,90	1,08	1,23	1,38	1,89	2,25	2,52	2,73	2,91	3,00	3,09	3,15	3,15
2000	—	0,45	0,63	0,75	0,87	0,96	1,35	1,59	1,80	1,95	2,04	2,13	2,19	2,22	2,22
3000	—	0,36	0,51	0,63	0,72	0,81	1,11	1,29	1,47	1,59	1,68	1,74	1,80	1,83	1,83
4000	—	0,30	0,45	0,54	0,63	0,69	0,96	1,14	1,26	1,38	1,44	1,50	1,56	1,56	1,59
5000	—	0,27	0,39	0,48	0,54	0,63	0,84	1,02	1,14	1,23	1,29	1,35	1,38	1,41	1,41
10000	—	0,21	0,27	0,33	0,39	0,45	0,60	0,72	0,81	0,87	0,93	0,96	0,99	1,00	1,00
15000	—	0,15	0,24	0,27	0,33	0,36	0,48	0,57	0,66	0,72	0,75	0,78	0,80	0,81	0,81
20000	—	0,15	0,21	0,24	0,27	0,30	0,42	0,51	0,57	0,60	0,66	0,66	0,69	0,69	0,72
25000	—	0,12	0,18	0,21	0,24	0,27	0,39	0,45	0,51	0,54	0,57	0,60	0,63	0,63	0,63
30000	—	0,12	0,15	0,21	0,24	0,24	0,36	0,42	0,45	0,51	0,54	0,54	0,57	0,57	0,57
40000	—	0,09	0,15	0,18	0,21	0,21	0,30	0,36	0,39	0,42	0,45	0,48	0,48	0,51	0,51
50000	—	0,09	0,12	0,15	0,18	0,18	0,27	0,33	0,36	0,39	0,42	0,42	0,45	0,45	0,45
100000	—	0,06	0,09	0,12	0,12	0,15	0,18	0,24	0,24	0,27	0,30	0,30	0,30	0,31	0,33

a) Number of points ( $\Delta$  segments); b) Content of phase F, %

of which should not exceed the earlier ~~value~~ value  $\Delta$ , then based on this value and the approximate content of <sup>the</sup> component F being analyzed (appraised visually), we find from Table 15 the appropriate number of segments which need to be measured.

If it is required that we assure the obtainment of a fixed value of error  $\Delta$  with a higher degree of reliability than the probable error, we can use the data in Table 16.

If the result of analysis differs substantially from that value which we estimated visually, determining the necessary number of segments, we should make the appropriate correction, taking into account more reliable data obtained as a result of analysis.

Table 15  
 Minimum Number of Points or Segments Needed for Obtaining Probable  
 Error Not Exceeding  $\Delta$ , during Point and Linear Analysis

a)	b)													
	1 99	2 98	3 97	4 96	5 95	10 90	15 85	20 80	25 75	30 70	35 65	40 60	45 55	50
0,1	4400	8700	12932	17065	21109	59936	56661	71104	83325	93324	101101	106636	109989	111111
0,2	—	2178	3233	4266	5277	10000	14165	17776	20831	23331	25275	26664	27497	27775
0,3	—	968	1438	1897	2347	4446	6299	7904	9263	10374	11239	11856	12222	12350
0,4	—	—	809	1068	1321	2592	3545	4448	5213	5838	6325	6672	6881	6950
0,5	—	—	518	694	846	1612	2270	2848	3338	3738	4050	4282	4406	4450
1	—	—	—	—	—	400	567	711	833	933	1011	1067	1100	1111
2	—	—	—	—	—	—	142	178	208	233	253	267	278	278
3	—	—	—	—	—	—	—	79	93	104	112	119	122	124
4	—	—	—	—	—	—	—	—	—	58	63	67	69	70

a) Absolute error  $\Delta$ , %; Content of phase F, %

In the calculation of  
 Tables 13 - 16, the factor K  
 was assumed to equal 1.  
 Analyzing the structures, the  
 nature of which does not  
 depend upon the direction  
 (in the plane of cut), we get  
 a factor K which is always less  
 than unity. ~~The~~ <sup>This</sup> mean value can  
 be assumed to equal 0.65, as  
 follows from the earlier  
 presented test data. Equation  
 (15.11) indicates that the  
 required number of segments  
 is proportional to the square  
 of the factor K. ~~TKMK~~ Therefore,  
 the number of segments which  
 is determined based on tabular  
 data can almost always be  
 considerably decreased by  
 multiplying it times the  
 square of the factor K, that  
 is by 0.42, if only the

Table 16  
 Minimum Number of Points or Segments during Point and Linear Analysis Necessary  
 for Obtaining an Error not Greater Than  $\Delta$ , with Probability of 0.9544

a)	b)														
	1 99	2 98	3 97	4 96	5 95	10 90	15 85	20 80	25 75	30 70	35 65	40 60	45 55	50	
0,1	39600	78400	116400	—	—	—	—	—	—	—	—	—	—	—	
0,2	9900	19600	29100	38400	47500	90000	127500	—	—	—	—	—	—	—	
0,3	4400	8711	12933	17064	21111	40000	56666	71111	83333	93333	101111	—	—	—	
0,4	2475	4900	7275	9600	11875	22500	31875	40000	46875	52500	56875	60000	61875	62500	
0,5	1584	3136	4656	6144	7600	14400	20400	25600	30000	33600	36400	38400	39600	40000	
1	—	784	1164	1536	1900	3600	5100	6400	7500	8400	9100	9600	9900	100 00	
2	—	—	—	384	475	900	1275	1600	1875	2100	2275	2400	2475	2500	
3	—	—	—	—	—	400	567	711	833	933	1011	1067	1100	1111	
4	—	—	—	—	—	225	319	400	469	525	569	600	619	625	
5	—	—	—	—	—	144	204	256	300	336	364	384	396	400	
6	—	—	—	—	—	—	142	178	208	233	253	267	275	278	
7	—	—	—	—	—	—	104	131	153	172	186	196	202	204	
8	—	—	—	—	—	—	—	100	117	130	142	152	155	156	
9	—	—	—	—	—	—	—	79	93	104	112	118	122	124	
10	—	—	—	—	—	—	—	—	75	84	91	96	99	100	

a) Absolute error  $\Delta$ , %; b) Content of phase F, %

structure is isotropic (isometric) and uniform. If the structure is banded, and the ~~XXXXXXXX~~ secants are located perpendicularly to the direction of the striation, the required number of segments then decreases still more. In this case, the value of the factor K can be assumed to equal 0.4 and hence the necessary number of segments found from the tables can be multiplied by 0.16. For instance, if at ~~the~~ content of analyzed component ~~equaling~~ 20%, and ~~a~~ probable error not surpassing 1%, we are required to measure 711 segments (see Table 13), in ~~the~~ case of banded arrangement of the component being analyzed and with secants directed perpendicularly to the striation, then for getting the same accuracy of analysis, it is sufficient to measure a total of  $711 \times 0.4^2 = 114$  segments, namely six times less.

If the objects of analysis are at the same time several components, in an analysis on the same length of secants, then the error of determination of each of the components will differ, since their content in the alloy, dimensions and form of microparticles are different. Therefore the calculation of error needs to be made for each of the structural components separately.

~~XXXX~~ The linear method of determining the structural or phase composition of an alloy, owing to the possibility of using various devices, especially integrators, is very effective both in accuracy and in speed. It is especially effective in the analysis of structural components having a banded arrangement, since here we are required to measure the minimum number of segments to get sufficient accuracy. In particular, it is feasible to determine by such a method the very small amounts of structural components, having a linear orientation (for instance, content of extended nonmetallic inclusions in a lengthwise cut), by the method of stationary microsection. We should recall that in the use of lengthwise cuts, the mean

suspended volumetric content of phase should be computed on the basis of eq.(11.3) (see Section 11).

For analysis of the metallic structures, it is convenient to use the linear method. Determining by this method the structural composition, it is easy to compute (with the measurement and summation of lengths of segments) the number of segments, especially since this is necessary also for a determination of accuracy of the analysis conducted. This number of segments, referred to a unit ~~of~~ length of secants, along which they were measured, provides the possibility of determining the second most important parameter of spatial structure of <sup>an</sup> alloy, namely the  $\Sigma X$  value of specific surface of the structural component under analysis.

In an electric ~~XXXXXXXXXX~~ integrating instrument, the diagram of which is shown in Fig.38, the number of segments is not computed; however, this can easily be done by modifying the system slightly. Such a type of device was proposed by A.A.Glagolev in one of the designs of the integrators developed by him (Bibl.50).

In conclusion, we present an example of incorrect use of linear analysis. Determining the content of ~~XXXXXXXXXXXXXXXXXX~~ carbides of chromium, niobium, and tantalum in various alloys by the linear method and striving for exceedingly high accuracy of determination, namely 0.01%, J.R.Lane and M.J.Grant could not detect changes in structure in the process of ~~XXX~~ aging of alloys (Bibl.78). Actually, if we assume the probable error as equaling 0.01%, at content of about 5% of the given type of carbides, we are then required to measure more than two million segments. Naturally, this could not be done, although the ~~XXXXXXXXXX~~ process of linear analysis, according to the testimony of authors, lasts for several days. It is quite evident that it is necessary to reckon with the possibilities ~~XXX~~ of each type of analysis. The data presented in this paragraph permit one to compute in



of the sectors, then using the same law of proportionality, we can determine the areas of sectors. This proposition forms the basis of the point counting method.

From the theory of probability it is known that if we draw a point at random in the area G, the probability of the occurrence of the point in any part of this area is proportional to the size of this part (length, area, etc.) and does <sup>not</sup> depend upon its location and shape (Bibl.101). Therefore, if the area is a plane, the area of which equals G, the probability of placing at random a sketched point on the part of the surface, the area of which equals g, will equal

$$p = \frac{g}{G}$$

wherein this probability is ~~XXX~~ independent of the shape and ~~XXXXXX~~ location of the part of surface g. Specifically, this part can consist of a large number of individual sectors, the total area of which equals g.

on  
If ~~XX~~ the surface being considered we draw not one but a large number of points z, then ~~XX~~ sector g of the surface there will fall x points, wherein the number x tends towards the value pz and the ratio of values pz and x are all the closer to unity, the greater <sup>the</sup> number of points ~~that are~~ drawn on the surface. Therefore the part of area of sector g on the surface G will be ever ~~XXX~~ closer to the value  $\frac{g}{G} = \frac{x}{z}$ , the greater the value for z (and hence for x).

With reference to the quantitative microanalysis, the point counting method reduces to a jumplike movement of the cut in the field of view of the microscope, wherein ~~XX~~ in each new position of the cut, it is noted just which of the structural components is located in the point of <sup>the crossing</sup> ~~XXXXXXXXXX~~ of the eyepiece with the cross hairs. Let us assume that the structure under consideration contains three components, which we designate by A, B and C. If in the process of examining the cut in 1000

fields of view, the point of cross-hair (reticle) fell 204 times on component A, 33 times on component B and 708 times on C, the relative content of these components in the area of cut, and also in the volume of alloy then comprises in %:

A . . . . .	20.4
B . . . . .	8.8
C . . . . .	70.8
	<hr/>
	100.0

In the point analysis the points on the microsection can be arranged, by continually moving the cut by the same amount (for instance, by 0.2 mm) with the aid of slides mounted on the microscope stand. Having finished one series, we ~~may~~ move to a second parallel series, etc. As a result, the points prove to be located in the nodes of a quadratic or rectangular grid. In petrographic analysis, there is used the special ~~band~~<sup>stage</sup> developed by Glagolev, with the aid of which the cut is moved along a spiral line, by the same amount each time. The observance of ~~it~~ a fixed geometric regularity of placing the points is quite unnecessary, if the main requirement is fulfilled, namely uniformity of their distribution. However, this last requirement is assured most reliably at a regular arrangement of points over the entire field of the cut. The important advantage of the point counting method ~~XXXXX~~ consists in that <sup>it</sup> can be used without any kind of special equipment. Even in the use of the simplest method, the movement of the cut by hand and a recording of results, ~~XXXXX~~ one can conduct an analysis of structure in a total of only 30 - 40 min.

~~XXXX~~ The point counting method of analysis permits the mechanization of the process of moving the cut and the computation of points, which considerably simplifies and speeds up the analysis, at the same time increasing its ~~XXXX~~ precision. A device for point analysis, called a push integrator was proposed by Glagolev in several

variants, the first of which was developed in 1931 (Bibl.50). In simplest form, the push integrator is a recorder consisting of several mechanical counters of ordinary type. The counters count off the number of presses made on a key, each of which is intended for a fixed structural component. Simultaneously with pressing on any key, by means of a flexible lead (for instance the trigger from a camera), a jolt is given to the micrometer screw of the slides of the microscope ~~stand~~ <sup>stage</sup> or of a two-coordinate conveying tube, which displaced the cut into a new position.

At the start of analysis, all counters are zero-set. The observer working with the push integrator, observing the structure in the eyepiece, presses on that key which is dented for counting the number of points falling in the structural component, located at the given position of cut in the center of field of view (i.e. in the point of reticle of the eyepiece). During pressure, the microscope stand is moved into a new position ~~XXXX~~ and the observer again presses the key, corresponding to this new position, etc. In the process of the entire analysis, there is ~~XXX~~ no need to look away from the eyepiece, which has to be done many times in working without a push integrator and which has a bad effect upon vision. In certain models of the push integrator, there are special devices which automatically indicate the attainment of a fixed total number of points, set beforehand depending upon the required accuracy of analysis. After examining by the described sequence the entire area of cut, the number of pressures (recorded by the counters) on each of the keys are proportional to the content of the corresponding structural components in the alloy; therefore, the calculation of percentual composition of alloy requires no more than several minutes. Thus, the push integrator permits one to determine simultaneously the content of all structural components of the alloy, the number of which rarely surpasses 6, wherein

the duration of analysis in case of 1000 points reduces to 15 - 20 min, also including the calculation.

The point counting method is quite useable in the analysis of highly dispersed structures when the linear method of ~~XXX~~ analysis cannot be used as a result of ~~XX~~ very short lengths of the segments being obtained, which therefore cannot be measured with enough precision, even using maximum magnifications. In the work with the point counting method, high skill of <sup>the</sup> observer is not needed, since all the determination reduces to a ~~XXXXXXXXXXXXXXXXXXXX~~ recognition of the structural component in the point of cross-hair of the eyepiece and pressure on the ~~XXXXXX~~ appropriate key of the recorder. Therefore the point counting method of analysis should be given preference over other methods of determining the structural composition of alloys (with the exception of individual specific cases, which were discussed in Sections 13 and 15).

Glagolev's point counting method was ~~XXXX~~ recognized and widely used in the practice of petrographic analysis in the Soviet Union as well as abroad, although this was considerably delayed. For instance, in ~~XXXXXX~~ <sup>the USA</sup> the description of the Glagolev point counting method, with a reference to its early publications (1933 - 1934) was given only in 1949 by F.Chayes (Bibl.102). Basing on the experience of conducting around 300 analyses of microsections of rocks, Chayes gives a very high appraisal of the point counting method, although he was evidently unaware of the monograph published in 1941 by Glagolev (Bibl.50), describing improved devices and methods of analysis using the point counting method. Chayes remarks that the device for point analysis, which can easily be assembled from manufactured parts being used in microscope technology (mechanical ~~stage~~ <sup>stage</sup> for the microscope and counters of ~~the~~ conventional type), exceeds all other devices

intended for determining the structural composition, in economy, rapidity of analysis, and accuracy of results obtained. Comparing the speed of analysis in the point counting and linear methods of analysis, Chayes adduces the following data: duration of analysis ~~in case of the integrational method of Wentworth~~ when using the Wentworth integrating stage comprises 1 hr, in the electrical counter used by Hurlbut, the analysis is conducted in 30 min, while in the point counter (primitive construction) it takes but 15 min. Subsequently, conducting over 600 analyses of rocks by the point counting method, Chayes confirmed his initial estimation of this means of analysis (Bibl.103).

The accuracy and reliability of results of analysis conducted by the point counting method are determined in a well-defined manner (for the given structure) by the total number of points, computed in the process of analysis. In distinction from the linear method, where we use empirical ~~formulas~~ formulas, in case of the point analysis, the geometrical probability of the falling of a point in one or the other structural component is easily subjected to calculation. Therefore, basing on data of the probability theory and specifically the ~~Laplace~~ Laplace theorem, ~~we~~ one can determine computationally the conditions of analysis assuring the obtainment of an error not in excess of that assigned, with an earlier established reliability.

Let us assume that one of the structural components, the content of which we desire to identify, occupies on the cut  $F\%$  of ~~KK~~ its entire area, which is taken to equal 100%. If we take a sufficiently large number of points  $z$ , distributing them randomly but uniformly over the entire area of the cut, the probability of the occurrence of an individual point on the structural component of interest to us will equal  $p$ , wherein, as was stated above,

$$p = \frac{F}{100} .$$

The chance of ~~XXXX~~ the opposite occurrence, i.e. of the falling of a separate, randomly selected point on an area occupied by all the other structural components (other than ~~XXXX~~ that of interest to us), we ~~signify~~<sup>denote</sup> by  $q$ . Then obviously,

$$q = \frac{100 - F}{100}.$$

If we ~~signify~~<sup>denote</sup> the number of points (from the total number of points  $z$ ), which have fallen on the area of the cut, occupied by the measured structural component, by  $x$ , ~~XXXX~~ then the error of determination will equal

$$\delta = \frac{x}{z} - p,$$

while the absolute error of determination, expressed in percents of an area of cut,  $\Delta$  will be 100 times larger:

$$\Delta = 100\delta = 100 \frac{x}{z} - F.$$

The probability theory provides the following relationship between the value of error of determination  $\delta$ , the number of measurements for countings made during ~~the~~<sup>test</sup> (in the given case, the number of points)  $z$ , and the probabilities  $p$  and  $q$ :

$$\delta = t \sqrt{\frac{p q}{z}} \quad (16.1)$$

or substituting instead of  $\delta$ ,  $p$  and  $q$  their value is expressed in percentages of area of cut:

$$\Delta = t \sqrt{\frac{F(100 - F)}{z}} \quad (16.2)$$

The coefficient  $t$  entering ~~XXXX~~ eqs.(16.1) and (16.2) ~~is~~<sup>shows</sup> the same standard ~~an~~ deviation, which we mentioned above (see Section 15). It is

connected with the reliability of the obtained result of analysis by eq.(15.6),

and the appropriate numerical data are adduced in Table 12.

To determine the error of analysis  $\Delta$ , it is necessary to know <sup>the</sup> values  $F$  and  $z$  and to assign a definite reliability of result of determination  $P$ , according to which there is found the corresponding value of standard deviation  $t$  (from Table 12).

In the practice of quantitative microanalysis, ~~XX~~ two types are possible: ~~XXXXXXXX~~

a) *a posteriori* determination of error of already conducted analysis, when we already know the values listed above and b) preliminary calculation of conditions of analysis

(i.e. of required number of points), assuring the obtainment of an error not surpassing that assigned beforehand. In the latter case, the unknown content of the structural component  $F$  being analyzed is determined approximately in advance, visually, and after <sup>completion</sup> ~~conduct~~ of analysis, a refined calculation of error is conducted.

Let us assume that we have conducted by the point counting method an analysis of an alloy, wherein of the examined 1200 points, 452 fell in the assigned structural component, while 748 fell in all the remaining components of the structure. Hence the unknown content of the assigned component of the structure will equal (in percents of area of cut or volume of alloy):

$$F = \frac{452}{1200} 100 = 37,7\%$$

We find the error of determination according to eq.(16.2), having substituted in it the derived values:

$$\Delta = t \sqrt{\frac{37,7 \cdot (100 - 37,7)}{1200}} = 1,40\% \cdot t$$

Having assigned to the ~~XXXX~~ standard deviation  $t$  various values, corresponding to

fixed values of reliability of ~~XXXX~~ analytical results, we get actual values of certainty. error for each ~~reliability~~ <sup>certainty</sup>. For instance, if  $t = 0.6745$ , the ~~reliability~~ <sup>certainty</sup> of obtaining error, not surpassing the value

$$1,40 \cdot 0,6745 = 0,94\%$$

then equals 0.50 or 50% (see Table 12). In other words, in the conduct of a large number of independent analyses, according to 1200 points in each analysis, in 15% of the analyses the error does not surpass 0.94% of the area of the cut. The error obtained with ~~reliability~~ <sup>a certainty of</sup> 0.50 or 50% is called the probable error and its value ~~is~~ most often ~~XXXXXX~~ typifies the accuracy of determination being realized by this or another method.

If we assign a higher ~~reliability~~ <sup>certainty</sup>, equaling e.g. 0.99 or 99%, for which the standard deviation equals 2.5758, then only in one case out of 100 analyses (with 1200 points in each) can the absolute error somewhat ~~surpass~~ <sup>exceed</sup> the value

$$1,40 \cdot 2,5758 = 3,6\%$$

In the calculation of the minimum necessary number of points, in order to get the required accuracy of analysis, we use the formula obtained from eq.(16.2):

$$z = t^2 \frac{F(100 - F)}{\Delta^2} \quad (16.3)$$

To compute the number of points  $z$ , we assign in advance the values  $\Delta$  and  $t$ , proceeding from the purpose and importance of the analysis, while we determine  $F$  in first approximation visually. From eq.(16.3), it follows that the required number of points quickly increases with a ~~XXXX~~ decrease in the permissible absolute error of determination  $\Delta$  and with <sup>an</sup> increase in <sup>the</sup> reliability of result of analysis, being determined by <sup>the</sup> value of standard deviation  $t$ , ~~XXX~~ since these two values enter the formula in the second power.

Let us examine the above presented example when the content of ~~XXX~~ structural component being analyzed in the alloy equals 37.7%. The probable absolute error, exceeding 1% of area of volume of cut, may be obtained at number of points  $z$ , being determined by eq.(16.3):

$$z = (0,6745)^2 \frac{37,7 (100 - 37,7)}{(1,0)^2} = 1069.$$

Conducting a determination with the same reliability, but with a permissible error not surpassing 0.5% of volume of alloy, we get the necessary number of points exceeding the former by 4 times:

$$z = (0,6745)^2 \frac{37,7 (100 - 37,7)}{(0,5)^2} = 4276.$$

If at the same permissible error, we increase the reliability of result of analysis from 50% to 95% (at which the standard deviation  $t$  equals 1.9600), the number of points which need to be calculated will increase to

$$z = (1,9600)^2 \frac{37,7 (100 - 37,7)}{(0,5)^2} = 9023.$$

The numerator of the eq.(16.3) acquires maximum ~~XX~~ importance when the given structural component takes up exactly ~~1/2~~ half of the volume of <sup>the</sup> alloy and symmetrically decreases at <sup>a</sup> decrease of its content to zero or at <sup>an</sup> increase to 100%, as is evident from the data in Table 17. However, the required number of points, at small contents of the component being analyzed nevertheless increases, in spite of the corresponding decrease in the numerator, since the lower the content of assigned component in the alloy, the smaller should be the value of permissible absolute ~~XXXX~~ error  $\Delta$ , which enters the denominator of eq.(16.3) in squared form. Thus if, at <sup>a</sup> content of <sup>the</sup> given component equaling 50%, even in case of a high requirement for accuracy of analysis, an error of 0.5% of the volume is quite acceptable (relative

error equals 1%), then at <sup>a</sup> content of <sup>the</sup> component being analyzed equaling 0.5% of volume of alloy, the absolute error should be counted in hundredths of a percent of volume of <sup>the</sup> alloy. Accordingly there also increases the number of points required for obtaining such an accuracy.

Table 17

F, %	F (100-F)	F, %	F, %	F (100-F)	F, %
1	99	99	26	1924	74
2	196	98	27	1971	73
3	291	97	28	2016	72
4	384	96	29	2059	71
5	475	95	30	2100	70
6	564	94	31	2139	69
7	651	93	32	2176	68
8	736	92	33	2211	67
9	819	91	34	2244	66
10	900	90	35	2275	65
11	979	89	36	2304	64
12	1056	88	37	2331	63
13	1131	87	38	2356	62
14	1204	86	39	2379	61
15	1275	85	40	2400	60
16	1344	84	41	2419	59
17	1411	83	42	2436	58
18	1476	82	43	2451	57
19	1539	81	44	2464	56
20	1600	80	45	2475	55
21	1659	79	46	2484	54
22	1716	78	47	2491	53
23	1771	77	48	2496	52
24	1824	76	49	2499	51
25	1875	75	50	2500	50

For instance, if we conduct a determination of the component of structure occurring in a total of 0.5% by volume, while the value of absolute error should not surpass 0.025% (which ~~XXXX~~ corresponds to the relative error equaling 5%) at a probability of 50%, then the required accuracy is assured by calculating the following number of points:

$$z = (0,6745)^2 \frac{0,5(100 - 0,5)}{(0,025)^2} = 36214.$$

~~XXX~~ Practice indicates that in one minute, one can compute 75 - 100 points (Bibl.102). Hence for computing 36, 124 points, more than 6 hrs would be required,

i.e. ~~XXXXXXXXXX~~ practically an entire ~~work~~ working day.

In such cases, it is advantageous to use the ~~XXXXXXXXXX~~ "method of fields", proposed by Glagolev (Bibl.50). According to the method of fields, in one field of view there is examined not one point of crossing of the eyepiece with the cross-hair, but ~~XXXXXXXXXX~~ several hundred ~~XXXXXX~~ <sup>nodal</sup> points of the grid of the eyepiece. Moving the cut in the field of view of the microscope, at each new position of it there is computed the number of ~~XXXXXX~~ <sup>nodal</sup> points of the grid of the eyepiece, falling in the structural component being analyzed. For instance, in the determination of content of component, present in the alloy in the amount of 0.5% in all, let us use the square-grid eyepiece, shown in Fig.14 which has 289 ~~XXXXXXXXXX~~ nodal points (17 × 17). Conducting the calculation in about 125 fields of view, distributed evenly over the entire field of cut, we already get the required total number of points:

$$125 \cdot 289 = 36125.$$

This calculation may be done quite rapidly, since in all 125 fields of view, in the analyzed structural component, there fall ~~approximately~~ approximately

$$36125 \frac{0.5}{100} = 180 \text{ points}$$

which we also have to compute, and this takes up 10 - 15 min in all. Hence, the Glagolev method of fields permits one to expand considerably the area of efficient use of the point counting method for cases of low content of components of structure being analyzed. However, it must be kept in mind that in the use of the method ~~of~~ of fields, one gets a ~~XXXXXXXXXX~~ grouped, congested arrangement of points and hence the principle of uniform distribution of points over the entire area of the cut, placed at the basis of the conclusion of eq.(16.2), is disrupted. Therefore the accuracy of the method depends not only upon the total number of points,

but also upon fluctuation in content of <sup>the</sup> component being analyzed in various fields of view. As a result of this, the actual error will exceed the computational one to an ever greater degree, the more irregular the distribution of the analyzed component over the field of the cut.

If the content of structural component is less than 0.1% of the volume of alloy, the number of required points increases to such an extent, that even the use of ~~XX~~ the method of fields does not permit the attainment of a practically acceptable duration of microanalysis. In such a case, as noted above (see Sections 13 and 15), it is more feasible to use the planimetric or linear methods.

In order to avoid the need for calculations using eq.(16.3), one can use compiled reference tables. It is easy to see that eq.(16.3) for the point counting method is quite identical to eqs.(15.10) and (15.11) for the linear method, adduced in Section 15, under the condition that the factor K in the latter ones is equal to 1. Since Tables 13 - 16 were computed under the observance of this condition, they are ~~quite~~ quite applicable not only for the linear but also for the point counting method. In the latter case, the number of segments is equivalent to the number of points.

The above-presented calculations of error take into account the random errors of statistical analysis. In addition to these errors, there can occur a systematic error, caused by the fact that the point of crossing of the eyepiece with the cross-hairs and the nodal points of the square-grid eyepiece are not geometric points but have fixed, although small, dimensions. This systematic error is coupled with the random ~~error~~ error and as a result the total error of analysis may prove in certain cases to be quite considerable, as this was indicated by A.C.Spektor (Bibl.104). In Fig.42, we show systematically the effect of width of lines forming a ~~point~~ point

upon the obtainment of a systematic error. If the width of lines equals  $a$ , while the diameter of sections of microparticles, having a spherical form, which for simplicity we will assume of equal size, equals  $d$ , then the "point" partially or completely falls on all sections of microparticles, the centers of which prove to be located within the contour A (Fig.42,a). However, if the ~~XX~~ point is geometric, not having dimensions, it can fall only in those sections of microparticles, the centers of which prove to be located within the circumference with a diameter  $d$ , with a center in the point of the crossing (Fig.42,b). Hence, the actual "point" always will fall on the structural component being analyzed, in a greater number of cases than the ideal point. As ~~XXX~~ is evident, the error will be all the greater, the less the diameter of sections of microparticles  $d$  in comparison with the size of "point"  $a$ , i.e. the more dispersed the structural component being analyzed.

Spektor determined the content of nonmetallic ~~XXXXXXXXXX~~ inclusions in type ShKh15 steel in a ~~XXXXX~~ transverse microsection. The determination was made by the method of fields, wherein the total number of points comprised 1,770,000, of which 580 points fell in the nonmetallic inclusions. If we disregard

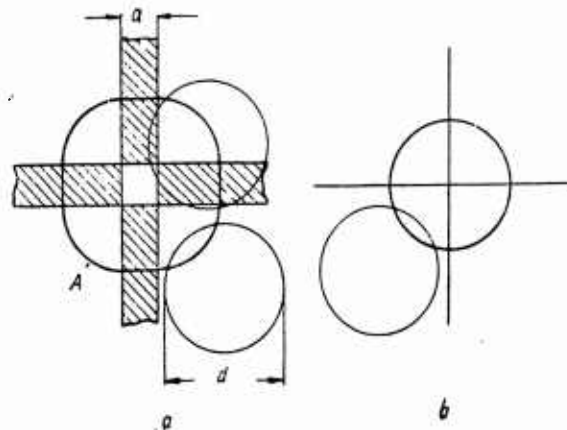


Fig.42 - Effect of Width of Lines Forming the Point of Cross-Hair of Eyepiece, during Point Counting Method of Analysis [after Spektor (Sibl.104)]

the dimensions of nodal "points" of the eyepiece grid, the volumetric content of nonmetallic inclusions in steel is determined by the figure

$$\frac{580}{1770000} 100 = 0,0328\%$$

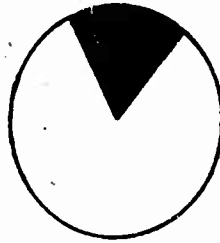


Fig.43 - Eyepiece Insert with Dark Sector Replacing the Eyepiece with Cross-Hairs, and Free of Systematic Error

~~The~~ width of projection of lines of the grid of eyepiece on the surface of the cut was found as equal to one micron, while the average dimension of sections of round nonmetallic ~~inclusions~~ <sup>inclusions</sup> was 4 microns. The calculation of content of nonmetallic

inclusions, conducted by Spektor with a correction, taking into account the effect of actual width of lines of the eyepiece grid, yielded a result almost <sup>twice as</sup> small as that obtained without correction, namely 0.0176%. A control analysis, conducted by the planimetric method, yielded a figure very close to the latter, that is 0.0174%. According to the ~~Spektor~~ Spektor data, one should never disregard the dimensions of the "point", even in the case when its cross section is 20 times less than the mean diameter of sections of microparticles (in the example considered, the cross section of the "point" is 4 times less than the mean diameter of inclusions in the cut).

In an analysis of the dispersed structure by the point method, we can use a correction coefficient, for calculation of which we need to know the width of lines forming the "point", the mean diameter of sections of microparticles and their number per unit ~~area~~ <sup>correction</sup> area of the cut. The method of computing this ~~coefficient~~ <sup>coefficient</sup> was developed by A.S. Spektor (Bibl.104); however, we do not present it here because it is fairly unwieldy and requires determination of a number of additional parameters of

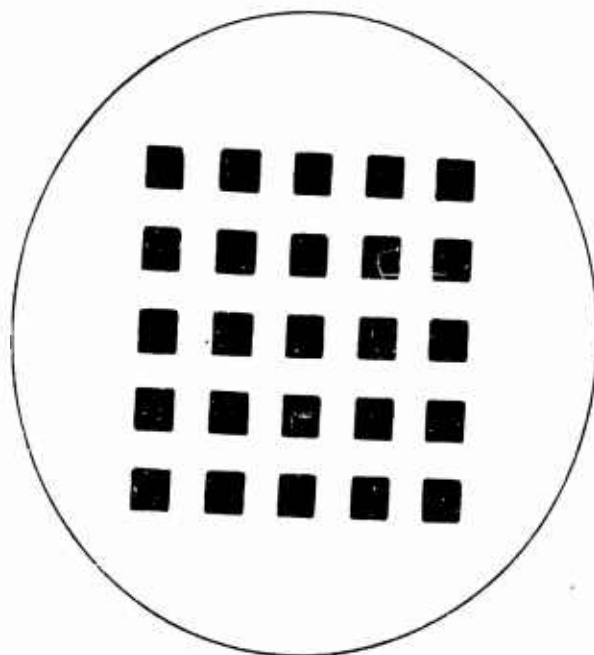


Fig.44 - Eyepiece Insert, Replacing the Square-Grid Eyepiece during Point Counting Analysis, Free of Systematic Error

microstructure ~~XXX~~ (~~the~~ average diameter of inclusions, and their quantity).

We show in Fig.43 an eyepiece insert with a dark sector. The point of the peak of this sector is a geometric point and therefore, using such an insert, one can be rid of systematic error. In Fig.44, we show another insert, containing a number of dark squares, replacing the square-grid eyepiece for purposes of point analysis by the method of fields. In the analysis, there is ~~XXXXX~~ identified the structural component, on which there falls each of the points of ~~points~~ <sup>vertices</sup> of the squares.

Section 17. Structural and Chemical Composition of Alloy

The ~~XXX~~ result of quantitative metallographic analysis conducted by planimetric, linear or the point counting method, is the complete or partial structural composition of alloy, expressed in percentages or fractions of area of ~~XXX~~ cut or of volume of alloy (which has the same meaning at proper choice of surface of cut). Frequently

it is feasible to convert the structural composition to chemical or vice versa; this permits not only a checking of results of both types of analysis by way of their comparison, but also develops additional data on the composition of individual phases and structural components.

In the formulas connecting the chemical and structural composition of the ~~XXX~~ alloy, ~~XXXX~~ mandatorily enter the values of specific weights of phases and structural components, and also of the alloy as a whole. Therefore a valuable supplement to the data of structural and chemical compositions of alloy is the amount of specific weight of the alloy itself. This value can be determined experimentally with high accuracy and is very simple methodologically.

The specific weight of individual phases and structural components of alloys ~~are~~<sup>is</sup> far from being known in every case. However if we have access to data both of structural and chemical composition of alloy, then we can determine by a computational method the specific weight of any phase and structural component, which it is not possible to differentiate in a pure form for the test determination of its specific weight.

Since in the future it is necessary to deal with a number of values, expressing the structural and chemical composition of alloy, the chemical composition and specific weight of individual phases and ~~XXXXXXXXXX~~ structural components, we introduce the following symbols:

1. Individual phases and ~~XXX~~ structural components of alloy . . . . . a, b, c
2. Content of ~~XXXX~~ phase or structural component in alloy,  
in percents of area of cut or volume of alloy . . . . .  $F_a, F_b, F_c$
3. Fraction of volume of alloy occupied by phase or structural  
component,  $\text{mm}^3/\text{mm}^3$  or  $\text{cm}^3/\text{cm}^3$  . . . . .  $\Sigma V_a, \Sigma V_b, \Sigma V_c$
4. Content of phase or structural component in alloy, in weight  
percentages . . . . .  $G_a, G_b, G_c$

5. Specific weight of individual phase or structural component,  $\gamma$   
 gm/cm<sup>3</sup> . . . . .  $\gamma_a, \gamma_b, \gamma_c$
6. Content in individual phase or in structural component of any  
 element (for instance, of carbon), in weight percentages . . . .  $G_a, G_b, G_c$

In the case of ~~XXXXXX~~ <sup>iron-</sup> ~~ferrite~~-carbon ~~alloys~~, the <sup>subscripts</sup> indexes a, b, c replace the indexes signifying the actual structural components of steels and irons: F (ferrite), P (pearlite), Ts (cementite), G (graphite), M (martensite), T (troostite), S (sorbite), etc. The content of ~~any~~ phase expressed in volumetric ~~percentages~~ percents,  $F_a$ , is equal to the fraction, magnified 100 ~~times~~, of volume of alloy being occupied by the same phase  $\sum V_a$ .

If we know the full structural composition of the alloy, the weight content of any of ~~its~~ structural components is then found according to the equation:

$$G_a = \frac{\gamma_a \sum V_a}{\gamma_a \sum V_a + \gamma_b \sum V_b + \gamma_c \sum V_c + \dots} 100\% \quad (17.1)$$

If the actual specific weight of the alloy itself is known, we can substitute its value in the denominator of the formula, since the denominator equals the specific weight of the alloy as a whole. This permits one to compute the weight content of any phase or ~~any~~ component of the structure of the alloy, if we know the volumetric content of the given ~~any~~ structural component and its specific weight.

The unknown specific weight of <sup>a</sup> structural component is easy to find based on the same formula, if we know its weight content  $G_a$ , the volumetric content  $\sum V_a$  and the actual specific weight of <sup>the</sup> alloy, comprising the denominator of ~~any~~ eq.(17.1). As an example, we determine the specific weight of <sup>the</sup> graphite component of six samples of gray and malleable iron, using the test data of G.I. Pogodir-Alekseyev (Bibl.105), adduced in Table 18. Samples 1 - 3 represent malleable iron with a ferrite or

pearlite base, while samples 4 - 6 refer to ~~XXXX~~ gray iron, of which the metallic base ~~XXXX~~ consists of pearlite or of pearlite combined with cementite. The volumetric content of graphite was determined by planimetry based on photomicrographs, determining the sectors of cuts with average graphite ~~XXXX~~ content for ~~XX~~ each sample, wherein the accuracy of determination was low. The weight content of graphite was determined by the difference between the content of total carbon and ~~banded~~ <sup>found</sup> carbon; these contents were presented by Pogodin-Alekseyev for all six samples.

Table 18

a)	b)			f)	g)
	c)	d)	e)		
1	2,71	0,18	2,53	8	7,384
2	3,18	0	3,18	10,5	7,282
3	2,80	0,92	1,88	6	7,459
4	3,30	1,24	2,06	7	7,440
5	2,86	1,12	1,74	6	7,505
6	2,76	0,89	1,87	6	7,466

a) No. of sample; b) Carbon ~~XXXX~~ content, % (by weight); c) C<sub>total</sub>; d) C<sub>~~banded~~ <sup>found</sup></sub>; e) C<sub>graphite</sub>; f) Content of graphite, % (by volume); g) Specific weight of iron, gm/cm<sup>3</sup>

The calculation was done on the basis of eq.(17.1). The specific weight of ~~the~~ graphite component is not known. The left side of the equation is set equal to the weight content of graphite in iron. Thus, for the first sample, we set up the equality:

$$2,53 = \frac{0,08 \gamma_g}{7,384} 100,$$

from which we find  $\gamma_g = 2,34 \text{ gm/cm}^3$ . Similarly for all six samples we get, gm/cm<sup>3</sup>:

1 . . . . .	2,34
2 . . . . .	2,21
3 . . . . .	2,34
4 . . . . .	2,19
5 . . . . .	2,18
6 . . . . .	2,33
mean . . . . .	2,27

Based on literature data (Bibl.106, 107, 108, 109), the specific weight of graphite ~~changes~~<sup>varies</sup> quite inconsistently between ~~2~~, 20 and 2.55, while the theoretical calculation based on parameters of ~~the~~<sup>the</sup> crystal lattice provides the figure 2.24.

In spite of the above-mentioned low accuracy of determining the volumetric content of graphite, the results of all analyses are very close to results obtained by other methods and deviate but little from the mean value (not more than by 3 - 3.5% of the value being determined).

Since in the example considered, the phase under analysis is a pure element, its weight content determined by chemical analysis may be equated to ~~XXXX~~<sup>the value</sup> computed on the basis of eq.(17.1). In a similar way, we can find the dependence between the weight and volumetric content of graphite in iron. In conformity with the above-adduced data, the specific weight of graphite can be assumed to equal 2.25 gm/cm<sup>3</sup>. The specific weight of the ferrite base depends upon the content of admixtures dissolved in the ferrite. The specific weight of pure ferrite, containing not over 0.01% of impurities, equals 7.874 gm/cm<sup>3</sup> (Bibl.110). The specific weight of silicic ferrite of malleable and gray iron~~s~~ is ~~all~~ the lower, the higher the silicon content in them: at 1% Si, the specific weight of ferrite can be assumed to equal 7.79 ~~XXXX~~ gm/cm<sup>3</sup>, while at 2% Si, it is 7.70 gm/cm<sup>3</sup> (Bibl.111).

Using these data, it is easy to formulate an equation for the case of ~~ferrous-carbon~~<sup>iron</sup> alloys, containing 2% silicon and having a ferrite metallic base:

$$G_g = \frac{2,25 \Sigma V_g}{2,25 \Sigma V_g + 7,70 \Sigma V_f} 100\% \quad (17.2)$$

Since the fractions of volume, taken up by ferrite and graphite, are equal to 1 as a total, eq.(17.2) provides a clearly defined dependence between the weight and volume content of graphite. The specific weight of cementite, based on data of K.Khond and his researchers equals  $7.662 \text{ gm/cm}^3$  (Bibl.112), that is, almost exactly coincides with the specific weight of siliceous ferrite, containing 2% silicon. Therefore eq.(17.2) proves ~~XXXX~~ valid not only for iron with a ~~XXXX~~ ferrite base, but also for iron with a base ~~made~~ of pearlite or of pearlite ~~XXXXXX~~ combined with cementite. In Fig.45, the dependence being determined by eq.(17.2), is shown graphically by a solid line (for alloys, containing 2% silicon). The broken line

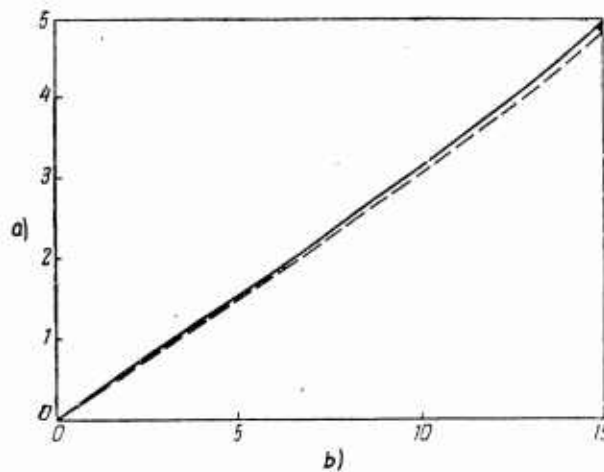


Fig.45 - Dependence between Volume and Weight Content of Graphite Contained in ~~Iron-~~ <sup>Iron-</sup>Carbon ~~Alloys~~ Alloys Containing 2% Silicon (solid line) and with 0% Silicon (broken line)

a) Carbon, weight in %; b) Graphite, volume in %

corresponds to pure ~~ferrous-carbon~~ <sup>iron-</sup> alloys, and as we see, almost coincides with the line for alloys containing silicon.

The denominator in eq.(17.2) determines the specific weight of alloys as a

whole. The dependence of specific weight of <sup>the</sup> alloy upon <sup>the</sup> content of graphite, expressed in weight percents, is presented in Fig.46. Line (1) in this drawing corresponds to pure <sup>iron</sup> ferrous-carbon alloys, while line (2) corresponds to alloys containing 2% silicon. The points located between these lines correspond to test data obtained for steels and irons with a varying content of silicon, by Pogodin-Alekseyev and N.T.Gudtsov with their coworkers (Bibl.105).

In those cases when the structural component of interest to us is a chemical compound or a complex formation (eutectic, eutectoid), the weight content of component obtained by eq.(17.1) can by no means be compared directly with chemical analysis data. The weight content determined by the equation must be first multiplied by the value determining the weight content of the element of interest

to us in the given structural component, and be divided by 100.

Let us assume that the structure hypoeutectoid of ~~hypoeutectoid~~ steel consists only of ferrite and pearlite. Just as above, the specific weight of ferrite is assumed to equal 7.874, while that of pearlite is 7.848 gm/cm<sup>3</sup> (the calculation of this last value is given below). The carbon content in ferrite is assumed to equal 0.006%, while in pearlite, it is assumed to be 0.8% [according to I.I.Kornilov (Bibl.21)].

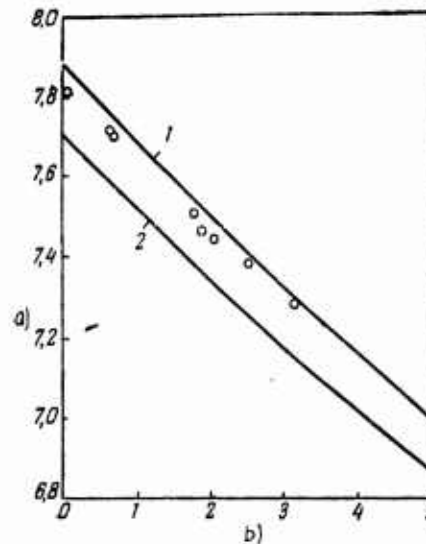


Fig.46 - Dependence of Specific Iron-Carbon Weight of ~~Ferrous-Carbon~~ Alloys upon Content of Graphite  
a) Specific weight of iron, gm/cm<sup>3</sup>;  
b) Graphite, wt.%

The weight content of structural components, in conformity with eq.(17.1), is determined by the values:

$$G_f = \frac{7,874 \Sigma V_f}{7,874 \Sigma V_f + 7,848 \Sigma V_p} 100\%$$

$$G_p = \frac{7,848 \Sigma V_p}{7,874 \Sigma V_f + 7,848 \Sigma V_p} 100\%$$

Since in the given case, carbon is contained in both components of the structure, its total computed content in steel, expressed in weight percents, will equal

$$\%C = \frac{7,874 \cdot 0,006 \Sigma V_f + 7,848 \cdot 0,8 \Sigma V_p}{7,874 \Sigma V_f + 7,848 \Sigma V_p} \quad (17.3)$$

Since in the total, ~~XXXXXXXXXXXX~~ the fractions ~~XXXXXXXXXXXX~~ being of volume of alloy/ occupied by ferrite and pearlite equal unity, eq.(17.3) permits one to determine unequivocally the content of carbon in steel based on <sup>the</sup> quantity of pearlite in its volume (or in the ~~XXXXX~~ area of cut). The dependence is considerably simplified if we disregard the difference of specific weights of ferrite and pearlite, and also the content of carbon in ferrite, as is usually done in metallographic practice, then

$$\% C = 0,8 \Sigma V_p \quad (17.4)$$

From Table 19, it is evident that the difference in results computed according to eqs.(17.4) and (17.3) is slight.

Table 19

a)	b)	
	c)	d)
0	0,006	0
0,1	0,085	0,08
0,2	0,164	0,16
0,3	0,244	0,24
0,4	0,323	0,32
0,5	0,402	0,40
0,6	0,482	0,48
0,7	0,561	0,56
0,8	0,641	0,64
0,9	0,720	0,72
1,0	0,800	0,80

a) Fraction of pearlite in volume of steel; b) Carbon content, %; c) By exact formula; d) By approximate formula

hypereutectoid  
For ~~XXXXXX~~ steel, the calculation of weight content of carbon based

on microanalysis data is conducted according to the equation:

$$\% C = \frac{7,848 \cdot 0,8 \Sigma V_p + 7,662 \cdot 6,69 \Sigma V_c}{7,848 \Sigma V_p + 7,662 \Sigma V_c}, \quad (17.5)$$

in which the ~~XXXX~~ figure 6.69 denotes the carbon content in cementite\*. Disregarding the difference of specific weights of pearlite and ferrite, we get

$$\% C = 0,8 \Sigma V_p + 6,69 \Sigma V_c. \quad (17.6)$$

The determination of carbon content by structure is less accurate ~~XXX~~ in hypereutectoid steel, in comparison with hypoeutectoid. In general the accuracy of microanalysis decreases with an increase in the content of <sup>the</sup> element of interest ~~in~~ in the structural component being measured. In ferrous alloys containing carbon, therefore, ~~XXXX~~ the maximum accuracy is achieved during measurement of the pearlite component, slightly less accurate in measuring the cementite component, and still less accurate in measuring the volume of free graphite. If, in the determination of volume of structural component, there is admitted the same absolute error, the error of calculational determination of content of carbon then will be proportional to 0.8 in case of pearlite structure, and 6.69 in case of cementite and 100 in case of graphite.

As is known, the carbon content in pearlite can often deviate considerably from the ~~XXXXXX~~ <sup>canonical</sup> figure as a result of formation of quasi-eutectoid structures. This however does not interfere with the establishment of actual carbon content in

---

\* Usually the carbon content in cementite is assumed to equal 6.67%. However, the calculation conducted ~~XXX~~ on the recent data of values of atomic weights yields ~~XXXXXX~~ the figure presented in the text.

only  
 such pearlite and its specific weight, if/there are several samples of steel with varying content of pearlite identical in internal structure, and hence with varying content of carbon in the steel. For instance, if there are two samples of steel containing pearlite of homogeneous structure, the carbon content in which is known, as well as the volume content of pearlite, determined by one of the methods of quantitative microanalysis, one can then compute the unknowns, namely the specific weight of pearlite and content of carbon in it. Disregarding the carbon content in ferrite, we formulate for each of the samples individually an equation of the following type:

$$\%C = \frac{C_p \gamma_p \cdot \Sigma V_p}{7,874 (1 - \Sigma V_p) + \gamma_p \cdot \Sigma V_p} \quad (17.7)$$

In these equations, only two values are unknown to us, namely the carbon content in the quasi-eutectoid  $C_p$  and its specific weight  $\gamma_p$ . Therefore, having at ~~XXX~~ our disposal two equations with two unknowns, we easily find both unknowns.

If we were also interested in the values which we disregarded in the above calculation, namely the carbon content in ferrite and the specific weight of ferrite, then we would have needed not two but four samples with ~~XXXXX~~ varying carbon content, but with identical pearlite structure. Such a method of calculation can prove quite effective for investigating the structure and properties even of submicroscopic elements of structure, for instance the metal of intercrystallite zones.

If a determination of structural composition by methods of quantitative metallography becomes difficult or unrealizable by way of direct experiment, as a result of high dispersed state of structure being analyzed, we can get the data of interest to us by way of calculation. For instance, the volumetric composition of

stratified pearlite is quite difficult to determine by direct measurement of <sup>the</sup> content of ferrite and cementite, as a result of a number of difficulties of a technical nature, which we mentioned in Section 12. Nevertheless, having at our disposal values of specific weights of ferrite and cementite, the content of carbon in them, and knowing the carbon content in pearlite, we can formulate an equation similar to eqs.(17.3) and (17.5):

$$0,8 = \frac{7,874 \cdot 0,006 \Sigma V_f + 7,622 \cdot 6,69 \Sigma V_c}{7,874 \Sigma V_f + 7,662 \Sigma V_c} \quad (17.8)$$

in which there is contained but one unknown,  $\Sigma V_{tS}$ , since the fractions of volume of pearlite occupied by ferrite and cementite are equal to unity in the total. Solving this equation, we find the volumetric content of ferrite and cementite in the pearlite:

$$\Sigma V_c = 0,122 \quad \text{or} \quad 12,2\%, \quad \Sigma V_f = 0,878 \quad \text{or} \quad 87,8\%.$$

The specific weight of pearlite, being determined by the law of displacement, is equal to the denominator in eq.(17.8), specifically 7.848 gm/cm<sup>3</sup>. This figure correlates well with the literature data, according to which the specific weight of normal pearlite equals ~~XXXX~~ 7.846 - 7.85 gm/cm<sup>3</sup> (Bibl.109, 107). The ratio of volume of ferrite to the volume of cementite in pearlite, in conformity with derived data, equals:

$$0,878 : 0,122 = 7,2.$$

In a series of researches, there was proved the inconstancy of chemical composition of cementite (Bibl.85, 113). If ~~XXXX~~ this is so, the calculation based on eq.(17.8) is not rigorous. In particular, ~~XXA~~ A.N.Rozanov conducted direct measurements <sup>of</sup> ~~the~~ thicknesses of ferrite and cementite plates of pearlite of eutectoid steel in a microsection pickled with ~~XXX~~ sodium picrate, wherein the ratio of these thicknesses (identical to the ratio of volumes of ferrite and cementite in pearlite)

proved to equal 5.68, but not 7.2 as was computed by us, and not 7.0 as ~~XX~~ was found by other ~~XXX~~ researchers (also by way of calculation). The author also showed that the carbon content in cementite increases with temperature, while the hardness of cementite changes during tempering, depending upon the temperature of heating (Bibl.114).

Using the data of quantitative microanalysis and of share of pure metals found experimentally, one can determine by calculation the share of metal in the intercrystallite zones. The samples should differ from one another by ~~XXX~~<sup>the</sup> value of specific surface of grains (or ~~XX~~ value of grain). Using an electron microscope, Gardin showed that one can determine ~~XXX~~<sup>quite</sup> precisely the volume of the intercrystallite zones (Bibl.115). For ~~XX~~ a specimen of technical iron, he found that the specific volume of intercrystallite zones equals  $0.03 \text{ mm}^3/\text{mm}^3$ , or 3% of the total volume of metal. The specific surface of grains of this specimen equaled  $120 \text{ mm}^2/\text{mm}^3$ , while the average thickness of ~~the~~<sup>the</sup> boundary zone amounted to 0.25 micron. Determination of specific weight of samples can be conducted with great accuracy and is quite simple methodologically.

The calculation of specific weight of metal as a whole is conducted, as normally, based on the rule of displacement according to the formula:

$$\gamma_f = 0.97 \gamma_k + 0.03 \gamma_m, \quad (17.9)$$

where  $\gamma_k$  and  $\gamma_m$  are respectively the specific weight of intracrystallite and

intercrystallite metals (unknown to us);

$\gamma_f$  is the calculated value of specific weight of metal as a whole,

which is equated to the value found from experience.

Since the specific weights of two samples can be determined experimentally, there remain two unknowns  $\gamma_k$  and  $\gamma_m$ , which we also find from the two equations.

The introduction (into the calculation of structural composition) of values of specific weight determined from experiment is quite efficient, since the specific weight is very sensitive to the least changes in the ~~XXXXXX~~ structure of the alloy. However, it is noteworthy that the value of specific weight is also affected by differences <sup>the</sup> in value of specific volume of intercrystallite zones and of change ~~XX~~ in structure as a result of cold plastic deformation (of cold-~~working~~), ~~hardening~~). This needs to be kept in mind and considered in the production of precise calculations.

For instance, K.Mayer determined by test that the specific weights of ~~mono~~<sup>single</sup>crystal and polycrystal of copper ( $\text{gm/cm}^3$ ) differ considerably, as this is apparent from the following figures,

Monocrystal . . . . .	8.95235
Polycrystal . . . . .	8.94153

The specific weight of polycrystal is lower by 0.12% owing ~~XX~~ to the presence in the structure of a lighter metal of intercrystallite zones (Bibl.45).

M.G.Oknoy showed that cold plastic deformation of metal is accompanied by a decrease in its specific weight. The swaging of samples of annealed steel, containing from 0.23 to 1.67% C, in which the height of samples decreased from 15 to 10 mm, was accompanied by a decrease in <sup>the</sup> specific weight of steel by values ranging from 0.02 to 0.16%. In alloyed steels, especially austenitic, there occurred a ~~XXXX~~ decrease in specific weight by 0.45 - 0.52%. Subsequent annealing of cold-hardened metal is accompanied by an increase in specific weight. Thus, the specific weight of steel wire (0.1% C), decreased by stretching from 4 mm to 0.7 mm without intermediate annealing, as a result of later annealing increased by 0.24% (Bibl.116).

According to data of T.Ishigaki, the specific weight of a steel sample, which had broken during a tensile test, was lower by 1.08% in the breaking zone than in the undeformed one during the testing of a part of the sample [~~the~~ heading (Bibl.117)].

Although <sup>the</sup> changes in specific weight of steel during plastic deformation and annealing are not great, in certain cases of combined calculation, ~~which~~ they should still be taken into account.

According to data of quantitative microanalysis, chemical analysis and of determination of specific weight, combined calculation can prove quite effective in many cases of research, having the purpose of explaining the chemical composition, physical properties and structure of individual components of structure. Since at present, such ~~an~~ a method is used relatively rarely, it is feasible to expand its use in metallographic practice. The reader can find additional information in the report by M.Ye.Blanter (Bibl.118).

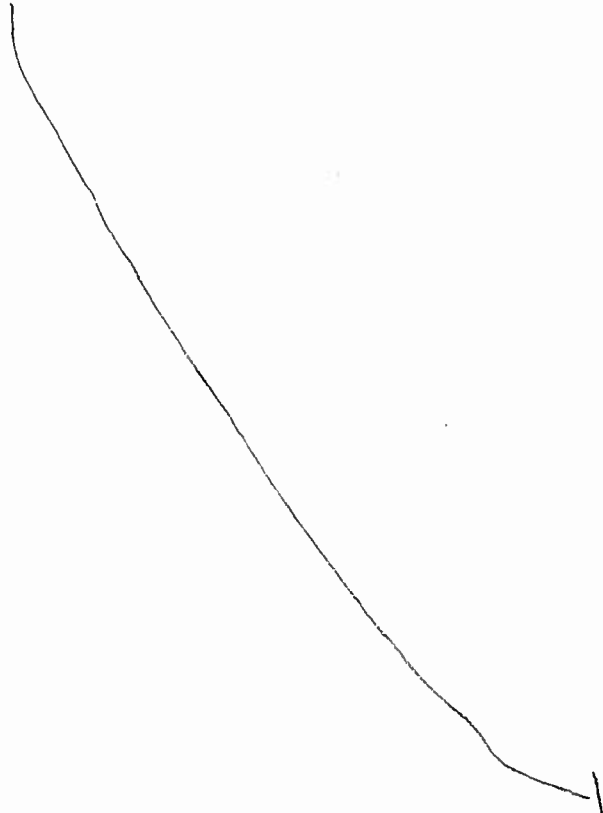


Table 20

Specific Weights of Pure Metals and of Certain  
Structural Components

Name	$\gamma$ gm/cm <sup>3</sup>	Source
Ferrous-Carbon Alloys		
Ferrite . . . . .	7,874	[110]
Cementite . . . . .	7,662	[112]
Graphite . . . . .	2,25	[109]
Pearlite . . . . .	7,848	—
Ferrous phosphide . . . . .	6,74	[26]
Binary phosphide eutectic(σ <sub>Fe</sub> Fe <sub>3</sub> P), . . . . .	7,14	[26]
Ferrous sulfide . . . . .	4,30	[71]
Manganese sulfide . . . . .	3,99	[26]
Silica . . . . .	2,26—2,31	[247]
Alumina . . . . .	3,85—4,10	[247]
Manganese orthosilicate (2 MnO · SiO <sub>2</sub> ) . . . . .	3,58—3,70	[247]
Ferrous orthosilicate (2 FeO · SiO <sub>2</sub> ) . . . . .	4,35	[247]
Alumina silicate (Al <sub>2</sub> O <sub>3</sub> · SiO <sub>2</sub> ) . . . . .	3,05	[247]
Magnesium oxide . . . . .	3,50—3,65	[247]
Manganese oxide . . . . .	4,73—5,50	[247]
Pure Metals		
Aluminum . . . . .	2,7	[248]
Beryllium . . . . .	3,5	[248]
Vanadium . . . . .	8,97	[248]
Bismuth . . . . .	21,33	[248]
Tungsten . . . . .	9,58	[248]
Cadmium . . . . .	12,99	[248]
Cobalt . . . . .	8,90	[248]
Silicon . . . . .	2,4	[248]
Manganese . . . . .	7,44	[248]
Copper . . . . .	8,94	[248]
Molybdenum . . . . .	10,2	[248]
Nickel . . . . .	8,9	[248]
Tin . . . . .	7,3	[248]
Lead . . . . .	11,34	[248]
Antimony . . . . .	6,62	[248]
Tantalum . . . . .	16,6	[248]
Titanium . . . . .	4,5	[248]
Chromium . . . . .	7,14	[248]
Zinc . . . . .	7,14	[248]

a) Name; ~~XXXXXXXX~~ b) Source

In conclusion, in Table 20 we adduce values of specific weights of a number of metallic and nonmetallic structural components of alloys, mainly ~~XXXXXXXX~~

*iron -*  
~~XXXXXXXX~~ carbons, which can be used in the calculations.

### Chapter III. Measurement of Boundary Surfaces of Grains, Phases, and Structural Components

#### Section 18. Specific Surface and Special Methods for Its Determination

In pure polycrystalline metals, boundaries separating crystallites appear as continuous surfaces similar to a film of soap suds in a cylinder. In contrast to the latter, the facets of cells of the boundary surface in metals are not flat but more or less curved, just as the edges of the cells. In alloys the interfaces of different phases or structural constituents may be shaped as continuous surfaces. However, closed contours, which limit the volume of individual microparticles are also frequently observed.

In certain structures, closed surfaces, which limit the volume of individual microparticles, may have a more or less irregular geometrical configuration approximating the shape of a sphere, a flat platelet, etc. The thickness of all interfaces, which would show this separately, was quite insignificant in comparison to their extent through space. For this reason they may be considered as geometrical surfaces.

The extent (or amount) of interfaces of grains of pure metal, measured in units of area, divided by the unit volume of metal is called the specific surface of grains. In alloys, too, the surfaces of various phases or structural constituents may be characterized by a definite value of the specific surface of each one of them. Generally speaking, the total specific surface in an alloy is not equal to the sum of specific surfaces of constituent structures, for they are partially superimposed. For example, in hypereutectoid steel, the surface of the pearlite constituent is coincident with the surface of cementite. For this reason the total specific surface is equal to the specific surface of any constituent and, consequently, in this case the surfaces are completely superimposed. In low carbon steel the surface of ferrite grains partially coincides with the surface of pearlite

formations. Further in this article, we shall measure the value of the specific surface in all cases in  $\text{mm}^2/\text{mm}^3$ .

Even during the initial stage of development of this science of metals, interfaces attracted the attention of scientists, for they are precisely the region where the initial stages of the formation of new structures are localized during structural modifications. Moreover, the size of the specific surface is directly related to the dispersity of the structure which essentially affects the most diversified properties of metals and alloys. The interest in interfaces in metals increased particularly after 1912, when W. Rosenhain applied to them the hypotheses of G. Beilby on the amorphous structure of fine metal films. Despite that, the methods of quantitative evaluation of the extent of interfaces were developed considerably later.

The specific surface of crystallites in a pure metal, and the specific surface of any group of microparticles in an alloy, are dependent (1) upon the average size of the crystallite or microparticle, (2) upon the shape of crystallites or microparticles and (3) upon the degree of fluctuation of their sizes. Therefore, when determining the magnitude of the specific surface, all of the aforementioned factors should be taken into account.

A method for determining the specific surface was developed for the first time by N. T. Belaiew in 1922. It is applicable to one specific structure, lamellar pearlite. N. T. Belaiew utilized the peculiarities of the geometrical structure of lamellar pearlite, which may be considered, with a certain degree of idealization, as a block of plane-parallel platelets of ferrite and cementite having a different spatial orientation in each individual grain of pearlite. It is assumed that platelets of ferrite and cementite are of equal thickness throughout the entire volume of pearlite subjected to a similar heat treatment.

Inasmuch as the carbon content in the cementite, ferrite, and normal lamellar pearlite is stable, the ratio between the thicknesses of ferrite and cementite platelets remains constant regardless of the fineness of the pearlite structure. The dispersity of pearlite is

characterized by the total thickness of a single pair of ferrite and cementite platelets. It is measured in microns and is known as interlamellar distance  $\Delta_0$ . On a microsection the apparent interlamellar distance differs with each grain of pearlite, for the plane of the microsection intersects pearlite grains forming different angles with the planes of ferrite and cementite in each individual grain. It is obvious that the actual interlamellar distance coincides with the interlamellar distance which is the minimum one of all interlamellar distances visible in the microsection; i. e., it coincides with the visible interlamellar distance of those pearlite grains in which the platelet planes happen to be perpendicular to the plane of the microsection.

Let us mentally cut out a cube from the individual grain of lamellar pearlite, so that its two opposite faces are parallel to the surfaces of ferrite and cementite platelets. The edge of the cube we shall take as unity. In that case the total number of pairs of ferrite and cementite platelets, found within the cube, would be

$$z = \frac{1}{\Delta_0}.$$

Since each pair of platelets has two planes which separate ferrite and cementite, and the area of each plane is equal to unity (inasmuch as the edge of the cube is unity), the total surface of phase interfaces within the cube, i. e., within the volume equal to unity, will be defined by the formula:

$$\Sigma S_{\phi} = \Sigma S_{\eta} = \frac{2}{\Delta_0} \text{ mm}^2/\text{mm}^3. \quad (18.1)$$

In practice, in order to determine the specific surface of phase interfaces in lamellar pearlite, it is necessary to know only the value of the interlamellar distance  $\Delta_0$ .

The determination of the interlamellar distance by the method described becomes more difficult with increasing dispersity of pearlite. When the interlamellar distance is very small, it is impossible to

measure it, since even at high magnification the internal structure of pearlite is not resolved precisely in those grains in which the measurement has to be made. At the same time, even in the pearlite with a very fine structure there are always observed individual grains in which the microsection plane forms a small angle with the planes of platelets and, for this reason, it is possible to measure only the apparent interlamellar distance which, however, is not equal to the actual one but is always greater than the latter.

Let us examine again the internal structure of an individual grain of geometrically ideally constructed lamellar pearlite. The number of cementite platelets, intersected by an intercept of a definite length directed normally to the surface of platelets, we assume to be 100 per cent. At any other angle between the intercept and the surfaces of platelets, the intercept of the same length would intersect a smaller number of platelets than at the angle of 90 degrees. According to N. T. Belaiew, the relationship between the number of intersected platelets and the angle formed by the intercept and the surface of platelets is given by the following numbers [55, 56]:

<i>angle of incidence -</i>	90	64	53	45	36	30	24	17	12	6
<i>No. of lamella %</i>	100	90	80	70	60	50	40	30	10	5

In accordance with the numbers presented above, the apparent interlamellar distance will be the greater the smaller the angle between the platelets of a given pearlite grain and the plane of the microsection. The nature of the internal structure of the grain remains constant, until this angle reaches the value of about 17 to 12 degrees, although the pearlite appears to be increasing the "cores" as the angle decreases. However, if the angle is less than 6 degrees, the appearance of the internal structure of the pearlite grain changes quite characteristically: the cementite platelets become curved and broken. This circumstance was noted by N. T. Belaiew, who utilized it to measure the interplatelet distance in dispersed pearlite, when this distance cannot be measured in those grains where its value is minimum. The author of this method postulated that with practice it

is possible to determine with sufficient accuracy the angle at which the plane of the microsection intersects the platelets of a given pearlite grain from the nature of the disposition and the shape of cementite platelets. However, if we know this angle and also the apparent interlamellar distance in a given grain, the actual interlamellar distance can be calculated on the basis of an elementary geometrical construction. For this reason, if dispersed pearlite contains at least several grains in which ferrite and cementite platelets are distinguishable, the actual interlamellar distance may be determined by the method described [55,56]. The characteristic change in the arrangement of cementite platelets in the pearlite grain, when they are almost parallel to the surface of the microsection, may be explained by a certain space curvature of cementite platelets, which for the first time was noted by N. G. Okanov [119] and after that confirmed by the investigations of N. T. Belaiev [55, 56] and K. F. Starodubov [120].

The method, developed by N. T. Belaiev in 1920 to 1925, was comparatively recently verified and applied by G. Pellissier and his associates [121]. By means of direct experimentation they found that a special arrangement of cementite platelets in the pearlite grain does exist when the angle between the platelets and the plane of the microsection is less than 7 degrees. Therefore, having measured the apparent interlamellar distance in pearlite grains of this type, the actual interlamellar distance is calculated by using the formula:

$$\Delta_0 = \Delta_k \sin 7^\circ, \quad (18.2)$$

where  $\Delta_k$  is the apparent interlamellar distance.

Having determined the unknown value of the actual interlamellar distance,  $\Delta_0$ , the specific surface of phase interfaces is determined in pearlite from Formula (18.1).

The actual interlamellar distance in pearlite grains, the platelets of which are perpendicular to the plane of the microsection, may be determined more readily and accurately. Even when the angle between the platelets and the plane of the microsection is 10 degrees greater than a right angle, the error is only 1.5 per cent. The

shortcoming of this method is its applicability only to pearlite with a relatively coarse structure, when ferrite and cementite platelets are resolvable in all pearlite grains.

The situation is different in the second case when the apparent interlamellar distance is measured in grains with a very small angle between the platelets and the plane of the microsection and Formula (13.2) is used for calculations. In this case a change in the angle of intersection of only 1 degree produces considerable error. For example, if the specific change in the type of the pearlite grain occurs not at 7 degrees but at 6 degrees, the sine of the angle of intersection would change from 0.122 to 0.105 and the error would be 14 per cent.

In view of the aforesaid it is more expedient to determine the interlamellar distance in pearlite of high dispersity by the method developed by M. Gensamer and his associates [122]. In accordance with their method, the interlamellar distance is measured on a microsection in several grains of pearlite along directions ranging between directions perpendicular to the platelets and directions parallel to them, and the mean value is taken. In other words, if a straight line of a definite length is drawn across the structure of lamellar pearlite (on the microsection or photomicrograph), which intersects cementite platelets in several grains at all possible angles, ranging between 0 and 90 degrees, and after that if the length of the line is divided by the number of cementite platelets intersected by it, the resulting mean length of an intercept between adjacent cementite platelets will be precisely the initial value of  $\Delta$  needed for calculations. Gensamer and his associates experimentally determined that the value derived in this manner is proportional to the actual interlamellar distance:

$$\Delta = k \Delta_0 \quad (13.3)$$

and that the coefficient  $k$  is found within the limits 1.9 and 2.0.

This relationship is a special case of a general method for the determination of this specific surface, the method of random sections,

which will be described further in this book. In agreement with the method of random secants, the coefficient in Formula (18.3) must be precisely 2, which can be proved mathematically. Therefore, the corrected formula of M. Gensamer must have the following form:

$$\Delta_0 = 0.5\Delta. \quad (18.4)$$

The specific surface of the phase interface in lamellar pearlite is calculated from Formula (18.1), using the value found for the actual interlamellar distance,  $\Delta_0$ .

M. Gensamer's corrected formula (18.4) has been used by A. I. Gardin in an extensive structural study of the products of isothermal decomposition of austenite, including highly dispersed products [87, 123]. Among the structures investigated under the electron microscope were decomposition products with the magnitude of specific surface reaching  $25,000 \text{ mm}^2/\text{mm}^3$ , for which the actual interlamellar distance is only 800Å. Even under such disadvantageous conditions, the Formula (18.4) was quite valid and the method reliable.

Thus, for the determination of the specific surface of the phase interface in lamellar pearlite there exists simple specific methods verified in practice:

1. The method of direct measurement of interlamellar distance, developed by N. T. Belaiew, which is suitable for relatively coarse lamellar pearlite, and
2. The method of measuring the mean length of the intercept between adjacent platelets of cementite on a straight line intersecting a number of pearlite grains with differently oriented platelets.

The latter method was developed by M. Gensamer and his associates, and the formula used for calculating the interplatelet distance has been defined by us. The second method is suitable for pearlite of any dispersity but requires magnification sufficient for resolving the internal structure of all pearlite grains.

A second type of structure, possessing a definite geometrical regularity, which permits the application of special methods of deter-

mination of specific surface, is a structure consisting of a multitude of microparticles of spherical shapes belonging to one phase, which microparticles are uniformly distributed through the volume of the second phase (matrix). Typical structures of this type are granular pearlite or granular cementite in ferrite, the structure of magnesium cast iron with spheroidal graphite inclusions, the structure of steel containing non-metallic inclusions of spheroidal shapes, and certain others.

In structures containing spheroidal microparticles, both the total number of particles per unit volume of metal and their size distribution (with respect to the size of diameter) may be calculated by methods presented in the following chapter. In the case where we know the number of particles of each size per unit volume of metal, the calculation of the total surface of microparticles is reduced to simple arithmetic. However, the technique of determining the number of microparticles and their size distribution is one of the most effort-consuming processes of quantitative metallographic analysis. For this reason, it is not reasonable to use this technique for the special purpose of determining this specific surface, particularly since there is available a quite simple and accurate method, the method of random secants.

Here we shall consider two approximate methods. The first of these, proposed by us, is based on the assumption that all spheroidal microparticles are of equal size [124]. If the diameter of these microparticles is  $D$  mm and their number in  $1 \text{ mm}^3$  is  $N$ , then the specific surface of microparticles will be:

$$\sum S = \pi D^2 N \text{ mm}^2/\text{mm}^3. \quad (18.5)$$

At the same time the total volume of all microparticles in  $1 \text{ mm}^3$ , i. e., the fraction of the volume of alloy occupied by them, will be defined by the quantity:

$$\sum V = \frac{\pi D^3}{6} N \text{ mm}^3/\text{mm}^3. \quad (18.6)$$

By simultaneous solution of Formulas (18.5) and (18.6) we derive:

$$\Sigma S = \frac{6 \Sigma V}{D} \text{ mm}^2/\text{mm}^3. \quad (18.7)$$

The fraction of the alloy volume occupied by the phase consisting of spheroidal microparticles, may be determined directly by one of the methods of stereometric metallography presented in Chapter 2. If this phase is cementite or graphite, then its volumetric content may be readily calculated from the data of chemical analyses, as described in Section 17. The diameter of spheroidal microparticles of equal size may be determined directly on the microsection, for the section diameter of maximum size is, of course, the actual diameter of the volumetric microparticles. Having obtained the values of both quantities found in Formula (18.7), by the method described, it is possible also to calculate the value of the specific surface.

The number of sections of microparticles per unit area of the microsection,  $n$ , may be substituted into Formula (18.7) for the diameter of microparticles of equal size. For this purpose we shall use the expression which correlates the diameter of spheroidal microparticles of equal size,  $D$ , and their number per unit volume,  $N$ , and the number of sections per unit area,  $n$ :

$$n = DN. \quad (18.8)$$

Having squared both sides of equation (18.5), by means of simple conversions which take into account relationship (18.8), we derive:

$$\Sigma S = \sqrt{6 n V} = 4.34 \sqrt{n V}. \quad (18.9)$$

Consequently, on the assumption of equal size of all spheroidal microparticles of a given phase, we derive Formulas (18.7) and 18.9) for the calculation of the specific surface of this phase. This does not account for fluctuations in article size. Therefore from Formulas (18.7) and 18.9) we derive approximate and always high values.

Another type of approximate formula for the calculation of the specific surface (as applied to granular cementite) was proposed by F. S. Dolshteyn [125, 126]. If the total volume of all spheroidal

microparticles of a given phase per unit volume of the alloy is  $\Sigma V$ , and their number is  $N$ , then the mean volume of an individual microparticle will be

$$V = \frac{\Sigma V}{N}. \quad (18.10)$$

The surface of an individual microparticle may be expressed by its volume and diameter in the following fashion,

$$S = \pi D^2 = \frac{\pi D^3}{6} \cdot \frac{6}{D} = \frac{6V}{D}, \quad (18.11)$$

and, consequently, the total surface of all microparticles in the unit volume of the alloy will be

$$\Sigma S = SN = \frac{6V \cdot N}{D} = \frac{6\Sigma V}{D}. \quad (18.12)$$

Applying the precise calculation of the total number of microparticles and their distribution by the complex method of E. Schoil, I. L. Mirkin showed in one of his papers that the mean diameter  $\bar{d}$  of sections of spheroidal microparticles, measured on the plane of the microsection, may be substituted for the value of the diameter of the volumetric microparticles,  $D$ , in Formula (18.8). This substitution, according to I. L. Mirkin, introduces an error which does not exceed 7 per cent [127].

Replacing the diameter of volumetric microparticles,  $D$ , by the mean diameter of their cross sections,  $\bar{d}$ , we finally derive the approximate formula of S. Z. Bokshateyn:

$$\Sigma S = \frac{6\Sigma V}{\bar{d}}. \quad (18.13)$$

The formula of S. Z. Bokshateyn also produces high values of the specific surface. Accounting for the fluctuation of size of volumetric grains, the formula (18.13) would appear as:

$$\Sigma S = \frac{6\Sigma V}{\bar{d}} \left( \frac{\pi}{4} \cdot \frac{1}{1 + \delta^2} \right), \quad (18.14)$$

where  $\delta$  is the ratio of the root-mean-square deviation of the diameter of volumetric microparticles,  $\sigma\{D\}$ , to their mean diameter,  $\bar{D}$ .

This ratio for ordinary structures quite frequently varies between 0.2 and 0.5. The correction coefficient for S. Z. Bokshsteyn's formula (18.13) has the following values, depending upon the value of  $\beta$  [in agreement with Formula (18.14)]:

0	0.785
0.1	0.778
0.2	0.756
0.3	0.720
0.4	0.677
0.5	0.628
0.6	0.577

Moreover, there is a formula which was used by L. S. Moroz in his studies to calculate the total surface of spheroidal grains of a carbide phase [12]:

$$\Sigma S = 1.68 \sqrt{C_k n}, \quad (18.15)$$

in which  $C_k$  is equal to the ratio of total volume of carbides per unit volume of steel to the carbon content of the carbide in weight per cent, 6.68.

All of the approximate formulas include some two parameters, the values of which must be found experimentally. Therefore, it should be remembered that the simpler and more accurate method for the determination of the specific surface is the method of random sections.

## Section 19. Approximate Methods for Determining the Specific Surface of Polyhedral Structures

The first attempt to determine experimentally the magnitude of the specific surface of crystallites of a single-phase polyhedral structure was made by I. P. Lipilin in 1937 [129]. The aim of I. P. Lipilin's studies, for which he developed his method, was to determine the influence of the magnitude of the specific surface of austenite grains on the isothermal decomposition time. I. P. Lipilin's reasoning was based on the assumption that the unknown quantity of the grain surface per unit volume of steel is directly proportional to the length of grain boundaries per unit area of polish. This assumption, quite valid in the case of equiaxed grains, is accepted by I. P. Lipilin without any proof, as we shall see later. The length of boundary line, which could be measured experimentally and directly (for example with the aid of a curvimeter from the photomicrograph), was determined by I. P. Lipilin indirectly from the number of planar grains per unit area of polish.

If various isoonal grids are examined on a plane, that is, grids constructed from figures (or groups of figures), which are equivalent and identical, with respect to shape, then for the general case the total linear extent of perimeters of these figures per unit area,  $\sum P$ , and the number of plane figures on the same area,  $n$ , are related by an equation of the following type:

$$\sum P = a \sqrt{n} \quad , \quad (19.1)$$

where the coefficient  $a$  is dependent only upon the shape of the figures constituting the grid. For example, for an isoonal grid, consisting of regular and equivalent triangles, this coefficient is 1.86. For a grid of identical squares, this coefficient is 2.00 and for a grid of regular hexagons it is 2.20.

For his calculations, I. P. Lipilin arbitrarily assumes that the coefficient  $a$  is 2 and that the number  $n$  in each individual case is equal to the actual number of austenite grains per unit area of polish. Consequently, it is not the specific surface of austenite grains that

is determined by the method, accepted by I. P. Lipilin, but a value which is proportional to it, the total perimeter of plane grains per unit area of polish. Moreover, substituting the calculation from Formula (19.1) for the direct measurement of this perimeter, the author of this method disregards a number of factors which essentially affect the value of the specific surface, such as the difference in the curvature of grain surfaces and the degree of variation of their size within the volume of steel subject to investigation. At the same time, in different specimens of steel with the same size of planar grain, the values of specific grain surfaces may differ precisely due to the difference in the aforementioned quantities which the method does not consider.

Nevertheless, I. P. Lipilin succeeded in establishing the fact that the rate of austenite decomposition is a linear function of the length of grain boundaries per unit area of polish and, consequently, a linear function of the value of specific grain surface of austenite, proportional to it. It should also be noted that the value of the coefficient in Formula (19.1), chosen by I. P. Lipilin, is quite close to the mean value which is usually observed. However, generally speaking, this coefficient is not a constant value but is dependent upon the aforementioned factors.

Sometime after publication of the paper by I. P. Lipilin, Rutherford, Aborn and Bain published their studies. Their aim was also to determine the quantitative relationship between the parameters of plane and spatial structures, specifically, the specific grain surface. These studies differ in principle from Lipilin's work in that the authors assumed the crystallites to have equivalent and geometrically regular bodies, which differs from the real structure of metals [57]. There are known five geometrically regular bodies, shown in Figure 47, which are capable of completely filling space. Of these the authors investigated the cubic octahedron with 14 faces of which 8 are regular hexagons and 6 are squares (see Figure 47e). All edges of the cubic octahedron are equal. According to the data of W. Kelvin, the cubic octahedron with 14 faces is a body which has a minimum

surface for a given volume (among the bodies which fill the space). For this reason, the authors assume that in a state of equilibrium the crystallites of metals precisely conform to the shape of a 14-face cubic octahedron. This has been confirmed by the observation according to which the crystallites of thoroughly annealed metals have 9 to 19 faces; on an average about 14 faces.

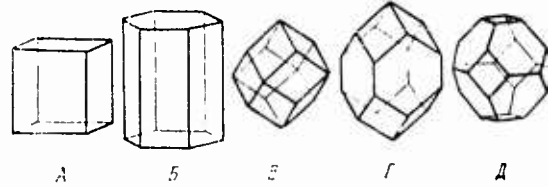


Fig. 47. Geometrically regular bodies, capable of completely filling space.

A cube B hexagonal prism C rhombic dodecahedron D elongated dodecahedron E cubic octahedron

Different sections of a geometrically regular body are examined for the possibilities of obtaining polygons, with different numbers of angles, on a plane. The authors also calculate the mean area of a section of cubic octahedron and after that equate it to the area of grains corresponding to different numbers of the standard ASTM grain size scale. Values of specific surface of equivalent cubic octahedrons are calculated respectively for each number of the grain size. They are listed in Table 21. It is possible to agree with a choice of a cubic octahedron as an idealized shape of a crystallite, since actually the mean number of faces, separated from the metal aggregate of crystallites, is close to 14 (see for example Figure 5.). However, in reality the crystallites are not equivalent and, moreover, have curvilinear edges and faces with different curvature. Therefore, these assumptions reduce the method and the results, calculated by it, to an extremely tentative state.

1. Номер зерна по шкале ASTM	2. Удельная поверхность, мм <sup>2</sup> /мм <sup>3</sup>	3. Номер зерна по шкале ASTM	4. Удельная поверхность, мм <sup>2</sup> /мм <sup>3</sup>
1	4.7	6	51.4
0	6.7	7	75.6
1	9.5	8	107
2	13.4	9	151
3	18.9	10	214
4	26.7	11	302
5	37.8		

1. No. of grains per ASTM Scale.  
 2. Specific surface of grains, mm<sup>2</sup>/mm<sup>3</sup>.  
 3. same as 1.  
 4. same as 2.

Table 21

In 1938, Kaiser [45] calculated the limiting value of the specific surface. Kaiser's calculations are based on Ya. S. Fedorov's notions that in approximation polycrystals may be regarded as a system of equivalent polyhedrons, closely packed in space. Kaiser considers four basic types of polyhedrons which can fill space: a cube, a hexagonal prism, a rhombic dodecahedron, and a cubic octahedron. For all types of polyhedrons, Kaiser determines the specific grain surface as a function of the number of grains (polyhedrons) per unit volume:

$$\Sigma S = \rho \sqrt[3]{N}, \quad (19.2)$$

where the coefficient  $\rho$  is dependent on the type of the polyhedron, which we assume to be the shape of metal crystallites. According to Kaiser, the coefficient  $\rho$  has the following values:

For the cube	3.000
For the hexagonal prism	2.866
For the rhombic dodecahedron	2.673
For the cubic octahedron	2.659

Inasmuch as Formula (19.2) defines the specific surface through the quantity  $N$  (the number of crystallites per unit volume of metal), which is unknown to us, Kaiser carries his calculations only for the limiting case, assuming that the minimum possible crystallite size is of the same order as the block size of mosaic structure. Accepting, as it is assumed by Kaiser, that the order of volume of 1 mosaic block is  $10^{-11} \text{ mm}^3$  and that accordingly the number of blocks per unit volume is  $10^{11}$ , we find the limiting values of the specific surface ranging between  $12,3000 \text{ mm}^2/\text{mm}^3$  (for a cubic octahedron) to  $13,900 \text{ mm}^2/\text{mm}^3$  (for a cube). As has been calculated by Kelvin, the minimum surface of equivalent crystallites corresponds to the shape of a cubic octahedron. If the shape of microparticles differs from equiaxed, the limiting values of the specific surface may be considerably higher than those calculated. For example, we have already mentioned that the specific area of the interfacial surface of lamellar pearlite has been experimentally measured to be  $25,000 \text{ mm}^2/\text{mm}^3$ .

The desire to approach the real structural shapes of polycrystalline metallic aggregates, prompted some investigators to attempt

the assumption of the equal size and identical shape of all its constituent crystallites. D. Meijering determined analytically the parameters of the spatial structure of a metal polycrystal, which is formed by means of simultaneously commencing growth of all crystallites at an equal and constant rate of growth in all directions (spherical syngene of growth), with the centers of crystallization randomly arranged in the volume [130]. For the specific surface area, he derived the following relationship as a function of the number of crystallites per unit volume (or the number of centers of crystallization):

$$\Sigma S = 2.91 \sqrt[3]{N} . \quad (19.3)$$

Other conditions for the formation of a polycrystalline structure have been considered by Johnson and Mehl. The authors' reasoning is based on the postulate that crystallites grow from centers which nucleate gradually and uniformly in time, at a rate constant the entire process at a spherical syngene of growth. If the nucleation rate of crystallization centers is a  $\text{cm}^{-3} \text{sec}^{-1}$ , and the linear growth rate is  $v \text{cm sec}^{-1}$ , then the final number of crystallites per unit volume can be determined from the formula [130]:

$$N = 0.8960 \left( \frac{a}{v} \right)^{3/4} , \quad (19.4)$$

and the specific interfacial area of crystallites will be:

$$\Sigma S = 2.479 \left( \frac{a}{v} \right)^{1/4} \quad (19.5)$$

From these two formulas, eliminating the value of crystallization parameters, we find the relationship between the specific area and the number of crystallites per unit volume of metal:

$$\Sigma S = 2.572 \sqrt[3]{N} . \quad (19.6)$$

The conditions for the formation of a polycrystalline aggregate, accepted in D. Meijering's model, as well as in calculations of W. Johnson and R. F. Mehl, do not correspond to the real course of the process. Although the growth of crystallites does commence practically simultaneously, as is assumed by D. Meijering, the process of

crystallite impingement, which has not been reflected in any of the considered schemes, commences simultaneously with the crystallite growth and continues to the end of crystallization (and under certain conditions even after it).

Nevertheless, from a comparison of the coefficients of Formulas (19.6), and (19.2) for the case of the cubic octahedron, it follows that for a given number of crystallites per unit volume none of the polycrystalline aggregates with equivalent grains have a minimum specific area and, consequently, a maximum thermodynamic stability.

Section 20. The Method of Random Secants on a Plane. Isometric Systems of Lines on a Plane, and Determination of Their Lengths

The method of random secants, developed by us in 1945 [58, 131, 59], is a universal method of direct determination of actual specific surface of grains, phases and structural components by means of measurements carried out upon a flat section (microsection). In this case, no assumptions of any kind are made on the shape and disposition of boundary surfaces in space, as it was done in methods reviewed in Section 19; a true interface is measured just as it is in reality. The measurement of the total length of a system of lines per unit area of the plane upon which they are located. The measurement of the specific surface is carried out by the method of random secants in space and the specific length of lines in a plane is measured by the method of random secants in a plane.

In two-dimensional and three-dimensional problems it is necessary to do identical measurements on a plane. However, operations carried out within a two-dimensional problem are more illustrative and the results obtained may be directly verified by other methods of measurement, which cannot be done in a three-dimensional variant. For this reason, we start the description of the method by describing its application between the solution of a two-dimensional problem and after that we shall consider a problem for space.

We shall begin the analysis with an isometric system of lines; i. e., a system of lines on a plane such that the properties are identical in any direction. Boundary lines of cementite and ferrite in the structure of granular pearlite may serve as examples of such systems on a plane called a microsection; also, lines which separate the graphite constituent and metal base in cast irons with laminar or globular graphite, boundary lines of grains of a single-phase polyhedral structure, etc. It is not important whether the lines of a system form bound contours on a plane (just as in the first two examples) or appear as a continuous grid without breaks in it, as in the case of the polyhedral structure of a pure metal or a solid solution,

which structure consists of equiaxed flat grains. The system will be isometric if separate groups of lines in it have a definite directivity and it is not duplicated in other groups of lines. For example, in the structure of lamellar pearlite on a plane of a microsection, lines which separate the cementite and ferrite phases have a strict directivity to each individual grain. However, this directivity differs for each individual grain of pearlite and, if we are to examine a sufficiently large group of lamellar pearlite grains, that is, its structure as a whole, we shall find no definite direction in which the line of platelets division are preferentially oriented.

The notion of the isometric system may be characterized in a somewhat different way. If all the lines of the system, which generally speaking are curves, are divided into infinitely small intercepts of equal length and all intercepts are grouped with respect to their directivity, then it will happen that each group will have a statistically constant number of intercepts.

The method of random secants on a plane is based on the case of geometrical probability of intersecting a randomly drawn line by a system of lines on a plane (nonisometric case), which in the theory of probability is known as "Buffon's needle problem". In essence, it consists in the following.

A system of equally spaced lines, with the distance between them  $a$  are drawn on a horizontal plane. An intercept of a straight line ("needle") is randomly located in the ruled plane. The length of this intercept,  $l$ , is smaller than the distance between parallel lines,  $l < a$ . Speaking of random location, we have in mind the fact that the middle point of the intercept (the center of the needle) has an equal probability of being at any distance from any line on a plane, and any angle between the needle and the direction of these lines is equally probable. The needle, tossed randomly on a plane as described, may either intersect or not intersect any of the parallel lines on the plane. Inasmuch as the needle is shorter than the distance between the straight lines,  $a$ , it cannot simultaneously intersect more than one straight line (Figure 48).

Thus, as a result of one random toss of a needle, we can demonstrate either the facts of intersection or its absence. It is necessary to determine the probability of intersection by the needle with one of the straight lines on the plane.

In the theory of probability, this problem is solved on the basis of elementary geometrical considerations, which in our opinion would be superfluous here and which are found in any textbook on the theory of probability [101]. The probability of intersection is defined by the formula:

$$p = 2l/\pi a \quad (20.1)$$

If the number of repeated tosses of the needle is large, the number of its intersections with the straight lines on the plane will be defined by the equation:

$$t_1 = pt = (2l/\pi a)t, \quad (20.2)$$

where  $t$  is the total number of tosses of the needle on the plane,  $t_1$  is the number of intersections of the needle with the straight lines on the plane. If we know the distance between the parallel lines on the plane,  $a$ , and the length of the needle,  $l$ , then the validity of formulae (20.1) may be confirmed by experimental determination of the quantity  $\pi$  found in the formula, by repeated tossing of the needle. This was done at different times by several experimenters. The values of  $\pi$  obtained by us, are presented in Table 22 [132].

<i>Experimenter</i> ↑ Экспериментатор	<i>Total no. of throwing needles</i> ↑ Общее число бросаний иглы	<i>Found by an experiment of value of the number of π</i> ↑ Найденное из опыта значение числа π	<i>year</i> ↑ Год
1. <i>Wolf</i> Вольф . . . . .	5000	3,1596	1850
2. <i>Smith</i> Смит . . . . .	3204	3,1553	1855
3. <i>Foks</i> Фокс . . . . .	1120	3,1419	1894
4. <i>Laццарини</i> Лаццарини . . . . .	3408	3,1415929	1901

Table 22

The absolute deviation of experimentally obtained values of  $\pi$  from its true value does not exceed 0.018, that is, about 0.6 per cent of the value which is being determined.

From the viewpoint of the theory of probability, the end result is independent of the shape and location of lines drawn on a plane. The location of lines shown in Figure 48, was needed to obtain the possibility for calculating the geometrical probability of the number of intersections, which would not change as long as the total length of line per unit area of our plane remains the same.

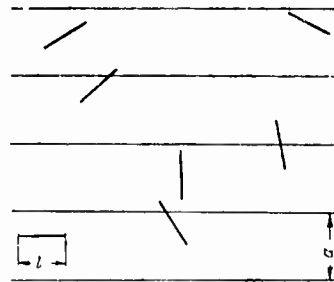


Figure 48. Diagram for Buffon's proposition "about the needle"

It is equally true that an intercept of a straight line (a needle), which is placed on a plane, may be replaced by a line of any length or curvature, or by any rigid contour being rectilinear, curvilinear, smooth or broken, bound or open; it is absolutely the same.

From Equation (20.2) it follows that the mathematical expectation (M. E.) of the number of intersections,  $A$ , when tossing on a plane with a system of parallel equidistant lines (Figure 48), a needle with length  $l$  and the number of tosses of the needle  $t$ , is equal to:

$$M. E. (Z) = (2l/\pi a)t. \quad (20.3)$$

When a rigid contour (or any other straight line) the length of which is equal  $L$ , is substituted for the needle, we can subdivide the former into elementary sections of length,  $l$  each. According to the law of condition of probability, the mathematical expectation of the number of intersections of the contour with the straight lines on a plane is dependent only upon its length and the number of tosses of the contour

on a plane (with a system of lines on the plane being the same) and will be defined by the formula:

$$M. E. (Z) = 2Lt/\pi a \quad (20.4)$$

It is obvious that the product  $Lt$  is equal to the total length of lines intersecting the system of lines on a plane for any number of tosses on it of a rigid contour or any other line of length  $L$ . Here and further in this article we shall designate as  $m$  the number of intersections per unit of the total lengths of the contour (or generally speaking, by any lines, which we shall call random secants) of lines drawn on a plane by lines of the rigid contour (i. e., per unit length of secants). In this case, this number will be defined by the formula:

$$m = \frac{M. E. (Z)}{Lt} = \frac{2}{\pi a} \quad (20.5)$$

It should be noted that in all formulas presented above the value  $1/a$  is the total length of parallel lines drawn on a plane divided by unit area, i. e., the specific length of lines on a plane. Actually, if a square, the side and the area of which equal unity, is isolated on a plane, and two sides of the square are parallel to the grid of lines drawn on a plane, then the length of each intercept of these lines found within the square will be equal to unity and their number within the square will be equal to  $1/a$ . The number of intercepts, other conditions being equal, is determined only by the total length of the lines of the system per unit area, which is also equal to  $1/a$ , and which further in this article we shall designate as  $\Sigma P$  (the total perimeter of lines per unit area measured in  $mm/mm^2$ ). On the basis of the aforesaid, we can rewrite formula (20.5) as follows:

$$m = (2/\pi) \Sigma P = 0.6336 \Sigma P \quad (20.6)$$

Correspondingly, the total length of the lines of the system per unit area will be defined by the formula which further in this article we shall call the basic formula of the method of random secants for a plane:

$$\Sigma P = \frac{\pi}{2} m = 1.571m \quad (20.7)$$

For the actual number of intersections of the lines of a system on a plane by secants, we shall take with respect to  $l$  mm of the total length of all secants. For this reason, the average number  $m$  of intersections per unit length of the secants, obtains the dimension of  $\text{mm}^{-1}$ . The total length of a system of any lines on the plane of a microsection per unit of its area is measured in  $\text{mm}/\text{mm}^2$ , that is, it has the same dimensionality as the number  $m$ . Values  $\sum P$  and  $m$  do not have to be necessarily expressed in millimeters. However, the unit measurements of these two values must be identical. When taking measurements on photomicrographs, it is necessary to consider the actual linear magnification.

Let us derive the basic formula of the method of random secants for a plane.

Let a secant possess a certain <sup>disappearing</sup>  $\lambda$  small width  $\Delta$ , that is, let us consider the large number of extremely narrow bands of equal widths  $\Delta$ , instead of secants on a microsection. The location of these narrow bands is absolutely random but statistically uniform over the entire area of the microsection. They are directed randomly, that is in such a manner that any direction of a band is equally probable. Let us designate the total length of all bands as  $L$ . Inasmuch as their width is equal to  $\Delta$ , the total area of the microsection covered by the band, will be equal to  $L \Delta$ . In this case we are ignoring those sections of the microsection in which bands are superimposed, since the areas of the sections are insignificantly small of the order of  $\Delta^2$  and are numbered as finite and relatively small.

By intersecting the lines of grain boundaries (or some other microparticles), the bands form intercepts these lines which we can accept as straight, inasmuch as the width of bands,  $\Delta$ , is disappearingly small. When in the limit this width becomes zero, the band itself would transform into lines, secants. If the acute angle formed by the direction of bands and lines of grain boundaries, which they intersect, are designated as  $\alpha_1, \alpha_2, \alpha_3 \dots$ , and the length of intercept on the lines of grain boundaries are as  $\lambda_1, \lambda_2, \lambda_3 \dots$ , respectively, then for each of the intercepts it is possible to write an equation of the type:

$$\Delta = \lambda_i \sin \alpha_i. \quad (20.8)$$

For this reason the total length of all intercepts per unit area of the microsection will be called :

$$\sum \lambda/L \Delta = (1/L) \sum_{i=1}^Z \frac{1}{\sin \alpha_i} \quad (20.9)$$

Let us divide and multiply the right half of the latter equation by the number of all intersections,  $Z$ . Here we take into consideration the fact that the ratio  $Z/L$  at a large number of intersections,  $A$ , in the limit at  $\Delta = 0$ , is equal to the average number of intersections of boundary lines by secants per unit length of the latter, that is, it is equal to the number  $m$ , and the ratio  $\sum \lambda/L \Delta$  is equal to the total length of boundary lines per unit area of the microsection, that is, it is equal to  $\sum P$ . Making appropriate changes in the formula (20.9) we derive:

$$\sum P = \frac{m}{Z} \sum_{i=1}^Z \frac{1}{\sin \alpha_i} = Am. \quad (20.10)$$

The quantity, which in formulas (20.10) has been designated as  $A$ , is the average value of the reciprocal of the sine of the angle for all possible values of this angle on the plane with each value being equally probable.

Let us find the value of quantity  $A$  under the condition of equal probability of any value of angle within the limit of zero to  $\pi/2$ .

Let us take a circle, the diameter of which is equal to unity, and the center at the origin of rectangular coordinates. The angle between the shifting radius of the circle and  $x$  axis we shall designate as  $\alpha$ .

Then:

$$y = \sin \alpha = \sqrt{1 - x^2}, \quad (20.11)$$

and the reciprocal value of the sine of angle  $\alpha$  is equal to:

$$1/\sin \alpha = 1/\sqrt{1 - x^2}. \quad (20.12)$$

The unknown quantity  $A$  is equal to the mathematical expectation of the function (20.12) with  $x$  varying between zero and unity. For this reason, by integrating we derive:

$$A = M. O. \left( \frac{1}{\sin \alpha} \right) = \int_0^1 \frac{dx}{\sqrt{1 - x^2}} = \frac{\pi}{2}. \quad (20.13)$$

By inserting the thus calculated value of quantity  $A$  into Equation (20.10) we have the basic formula of the method of random secants for a plane derived analytically:

$$\sum P = \frac{\pi}{2}m = 1.571 m.$$

In the analytical derivation of Formula (20.7), we substituted bands for secants. The width of the bands is the disappearingly small width  $\Delta$ , which in the limit becomes zero and bands become secants. Inasmuch as the width of the bands is disappearingly small and approaches zero, the course of the proof obviously will not be changed if curves, for example, rings with a disappearingly small width but with a finite diameter, are substituted for straight lines (bands). If we can accept  $\Delta \rightarrow 0$ , without committing an error, then the area of the ring is equal to the length of its circumference multiplied by the width  $\Delta$ . This assumption would not change the end result nor change the course of the proof. Hence, it follows that secants may be replaced by any curves and the average number of intersections per unit of their length,  $m$ , is independent of the shape of secants.

It is very important to note a very important prerequisite condition for the analytical derivation of Formula (20.7). The equal probability of all possible values of angle  $\alpha$ , i. e., of the angle at which the secant intersects the line of the system which has been measured. The formula is not applicable if this condition is not observed. This prerequisite condition is fulfilled in the following three instances:

- a. The system of lines on a plane is isometric. Then secants may run in any direction, including a series of usually parallel straight lines disposed at any angle.
- b. The system of lines on a plane is not isometric, i. e., the lines have a definite preferential directivity, but secants are randomly located, i. e., all directions of secants are equally probable.
- c. The system of lines on a plane is isometric and directions of secants are random and any of these directions are equally probable.

In practice, it is frequently convenient to use a circumference or a spiral instead of a straight secant. The convenience of this substitution consists in that the secant conveniently changes its direction with respect to the system of lines on a plane and for this reason any angle at which the secant intersects the lines of the system automatically becomes equally probable, even in the case when the location of the lines on the plane is not random (is oriented) but have a certain directivity (orientation).

Now let us consider cases of practical application of the method of random secants on a plane and of formula (20.7). An ordinary polyhedral structure (ferrite) is shown in Figure 49, linear magnification 100, which completely satisfies the notion of isometricity.

<i>1. Число пересечений <math>m_i</math></i>	<i>2. Число случаев <math>x_i</math></i>	<i>3. Произведение <math>m_i x_i</math></i>
7	—	—
8	4	32
9	10	90
10	24	240
11	32	352
12	34	408
13	22	286
14	2	168
15	4	60
16	3	48
17	1	17
18	—	—
<i>4. Всего</i>	146	1701

Table 23

The true area of the drawing, that is on the plane of a microsection (is one square millimeter). A secant, 100 millimeters long, corresponding to a true length of 1 millimeter is drawn across the area. This straight line intersects the grain boundary lines at 8 points. It is apparent that the number of intersections may be somewhat different at different positioning of the line. However, for each given structure there exists a definite concrete mean value of the number of intersections, which is dependent upon the total length of lines per unit area.

If a straight line is randomly drawn across Figure 49 a large number of times, each time recording the number of intersections between the straight line and the grain boundaries  $m_i$ , it would give a series of values for the number of intersects. The results of 141 "tossings"

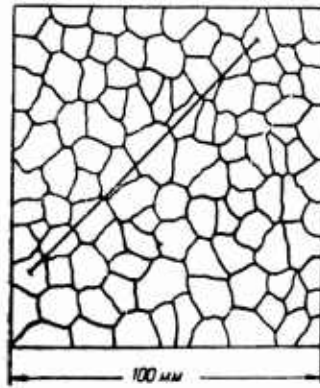


Fig. 49

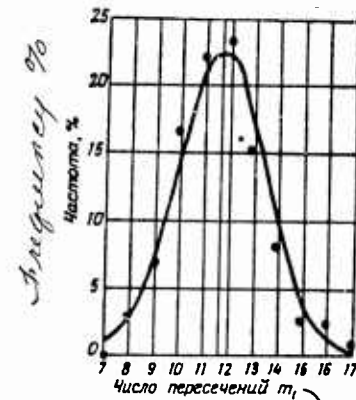


Fig. 50

*Σ n. of intersections m<sub>i</sub>*

Fig. 49. Polyhedral structure and random secant intersecting boundary lines at 8 points

Fig. 50. Curve of frequencies of the ~~numbers and intersections~~ number of intersections by the random secant with the boundary lines of the polyhedrons of Fig. 49

are shown in Table 23. The lines were disposed across the area of the drawing randomly in random directions. The mean number of intersections of secants and boundary lines, according to the data obtained, is equal to

$$\sum L \frac{\pi}{2} m = 1701 : 146 = 11.6 \text{ mm}^{-1}$$

Here the number of intersections,  $m$ , is no longer a random value, which it is when tossing a needle. At a sufficiently high total number of intersections, the number  $m$  approaches a quite definite quantity, the value of which follows from formula (20.7). The frequency curve for the number of intersections, constructed from the data in Table 23, is shown in Figure 50. It is a typical curve of statistical distribution. Consequently, the value of  $m$  may be determined with any accuracy for any concrete system of lines on a microsection. This accuracy is dependent upon the total number of intersections calculated in the course of analyses. It is obvious that this number is proportional to the total length of secants. For this reason, the accuracy for each given structure is singularly determined by a length of the secant. In the example considered above, the number of intersects was 1701 for the length of 146 millimeters (under real conditions, on the plane of the microsection), which is apparent in Table 23.

If the value of the mean number of intersections length of secants,  $m$ , is determined with required accuracy, we further find from formula (20.7) the total length of ferrite boundaries per unit area of the microsection:

$$\Sigma L_{\text{fer}} = \frac{\pi}{2} m = 1.571 \cdot 11.6 = 18.2 \text{ mm/mm}^2.$$

Inasmuch as we have considered the secant as if found in the plane of the microsection and for this reason have assumed its length equal to 1 millimeter (accounting for the magnification), the value obtained is also related to the area of the microsection, that is, it is real. In Figure 49, the length of the secant is 100 millimeters, therefore, the total length of lines in the drawing is 100 times greater than the calculated one and is 1820 millimeters. This may be readily verified with the aid of a curvimeter.

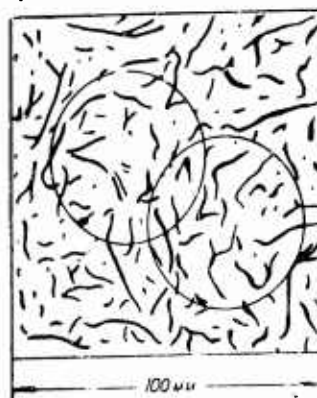


Fig. 51. Circular secants intersecting the graphite ~~precipitations~~ precipitations of grey cast iron

In order to use a circular secant, a circle is marked on cellophane and the diameter of which is measured as accurately as possible. After that, the cellophane is superimposed on the drawing or microphotograph of the structure which is being analyzed and the number of intersections of the circumference with the system of lines, which is of interest to us, is calculated. Calculations are repeated, each time shifting the circumference over the photomicrograph.

Calculations, similar to the one described, was done by us for the structure of graphite flakes in grey cast iron and are shown in Figure 51, and the magnification of 100, the aid of circular secant 50 mm in diameter on a drawing or 0.5 mm in diameter on a microsection. We wish to underline the fact that in this case we calculated precisely

the number of intersected flakes and not the interface boundaries "metal base--graphite." For this reason in our further calculations we shall derive a value for the total length of cross sections of graphite flakes and not the length of interface boundaries which will be approximately twice as large as the one found.

The mean number of intersections of the circumference and cross sections of graphite flakes, on the drawing, was 15.6, the number of different positions of the circumference being 170.

Taking into consideration the fact that the length of the secant in this case is equal to the perimeter of the circumference, the real diameter of which is 0.5mm, we find the mean number of intersects per 1 mm of length of secants, is

$$m = \frac{15.6}{0.5\pi} = 10.0 \text{ mm}^{-1}$$

Further, from Formula (20.7) we find the unknown value of the total length of cross sections of graphite flakes per unit area of the micro-section:

$$\Sigma L_{gr} = \frac{\pi}{2} m = 1.571 \cdot 10.0 = 15.71 \text{ mm/mm}^2 .$$

In order to determine the length of lines, which separate the graphite and metal base in cast iron, the number of intersections obtained should be doubled. Therefore, the total length of boundary lines "metal base - graphite" will be 31.42 mm/mm<sup>2</sup> of the microsection.

The examples considered demonstrate the application of the method of random secants for the determination of the length of lines on structural sketches or photomicrographs. For a structural analysis directly under the microscope, which in practice is most common, one of the following methods is used.

By the first method, one field after another of the structure is examined through the ocular-micrometer (Figure 13) and the number of intersections between the diameter line of ocular scale and lines of the structure, which is of interest to us, is calculated in each field of vision in the microsection. The fields of vision in this case must

be disposed uniformly over the field of the microsection and should encompass its entire area. After that, having determined the length of the image of the ocular scale on the plane of the microsection,  $\lambda$  in mm, with the aid of the object-micrometer, and knowing the fields of vision,  $Z$ , which have been examined in the course of the analyses, we find the total length of secants,  $\lambda Z$ . After that, the total number of intersections calculated for all examined fields of vision, is divided by  $\lambda Z$  and the mean number of intersects per 1 mm of secants,  $n$ , is obtained. Further, from Formula (20.7) the specific length of boundary lines on the microsection is calculated.

By the second method, the structure is examined through the ocular with a cross hair. By continually shifting the microsection along a straight line, using the micrometer screw of the carriage on the microscope stage, we simultaneously calculate (in the head or with the aid of an ordinary counter) the number of times the boundary lines, which are of interest to us, pass the point of the cross hair of the ocular. Having completed the examination along one line of one edge of the microsection to another, the length of the path, recorded by this scale and by the head of the micrometer screw, is jotted down and the operation is repeated along the second line, etc. Thus, the examination uniformly encompasses the entire area of the microsection. Having divided the total number of intersects, calculated for the entire analyses, by the total length of microsection displacement, we derive the number  $n$ , after which we calculate the specific length of boundary lines on the microsection from (20.7).

By the third method, a straight line, a circumference, or a spiral is marked on the ground glass of the microscope camera and the determination is carried out in the same manner as on a photomicrograph or a sketch.

From the examples described, it is possible to compute that the method of random secants is one of the least effort consuming methods among other methods of stereometric metallography. Of the methods considered above, the second method, which is reduced to a simple displacement of the microsection and simultaneous calculation of the

number of intersects, is the most effective. Calculations may be carried on at a rate of an ordinary oral count. When using a counter, they may be even more rapid. In one minute it is possible to record 100 to 120 intersections. For this reason, an analysis, for example, of 1,000 points, takes up only about 10 minutes. As we have already mentioned, the total number of intersections obtained during the analysis determines the accuracy of the obtained results. A technique for choosing the required number of intersections, varying with requirements of precision and reliability of the analysis by the method of random secants, will be presented further in this article.

Section 21. Nonisometric Systems of Lines on a Plane and Their Characteristics

The systems of boundary lines, which separate the crosssections of microparticles on a plane of microsections and which are <sup>practically</sup> observed in alloys and <sup>pure metals</sup>  $\Lambda$ , are far from being always isometric. Cold plastic deformation of metal and frequently hot deformation at sufficiently temperature, (of directed crystallization) transcrystallization (certain other causes are responsible for the presence of certain preferential directivity or orientation of boundary lines on a plane. In contrast to isometric systems, these systems of lines we shall call oriented. Moreover, systems may be completely oriented or oriented only partially. If lines of an oriented system are divided into elementary sections of a very small but equal length, which we shall assume to be straight, then it may happen that all sections are parallel to one or several definite lines which we shall call the orientation axes of a system of lines on a plane. In this case, a system of lines is regarded as completely oriented on one or in several directions, that is along one or several orientation axes.

Several different variants of completely oriented systems of lines, having one orientation axes, are schematically drawn in Figure 52. In this case all lines are usually parallel, which is the only condition which defines a system as completely oriented with one axis. The lines themselves may be continuous or interrupted and the distance between parallel lines may be either constant or not constant. One type of a completely oriented system of lines with the one orientation axes is, specifically, a system of equidistant parallel straight lines, shown in Figure 40A.

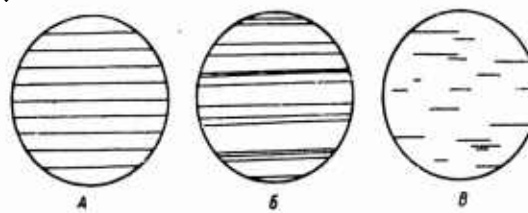


Fig. 52. Completely oriented systems of lines on ~~MM~~ a plane with one axis of orientation

Among the structural elements of metal alloys, the case of the complete orientation where one axis has been observed relatively infrequently. For example, usually parallel rectilinear fine fibers of plastic nonmetallic inclusions, elongated by rolling or drawing, may be cited. They may be observed in the longitudinal cross section of a rod or wire.

A system of boundary lines of nonmetallic inclusions <sup>in</sup> a free-cutting steel corresponds almost precisely to a diagram shown in Figure 52C. The axes of a rod is the orientation axis in such structures.

Another type of complete orientation of lines on a plane, with two orientation axes, is shown schematically in Figure 53. The angle formed by the orientation axes may be a right angle or an acute angle. The distance between the lines, parallel to one of the orientation axes, may be constant or may vary. Lines themselves may be continuous or interrupted. In this case, a system of lines may be regarded as consisting of two completely oriented systems with one orientation axis (Figure 52) which are superimposed in such a manner that the orientation axes form at an <sup>appropriate</sup> angle.

The type of the system of lines oriented in two directions described above, has been observed almost in its pure form in metal structures in individual grains during their recrystallization when the dendrite axes of different orders form a definite angle in the plane of the microsection. Another case of almost complete orientation along two usual perpendicular lines may be observed in several photomicrographs in Ya. R. Raucin and Sh. R. Zheleznyakova's studies [133].

Further, let us consider a case of complete orientation along three axes disposed at an angle of 120 degrees to each other. The regular geometrical systems of lines of this kind, an isogonal grid of regular hexagons deserves attention. It was used by a laboratory of Timken plant for constructing a first scale for the grain size of steel [134]. Here the size of the hexagons that appear as 3 systems of equidistant, parallel, interrupted straight lines, which are superimposed in such a way that the orientation axes of any one system form an angle of 120 degrees with the other two axes. An absolutely similar orientation is

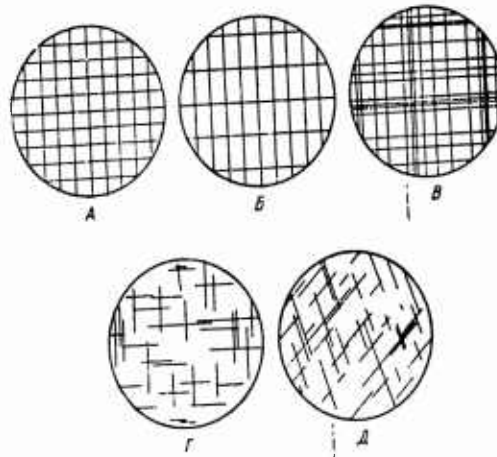


Fig. 53 ~~CM~~ Completely oriented systems of lines on a plane with two axes of orientation.

found in a grid constructed from regular triangle. It differs from the preceding one in that the lines which form it are continuous. The length of lines are oriented in three directions, is the same with both of these systems shown in Figures 54A and B. At the same time, with the number of orientation axes exceeding one, there is always a possibility of a relatively greater length of lines in one or several directions than in other directions. Generally speaking, a different degree of orientation is possible along each axis which exists in a given system. These is, for example, the isogonal grid, shown in Figure 54C, also with 3 orientation axes, but the length along two axes perpendicular to each other is less than the length along the third axis which is disposed at an angle of 45 degrees to the first two axes [135].

The greater number of orientation axes in a system, the closer it is to the isometric plane of the line systems which may be regarded as having an infinitely large number of orientation axes. Thus, for example, when isogonal grid, shown in Figure 55, having only 6 orientation axes, resembles a system of boundary lines of an ordinary polyhedral structure with equiaxed grain (see Figure 49).

In plane crosssections of real structures, the boundary lines of microparticle crosssections are usually either isometric or only par-

tially oriented systems. Completely oriented boundary line systems occur as an exception. The partial orientation of a system of lines on a plane we understand to mean such systems of lines in which only a part of the total length of lines is oriented in a definite line, or more frequently being parallel only to one orientation axes. Thus, Figure 56 shows structures of hot rolled steel annealed at different temperatures. It is quite obvious that in both cases a quite definite directivity of grain boundary lines of ferrite may be observed. However, this orientation is incomplete in contrast to the schemes as shown in Figures 52, nor does it approach completeness in any way. A typical example of a partially oriented system of lines on a plane, when not all lines of a system but only a certain portion of the total length of grain boundary lines of ferrite is parallel to the orientation axis, which axis in this case corresponds to the direction of rolling, is shown in Figure 56.

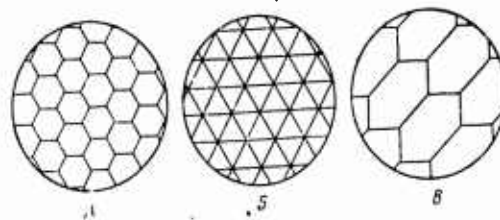


Fig. 54. Completely oriented systems of lines on a plane with three axes of orientation

Besides the fact that partial orientation of boundary lines is present in both structures, shown in Figure 56, we also note that the relative length of the oriented portion of lines in the structure in the drawing at the left is considerably greater than in the drawing on the right. In other words, the degree of orientation of boundary lines in steel annealed at 600 C is notably greater than in steel annealed at 350 C.

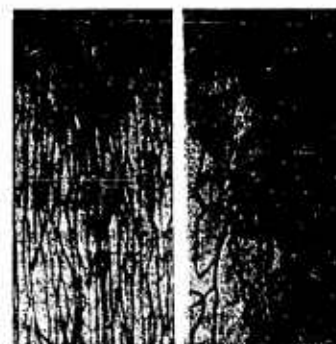
Quantitative determination of the degree of partial orientation

is quite effective and many times attracted the attention of the metallographers. As far back as 1900 studying the deformation of mild steel in the cold state from Y. Geyn measured the visible length and width of ferrite grains [136]. Later, F. Rapaggs made an attempt to determine the magnitude of a reduction of alloyed steel by forging from the degree of deformation (elongation) of the carbide which was characterized by a ratio between the length of cells on the network and their width [137]. F. Rapaggs correlated the value of this ratio of to the degree of the reduction through a special formula.

The degree of orientation of a system of lines in a plane may be estimated quantitatively by a value which is the ratio of the oriented portion of lines to their total length; this evaluation seems natural. This is necessary to have a possibility to determine separately the aforementioned values, whereas the method of random secants makes it possible to determine only the total length of lines of a system in its area.



55



a

b

56

Fig. 55. Isogonal lattice with 6 axes of orientation

Fig. 56. Examples of partial orientation of lines of grain boundaries of industrial iron tempered at 600° (a) at 850° (b) [217]

If the oriented portion of lines is removed, then the remaining portion of lines of the system will be isometric. The validity of this supposition and its hardnability, at least for practical purposes of geometric metallography, has been demonstrated by us on a number of examples [138]. For this reason, a partially oriented system of

lines on a plane may be regarded as consisting of two superimposed system, of which one is particularly oriented and the second is completely isometric. For this case, the numerical expression for the degree of orientation of the system of the lines of a plane, providing it has one orientation axis, will be determined in per cent from the formula

$$\alpha = \frac{\sum P_{or}}{\sum P_{or} + P_{is}} 100\% \quad (21.1)$$

where  $P_{or}$  is the specific length of the oriented portion of lines,  $\text{mm}/\text{mm}^2$ ;  $P_{is}$  is the specific length of the isometric portion of lines,  $\text{mm}/\text{mm}^2$ .

It should be noted that when dividing the lines of a system into elementary sections of equal length, for the purpose of determining which of them are oriented and which are isometric, we can assume these elements infinitely small as to length. For this reason, predetermination of the degree of orientation by the method described above, is applicable not just to systems in which the rectilinear sections of boundary lines, parallel to each other (as in Figure 56), are clearly distinguishable. The degree of orientation may be also determined in such systems of lines which consist of small curves *not containing* rectilinear elements, for example, in a system of ellipses on a plane, the large axes of which are usually parallel.

A method for measuring the total linear length of lines of any system on a plane by the method of random secants is presented in Section 20. Now, the notion "isometricity" of a system of lines may be elaborated from the viewpoint of this method. If from any random point on a plane, on which a system of lines is drawn, straight lines (secants) are drawn in all possible directions, then the mean number of intersections per unit length of each straight line would have the same mean, statistically constant, value as an isometric system of lines on a plane. In other words, the mean number of intersections per unit length of secants in an isometric system of lines is independent of the direction of the secant.

The more visual characteristics of the orientation of the system

of lines on a plane is afforded by "the rose of the number of intersections" which shows the actual relationship between the mean and number of the intersections per 1 mm of length of the secant and its direction, constructed in polar coordinates. From the aforesaid, it is obvious that for any isometric system of lines on a plane the rose of the number of intersections is described by a circumference with its center at the origin of polar coordinates.

The shape of the rose of the number of intersections is quite sensitive to the presence of *small* preferential directivity of line systems. In those cases when the degree of directivity is insignificant and cannot be observed visually, the rose of the number of intersections doesn't deviate from its circular shape.

The experimental construction of the rose of the number of intersections is quite simple. A series of initially parallel secants, forming a definite angle  $\alpha$  with the orientation axis, is drawn upon a microsection or a photomicrograph, providing that the direction of the axes may be clearly determined by visual observation or the topography of the plane of the microsection. Thus, for example, it is possible that to assume that the orientation axes on the longitudinal microsection of a rod or a wire coincides with their geometrical axes. Secants of a given group are randomly distributed but uniformly over the entire surface of the microsection or over the area of the photomicrograph; directions of all secants must be exactly the same with the respect to the orientation axis. Having determined the mean number of intersections per 1 mm of secants in a given direction,  $m_{\alpha}$ , the next group of secants is drawn but in a different direction, etc. Having derived a number of values of mean numbers of intersections for many directions of a plane, the rose of the number of intersections is constructed. For this purpose, the radii-vectors, which form the same angles with the O-O axis as were formed by individual groups of secants and the orientation axes, are drawn from the origin of coordinates. The length of each radius-vector expresses, on a definite scale, the values of mean numbers of intersections for corresponding directions of secants.

After that, the ends of radii-vectors are connected by a smooth curve which is precisely the rose of the number of intersections constructed from the data of the experiment.

The rose of the number of intersections for the polyhedral structure of almost pure iron with equiaxed grains is shown in Figure 57. The circular shape of the rose indicates that the system of boundary lines of ferrite in this case is actually isometric. The rose of the number of intersections was constructed similarly for the system of ferrite lines of rolled sheet, on a microsection, the plane of which was perpendicular to the plane of the sheet, has an entirely different shape. In this case, the O-O axis of the graph coincides with the direction of rolling, which is precisely the orientation axis of ferrite grain boundaries. The rose, shown in Figure 58, has one maximum of the number of intersections in the direction perpendicular to this axis, (that is, to the plane of the sheet) and one minimum in the direction that which coincides with the orientation axis O-O, as shown by the values of the respective radii-vectors.

Upon the basis of our assumption, according to which partially oriented system of lines may be regarded as consisting of two superimposed systems, of which one is completely oriented and the second is completely isometric, the plot of the rose of the number of intersections may be calculated.

For this purpose it is necessary to measure how many microsection mean and numbers of intersections on the in tool and not in many directions (as is the case in a system of lines with one orientation axis, which is a more common case in real structures on plane).

The orientation of lines of a system on a plane may be characterized not graphically, not by the shape of the rose of the number of intersections, which generally speaking, is practically inconvenient, but by one definite number which characterizes the degree of orientation in conjunction with Formula 21.1. Two groups of secants, forming a right angle (in systems with one orientation axis), are used both for calculating the plot of the rose of the number of intersections and for determining the degree of orientation. Inasmuch as in this method

the secants are not randomly directed, but have a quite definite direction, we have called the method of using these secants the method of directed secants.

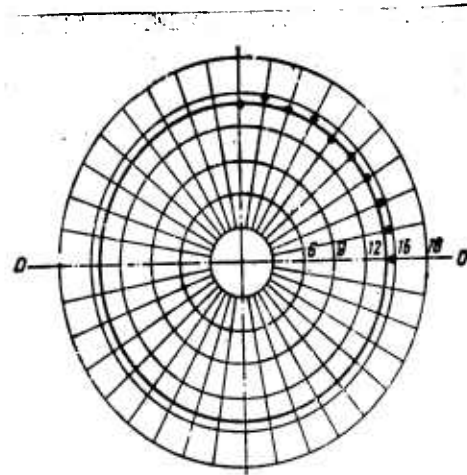


Fig. 57. Plane rose of the number of intersections for the system of boundary lines of the grain of industrial iron with equiaxial grain

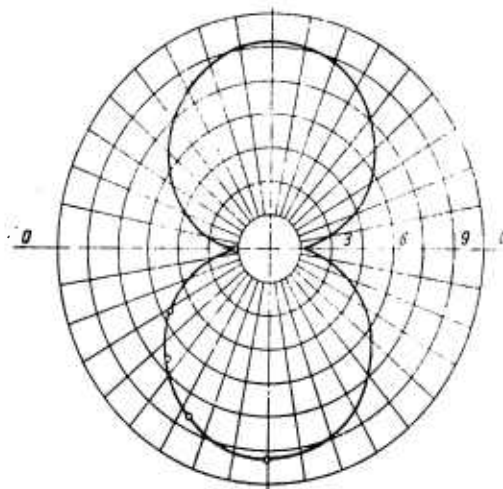


Fig. 58. Plane rose of the number of intersections for the system of boundary lines of the grain of industrial iron deformed by rolling (on a microsection of sheet iron)

Section 22. The Method of Directed Secants and the Analyses of  
Partially Oriented Structures on a Plane

Let us consider a system of mutually parallel and equidistant lines, shown in Figures 48 and 52A. There the number of intersections of the secant and the grid lines of the system, depending upon the angle formed by the secant and the orientation axis, is expressed by the formula

$$m = \frac{\sin \alpha}{a} - mm^{-1}, \quad (22.1)$$

where  $a$  is the distance between parallel lines and  $\alpha$  is the angle formed by them and the secant.

Secants directed parallel to the orientation axis would not run into a single line of the system and for this reason the number of intersections  $m_0$  or  $m$  will be zero. Conversely, secants directly perpendicular to the orientation axis will run into the greatest number of lines of the system and a number of intersections,  $m_{90}$  or  $m_1$ , will happen to be greater than at any other direction of secants. The graph of the relationship, expressed by the Formula (22.1) is plotted in polar coordinates in a form of two circumferences of equal diameter opposite to each other and the orientation axis 0-0 at the origin of coordinates, as shown in Figure 59. The shape shown in Figure 59 is the rose of the number of intersections for the given case and the diameters of circumferences, which comprise it, correspond to the maximum number of intersections per 1 mm of the secant,  $m_{90}$  or  $m_1$ . The rose of the number of intersections of this type occurs for all systems of lines on a plane which are completely oriented and possess only one orientation axis (Figure 52 a, b, and c).

For a system of lines which has two orientation axes located at right angles to each other forming a continuous grid of identical squares (Figure 53A), or rectangles (Figure 53B), may be regarded as consisting of two systems of parallel and equidistant straight lines, the orientation axes of the systems being usually perpendicular. For each system separately the number of intersections, which is dependent upon the di-

rection of the secant, is expressed by the Formula (22.1). By applying the rule of the addition of means, for the entire system, we derive a relationship between the number of intersections and direction:

$$m_{\alpha\beta} = \sin\alpha/a + \sin\beta/b \text{ mm}^{-1} \quad (22.2)$$

where a and b are the distances between parallel lines in each system;  $\alpha$  and  $\beta$  are angles formed by the secant and corresponding orientation axis of both systems.

If degrees of orientation are identical in directions of both axes, that is, the system is a grid composed of squares (Figure 53A) values of a and b are equal. Moreover, taking into consideration, the fact that there is perpendicularity of orientation axes, the sum of  $\alpha$  and  $\beta$  angles is 90 degrees. We simplify the Formula (22.2) for the case of square grid:

$$m_{\alpha} = (1/a) [\sin\alpha + \sin(90-\alpha)] \text{ mm}^{-1} \quad (22.3)$$

The rose of the number of intersections for a square grid (Figure 53A), calculated from this formula, is shown in Figure 60.

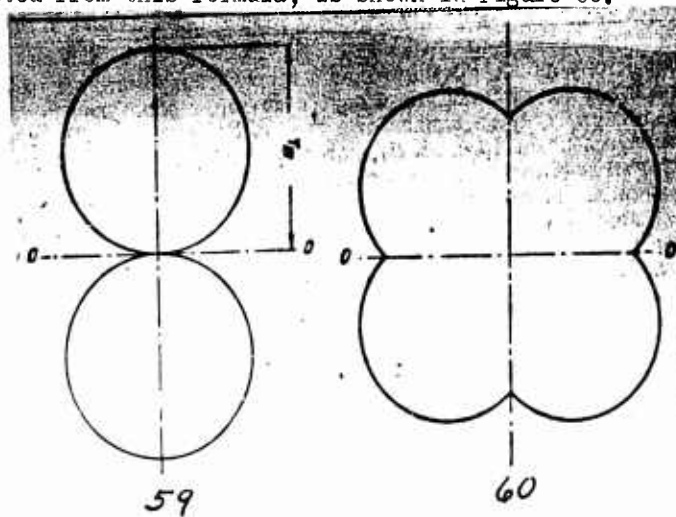


Fig. 59. Plane rose of the number of intersections for the completely oriented system of lines with one axis of orientation

Fig. 60. Plane rose of the ~~MMMM~~ number of intersections for the completely oriented system of lines with two mutually perpendicular axes or orientation with identical degree of orientation along both axes (square lattice)

The maximum number of intersections occurs in the direction which forms an angle of 45 degrees with both orientation axes.

The rose of the number of intersections for a system of lines, formed by different, oriented groups of mutually parallel and equidistant

straight lines, may be readily constructed graphically without calculations from Formulas (22,1)-(22,3). For example, let us consider the construction of the rose of the number of intersections for the system of regular rectangles, shown in Figure 53B. The distance between horizontal straight lines we shall designate as  $a$  and the distance between vertical lines as  $b$  ( $a > b$ ). First let us construct two separate roses for the number of intersections for each system of straight lines, horizontal and vertical.

For the system of horizontal lines, the rose of the number of intersections will be comprised by two circumferences with diameters  $a$ , which will be tangent to each other and to the axes of horizontal orientation, at the origin of coordinates. Similarly, the rose of the number of intersections for the system of vertical lines formerly described by two circumferences, the diameters of which are  $\frac{1}{b}$ , is tangent to each other and the axis of vertical orientation at the origin of coordinates.

rose of the number of intersects shown in Figure 61, where two circumferences (1) are for the system of horizontal lines and two circumferences (2) are for the system of vertical lines. Further, we add the radii-vectors of both roses of the number of intersections for each direction and thus obtain the radii-vector, the length of which correspond to the total number of intersections in the same direction. By connecting the ends of the total radii-vectors with a smooth curve, we obtain curve three which is precisely the contour of the rose of the number of intersections for a system of lines forming a plane grid of rectangles (in plotting, the ratio of the height of rectangles to their width was taken  $\frac{a}{b} = 2$ ).

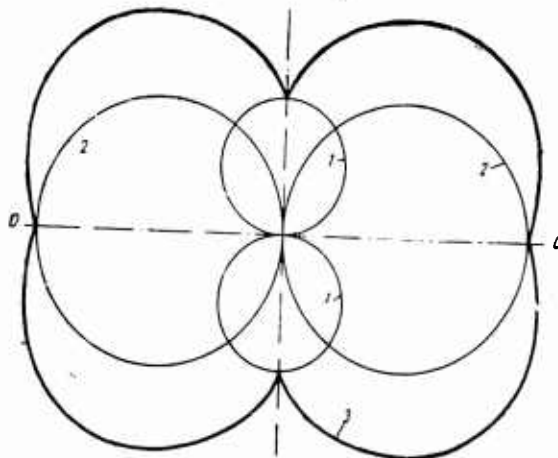


Fig. 61. Graphic construction of the flat or plane rose of the number of in-

tersections for the completely orientated system of lines with two mutually perpendicular axes of orientation. The orientation along each of the axes is different (rectangular lattice)

A graphic plotting of the rose of the number of intersections, similar to the one just described, was made by us for the case of uniform orientation of lines of a system with three orientation axes located at an angle of 120 degrees to each other. This plot, which is valid for isogonal grids made up of regular hexagons (see Figure 45A) or triangles (Figure 54B), is shown in Figure 62.

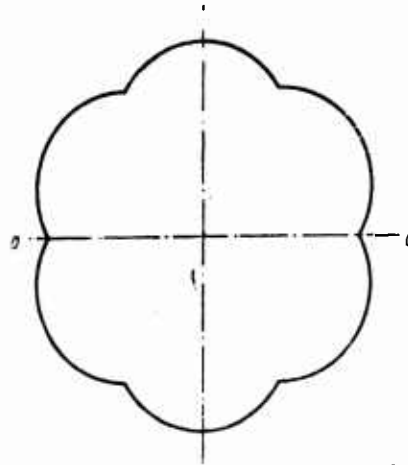


Fig. 62. Plane rose of the number of intersections for the fully oriented system of lines with three axes of orientation placed at an angle of 120°. The degree of orientation along all three axes is identical. (lattices from regular hexagons or triangles)

As the number of orientation axes is increased further, the shape of the rose of the number of intersections approaches still closer to a circumference. Therefore, an isometric structure may be regarded as one that does not have orientation axes, as well as one that has an infinitely large number of axes.

Let us examine the analytical and the graphical construction of the rose of the number of intersections partially oriented structures and their types for systems of lines of this type, which are more commonly encountered in practice.

Let a partially oriented system of lines be comprised of two systems, the oriented system and the isometric system. The number of intersections of the secant with the oriented portion of lines of the system is defined, depending upon the direction, by Formula (22.1). It is known (See Section 20) that the value of  $\frac{1}{a}$  is equal to the specific length of the oriented portion of the lines of the system,  $P_{or}$  mm/mm<sup>2</sup>. Therefore, we can rewrite Formula (22.1) as follows:

$$m'_{\alpha} = \sin \alpha \cdot \sum P_{or} \text{ mm}^{-1} \quad (22.4)$$

where  $m'_{\alpha}$  is the number of intersections of the secant with only the oriented portion of lines per 1 mm of its length.

The number of intersections of the secant and the isometric portion of the lines of the system is defined by the Formula:

$$m'' = \frac{2}{\pi} \sum P_{is}. \quad (22.5)$$

In that case the total number of intersections in a given direction will be:

$$m_{\alpha} = m'_{\alpha} + m'' = \sin \alpha \cdot \sum P_{or} + \frac{2}{\pi} \sum P_{is}. \quad (22.6)$$

From Formula 22.6 it is possible to plot the rose of the number of intersections, knowing the length of the oriented and isometric portion of a system of lines.

The graphical plot of the rose of the number of intersections for partially oriented systems of line is even simpler. For this purpose we have to know two values, measured on the plane of the microsection — the mean number of intersections of the oriented portion of lines of a system with the secant perpendicular to the orientation axis,  $m'_{90}$ , and the mean number of intersections for the isometric portion of lines of a system,  $m''$ . If we know the specific lengths of both portions of lines of a system,  $\sum P_{or}$  and  $\sum P_{is}$ , we can calculate the values we need from Formulas (22.4) and (22.5), respectively.

From the first of these values, we plot the rose of the number of intersections for the oriented portion of lines. It will be described by two circumferences, the diameters of which are  $m'_{90}$  tangent to the orientation axis at the origin of coordinates (see Figure 59).

In using the second value, we plot the rose of the number of intersections for the isometric portion of lines of the system. It will be a circumference with its center at the origin of coordinates. The radius of the circumference will be  $m''$  (see Figure 57).

The rose of the number of intersections for a partially oriented system of lines, as a whole, we shall derive just as before by adding

radii-vectors of the plotted auxiliary rose for each direction. In the plot shown in Figure 63, it has been assumed that the specific length of the oriented portion of the lines is  $3/4$  and that of isometric portion is  $1/4$  of the total specific length of the lines of the system as a whole.



Fig. 63. Graphic construction of the plane rose of the number of intersections for the partially oriented system of lines in accordance with the the numbers of intersections on secants parallel and perpendicular to the axis of orientation.

To have an accurate comparison between contours of theoretically calculated and experimentally plotted roses of the number of intersections for partially oriented systems of lines, it is necessary to determine directly on the microsection the mean numbers of intersections of secants with oriented and isometric portions of lines of a system separately.

Let us examine the partially oriented system of ferrite boundary lines shown in Figure 56. Secants, directed parallel to the orientation axis of boundary lines, do not intersect those elements of boundary lines which are parallel to these secants, i. e. is, they have the same direction as the orientation axis of the system. Hence, it follows that secants directed parallel to the orientation axis intersect only the lines of the isometric portion of considered systems of boundary lines.

Therefore, the number of intersections determined on the secants parallel to the orientation axis, will be the actual number of intersections with the isometric portion of lines of a system in any direction and, in accordance with the symbols accepted previously, will equal:

$$m'' = m_{\parallel} \text{ mm}^{-1},$$

where  $m_{||}$  is the mean number of intersections of the directed secant, parallel to the orientation axis, per 1 mm of its length.

On the basis of this value it is possible to determine directly the length of the isometric portion of lines of a partially oriented system on a plane:

$$\sum P_{is} = \frac{\pi}{2} m_{||} = 1.571 m_{||} \text{ mm/mm}^2. \quad (22.8)$$

The second group of secants are directed perpendicularly to the orientation axis and the mean number of intersections per 1 mm of their length is designated as  $m_{\perp}$ . This number is obviously made up of the number of intersections of the isometric portion of lines of the system,  $m_{\perp}$ , and with the oriented portion of lines,  $m'_{90}$ . Therefore, the number of intersections with only the oriented portion of lines and the secant directed perpendicular to the orientation axis will be

$$m'_{90} = m_{\perp} - m_{||} \text{ mm}^{-1} \quad (22.9)$$

Later we shall prove that the specific length of lines, completely oriented along one orientation axis of a system, is precisely equal to the mean number of intersections per 1 mm of length of the secant directed perpendicular to the axis, that is

$$\sum P_{or} = m'_{90} = m_{\perp} - m_{||} \text{ mm/mm}^2. \quad (22.10)$$

Thus using two groups of secants, of which one is directed parallel to the orientation axis and the second is perpendicular to it, will determine independently the mean number of intersections for lines of the oriented and isometric portions of a system. Formulas 22.8 and 22.10 make it possible to measure separately the specific length of the oriented and the isometric portions of lines of the system themselves. The total length of all lines of a partially oriented system of lines on a plane will be defined by the Formula:

$$\sum P = \sum P_{is} + \sum P_{or} = m_{\perp} + 0.571 m_{||} \text{ mm/mm}^2. \quad (22.11)$$

Knowing the same two values, determined by calculating the intersections on the microsection in two mutually perpendicular directions,

$m_{\perp}$  and  $m_{\parallel}$ , it is possible also to calculate the degree of orientation of lines of a system using (Formula 21.1), taking into account Formulas (22.8) and (22.10), as converted to the following formula:

$$\alpha = \frac{P_{or}}{P_{or} + P_{is}} 100 = \frac{m_{\perp} - m_{\parallel}}{m_{\perp} + 0.571 m_{\parallel}} 100\% \quad (22.12)$$

Now we shall illustrate from a concrete example the application of the method of directed secants to a partially oriented system of boundary lines, which has been proposed previously. The system of lines is shown in Figure 64. It is a system of boundary lines of silicon ferrite grains on a microsection of transformer steel. The plane of the microsection is perpendicular to the surface of the steel sheet and parallel to the rolling direction. The number of intersections on secants lying perpendicular and parallel to the orientation axis:

$$m_{\perp} = \frac{792}{34} = 23.3 \text{ mm}^{-1} \quad \text{and} \quad m_{\parallel} = \frac{378}{50} = 7.6 \text{ mm}^{-1}. \quad (22.13)$$

1. *m. of inter-  
actions on  
1 cm secant*  $m_i$   
2. *m. of  
occurrences*  $x_i$   
3. *Product*  $m_i x_i$

1. Число пересечений на 1 мм секущей $m_i$	2. Число случаев $x_i$	3. Произведение $m_i x_i$	1. Число пересечений на 1 мм секущей $m_i$	2. Число случаев $x_i$	3. Произведение $m_i x_i$
А. Секущая перпендикулярна оси ориентации			Б. Секущая параллельна оси ориентации		
20	—	—	4	1	4
21	1	21	5	4	20
22	2	44	6	9	54
23	5	115	7	10	70
24	6	144	8	11	88
25	8	200	9	8	72
26	5	130	10	4	40
27	3	81	11	3	33
28	1	28	12	—	—
29	1	29	Всего	50	378
Всего	34	792			

A. Secant perpendicular to the orientation axis  
B. Secant parallel to the orientation axis.  
Table 24

Using Formula (22.8) we find the specific length of lines the positioning of which is isometric:

$$P_{is} = 1.571 \cdot 7.6 = 11.9 \text{ mm/mm}^2.$$

From Formula (22.10) we find the oriented portion of the boundary line per unit area of the microsection:

$$P_{or} = 23.3 - 7.6 = 15.7 \text{ mm/mm}^2 .$$

The total length of grain boundary lines is equal to the sum of separately determined values, that is  $27.6 \text{ mm/mm}^2$ . The degree of orientation of boundary lines, in Figure 64, we determine from Formula (22.12) :

$$\alpha = \frac{(23.3 - 7.6) 100}{23.3 + 0.571 \cdot 7.6} = 57\% .$$

Using here the values obtained for the mean numbers of intersections,  $m_x$  and  $m_y$ , we can plot the rose of the number of intersections for the structure shown in Figure 64, that is, we can determine graphically the relationship between the number of intersections per 1 mm of the directed secant and its direction, with respect to the orientation axis. The plot is shown in Figure 65. Only one quadrant of the polar system of coordinates is shown, inasmuch as the configuration of the rose of the number of intersections is symmetrical with respect to the coordinate axes.

The mean numbers of intersections in two mutually perpendicular directions can be measured as directly on the microsection. This can be carried out most conveniently in an apparatus for the determination of microhardness, PLT-3 with the ocular that has the cross hair.

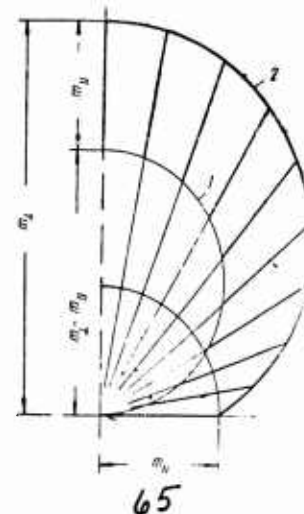
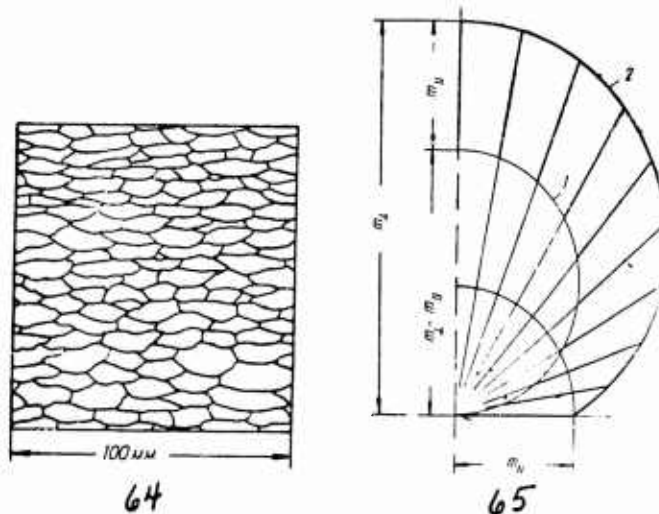


Fig. 64. Partially orientated system of lines of grain boundaries of silicon ferrite of sheet transformer steel

Fig. 65 Graphic construction of the plane rose of the number of intersections for the system of boundary lines of the grain of silicon ferrite (Fig. 64)

Section 23. The Rule of Total Projection for a Plane and the Verification of the Method of Directed Secants

For the verification of relationships between true parameters of a plane structure and parameters measured in quantitative microanalyses, what is frequently feasible is to calculate in advance the parameters subject to measurement and after that to compare the values obtained with actual measurements.

Let us assume that it is necessary to determine the total length of fibers of plastic nonmetallic inclusions, stretched out along the direction of rolling, on a longitudinal microsection. An area of a microsection, magnified one hundred times, is drawn schematically in Figure 66. The actual dimension of this area (on the microsection) is  $1 \times 1 \text{ mm}^2$ . Let us draw on this sketch a network of equidistant parallel lines perpendicular to the orientation axis of fibers. We assume that these lines are directed secants. The distance between adjacent lines is taken equal to  $\Delta$ . Thus, we have a number of narrow strips  $\Delta$  wide and 1 mm long. The number of strips (or secants) on the area in Figure 66 is obviously equal to  $\frac{1}{\Delta}$ .

Now let us calculate the number of intercepts of fibers of nonmetallic inclusions in each strip. If there shows only a fraction in the strip width, (that is, the end of fiber falls within the strip) we count it in providing that this fraction is greater than  $0.5 \Delta$ , and neglect it if it is not. Let us assume that the first strip has  $\alpha$  number of fibers  $n_1$ , the second one has  $n_2$ , the third has  $n_3$ , etc. In that case the sum of lengths of all intercepts of inclusions in the first strip is  $n_1 \Delta$ ; in the second it would be  $n_2 \Delta$ , etc. The total length of all fibers of nonmetallic inclusions in the area of Figure 66 (that is, per  $1 \text{ mm}^2$  of the microsection) would be:

$$\begin{aligned} \sum P_{\text{or}} &= \Delta (n_1 + n_2 + n_3 + \dots) = \\ &= \frac{n_1 + n_2 + n_3 + \dots}{(i : \Delta)} = \frac{n_1}{1} \text{ mm/mm}^2. \end{aligned} \quad (23.1)$$

The value  $\left(\frac{1}{\Delta}\right)$ , found in the denominator, is equal to the number and length of strips (secants) on the area of  $1 \text{ mm}^2$ ; in the numerator is the

total number of intercepts, which is equivalent to the total number of intersections of directed secants and fibers of nonmetallic inclusions in an area  $1 \text{ mm}^2$ . Hence, it follows that the total length of inclusions elongated by rolling per unit area of longitudinal microsection is equal to the mean number of intersections of inclusions and secants, directed perpendicular to the orientation axis of fibers, per 1 mm of length of these secants.

We have derived in Section 22 an equation, identical to Formula (23.1), for a system of parallel equidistant lines, where the validity of this relationship is obvious. Now we can see that the same relationship is valid for a system of parallel lines whose length and location on a plane may be random. Previously, when deriving Formula (22.10), we already used the relationship now obtained.

Let us consider another system of lines, consisting of a number of closed contours of different configurations and of other sections of straight lines and curves, disposed randomly, as shown in Figure 67. In Figure 67 we take the abscissa as the axis to which we project all the lines of the drawing. In this case we consider not ordinary projections of lines but their total projection, by which we mean the sum of lengths of projections of absolutely all elements of lines of the drawing, regardless of whether they are superimposed or not. Thus, for example, the total projection of a circumference is double its diameter. The total projection of lines on a plane, and also of planes in space, has a practical use in derivation and verification of methods of quantitative geometrical analyses of plane and spatial structures.

Just as in the preceding case, we draw a series of parallel equidistant lines in Figure 67, perpendicular to the base line of the drawing which we have chosen as the axis. It may readily be seen that the number of intercepts of the lines of the system in each strip will equal the number of their projections on the base line of Figure 67 in the same strip. Using the same logic as in the derivation of Formula (23.1), we come to the conclusion that the mean number of intersections per 1 mm of the straight lines perpendicular to the axis chosen by us, is precisely equal to the total projection, onto the same axis, of all lines of the

system found in unit area.

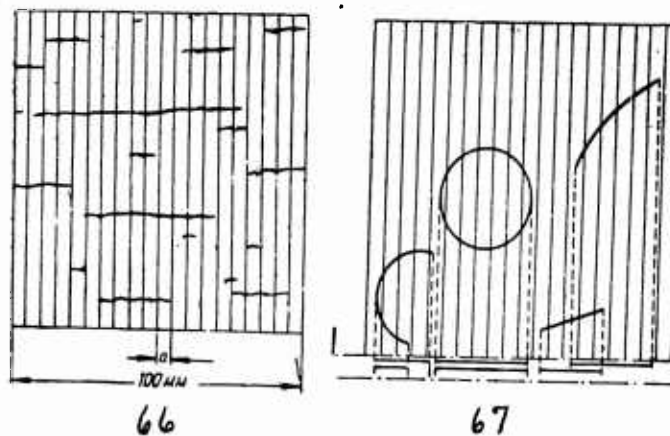


Fig. 66. Diagram of the derivation of the formula (23, 1)

Fig. 67. Diagram of the derivation of the rule for summary projection for a plane

Previously derived formula (23,1) is a specific case of this general rule inasmuch as in a system of lines similar to one shown in Figure 66, the notion of the total length of lines of a system is equivalent to the total projection of these lines onto the direction parallel to them (that is, perpendicular to directed secants.)

The rule of the total projection makes it possible to predetermine the mean number of intersections for a chosen geometrically definite system of lines. Thus, for example, if a  $1 \text{ cm}^2$  area of a microsection of granular pearlite contains a number of sections  $n$  of cementite grains, and their average diameter is  $d$ , then inasmuch as the total projection of each grain on an average will be  $\pi d$ , the mean number of intersections will be defined by the equation:

$$n = \frac{\sum F_c}{\pi d}$$

In this case the direction of secants is of no importance, for the magnitude of the total projection of a system of this kind on the axes of any direction is one and the same. The specific length of the boundary lines of cementite,  $\sum F_c$  is obviously  $\pi d \cdot n$ . For this reason the latter equation may be inserted into the preceding:

$$n = \frac{2}{\pi} \sum F_c$$

which is the basic formula of the method of random secants for a plane

(20.6).

Let us apply our rule of total projection to verify our assumption that a partially oriented system of lines may be divided into two systems, a system completely oriented and a system which is completely isometric. Let us examine a plane which contains a large number of identical ellipses, randomly disposed on the plane but oriented in such a manner that all large axes of the ellipses are mutually parallel. This system of elliptical lines on a plane, oriented in the manner described above, we regard as a partially oriented system of lines with the orientation axis parallel to the large axes of the ellipses. Let us designate the perimeter of each ellipse as  $P$ , the large half-axis as  $a$ , the small half-axis as  $b$ , and the number of ellipses per unit area as  $n$ .

The first group of secants is drawn perpendicular to the direction of large half-axes of ellipses. For this case, the mean number of intersections per unit length of secants, equal to the total projection of ellipses onto the direction of large axes, will be:

$$m_1 = 4 an \quad (23.2)$$

The average number of intersections per unit length of secants for the second group of secants, perpendicular to the secants of the first group, and, consequently, to the direction of a small axes of ellipses, will be:

$$m_{II} = 4 bn \quad (23.3)$$

The total length of perimeters of whole ellipses, per unit area can be found from the formula of the method of directed secants for a plane (22.12):

$$\sum P = m_1 + 0.571 m_{II} = 4n (a + 0.571 b),$$

from which we find the perimeter length of one ellipse:

$$P = 4 (a + 0.571 b). \quad (23.4)$$

The exact value of the length of the perimeter of an ellipse is expressed by the formula [139]:

$$P = \pi (a + b) k, \quad (23.5)$$

where the value of the coefficient  $k$  is defined by the infinite series:

$$k = 1 + (1/4)r^2 + (1/64)r^4 + (1/256)r^6 + \dots$$

with

$$r = (a - b) / (a + b).$$

We can calculate exact values of the perimeter length of an ellipse from Formula (23.5) and approximate values by the method of directed secants from Formula (23.4). The magnitude of error, expressed in per cent, versus the ratio of the lengths of the ellipse axes, is shown in Figure 68. The highest possible error, equal to a 6.8 per cent, occurs at the ratio of  $\frac{a}{b}$  of about 3. Beyond this narrow range the magnitude of the error rapidly decreases. The fact should be taken into consideration that an ellipse has smoothly changing curves, in which rectilinear elements are absolutely absent. At the same time even in this favorable case the method of directed secants was not sufficiently accurate. The shape of an ellipse was chosen to verify the accuracy of the method of directed secants, on the ground that some investigators accept the "grain shape" of an elongated volumetric grain as a figure of rotation of a longitudinal cross section, which is an ellipse. The results of another method of verification will be presented when considering the method of directed secants for a space.

If it is necessary to determine the total length of boundary lines on a plane, it is possible to apply an earlier variation of the method of directed secants [59]. The total length of lines in an isometric system is principally expressed by the equation of the method of random secants for a plane, the application of which is valid for any direction of secants on a plane:

$$\sum F_{i,r} = \frac{\pi}{2} m \text{ mm/mm}^2.$$

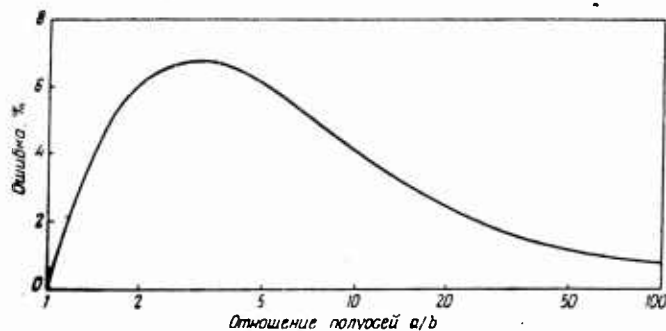


Fig. 68. Error in the determination of the perimeter of the ellipse by the method of directed secants as a function of the ratio of the lengths of the semiaxes of the ellipse

The length of lines of a completely oriented system is defined by Formula (22.4), and an appropriately different mean number of intersections is obtained for each direction of the secant with respect to the orientation axes:

$$\sum P_{or} = \frac{1}{\sin \alpha} m \times \text{mm/mm}^2 .$$

We cannot apply either of these formulas to the determination of the total length of boundary lines of a partially oriented system by the method of directed secants, for the coefficients of  $m$  in these formulas are different, and would tend not to classify the intersections obtained from oriented or isometric portions of lines of a system separately. However, for a definite value of  $\alpha$ , formed by the secants and the orientation axis, the coefficient in the latter formula may be made precisely equal to the coefficient of the basic formula for a plane, that is  $\frac{\pi}{2}$ .

In that case the need for separate computation of intersections with oriented and isometric portions of boundary lines is eliminated. We equate,

$$\frac{1}{\sin \alpha} = \frac{\pi}{2} = 1.571.$$

From this equation we find that it is necessary to maintain an angle  $\alpha$ , formed by directed secants and the orientation axis, of  $39.5^\circ$  or approximately  $40^\circ$ .

Consequently, if directed secants forming an angle of  $40^\circ$  with the orientation axis are used, and the mean number of intersections per 1 mm of length of these secants is determined, then the lengths of boundary lines of partially oriented systems may be calculated from the basic formula of the method of random secants (20.7). The conclusion just derived is verified for the structure shown in Figure (4). For 100 secants located at an angle of  $40^\circ$  to the orientation axis and actual length equal to 0.8 mm (80 mm in Figure (4)), a very fine agreement between the length of grain boundary with the length calculated from the basic formula is obtained.

The mean number of intersections per one secant is 14.05, and 17.6 intersections per 1 mm of the length of secants. The specific length of lines in Figure (4), calculated from the basic formula for a plane, will

be

$$\sum P = 1.571 \cdot 17.6 = 27.6 \text{ mm/mm}^2 .$$

Previously for the same structure we found the same value obtained by the method of separate determination of oriented and isometric portions of lines using 2 groups of mutually perpendicular secants (see the data in Table 24 on page 173). This absolutely identical agreement between the results is, naturally, accidental. The control measurement, carried out by the method of circular secants, gave a close figure, 28.2 mm/mm<sup>2</sup>. This shows that the method of secants, directed at an angle of 40 degrees to the orientation axis, or the method of oblique secants, assures correct results.

For the determination of the total specific length of lines of a partially oriented system on a plane we can use the method of random secants. The method of oblique secants on a plane is not the only one and is not even the best one for solving problems of this kind. It is, however, of interest, for it is possible to develop in analogy with it an appropriate method for spatial structures in which drawing of secants in all possible directions is practically impossible.

The method of directed secants, although it is not as rigorous from the mathematical viewpoint, it is quite valuable due to the fact that it is the only method permitting qualitative evaluation of the degree of orientation of systems of lines on a plane.

Section 24. The Method of Random Secants for Three-Dimensions; Systems of Boundary Surfaces in Three Dimensions

Considering the boundary surfaces of microparticles in three dimensions, we can approach their classification and characterization from different viewpoints. First of all, a given system of surfaces must be defined by the nature of the microparticles which they separate. In pure polycrystalline metals and in solid solutions, the crystallinity and the composition of microparticles (crystallites, grains) are the same; adjacent microparticles differ only as to crystallographic orientation of lattices in space. In more complex formations, surfaces may separate microparticles of different phases or structural constituents. In this case, the surface of one phase or structural constituent may coincide completely, partially, or not at all with the surface of the other phase or structural constituent. Thus, for example, in lamellar or granular pearlite, surfaces of both phases, of cementite and ferrite, are completely superimposed. In hypoeutectoid steel grain surfaces of ferrite and pearlite are only partially superimposed, for some surfaces of ferrite grains may coincide with the surface of other ferrite grains and not pearlite grains. For this reason, in hypoeutectoid steel there may occur surfaces of the following structural constituent pairs: ferrite-ferrite, ferrite-pearlite, pearlite-pearlite, excluding ferrite-cementite interfaces in the pearlite itself and surfaces of nonmetallic inclusions which have boundaries both with ferrite and pearlite (predominantly with the first one).

From the aforesaid it follows that systems of surfaces may be regarded either as the total surface of the given phase or structural constituents, or as an interface of two phases or two structural constituents. For this reason, in each concrete case it should be specified precisely what system of surfaces we wish to measure. Quantitatively the extent of a given system of surfaces in space is determined by the magnitude of the specific surface, that is, by the total surface area of the system divided by the unit volume measures in  $\text{m}^2/\text{mm}^3$ .

As to its configuration in space, a system of surfaces may consist of closed contours isolated from each other, or it may be one practically continuous surface, forming a three-dimensional similar network. Intermediate shapes are also possible.

Just as the systems of lines on a plane, the systems of surfaces are classified as isometric and partially or completely oriented. It is obvious that a greater variety of orientations are possible in three-dimensional space than in two-dimensional surface.

Let us imagine that all surfaces of a given system are broken up into a quite large number of elementary areas of equal size. By assuming that they are plane we erect normals to each area. If it happens that normals are oriented randomly, but statistically uniformly, i. e., the number of normals found in any solid angle is dependent only upon the magnitude of the angle and not upon the direction, we regard the system of surfaces as isometric space. Inasmuch as elementary areas are oriented randomly in space, by shifting them parallel to themselves, we can form a spherical surface from them under the condition that the system is isometric in space. The diameter of the spherical surface is determined by the magnitude of specific surface for a given system.

A system of grain surfaces of a polycrystalline aggregate is isotropic if the grains are equiaxed in space. Therefore, there is no ground to consider the "average shape" of equiaxed grains of so to spherical.

In some instances individual types of microparticles are geometrical bodies of quite irregular configuration. As, from Figure 3 it is apparent that microparticles of  $SrSO_4$  in  $FeSO_4$  are shaped as almost regular cubes and microparticles of  $Cu_2S$  phase are shaped as cylinders. In lamellar pearlite, microparticles of ferrite and cementite are platelets of regular shape. However, inasmuch as the axes of symmetry of many pearlite-type particles in a volume of an alloy have random directions, the system of their surfaces as a whole are isometric in space. Given that each group of particles has an identical spatial orientation, as e. g., a colony of alternating platelets of ferrite and cementite within the limits of a single grain of lamellar pearlite whose orientation does not coincide with the orientation of other colonies of same particles, the system as a whole is undoubtedly isometric.

The isometricity of a spatial structure may be given another definition. From some point within a volume of an alloy we direct straight lines in different directions *of* three-dimensional space. If the number of intersections of these lines with the surfaces of a system, which is of interest to us, divided by a length which is the same for all lines, is identical for all lines and independent of their direction in space, then this system of surfaces is isometric.

Since there may be a great number of different types of space orientation of boundary surfaces, we shall consider here the basic, the more typical ones which frequently occur in real structures. They are shown schematically in Figure 59. The schematic drawing in Figure 69a corresponds to the case of disoriented or isometric system of surfaces. It shows a three-dimensional structure of a polycrystalline aggregate with grains equiaxed in space. It is obvious that a structure may be more complex, for example, it may consist of many phases or structural constituents. Thus, surfaces of graphite precipitate in cast irons (except the so-called ~~XXX~~ "decomposition graphite"), surfaces of the cementite and ferrite phases in granular or lamellar pearlite, surfaces of twinning planes in copper or austenite, surfaces of brittle equiaxed particles of nonmetallic inclusions (although the particles themselves may be oriented as a "chain" in the direction of rolling) and many others may serve as examples of systems of isometric surfaces in space. In one and the same complex structure, surfaces of microparticles of certain phases or structural constituents may be oriented, whole surfaces of microparticles of other constituents may be isometric.

Plastic deformation, carried out at temperatures sufficiently low to produce residual strain of microparticles, is responsible for the appearance of space deformation of their surfaces, generally for a large group of microparticles or even for all microparticles without any exception. It should be noted that on a flat section we have frequently observed identical structure types of the orientation of grain boundaries, whereas the space orientation of corresponding boundary surfaces radically differs. Sometimes an isometric system of grain boundaries may be observed in a microsection, whereas the corresponding surfaces have a

clearly manifested spatial orientation. For example, on a transverse microsection of metal, deformed by drawing, we can observe an isometric network of boundary lines on a plane whereas the corresponding boundary surfaces possess a quite considerable spatial orientation. Hence it follows that it is important to correctly choose planes of a microsection in the case of oriented structures. For example, from a transverse microsection of metal, deformed by drawing or by rolling, we cannot form a correct idea either about the true grain size or about their shape. In some cases one microsection is not sufficient at all, in order to form an idea on a three-dimensional structure of an alloy.

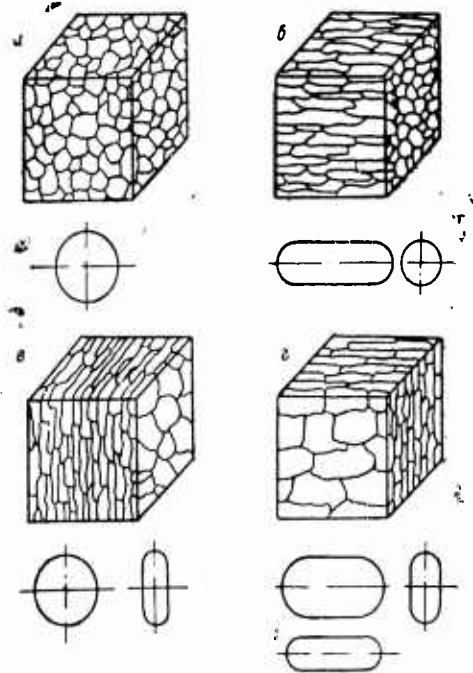


Fig. 69. Diagram of the kinds of orientation of the systems of the boundary surfaces in space.  
 a--isometric system; b--linearly oriented; c--oriented in a plane;  
 d--linearly oriented and plane-oriented system of surfaces

The shape of grains subjected to various types of plastic deformation changes to quite a degree. Drawing or rolling of rods of approximately equiaxed cross section modified the spherical shape of the grain surface, elongating it in the direction of drawing or rolling, whereas the cross section of grains in the plane perpendicular to this direction is reduced. As a result, grains acquire shapes of more or less elongated fibers. In this case of deformation, the system of surfaces of micro-particles acquires the orientation, the nature of which is illustrated by the schematic drawing in Figure 69d. In this type of deformation,

a certain part of elements of surfaces of microparticles, which (elements) we regard as flat areas of an infinitely small but similar size, happen to be not disoriented but parallel to the axis of drawing or rolling. In a section perpendicular to this axis, the plane system of boundary lines appears isometric and grains appear equiaxed. A system of surfaces of this kind (Figure 69d) has a linear (axial) symmetry, the axis of wire or rolled product, of equiaxed cross section, being the axis of symmetry. The structure in any plane passing through the axis of symmetry is statistically identical.

A system of surfaces, similar to one analyzed, the elements of which have a preferred orientation parallel to one line, deformation axis (which we understand as the direction of action of the force causing the deformation), we shall call a system of surfaces with linear orientation. The same kind of orientation is observed in crystallized structures: the axis of symmetry of surfaces of columnar crystallites is the line perpendicular to the surface giving off heat.

The elongated shape of microparticles (Figure 69b) does not necessarily predetermine the linear orientation or their surfaces (for example, the structure of babbitt) (Figure 4). It is not the shape of microparticles that is important but the regularity of their orientation in space.

Basically the different type of orientation of surfaces is produced by compressive deformation (upsetting), which reduces the size of microparticles in the direction of action of the force and uniformly increases their sizes in directions perpendicular to the deformation axis. From the viewpoint of space symmetry, the shape of flat grains and the system of surfaces of grains deformed by compression (Figure 69c) have the same axial symmetry as the systems of surfaces with linear orientation, with the axis of symmetry being also the axis of deformation, that is the direction of action of external forces.

Just as in the case of systems of surfaces with linear orientation, plane systems of boundary lines in cross sections perpendicular to the axis of symmetry are isometric, the grains are equiaxed and in cross section, passing through the axis of symmetry or parallel to it, a statistically identical structure is observed. Nevertheless the difference in orien-

tation of surfaces of microparticles of the type shown in Figure 69b and c attracts attention: in the first drawing, in the first approximation, the oriented portion of the grain surface is cylindrical whereas in the second type it appears as plane areas. The principal difference between these two systems of surfaces (Figure 69b and c) is clearly manifest when the systems are regarded as broken down into elementary plane areas, as it was done previously. In the case of an isometric system of surfaces, these areas are completely disoriented in space; in systems with linear orientation a certain part of areas is oriented parallel to the axis of symmetry; in the latter case (Figure 69c) the oriented part of areas is disposed perpendicular to the axis of symmetry or to the direction of forces causing deformation. For this reason, this system of surfaces we shall call a system with plane orientation.

Speaking of systems with linear or plane orientations, we always have in mind only a partial orientation of a given type, since in practice a complete orientation is never encountered.

Schematic drawing of the system of surfaces, simultaneously corresponding to the presence of both considered types of orientation, linear and plane, is shown in Figure 69d. This type of a structure may be produced by forge rolling, by rolling as strip, etc., when microparticles are flattened and simultaneously widened but not to the same degree in the direction of rolling or forge rolling and perpendicular to it. In this case, microsections, made in all three planes (parallel to the surface of the strip, perpendicular to it and simultaneously parallel to the axis of rolling, and also perpendicular to the axis of rolling) have different plane structures.

From Figure 69 it is apparent that there is a great diversity of grain shapes and systems of surfaces of microparticles, which is determined by the type of plastic deformation and, naturally, by its degree. Previously we have examined only the simplest cases, whereas in practice there occur other, more or less complex, types of deformation and, correspondingly more or less complex types of orientation of surfaces (for example, in torsion, bending, removing of the chip by different types of cutting, etc.).

The type of orientation of boundary surfaces is the most important characteristic of nonisometric structures. With the plane structure being the same with respect to quality as well as quantity, the space structure and, consequently, the behavior and property of the metal, dependent upon this structure, may differ a great deal. For example, a structure, shown in Figure 64, may occur on a microsection of metal which may possess linear and plane orientations. The values of specific surface, the radius of its curvature and, consequently, the degree of thermodynamic stability of the structure, are precisely dependent upon the orientation present in a given case.

For this reason, the value of the grain axis ratio as a characteristic of a plane structure, as was proposed by Ye. Geyn, F. Rapatts, et al., is meaningless if we do not know the type of spatial orientation of microparticle surfaces. At the same time, many investigations frequently indicate the precise degree of deformation but without mentioning its type, which deprives us of the possibility of estimating the spatial orientation of surfaces at least from the type of deformation used and responsible for this orientation.

On the basis of the aforementioned consideration, we come to the conclusion that the magnitude of specific surface alone is not sufficient as the characteristic system of boundary surfaces. The quantitative evaluation of the degree of a given orientation in terms of the basic types, is also needed. It is all the more needed, for as we shall see further the determination of the value of specific surface itself requires that the type of the orientation be known.

Section 25. Measuring Specific Surface by the Method of Random Secants  
for Space

For the measurement of extent of surfaces in space we shall use the same principle which underlies the method of measuring the length of lines on a plane by the method of random secants. In space there also exists a singular relationship between the mean number of the intersects and the value of specific surface of a given boundary system. The solution of Buffon's 2-dimensional "needle" problem, which underlies the method of random secants on a plane must be revised to be applicable to a 3-dimensional space problem.

The analogy is confirmed by the complete agreement between the dimensionalities of quantities measured and calculated in both cases. Both on a plane and in space, the dimensionality of the mean number of intersections per unit length of secants is expressed in  $\text{mm}^{-1}$ . However, dimensionalities of these specific length of lines on a plane (measured in  $\text{mm}/\text{mm}^2$ ) and specific surface in space (measured in  $\text{mm}^2/\text{mm}^3$ ) are also expressed in  $\text{mm}^{-1}$ . Thus, the coefficient of proportionality between the mean number of intersections per 1 mm of lengths of random secants and the specific length of lines on a plane, or surfaces in space, is a non-dimensional quantity.

The derivation of the basic formula of the method of random secants for space, similar to the corresponding formula derived for a plane (20.7), may be based on any system of surfaces in space. The surfaces of a system may be plane or curved, with any curvature, continuous or interrupted, composed of individual surfaces isolated from each other bounding a definite section of space or leaving it open; the surfaces may intersect each other or not come into contact at all; the elementary areas, comprising surfaces of a system, may be completely oriented, that is, located parallel to one (or several) planes or lines; they may be oriented only partially for, finally, they may be completely disoriented. In other words, a system of surfaces may have an absolutely arbitrary shape as well as location of surfaces, that is, of its components. There is only one uniquely essential requirement; the magnitude of the total area

of a given system of surfaces in a unit of volume of the specimen, which is being analyzed, must be representative of the entire volume of the aggregate which is the object of studies.

A large number of straight lines (secants) are drawn through the volume of metal or alloy, their location being random and their direction random. Under these conditions, the mean number of intersections of random secants with surfaces of a given boundary system, in the structure of metal, divided by the unit length of secants (1 mm), which we shall designate as  $m$ , will be proportional to the value of total surface of boundaries in the unit volume of metal; i. e., it will be proportional to the value of specific surface; it will be dependent exclusively upon the latter. The relationship between these two values is expressed by the basic formula of the method of random secants for space:

$$\sum S = 2m \text{ mm}^2/\text{mm}^3 \quad (25.1)$$

Let us prove analytically the validity of Formula (25.1). For this purpose, we shall isolate a large number of cylinders leaving the volume of metal or alloy which is being investigated. The axes of these cylinders will be secants that we have drawn. The cross section of cylinders,  $F$ , is assumed to be disappearingly small, so that when the limit  $F$  approaches zero, the cylinders themselves become straight lines coinciding with the axes of cylinders; that is, secants. The total length of all random secants and, consequently, of all cylinders in the volume of metal in question we shall designate as  $L$ .

Surfaces of cylinders intersecting boundary surfaces of the metal structure, found in the volume in question, will carve out a large number of elementary areas from boundary surfaces, which we regard flat, inasmuch as the section of cylinders,  $F$ , approaches zero. In that case, the shape of these elementary areas will be elliptical. Let us designate the total number of these elementary ellipses as  $Z$ ; their areas as  $S_1, S_2, S_3, \dots, S_z$ ; and acute angles, formed by the areas to the axes of cylinders as  $\gamma_1, \gamma_2, \gamma_3, \dots, \gamma_z$ , respectively. Then we may write  $Z$  number of similar equations:

$$S_1 = \frac{F}{\sin \gamma_1}; S_2 = \frac{F}{\sin \gamma_2}; S_3 = \frac{F}{\sin \gamma_3};$$

and so on.

Hence we find the total area of all elementary areas carved out by the cylinders:

$$S_1 + S_2 + S_3 + \dots + S_z = F \left( \frac{1}{\sin \gamma_1} + \frac{1}{\sin \gamma_2} + \frac{1}{\sin \gamma_3} + \dots + \frac{1}{\sin \gamma_z} \right). \quad (25.2)$$

The total volume of all cylinders is obviously FL. Since a large number of cylinders were taken and they were located periodically and randomly throughout the entire volume subject to investigation, now we may believe that the total area of body surfaces found within the cylinders, divided by their total volume, corresponds to the value of specific boundary surface characteristic for the entire volume of metal in question, that is to the value of S. Therefore,

$$S = \frac{S_1 + S_2 + S_3 + \dots + S_z}{FL} = \frac{1}{L} \left( \frac{1}{\sin \gamma_1} + \frac{1}{\sin \gamma_2} + \frac{1}{\sin \gamma_3} + \dots + \frac{1}{\sin \gamma_z} \right).$$

In the limit, when the cross section of cylinders, F, is reduced to zero, the cylinders will be straight randomly directed lines (random secants) and the total number of elementary areas, Z, carved out by the cylinders, divided by the total length of all secants, L, will be equal to the mean number of intersections of the secants with surfaces of structural boundaries divided by unit length of secants; that is, it will be equal to m. For this reason,

$$\sum S = m \left[ \frac{1}{Z} \left( \frac{1}{\sin \gamma_1} + \frac{1}{\sin \gamma_2} + \frac{1}{\sin \gamma_3} + \dots + \frac{1}{\sin \gamma_z} \right) \right] = Bm. \quad (25.3)$$

Since the cylinders, carved out in space, are directed randomly and chaotically, any position of a cylinder axes with respect to elementary areas carved by it, estimated by angle  $\gamma$ , is equally probable. For this reason, the part of the equation (25.3) found in brackets and designated as B is the mean reciprocal value of the sine of angle  $\gamma$  formed by the axes of cylinders and elementary areas; this angle varies

between zero and  $\frac{\pi}{2}$ . Let us find the value of B, assuming that any value of angle  $\gamma$  is equally probable, with-in the afore-mentioned limits.

We choose a system of rectangular coordinates with axes x, y, and z, with the radius-vector (the length of which is equal to unity) through the origin of coordinates. The coordinates of the second, non-stationery end of the radius-vector, we shall designate as x, y, and z. Let the angles, formed by the radius-vector and coordinate planes yz, xz, and xy respectively, be equal to  $\alpha$ ,  $\beta$ , and  $\gamma$ .

Now, by simple geometrical relations we find the value of the sine of angle  $\gamma$  formed by the coordinate plane xy and the radius-vector, as a function of direction of the vector in space, determined by coordinates of its nonstationery end:

$$\sin \gamma = \sqrt{1 - x^2 - y^2}.$$

It is obvious that the choice of any of the three angles, formed by the radius-vector and coordinate axes, is equally correct, and identical results would be obtained in all three cases. The reciprocal value of the sine of the chosen angle will be equal;

$$\frac{1}{\sin \gamma} = \frac{1}{\sqrt{1 - x^2 - y^2}}. \quad (25.4)$$

The mean reciprocal value of the sine of angle  $\gamma$  we shall find by integrating the function (25.4) within the limits of the first octant of the coordinate system, using the theorem of the mean value of a function;

$$B = \frac{\int_0^1 \int_0^{\sqrt{1-x^2}} \frac{dx \cdot dy}{\sqrt{1-x^2-y^2}}}{\int_0^1 \sqrt{1-x^2} \cdot dx} \quad (=2) \quad (25.5)$$

As a result of integration of function (25.5) within the above-mentioned limits, we derive the exact figure w. By substituting this value of the coefficient B into Formula (25.3), we finally derive the basic formula on the method of random secants for space:

$$\sum S = 2m \text{ mm}^2 / \text{mm}^3,$$

exactly in the form presented (25.1).

This formula is applicable for any system of surfaces in space under the condition of equal probability of the direction of secants, for which addition was used as a basis for the derivation of values of coefficient B.

However, to satisfy this only requirement under conditions of 3-dimensional space is far from being simple, in contrast to the analyses by the method of random secants on a plane. The specimens used in metallographic investigations are not transparent. For this reason, it is impossible to draw random secants in the volume and to calculate directly the produced intersections between secants and boundary surfaces. It is true that it would be possible to prepare a quite large number of microsections, through the specimens of the investigation, locating them uniformly in all possible directions, and having drawn one or several secants on each microsection, we find the total mean value of the number of intersections per 1 mm of length of secants for all microsections, which mean value would be characteristic for the entire subject as a whole. However, this method is extremely inefficient, although it may be realized. For this reason, we have to find some means for the application of the derived basic formula, which would permit us to limit the analysis to the plane of the microsection instead of in space. In this case, the number of required microsections should be minimum.

The mean number of intersections,  $m$ , is independent of the shape of secants drawn in space; they may be not only straight but also curves having a bound or open contour line in the plane, or they may be space curves. The equal probability of the direction of secants, needed for the coefficient B to be equal to the value calculated by us, is absolutely identical to the requirement of equal probability for any angle with which the secant intersects the surface. If the angle with which the secant intersects the surface, assumes all possible values, then the validity of Formula (25.5) is completely retained. Let us examine under what conditions the equal probability of any angle, at which the secant intersects a small elementary area (into which we can break down any system of boundary surfaces), is maintained.

Let us assume that all elementary areas or at least a definite fraction of them have a regular spatial orientation, for example, para-

parallel to a certain one or several planes or lines. In that case the equal probability of any angle, at which the secants intersect elementary areas, is satisfied only in the case when any direction in space of secants themselves is equally probable. If all of the elementary areas are completely oriented in space, then a system of arbitrarily directed secants or even only one straight or curved secant, possessing a sufficient length, assures us that any angle of intersection with elementary areas may be obtained with equal probability. In other words, of the two systems which are simultaneously present in the space which is being examined (systems of elementary areas into which we broke down the analyzed boundary surfaces and systems of secants), at least one must be disoriented in space and randomly and periodically directed.

In a system of surfaces isometric in space, the mean number of intersects per 1 mm of length on any secant, directed arbitrarily, will be one and the same. Therefore, random secants may be arranged, in particular, in one plane and consequently, to limit the analyses only to one microsection.

By intersecting the isometric system of boundary surfaces by a plane we obtain a plane structure with equiaxed grains, similar to one shown in Figure 49. Traces of intersections of grain boundary surfaces on an arbitrarily located plane of the microsection create on it an isometric system of boundary lines. For this reason, the mean number of intersections per 1mm of length of secants, determined on several microsections the planes of which are arbitrarily directed, will happen to be the same for all the microsections and, consequently, the actual number of intersections,  $m$ , for a system of boundary surfaces of the subject as a whole.

Hence, it follows that the method of random secants for space and its basic formula (25.1) are directly applicable for the study of spatial isometric systems of boundary surfaces.

Therefore, in many instances, which occur in metallographic practice, the mean number of intersections may be determined on a single microsection, as has been described for plane systems of boundary lines. For example, for the afore-mentioned Figure 49, the mean number of intersections,  $m$ , on the plane of the microsection is found to be equal to 11.6

$\text{mm}^{-1}$  to  $-1$  (see Table 23). Therefore, the specific surface of grain boundaries in this case is

$$\sum S = 2 \cdot 11.6 = 23.2 \text{ mm}^2/\text{mm}^3 .$$

The area of graphite flakes in  $1 \text{ mm}^3$  of gray iron, the structure of which is shown in Figure 51, similarly happens to be  $20.0 \text{ mm}^2$  and the specific surface of graphite is  $40.0 \text{ mm}^2/\text{mm}^3$ .

Prior to applying the above-described methods and Formula (25.1), it is necessary to prove that the system of boundary surfaces, which is of interest to us, is actually isometric in space. Here it should be kept in mind that the isometricity of a given system of boundary lines on a microsection does not prove that boundary surfaces are spatially isometric. For example, the system of boundary lines on a transverse microsection of a round or a wire is isometric, but the spatial isometricity of boundary surfaces must be confirmed by the same isometricity of a system of lines on a longitudinal microsection.

We must warn that it remains to be shown that Formula (25.1) is valid and universal for any systems of surfaces in space, since the coincidence of the mean number of intersections determined on a plane of microsection, and the value  $m$ , which is found in Formula (25.1), occurs only for systems with isometric surfaces in space. For these systems, we can write:

$$m = \frac{\sum S}{2} = \frac{2 \sum P}{\pi} ,$$

as follows from Formulas (20.6) and (25.1). Hence it follows that

$$\sum S = \frac{4}{\pi} \sum P = 1.273 \sum P \text{ mm}^{-1} . \quad (25.6)$$

The latter relationship shows that the assumption made by I. P. Lipilin [129], as a first order approximation, that the total length of boundary lines on a microsection is proportional to the total grain surface in a volume, happens to be absolutely invalid. The condition for the validity of this postulate and for Formula (25.6) is the isometricity of a system of grain boundary surfaces (or of microparticles of structural constituents) in space.

The validity of the method of random secants and that of its basic

formula for a plane could be verified very nicely experimentally, since the length of lines on a plane may be measured by several different methods. The experimental verification of the method and formula (25.1) for the case of 3-dimensional space presents a different problem, for besides the method of random secants there are no other methods permitting control measurements of the length of complex surfaces. For this reason, the validity of the method for space cannot be verified experimentally on a wide number of surface systems characterized by different geometrical shapes and space distribution.

Besides the existing complete analogy with corresponding postulates for a plane, the validity of the method and of the formula of random secants for space is confirmed experimentally on two specific structures distinguished by a definite geometrical regularity which makes it possible to measure the specific surface by other methods. Such types of structures are structures of lamellar and granular pearlites, the methods for measuring the specific surfaces of these boundaries of which have been considered previously in Section 18.

For lamellar pearlite, Formula (18.1), based on considerations of the geometry of pearlite structure, consisting of alternating platelets of ferrite and pearlite each pair of which has the same thickness within the limits of a given volume, is valid:

$$\sum S_{\text{fer}} = \sum S_{\text{cem}} = \frac{2}{\Delta_0} \text{ mm}^2/\text{mm}^3,$$

where  $\Delta_0$  is the distance between the platelets, in mm. If the basic formula of the method of random secants is valid, then by comparing the latter formula with Formula (25.1) it is possible to establish the relationship between the mean number of intersections per 1 mm of length of secants,  $m$ , and the value of interlamellar distance:

$$m = \frac{1}{\Delta_0} \text{ mm}^{-1}. \quad (25.7)$$

The mean number of cementite platelets intersected by the random secants on a microsection of eutectoid steel, then equals  $Z$  per 1mm of length of secants. In this case we assume that the secants pass through a sufficiently large number of pearlite grains and roughly into platelets at all possible angles to their planes, since the structure of lamellar

pearlite is isometric in space. In that case, the mean number of intersections of secants with cementite-ferrite interfaces will be twice as large as the number of intersected platelets,  $Z$ , inasmuch as each platelet is intersected by a secant at two points of its plane. Therefore,

$$m = 2Z \cdot \text{mm}^{-1}. \quad (25.8)$$

Let us designate as  $\Delta$  the value of mean intercept of secants between the edges of adjacent cross sections of cementite platelets (or of ferrite), on planes intersected by secants at all possible angles, as shown in Figure 70. This value obviously is

$$\Delta = \frac{1}{Z} \text{ mm}. \quad (25.9)$$

Comparing  $\Delta$  with Formula (25.8) we derive:

$$m = \frac{2}{\Delta} \text{ mm}^{-1}. \quad (25.10)$$

Now, by removing the quantity  $m$  from Formulas (25.7) and (25.10) we find the relationship between the mean length of that intercept on secants,  $\Delta$ , measured on the plane of a microsection as shown in Figure 70, and the actual value of the interplatelet distance:

$$\Delta = 2 \Delta_0. \quad (25.11)$$

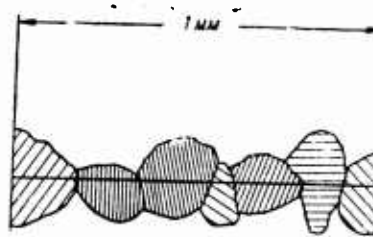


Fig. 70. Structure of laminar pearlite and an intersecting straight line.

The investigation carried out by M. Gensamer and his associates has established from the results of careful measurements that the mean distance between the edges of cross sections of adjacent cementite platelets on a microsection, which varies with the direction that may be perpendicular to the cross section of platelets or parallel to it, is 1.9 to 2.0 times greater than the actual interplatelet distance (directly measured

in the same grains of pearlite whose platelets are perpendicular to the plane of the microsection) [122]. *Wiggle* that the value measured by M. Gensamer, et al., is identical to the one which we have designated as .

The coefficient of proportionality between the quantity  $\Delta$  and interplatelet distance  $\Delta_0$ , experimentally found by M. Gensamer and his associates, is 1.9 to 2.0. Precise mathematical calculations, presented above based on the formula of the method of random secants for space (25.1), gives the value of this coefficient as 2. This agreement between experimental and calculated data concerns the validity of the method of random secants for a spatially isometric system of surfaces of phase boundaries in lamellar pearlite. It is obvious that the method applied by M. Gensamer and his associates is a specific case on the universal method of random secants.

When cementite or carbides in steel are spheroidal, their specific surfaces may be measured by several methods distinguished by a different degree of accuracy (see Section 18). The most accurate results are produced by calculations based on the number of carbide grains per unit volume and distribution of their size, which can be determined by the method of E. Scheil. Comparative measurement of specific surface by this method and by the method of random secants, carried out by M. Ye. Blanter, concerned the validity of the method for this type of structures [140]. Similar verification by producing the same results, was carried out by S. Z. Bokshtein [188].

Thus, experimental verification of the method of random secants for space, carried out on 2 types of structures, which permit measurements of specific surface by other methods, confirms the validity of the method itself and of its basic formula for space. It is noteworthy that over a short space of time, less than 10 years, the method of random secants for space has been developed three times [58, 59, 131, 43, 141]. This shows how great is the need for experimental measurement of metal science.

The experimental confirmation of Formula (25.1) also automatically confirms the validity of Formula (25.6), which establishes a direct proportionality between the values of the specific surface of boundaries

in space and the specific length of corresponding boundary lines on a plane, which is valid for surfaces that are isometric in space. On the basis of this relationship, the values of specific surfaces of grain boundaries have been determined for all eight numbers of grain size specified by the standard scale in GOST 5639-51. It should be kept in mind that the specific surface may differ, even if the number of planar grains per unit area of the microsection are the same, for there is no singular relationship between any two of these values. Therefore, the figures made by us and shown in Table 25 are valid only for concrete structures on a standard scale.

1. *№ of grains according to GOST 5639-51*  
 2. *Specific surface of grains мм<sup>2</sup>/мм<sup>3</sup>*

Table 25.

1. № зерна по ГОСТ 5639-51	2. Удельная поверхность зерен мм <sup>2</sup> /мм <sup>3</sup>	1. № зерна по ГОСТ 5639-51	2. Удельная поверхность зерен мм <sup>2</sup> /мм <sup>3</sup>
1	10	5	42
2	15	6	59
3	22	7	85
4	30	8	124

For a rapid, but approximate, determination, of the value of specific surface of grain boundaries we have developed a special scale. The evaluation of this scale is carried out by means of visual comparison of the picture, visible through the microscope or on a photomicrograph, and the scale shown in Figure 71. In contrast to the standard scale, which has a step-like representation, the proposed scale describes the structure with a continuously and smoothly changing value of the specific grain surface [142]. Values of the specific surface, given on the right, correspond to each horizontal section of the scale, if the magnification of the structure, which is being analyzed, is 100, 200, 1, and 500. At other magnifications the value of specific surfaces, derived from the scale, must be divided by 100 and multiplied by the actual magnification at which the structure was examined.

Facing 196

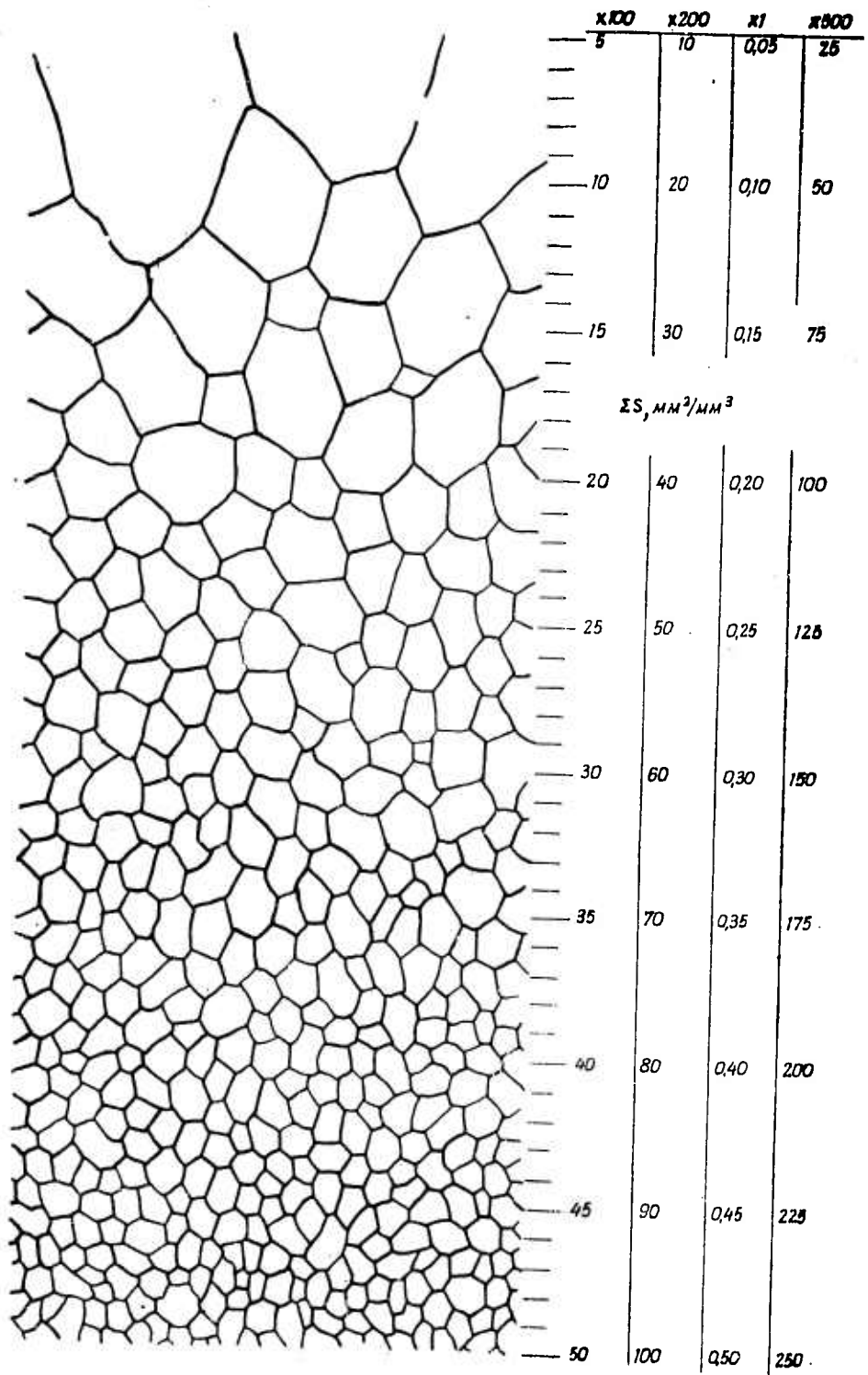


Fig. 71. Scale of comparison for the evaluation of the magnitude of the specific surface of the grain of polyhedral structure. The specific surface is shown in  $\text{mm}^2/\text{mm}^3 \times 100$ . S. A. Saltykov.

Section 26. Measuring the Specific Surface by the Method of Directed  
Secants for Space

As it has been previously mentioned, the basic formula of the method of random secants for space is universal and valid for any system of surfaces. However, its application for cases, when system of surfaces are not isometric in space, is difficult due to the fact that the determination of the mean number of intersections,  $m$ , requires that secants must be arranged in space in different directions. Therefore, to determine the mean number of intersections which would characterize the entire space system of boundaries as a whole, theoretically an infinitely large number of microsections with planes differently oriented in space, is needed; in practice the number of such microsections should be at least six. Although the application of formula (25.1) in the case of space oriented systems of surfaces is theoretically valid and permissible, due to the aforementioned reason in practice it is more expedient to use varieties of the method of random secants developed for the application to oriented systems of boundary surfaces. Such methods have been proposed by us [59, 60] and by A. G. Spektor [61]. When applying these methods, the secants are arranged not randomly but are directed in a definite manner and rectilinear secants are used exclusively. For this reason, methods of this kind, in contrast to methods of random secants, may be grouped together under the name of methods of directed secants.

The method of A. G. Spektor is intended for the measurement of specific surface of boundary systems having a special axis of symmetry. According to our classification (see Section 24) structures of this type belong to systems of boundary surfaces having either linear or plane orientation (but not both types of orientation simultaneously).

For systems of surfaces having an axis of symmetry, the mean number of intersections, just as for any other system, is singularly defined by the value of a specific surface in accordance with the basic formula:

$$m = \frac{1}{2} \sum S_{mn}^{-1} \quad (26.1)$$

Moreover, in this case the number of intersections at individual secants is the function of angle  $\beta$  formed by these secants and the axis

of symmetry.

The number of intersections per unit length of the secant, found within the elementary solid angle  $dw$ , the apex of which lies on the axis of symmetry, will be:

$$m = \frac{1}{2\pi} \int_0^{2\pi} m(w) dw. \quad (26.2)$$

The magnitude of the elementary solid angle  $dw$  is defined by the differentials of two angles, angle  $\beta$  formed by the secant and the axis of symmetry, and angle  $\varphi$ , which determines the rotation of the plane, in which the secant lies, about the axis of symmetry. In conformance with the rule of computation of mean values of directed quantities, we have:

$$m = \frac{1}{2\pi} \int_{\varphi=0}^{2\pi} \int_{\beta=0}^{\pi/2} m(\beta, \varphi) \sin \beta \cdot d\beta \cdot d\varphi. \quad (26.3)$$

Inasmuch as, for the type of surface systems in question, the structure is identical in any plane passing through the axis of symmetry (or parallel to it), the number of intersections is dependent only upon the magnitude of angle  $\beta$  and is independent of angle  $\varphi$ , which determines the rotation of the secant about the axis of symmetry. For this reason, expression (26.3) is converted into the following expression:

$$m = \frac{1}{2\pi} 2\pi \int_0^{\pi/2} m(\beta) \sin \beta \cdot d\beta = \int_0^{\pi/2} m(\beta) \sin \beta \cdot d\beta. \quad (26.4)$$

By bringing from Formula (26.4) the value of the mean number of intersections, derived for the case of axial symmetry of boundary surfaces, into the basic formula (26.1), we derive:

$$\sum_i S = 2 \int_0^{\pi/2} m(\beta) \sin \beta \cdot d\beta, \quad (26.5)$$

or in a more convenient form for calculations:

$$\sum_i S = 2 \int_0^{\pi/2} m(\beta) d[\cos \beta]. \quad (26.6)$$

The latter formula is the working formula for the measurement of specific surface of boundary systems with an axial symmetry by the

method of A. G. Spektor. The mathematical derivation of Formula (26.6) is rigorous without any approximations or assumptions which would reflect on the accuracy of calculations of the specific surface.

A microsection, whose plane intersects the axis of symmetry or is parallel to it, is used in practical applications of Formula (26.6). For articles, produced by rolling or drawing, which have an equiaxed cross-section profile, the plane of the microsection must intersect the axis of the rod, which is precisely the axis of symmetry of the structure. For sheets the plane of the microsection is arranged perpendicular to the surface on a sheet and the axis of symmetry is also perpendicular to the plane of the sheet; in the latter case Formula (26.6) is applicable if the system of measured boundaries is isometric in the plane of the sheet and the grains are equiaxed, that is, there is no linear orientation, but only plane orientation. In specimens deformed by upsetting, the plane of the microsection must coincide with the axis of the specimen (or with the direction of action of external compressive forces), which is precisely the axis of symmetry.

Several groups of secants are marked on the microsection, and a definite angle formed by the axis of symmetry and the direction of secants of a given group, is maintained in each group. Among chosen direction of secants, two must be always present, perpendicular and parallel to the axis of symmetry. In addition to these several other directions are chosen and the number of which is determined by the need for a smooth plotted curve. For secants of each group, a mean number of intersections per 1 mm of their lengths is calculated separately. A graph with coordinates "cosine of angle formed by secants and the axis of symmetry versus mean number of intersections in a given direction" is plotted from the data obtained. After that graphical integration is carried out: the area under the plotted curve is determined from the graph, which is equal to the mean number of intersections, defined by Formula (26.4) or to the half of the value of the specific surface, defined by Formula (26.6). By doubling the found value we find the unknown specific surface.

Let us consider an example given in the paper by A. G. Spektor [61]. The specific surface of the interface between pearlitic and fer-

ritic constituents was measured in the central portion of a cross section of preannealed steel wire after it had been drawn from 5.5 mm to 3.8 mm in diameter. The obtained mean number of intersections,  $m(\beta)$ , for each of seven directions, characterized by angle  $\beta$  formed by the intersection and the axis of the wire, are listed in Table 26. The graph of the relationship between the mean number of intersections and the cosine of angle  $\beta$  is given in Figure 72. The area under the curve, shaded in the drawing, is

$$m = \int_0^1 m(\beta) d[\cos \beta] = 252 \text{ mm}^{-1}.$$

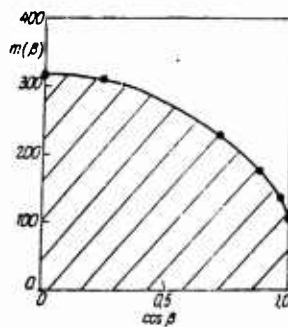
To find the specific surface, we double the latter figure and find:

$$\Sigma S = 2.252 = 504 \text{ mm}^2/\text{mm}^3.$$

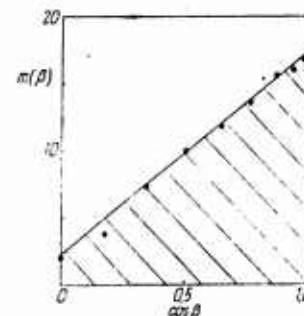
Table 26

<i>angle of inclination of secant to <math>\beta</math></i>	Угол наклона секущей $\beta$	$\cos \beta$	Число пересечений $m(\beta), \text{мм}^{-1}$	<i>№. of intersections <math>m(\beta), \text{mm}^{-1}</math></i>
	0	1.00	101	
	2.5	1.00	103	
	14	0.97	135	
	28	0.88	175	
	44	0.72	226	
	76	0.24	310	
	90	0.00	316	

In the example considered, the system of boundary surfaces between pearlitic and ferritic constituents is linearly oriented, according to our classification.



72



73

Fig. 72. Determining spatially the average number of intersections for the structure symmetrical relative to the axis (A. G. Spektor [61])

Fig. 73. Determining spatially the average number of intersections for the structure symmetrical relative to the axis (sheet rolling), by the method of A. G. Spektor.

Let us cite another example for a case of plane orientation. We

have carried out measurements on a specimen of sheet transformer steel with the structure of silicon ferrite, the grain surfaces of which have a plane orientation (that is, preferred orientation parallel to the surface of the sheet). In planes which are parallel to the surface of the sheet, the structure is isometric. In this case, the axis of symmetry of the structure, as well as the plane of the microsection, are disposed perpendicular to the surface of the sheet. The number of intersections was calculated on secants the direction of which with respect to the axis of symmetry varied with interval of 10 degrees. The obtained mean numbers of intersects for each direction are listed in Table 27. For graphical integration a graph has been plotted of the relationship between the number of intersections and the cosine of angle  $\beta$ , which, as it may be seen in Figure 73, may be regarded as rectilinear. The slope of the line is opposite to the one which took place in linear orientation (Figure 72), which is understandable: in a rod or wire the highest number of intersections occurs on secants perpendicular to the axis of symmetry (that is to the axis of the wire or rod), whereas in a sheet it occurs on secants parallel to this axis (that is perpendicular to the plane of the sheet). By measuring the area under the graph in Figure 73, which is made easier due to the fact that it is rectilinear, we find that the mean number of intersects is 9.6 mm<sup>-1</sup>. By doubling this number, we derive 19.2 mm<sup>2</sup>/mm<sup>3</sup>, which is the specific surface of grains of silicon ferrite.

In practice, calculations of the number of the intersections on different directed secants can be more readily conducted if the microscope has a rotating stage with a scale graduated in degrees, as for example microscopes M T -2, M T -3, and others. Satisfactory results are produced when an attachable rotating ring with a scale graduated in degrees is used. This ring goes with M T M-7 microscopes but can be used with any other metallographic microscope.

We have developed two variants of the analyses by a method of directed secants. One of these methods (the method of oblique microsections) makes possible to determine only the total value of the specific surface. The second method (the method of directed secants for space), besides that, makes it possible to estimate quantitatively

Table 27.

*Angle of  
inclination  
of Scurts  $\beta$*

Угол наклона секунд. $\beta$	$\cos \beta$	Число пересечений $n(\beta)$ , мм <sup>-1</sup>
0	1,000	17,0
10	0,985	16,8
20	0,940	16,0
30	0,866	15,5
40	0,766	13,6
50	0,643	11,8
60	0,500	9,9
70	0,342	7,3
80	0,174	3,8
90	0,000	2,3

*no. of inter-  
sections  $n(\beta)$ ,  
мм<sup>-1</sup>*

the orientation of surfaces of a system [59, 60]. Both methods are based on the assumption that a real system of oriented boundary surfaces may be regarded as consisting of two systems of which one is completely isometric and the second is completely oriented.

A. Linear Orientation of Boundary Surfaces

By breaking up boundary surfaces into equal, infinitely small elementary areas, in conformance with the original assumption, we take that a certain number of these areas are disposed parallel to the orientation axis, whereas the rest of areas are completely disoriented in space and, consequently, represent an isometric system. In rolling rounds of equiaxed cross section, in drawing rounds or drawing wire, the axis of orientation coincides with the axis of produced round or wire.

The total surface of the isometric number of elementary areas may be calculated from the basic formula of the method of random secants for space (25.1) under the condition that we know the mean number of intersections only and exclusively with those elementary areas which are disposed isometrically. Let us consider a case when the secants are directed precisely parallel to the orientation axis. Areas with linear orientation are also disposed parallel to this axis, therefore, secants of chosen direction cannot intersect them. Consequently, the mean number of intersections on secants, parallel to the orientation axis, is determined exclusively by the number of isometric areas. Therefore, having determined the mean number of intersections per 1 mm length of secants, parallel to the orientation axis which we shall designate as  $m_{||}$ , we can from Formula (25.1) find directly the specific surface of the isometric number of boundary surfaces:

$$S_{is} = 2 m_{||} . \quad (26.7)$$

Now, let us determine the specific surface of the oriented portion of boundary surfaces. Inasmuch as the elementary areas of this portion are parallel to the orientation axis, they are simultaneously perpendicular to any plane located at a right angle to this axis, that is, they are perpendicular to the plane of any transverse microsection of a round or wire. On a longitudinal microsection, the plane of which intersects the symmetry axis, or is parallel to the latter, traces of

areas with linear orientation form a system of lines parallel to the orientation axis. Let us place on the longitudinal microsection secants perpendicular to the orientation axis and let us determine the mean number of intersections per 1 mm of their length,  $m_{||}$ . These secants will intersect both the oriented and isometric elementary areas. However, inasmuch as we know the mean number of intersections with the isometric portion of areas,  $m_{\perp}$ , which is independent of direction, we can determine from the difference the number of intersections only with the oriented portion of areas. It will be

$$m_{\perp} - m_{||} . \quad (26.8)$$

Traces of areas with linear orientation form on the transverse microsection boundary lines, whose length will be defined by the basic equation of the method of random secants for a plane (20.7):

$$\sum P_{lin} = \frac{\pi}{2} (m_{\perp} - m_{||}) \text{ mm/mm}^2 . \quad (26.9)$$

On the basis that the length of traces of areas with linear orientation per 1  $\text{mm}^2$  of the area of transverse microsection is defined by the Equation (26.9) and that areas themselves are disposed perpendicular to the plane of the microsection, it is possible to conclude that

$$\sum S_{lin} = \sum P_{lin} \cdot 1 \text{ mm} .$$

Hence it follows that the specific surface of the portion of boundary surfaces with linear orientation is defined by the Formula:

$$\sum S_{lin} = \frac{\pi}{2} (m_{\perp} - m_{||}) \text{ mm}^2/\text{mm}^3 . \quad (26.10)$$

For this reason, in order to measure the specific surface of boundaries, with linear orientation, one longitudinal microsection would suffice, the plane of which intersects the orientation axis or is parallel to it. Correspondingly, two mean numbers of intersections,  $m_{||}$  and  $m_{\perp}$ , are determined. After that, the specific surface of the isometric portion of boundary is calculated from Formula (26.7): the portion of boundaries with linear orientation is calculated from Formula

(26.10). The total value of the specific surface, derived by adding the results obtained from both formulas, will equal:

$$\sum S_{\text{total}} = \sum S_{\text{is}} + \sum S_{\text{lin}} = 0.429 m_{\text{u}} + 1.571 m_{\text{l}} . \quad (26.11)$$

The degree of linear orientation of boundary surfaces is determined by the ratio of the specific surface of the portion with linear orientation to the total value of specific surface, expressed in per cent. From Formulas (26.10) and (26.11) it follows that the degree of linear orientation of surfaces,  $\alpha_{\text{lin}}$  is defined by the formula:

$$\alpha_{\text{lin}} = \frac{100 \sum S_{\text{lin}}}{\sum S_{\text{lin}} + \sum S_{\text{is}}} = \frac{100 (m_{\text{l}} - m_{\text{u}})}{0.273 m_{\text{u}} + m_{\text{l}}} \% \quad (26.12)$$

In the case of wire analyses, carried out by A. G. Spektor (see Table 26), the mean number of intersections on longitudinal and transverse secants was 101 and 316  $\text{mm}^{-1}$ , respectively. From our formula (26.11) we find that the total specific surface is  $540 \text{ mm}^2/\text{mm}^3$ , which differs approximately by 7% from the result obtained by A. G. Spektor, which is  $504 \text{ mm}^2/\text{mm}^3$ . From Formula (26.12) we determine that the degree of linear orientation of a given system of boundary surfaces is 62.6%.

#### B. Plane Orientation of Boundary Surfaces

Just as in the preceding case, we break down surfaces of a system into elementary areas. A certain number of these areas will be parallel to the orientation plane and others will form as isometric system of surfaces. Surfaces of grains of a rolled sheet, if sections of grains on microsections, parallel to the plane of the sheet, are equiaxed, serve as an example of a system with plane orientation. The plane of orientation is the plane of the sheet; perpendicular to this plane we locate the plane of the microsection subject to analyses.

Secants, parallel to the orientation plane, do not contain intersections with oriented elementary areas, for they and the secants are usually parallel. Consequently, the mean number of intersections per 1 mm length of secants, parallel to the orientation plane, will be determined exclusively by the length of the isometric portion of surfaces.

This mean number of intersections we shall designate as  $m_{\parallel}$ . Therefore, it is possible to write a formula which defines this specific surface of the isometric portion of boundaries in correspondence with the basic formula (25.1):

$$\sum S_{is} = 2 m_{\parallel} \text{ mm}^2/\text{mm}^3. \quad (26.13)$$

The second group of secants we arrange perpendicular to the orientation plane, designating the mean number of intersections per 1 mm of their length as  $m_{\perp}$ . If from this number of intersections are excluded those which are formed by the isometric portion of surfaces and the number of which per 1 mm of length of secants of any direction is  $m_{\parallel}$ , then the mean number of intersections only with oriented elementary areas, located perpendicular to secants, will be defined as the difference:

$$m_{\perp} - m_{\parallel} \text{ mm}^{-1}. \quad (26.14)$$

From the law of total projection for space, which will be presented further in this article, it follows that the total area of mutually parallel areas per unit volume of space is numerically equal to the mean number of intersections of these areas by secants directed at right angles to them, per unit length of secants. Using this postulate, we directly find:

$$\sum S_{pl} = m_{\perp} - m_{\parallel} \text{ mm}^2/\text{mm}^3. \quad (26.15)$$

From Formulas (26.13) and (26.15) it follows that the total magnitude of the specific surface of both portions of the system is:

$$\sum S_{total} = \sum S_{is} + \sum S_{pl} = m_{\perp} + m_{\parallel} \text{ mm}^2/\text{mm}^3. \quad (26.16)$$

The degree of plane orientation,  $\alpha_{pl}$ , is defined as the ratio of the portion of surfaces with plane orientation to their total specific surface expressed in per cent, that is:

$$\alpha_{pl} = \frac{100 (m_{\perp} - m_{\parallel})}{m_{\perp} + m_{\parallel}} \%. \quad (26.17)$$

From the aforesaid it follows that the analyses of structures with plane orientation also requires only 1 microsection, the plane of which must be perpendicular to the orientation plane. Two groups of secants

are marked on the microsection parallel to this plane and perpendicular to it. Correspondingly, two mean numbers of intersections,  $m_{\parallel}$  and  $m_{\perp}$ , are determined. After that, from Formulas (26.13) and (26.15) it is possible to calculate separately the specific surfaces of the isometric and plane-oriented portions of boundaries and their total length from Formula (26.16). The quantitative expression for the plane orientation we find from Formula (26.17).

In the above presented example of the analyses of transformer steel, which was carried out by us (see Table 27), the mean numbers of intersections on secants parallel and perpendicular to the orientation plane (which is perpendicular to the symmetry axis of the structure) were 2.3 and  $17.0 \text{ mm}^{-1}$ , respectively. From Formula (26.16) the total value of the specific surface is  $19.3 \text{ mm}^2/\text{mm}^3$ , which differs only by 0.5 per cent from the result obtained by the method of A. G. Spektor, which is  $19.2 \text{ mm}^2/\text{mm}^3$ . From Formula (26.17) we find that the degree of plane orientation of a given system of boundaries is 76.2 per cent.

#### C. Planar-Linear Orientation of Boundary Surfaces

As has been previously noted, this system of surfaces has no symmetry axis and, for this reason, the method of A. G. Spektor is not applicable in this case. A system of surfaces with a planar-linear orientation has one orientation plane and one orientation axis parallel to that plane. Elementary areas in such a system are subdivided into three groups: Areas of the first group are parallel both to the orientation plane and to the orientation axis simultaneously; areas of the second group are parallel only to the orientation axis, forming all possible angles with the orientation plane, each of which is equally probable; the arrangement of areas of the third group is isometric in nature, that is they are completely disoriented.

This type of orientation occurs, for example, in a sheet, strip or band, in which grains on microsections parallel to the plane of the sheet are not equiaxed but elongated in one preferred direction. For example, in a band the plane of the band is the orientation plane and its orientation axis is its longitudinal axis. In systems of the type in

question, schematically drawn in Figure 69d, quantitative analysis requires that not one but two microsections be prepared. The plane of the first microsection must be perpendicular to the orientation plane and parallel to the orientation axis. This microsection we shall call longitudinal. The plane of the second microsection is arranged perpendicular both to the orientation plane and orientation axis. We shall call this microsection the transverse microsection.

Inasmuch as in this case we have two types of orientation, which have been previously considered each separately, it is possible to apply formulas similar to formulas (26.7), (26.10), and (26.15). The only requirement is separate determination of mean numbers of intersections for each of the three aforementioned groups of elementary areas, which comprise a system of boundary surfaces with a planar linear orientation. Let us make an attempt to do just that.

Let us draw a group of secants on a longitudinal microsection, which secants are parallel to the orientation plane (that is to the plane of the band) and which are simultaneously parallel to the axis of linear orientation, inasmuch as the plane of the longitudinal microsection is also parallel to it. The mean number of intersections per 1 mm length of such secants, which we designate as  $m_{||}$ , is determined exclusively by areas with isometric orientation. Actually, under the given conditions, areas both with planar and linear orientations are parallel to secants and the latter cannot intersect them. Therefore, in accordance with the basic formula or Formula (26.7) we have:

$$\sum_i S_{is} = 2m_{||} \text{ mm}^2/\text{mm}^3. \quad (26.18)$$

The second group of secants we also draw parallel to the orientation plane (i. e., to the plane of the band) but on a transverse microsection the plane of which is perpendicular to the orientation axis. The mean number of intersections per 1 mm length of this group of secants we shall designate as  $m_{\perp}$ . Inasmuch as these secants are parallel to the orientation plane, they will not intersect the elementary areas with plane orientation. However, inasmuch as they are perpendicular to the orientation axis, they shall intersect areas with linear orientation

and, simultaneous with that, areas with isometric disposition. Therefore, if the mean number of intersections varies with areas of linear orientation, we shall find from the difference

$$m_1 - m_{11} \text{ mm}^{-1}, \quad (26.19)$$

and the specific surface of the portion of boundaries with linear orientation, in correspondence with Formula (26.10), will be defined by the expression:

$$\sum_{\text{lin}} = \frac{\pi}{2} (m_{\perp} - m_{11}) \text{ mm}^2/\text{mm}^3. \quad (26.20)$$

Third group of secants is arranged perpendicular to the orientation plane and orientation axis (i. e., perpendicular to the plane of the band). Secants may be drawn on any one of the two microsections, for the results will be identical. In this case, the secants will intersect all three groups of areas. The mean number of intersections with these groups per 1 mm of secants we shall designate as  $m_{\perp}$ . The mean number of intersections formed only by areas with plane orientation and secants, which are perpendicular to them, we shall find from the difference by subtracting mean numbers of intersections with isometrically disposed areas,  $m_{11}$ , and the areas with linear orientation, which is defined by the expression (26.19), from the number  $m_{\perp}$ . We derive:

$$m_{\perp} - m_{11} - (m_1 - m_{11}) = m_{\perp} - m_1 \text{ mm}^{-1}. \quad (26.21)$$

For this reason the specific surface of the portion of boundary surfaces with plane orientation, in correspondence with Formula (26.15), will be:

$$\sum_{\text{pl}} S_{\text{pl}} = m_{\perp} - m_1 \text{ mm}^2/\text{mm}^3. \quad (26.22)$$

Knowing how to determine separately the specific surfaces of each one of the three differently oriented portions of boundary surfaces, we can find without any difficulty the total specific surface by adding the right half of Formulas (26.18), (26.20), and (26.22). The degree of each type of orientation may be readily determined as the ratio of corresponding specific surfaces to their total magnitude expressed in per cent.

The method of oblique microsections [59, 17], first of developed

methods intended for the measurement of total magnitude of the specific surface of structures with linear and planar orientation, lost its importance after other methods, which had the same purpose and were described previously appeared. Therefore, it is necessary to discuss it here. Let us compare methods of analyses of oriented structures, described previously, and let us determine the scope of their application. As it has been already mentioned, the method of A. G. Spektor is rigorous from a mathematical viewpoint and may be applied for the size measurement of the total specific surface of systems of boundaries with axial symmetry. A shortcoming of this method is its inapplicability to the case of a more complex orientation, in the absence of axial symmetry, and the impossibility of quantitative estimation of the degree of orientation. Moreover, the method of A. G. Spektor, as compared with other methods, is more time consuming for it requires the determination of the mean number of intersections in several directions and subsequently graphic integration.

S. A. Saltykov's method of directed secants is approximate, but it has a number of advantages which are quite important in practice. It is applicable not only in the presence of axial symmetry but also in its absence. It also permits quantitative evaluation of the degree of various types of orientations of surface systems. Its procedure is simpler than that of A. G. Spektor's method and less time consuming, for average numbers of intersections are determined in only two (maximum three) directions and further, calculations use simple formulas. We shall show further that the procedural error of the method of directed secants, which is based on the assumption that any system of surfaces may be broken down into several systems with a definite type of orientation, does not exceed 5 per cent, which is quite acceptable for the great majority of carried-out measurements.

In conjunction with the aforesaid, the method of A. G. Spektor may be recommended for a more precise measurement of the total specific surface of boundary systems with axial symmetry, when the aim of the analyses is not the quantitative evaluation of the degree of orientation.

Section 27. The Rule of Projection for 3-dimensions and Verification of the Method of Directed Secants

Let us consider a system of mutually parallel and equidistant planes. Let us isolate within this system a cube with the edge equal to unity, so that two faces of the cube would be parallel and the rest perpendicular to the planes of the system. If the distance between parallel planes is  $\Delta$ , then the number within the volume of the cube will be  $\frac{1}{\Delta}$ , and the total area of planes within the cube, i. e., per unit volume, will be:

$$\sum S = \frac{1}{\Delta} (1.1) = \frac{1}{\Delta} \text{ mm}^2/\text{mm}^3. \quad (27.1)$$

In a more complex case we shall have a system of parallel plane areas of different dimensions and configurations, the planes of which will be disposed at different distances from each other, as shown in Figure 74. Let us break down the volume of the cube into several identical prisms, whose bases are squares with the side equal to  $a$ . These prisms will carve out from the planes of the system a number of areas, the maximum dimension of which may be equal to  $a^2$ . Let us arbitrarily agree to round off dimensions of areas, considering the dimension equal to a square if it exceeds half of this value, and equal to zero if it is less than this value.

Let us designate the number of these areas in each prism as  $m_1, m_2, m_3, \dots$ . Then the total surface of all areas within the cube along the edge of which is unity and two faces are parallel to the areas, will be:

$$\sum S = a^2 (m_1 + m_2 + m_3 + \dots). \quad (27.2)$$

Since the total number of prisms in the cube, the edge of which is unity, will obviously be  $\frac{1}{a^2}$ , then the mean number of areas in one prism will be:

$$\bar{m} = \frac{m_1 + m_2 + m_3 + \dots}{\frac{1}{a^2}} \text{ mm}^{-1}. \quad (27.3)$$

In the limit, when the cross section of prisms approaches zero and prisms themselves are transformed into secants, the mean number of

areas in one prism,  $m$ , will be equal to the mean number of intersections between plane sections of the system and secants perpendicular to them, per unit length of secants, i. e., it will be equal to  $m_1$ . Therefore, the specific surface of the system in question, in correspondence with Equations (27.2) and (27.3), will be equal to:

$$\sum S = m_1 \text{ mm}^2/\text{mm}^3. \quad (27.4)$$

This equation corresponds to the previously derived equation for a system of parallel equidistant planes (27.1), since the ratio  $\frac{1}{\Delta}$  precisely expresses the number of planes intersected per unit length of secants and directed perpendicular to the planes. Formula (27.4) has been used by us previously when deriving the relationship (26.15).

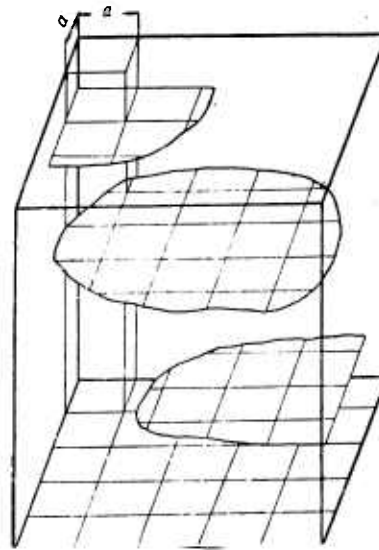


Figure 74.

Diagram to the derivation of the formula (27.4)

Besides the regularity determined here, we are also interested in the quantity which we shall call the total projection and which we understand to mean the sum of areas of superimposed projections, when projecting all surfaces found in a unit volume of the system in question, to some plane. In both cases, considered above, the systems consist of mutually parallel planes. For this reason their total projection on a plane parallel to them, obviously precisely coincides with the value of specific surface. Therefore, it may be stated that for the two considered specific cases the total projection of surfaces of a system onto a plane is equal precisely to the mean number of intersections per unit length of secants directed perpendicular to the chosen plane. Let us demonstrate that this postulate is general for any system of surfaces.

In the most general case, a system of surfaces may consist of surfaces that are open or bound, convex or concave, continuous or isolated from each other, plane or curves. Just as in the preceding case, in such a system (Figure 75) we break down the volume in question, which has a shape of a cube whose edge is unity, into a number of prisms whose bases are squares with the side  $a$ . Let us examine the projections of sections of the surface of the system, carved out by lateral faces of prisms, onto the base of a plane of a cube. Within each prism, those projections which are greater than  $a^2/2$  we round off to  $a^2$ , and ignore the others. The further course of logical consideration coincides with the derivation of Formula (27.4) for a system shown in Figure 74. For this reason we are not going to repeat it. The result is the law of projections for space, according to which the total projection onto any plane for any system of surfaces is precisely equal to the mean number of intersections between surfaces and secants directed perpendicular to chosen planes, per unit length of these secants.

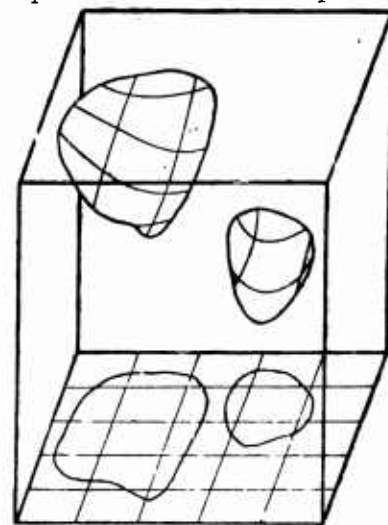


Fig. 75. Diagram to the derivation of the rule of the total projection for space.

This important law makes it possible in many instances to determine parameters of planar structures, for preselected dimensional systems of surfaces. As an example let us consider a group of spherical surfaces periodically but uniformly distributed through space. The diameter of spheres is  $D$  and the number per unit volume is  $N$ . The total projection of a sphere onto any plane is equal to twice the area of its central cross section, as follows from the definition of "total projection", which states that the projections of two half spheres are superimposed and the

areas of projections are added. For this reason the total projection of  $N$  spherical surfaces, which according to the law of projections is equal to the mean number of intersections formed by secants and surfaces, will be defined by the expression:

$$m = \frac{\pi D^2}{4} 2N = \frac{1}{2} \sum S \quad \text{mm}^{-1}. \quad (27.5)$$

This means that we derived the basic formula of the method of random secants for space (25.1) by other means. Further, using Formula (20.7), inasmuch as a system of spherical surfaces is isometric in space, we can find the specific of perimeters of cross sections of spherical surfaces from any plane intersecting a system of spheres:

$$\sum P = \frac{\pi}{2} m = \frac{\pi^2 D^2}{4} N = \frac{\pi}{4} \sum S.$$

We shall use the rule of total projection for determining the accuracy of the method of directed secants for space. For verification of this method we shall carry out a system of surfaces, representing identical ellipsoidal figures, which are periodically but statistically-uniformly distributed through space and arranged in such a manner that large axes of all ellipsoids are mutually parallel. Such a system is an example of a system of surfaces with linear orientation, in which the direction of large axes of ellipsoids is the orientation axes (also the symmetry axis). As compared with real structures, the system chosen for the verification of the method is not suitable for its evaluation, since in real systems of boundary surfaces there are always present sections parallel to the orientation axis (particularly at high degrees of orientation), whereas in this case oriented sections are absent. We assume that the large half axis of the ellipsoid is  $a$  and that the small half axis of the ellipsoid is  $b$  and that their number per unit volume is  $N$ .

In accordance with the method of directed secants, we mentally draw two groups of secants, parallel to the orientation axis and perpendicular to it. The mean number of intersections of these secants,  $m_{\parallel}$  and  $m_{\perp}$ , we shall determine by the rule of total projection. The ellipsoid is projected onto a plane, perpendicular to the first group of secants, as a circle the diameter of which is  $2b$ . Twice the area of  $N$  such circles will be equal to the mean number of intersections of secants parallel to the

orientation axes:

$$m_{\parallel} = \frac{\pi (2b)^2}{4} 2N = 2\pi b^2 N \text{ mm}^{-1}. \quad (27.6)$$

The ellipsoids are projected onto a plane perpendicular to the second group of secants (that is which is parallel to the orientation axis) as ellipses with half axes  $a$  and  $b$ . Twice the area of  $N$  such ellipses will be equal to the mean number of intersections on secants perpendicular to the orientation axis:

$$m_{\perp} = 2\pi abN \text{ mm}^{-1}. \quad (27.7)$$

Now putting at our disposal mathematically exact values of  $m_{\parallel}$  and  $m_{\perp}$ , we calculate the specific surface of the system of surfaces of rotation of ellipsoids, in question, the formula of the method of directed secants for the case of linear orientation (26.11):

$$\Sigma S = 1.571 m_{\perp} + 0.429 m_{\parallel} \text{ mm}^2/\text{mm}^3.$$

Substituting the values of the number of intersections, derived from formulas (27.6) and 27.7), and dividing both sides of the equation by the number of ellipsoidal sides per unit volume,  $N$ , we derive a formula which makes it possible to calculate approximately the surface of rotation as a function of the half axes:

$$S = 2\pi b (1.571a + 0.429b). \quad (27.8)$$

The verification of the derived formula unexpectedly revealed the following circumstance: its accuracy is approximately twice as high if the ratio of half axes of the ellipsoid is less than 3, and it becomes many times higher as this ratio increases, as compared with the approximation formula which is listed in reference books for the calculation of the surface of rotation of an ellipsoid. [143], [144]:

$$S = 2\sqrt{2}\pi b \sqrt{a^2 + b^2}. \quad (27.9)$$

The formula is coincidental with a positive error (the results of calculations happens to be greater than the actual value), and Formula (27.9) is coincidental with the negative error.

Under the most adverse conditions, the procedural error, which is due to the assumption that any system of surfaces may be broken down into elements isometrically arranged and oriented in a definite manner, does not exceed 5 per cent.

The principal of breaking down surfaces, which are being measured, into groups of elementary areas, oriented in space, in a definite manner (or disoriented), may be applied also in cases of a more complex orientation than the three types considered by us which are most commonly found in systems of boundary surfaces of metallic structures.

## Section 28. Orientation Analysis of Systems of Boundary Surface Areas

Besides the total extent (area) of boundary surface areas per unit volume of a metal alloy, their space orientation is also of great interest; the spatial orientation is generally dependent chiefly on the processes of plastic deformation or directional crystallization. Therefore, specifically, the orientation study of boundary surface areas, which is quite effective in determining local deformations, their heterogeneity and distribution in the volume of metal, is quite promising for the revealing and understanding of the mechanism of plastic metal flow in alloys. The spatial orientation of boundary surface areas may be considered from different viewpoints, on the basis of which appropriate methods of its quantitative characteristic are developed.

On the basis of purely geometrical notions, the orientation of an isolated elementary area may be defined by the size of angles which it forms with predetermined directions (axis, planes). From this viewpoint the orientation of complex systems of boundary surface areas may be estimated, for example, in the terms of relative fractions of elementary areas (or a fraction of these specific surface area), oriented in a definite manner. The method of this kind, developed by us [60], which permits numerical evaluation of lineal, plane and mixed lineal-plane orientations with the aid of coefficients of the degree of orientation, was described previously (see Section 26). Although this method is based on a certain assumption, its accuracy is quite sufficient for the most cases of orientational structural analysis. A rigid method for the estimation of orientation with the aid of a polar distribution diagram of the function of density of normals was developed by A. G. Spektor [146]. This method is applicable for systems of surface areas with axial symmetry, which according to our classification corresponds to lineal orientation or plane orientation.

From the other viewpoint, the orientation of boundary surface areas may be characterized by the density of their disposition in various special directions. The quantitative estimation of orientation, based on this notion, is expedient for several reasons. It is precisely the density of disposition of surface areas in various directions that determines the

anisotropy of properties of a metal or an alloy in the same measure in which it is dependent upon the interfacial boundaries of microparticles of like or unlike phases. The appearance of certain types of orientations of boundary surface areas is singularly connected with the regular disturbance of the initially uniform density of their disposition in various directions. Therefore, on the basis of the density of disposition of surface areas it is also possible to obtain, if it is necessary, a purely geometrical interpretation of their orientation. The method of estimating the orientation, based on the density of disposition of surface areas in various directions, is reduced to construction of a space rose of the number of intersections [138], similar to the plane rose of the number of intersections, described in Section 21.

Finally, it should be mentioned that it is possible to estimate indirectly the orientation of boundary surface areas by the ratio of lineal dimensions of microparticles (or their sections), measured in definite directions. The evaluation of oriented structures by the ratio of diameters of plane grains was proposed long ago by Ye. Geyn [136]. Inasmuch as this value almost always has a singular relationship to the degree of deformation of a given kind, it has been successfully used for the estimation of local deformation [145, 175]. It can be demonstrated that this characteristic of an oriented structure can be also derived from the density of disposition of areas in different directions, that is from the space rose of the number of intersections.

From the aforesaid it follows that the space rose of the number of intersections is a universal and comprehensive characteristic of orientation of surface areas, for it permits to calculate the value of the specific surface area and also to determine the quantitative indices of the orientation of surface areas of any interpretation which may seem more expedient to us.

If from any point within a system of surface areas rays are drawn in many directions, that is, secants with directions uniformly disposed in space, it is possible to calculate the number of intersections for each secant separately and to derive the mean number of intersections for each direction which is of interest to us. This postulate may be expressed

in a somewhat different way, which has a greater conformity with the method used in practice: the mean number of intersections for any given direction is determined by calculating the number of intersections for one group of mutually parallel secants, having had the same direction in space. Knowing the mean numbers of intersections for several directions, which obviously express the density of disposition of surface areas in these directions, we construct the space rose of the number of intersections in polar coordinates. The shape of the rose is singularly defined by the relative probability of intersection of surface areas of the system by secants in various directions, that is it is determined by the density of disposition of surface areas in these directions. For this reason the shape of the rose gives a complete characteristic of the orientation of these surfaces in space. The absolute dimensions of the rose, constructed on a definite scale, are singularly dependent upon the size of the specific surface area of a boundary system in question.

If a system of surface areas has an axis of symmetry, then the construction of the rose of the number of intersections is extremely simple. In such systems the structure is identical in all planes of polish which intersect the axis of symmetry (or are parallel to it). Therefore the rose of the number of intersections by corresponding boundary lines, constructed for any axial plane of polish on a plane, is obviously the axial intercept of the space rose. The shape of the latter is defined as the shape of the rotational body, obtained by rotating the grain rose of the number of intersections about the axis of symmetry.

For example, a system of parallel planes has the axis of symmetry perpendicular to them and in a section, which intersects this axis, it appears as a system of parallel lines. For the latter, the plane rose of the number of intersections is represented by two circumferences of equal diameter tangent at the origin of coordinates, the centers of which lie on the axis of symmetry (Figure 59). The rotation about the axis of symmetry makes it possible to produce a space rose of the number of intersections for a system of parallel planes, which is represented by two spheres tangent at the origin of coordinates, whose centers lie on the axis of symmetry of the system and whose diameters are equal.

In the case of space isometric system of surface areas, the mean numbers of intersections on secants of any direction coincide, just as it follows from the definition of the notion of isometricity itself. For this reason the space rose of the number of intersections is shaped as a sphere, the center of which is found at the origin of coordinates. The axial section of such a rose is identical with the shape shown in Figure 57.

If we accept our conjecture that it is possible to break down any system of surface areas into groups of identical elementary areas, of which areas of one group are arranged isometrically (completely disoriented in space) and areas of other groups are in one or another way completely oriented, the space rose of the number of intersections may be constructed by the method of adding vectors of each direction, as it is done on a plane (see Section 22). By this method a space rose may be constructed from mean numbers of intersections in few directions (two or three), both for systems with axial symmetry and for systems without it.

A series of sections of space roses of the number of intersections, intercepting the axis of symmetry (which is simultaneously the axis of rotation) is shown in Figure 76 for systems of boundary surface areas with the degree of plane orientation ranging between 0 and 100 per cent. A completely isometric system of surface areas is characterized by a spherical rose of the number of intersects (Figure 76,1). In the presence of plane orientation, "necking" appears which narrows down with increasing degree of orientation (Figure 77,2to 5). When a system of surface areas becomes completely oriented, the rose transforms into a pair of spherical surfaces tangent to each other (Figure 76, 6).

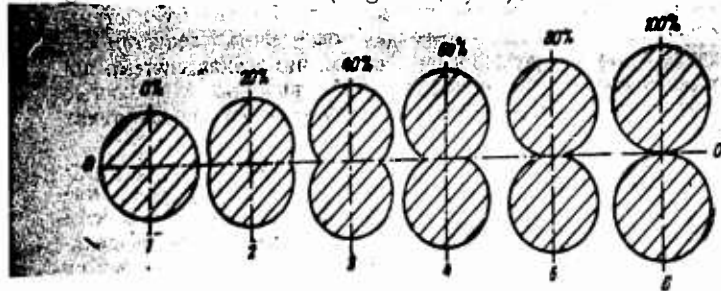


Fig. 76. Axial sections of space roses of the number of intersections with different degrees of plane orientation. The vertical axes are the axes of symmetry, and the axis O--O is the plane of orientation.

In the case of lineal orientation, the space roses of the number of intersections have different shapes. A series of axial sections of roses for systems of surface areas with the degree of lineal orientation, gradually increasing from 0 to 100 per cent, is shown in Figure 77. In contrast to the preceding case, here the initial sphere contracts with the increasing degree of orientation; contraction characterizes the isometric system along the axis of symmetry (Figure 77, 2 to 5). When a system becomes completely linearly oriented, the rose of the number of intersections becomes a torus, whose radius of the internal circle is equal to zero (Figure 77-6).

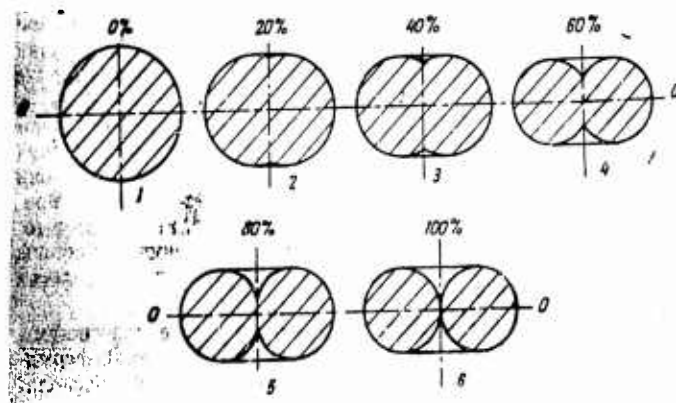


Fig. 77. Axial sections of space roses of intersections with different degrees of linear orientation. The vertical axes are the axes of symmetry and orientation.

In Figures 76 and 77, vertical axis of all shapes are simultaneously the axis of space symmetry of the structure and the axis of rotation for the formation of space rose from its section. In the case of a plane orientation, its plane is perpendicular to the axis of symmetry (Figure 77).

A rose of the number of intersections may be constructed by two methods: a simpler one based on measurements in a few directions (two to three) and by a more complex method using a large number of microsections. By comparing the shapes and sizes of roses, constructed by these methods for one and the same system of boundary surface areas, it is possible to determine the permissibility of our assumption that any system of surface areas

consists of completely isometric and completely oriented fractions. We shall cite certain results of such comparisons.

We have analyzed a system of interfacial surfaces of ferrite and pearlite constituents in a sized rod 9.5 mm in diameter from steel 30. The plane of polish coincided with the axis of the rod. The number of intersections between the secants and boundary lines, separating the ferrite and pearlite constituents, were counted in ten groups of secants (in ten directions) for every 10 degrees. The total length of secants in a group for each direction was taken such that the total number of intersections would be at least 1000. A total of more than 10,000 intersections were counted for the construction of the rose of the number of intersections. One quadrant of an axial section of the rose of number of intersections for a given case is plotted in Figure 78. The line which connects the points of the mean numbers of the intersections in various directions has been constructed graphically by our method of directed secants (see Figure 63), using the mean numbers of intersections of only two directions, parallel and perpendicular to the axis of symmetry (the latter is also the axis of the rod and the axis of orientation). Despite this, the rest of the points have a quite satisfactory agreement with the same curve, which lends evidence that the original postulate of our method of directed secants is permissible. The fact that when the direction of groups of secants varied between 0 and 90 degrees with respect to the axis of symmetry, they were disposed within a tenth to cover uniformly the entire area of the longitudinal plane of polish of the rod, should be taken into consideration. Nevertheless, it is possible that the scatter of points was produced by the essential difference in the magnitude of the specific surface areas in the periphery and central sections of the sized rod.

We have made similar measurements for a system of surface areas of silicon ferrite grains in sheet transformer steel (the thickness of the sheet 1 mm). Planes of polish were disposed perpendicular to the plane of the sheet. The control checking has shown that in the plane parallel to the plane of the sheet the ferrite grains were equiaxed, which gave evidence that axial structural symmetry was present. A total of about 1200 intersections have been counted for 10 directions. A graphic plot

of 1 quadrant of the axial section of the rose of the number of intersections is shown in Figure 79. Data obtained only for two directions, parallel and perpendicular to the axis of symmetry, have been used in this case for the construction. Nevertheless, Figure 79 shows that there is no need whatever to consider the mean numbers of intersections for all other directions, inasmuch as they have a fine agreement with the curve plotted only from two points. Consequently, in this case also the possibility of the original postulate of the method of directed secants, developed by us, is also confirmed.

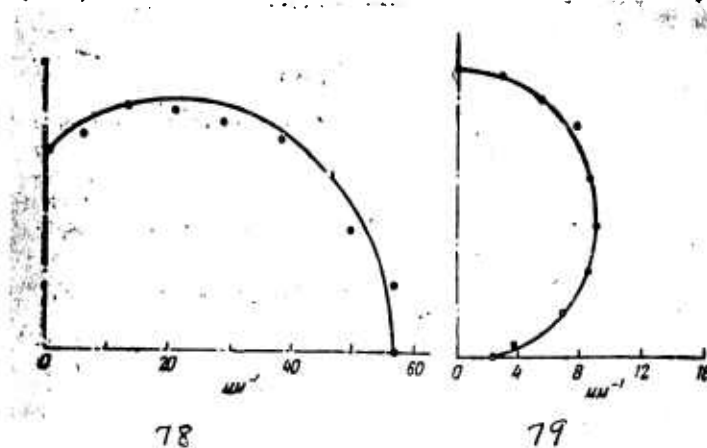


Fig. 78. Axial section of the space rose of the number of intersections for the system of surfaces of the portion of the perlite and ferrite components in a calibrated bar of steel of brand 30 (there is shown one quadrant of the section of the rose).

Fig. 79. Axial section of the space rose of the number of intersections for the system of the surfaces of the grain of silicon ferrite of sheet transformer steel (one quadrant of the section of the rose is shown).

The results similar to those shown in Figures 78 and 79 have been obtained by us for a number of specimens different as to types of orientation and structure. Roses of the number of intersections for grain boundaries of ferrite in sheet steel, for interfacial boundaries of ferrite and pearlite constituents in rolled rounds of different diameter, for interfacial boundaries in 2-phase brass rounds, for the same type of interfacial boundaries of ferrite and pearlite constituents in the rupture zone of the specimen deformed by stretching, etc., were constructed experimentally. In many cases a calculated curve has a fine agreement with experimentally found values of the mean numbers of intersections for different directions.

Let us consider a system of surface areas, with a plane orientation, having broken down the areas into two groups: a group of disoriented

elementary areas and a group of areas usually parallel. The number of intersections on the secants, which are parallel to the plane of orientation, will be determined by the size of the specific surface area of the group of disoriented areas only and it will be equal to  $m_{\parallel}$ . This number is independent of the direction of secants. The number of intersections with areas, disposed parallel to the plane of orientation, is dependent upon the angle between the secant and this plane. If the angle is 90 degrees, then we obtain the maximum number of intersections which is

$$m_{\perp} - m_{\parallel} = S_{or} \text{ mm}^{-1}$$

as it follows from Formula (27.4), inasmuch as the number of intersections with oriented areas only is equal to the total number of intersections minus the number of intersections with disoriented areas, which is equal to  $m_{\parallel}$ . It may be easily conceived that the mean number of intersections for any direction,  $m$ , will be defined by the expression:

$$m = (m_{\perp} - m_{\parallel}) \sin \alpha + m_{\parallel} \text{ mm}^{-1}, \quad (28.1)$$

where  $\alpha$  is the angle between the orientation plane and the direction of the secant. From the latter equation it follows that the graph of the mean number of intersections in different directions, versus the sine of angle  $\alpha$  must be a straight line. This is the same relationship expressed by the rose of the number of intersections but plotted in different coordinates. Deviation of experimentally found points from the straight line gives a more visible evidence of the error, due to the assumption on which our method of directed secants is based, than the plot of the rose in polar coordinates.

In Figure 80 line 1 shows the relationship for the same case, employing the same data which were used for plotting the rose of the number of intersections in Figure 78. Line 2 has been plotted using the same data as for the rose in Figure 79. Lines 3 and 4 were plotted by experimental data of A. G. Spektor for interfacial surface areas of ferrite and pearlite constituents in steel wire [61], with the scale on y axis 1/10.

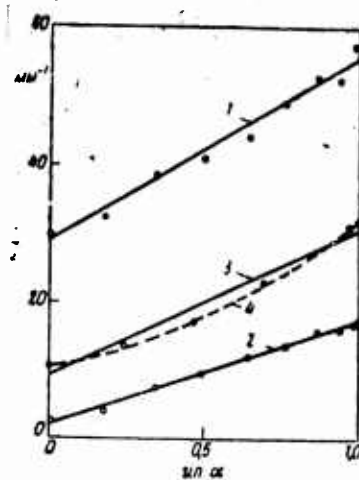


Fig. 80. Dependence of the average number of intersections on the sinus of the angle between the axis (or plane) of orientation and the direction of the intersecting straight line: 1--for calibrated rod of brand 30 steel; 2--for sheet transformer steel per our data; 3, 4--for wire per the data of A. G. Spektor (scale along the axis of the ordinates 1/10)

When discussing the results obtained the fact should be taken into consideration that the method of secants is a statistical method which definitely means that a number of intersections is determined with an unavoidable error. Moreover, scatter of points is possible due to nonuniform degree of orientation and the size of the specific surface area in external and in deeper layers of one and the same specimen. The mean angle formed by the secant and interfacial areas continually decreases as the direction shifts from perpendicular to parallel to the axis or plane of orientation. This possibly predetermines the systematic error, the magnitude of which is dependent upon the mean angle between the secant and interfacial surface areas and increases as the latter decreases.

Considering the aforesaid, it is possible to assume that rectilinear relationship between the mean number of intersections and the sine of the angle between the secants and the axis or the plane of orientation is quite justifiable for the purpose of practical application of the method of directed secants when it is necessary to estimate the orientation of boundary surface areas.

In summing up we arrive at the final conclusion that the quantitative evaluation of the more common types of orientations lineal and plane (occurring separately or together), is quite reliable and may be accomplished with sufficient accuracy by the coefficients of the degree of orientation, calculated by the method of directed secants with the aid of for-

mulas (26.12), (26.17) and formulas similar to them. In a case of a more complex orientation, a comprehensive and visible picture of the orientation of a surface areas system is given by the space rose of the number of intersections. This, however, is less convenient for it deprives us of the possibility of quantitative study of the relationship between the orientation of boundary surface areas and factors which affect it, inasmuch as the orientation is characterized not by concrete numbers but by a type of complex space shape, its projections or sections.

Now let us consider another method of estimating the orientation of boundary surface areas, proposed by A. G. Spektor [146]. The orientation of an elementary area with respect to any direction, defined by the straight line  $l$ , is characterized by the size of the angle  $(l, n)$  between this straight line and the normal  $n$  to the elementary area. Let us designate the size of the elementary area as  $dS$  and project all areas, comprising a system of boundary surface areas confined in a unit volume of metal, onto plane  $Q$ , perpendicular to a chosen direction, that is perpendicular to the straight line  $l$ . It is not difficult to see that the sum of all projected areas,  $dS_Q$ , is equal to the mean number of intersections of boundary surface areas with the unit length of the straight line  $l$ , that is it is equal to  $m_1$  (see Section 27). At the same time Formula (28.2)

$$m_1 = \int_S dS_Q = \int_S \cos (l, n) dS. \quad (28.2)$$

Hence it follows that Formula (28.3)

$$\cos (l, n) = \frac{m_1}{S}, \quad (28.3)$$

where the quantity  $S$  stands for the same thing as  $S$ , that is for the specific surface area.

Formula (28.3) gives the absolute value of the cosine of the angle between the normals to the surface area and the chosen direction, the weighted mean for the entire boundary surface area. For the direction it is more feasible to choose the symmetry axis of the structure. This value, which we shall call the mean cosine of the normals, according to A. G. Spektor is precisely the means for the estimation of the general orientation of boundary surface areas with respect to the axis of symmetry of the

structure, in particular, or with respect to a given straight line, in general. The mean number of intersections,  $m_1$ , in the direction parallel to the axis of symmetry, may be readily determined from the longitudinal plane of polish. The specific surface area,  $S$ , is calculated by the method of directed secants with the aid of graphic integration by Formula (26.6), for which purpose it is necessary to determine the relationship between the mean number of intersections and the direction of the secant with respect to the axis of symmetry of the structure on the longitudinal plane of polish.

Let us consider an example illustrating the calculation of the mean cosine of normals experimental data of A. G. Spektor, obtained for the interfacial surface area of pearlite and thorite constituents in steel wire drawn from 5.5 mm down to 3.8 mm in diameter. These data are listed in Table 26 and Figure 72. The mean number of intersections in the direction which coincides with the axis of symmetry is  $101 \text{ mm}^{-1}$  and the value of the specific surface area, found by graphic integration as in Figure 72, is  $504 \text{ mm}^2/\text{mm}^3$ . From these data we find the mean cosine of normals from the Formula (28.3):

$$\cos(l, n) = \frac{101}{504} = 0.20.$$

The limiting values of the mean cosine of normals determined by systems of surface areas completely oriented in the direction of the axis of symmetry (complete lineal orientation) and completely perpendicular to it (complete planar orientation). In the first case, the mean cosine of normals with respect to the axis of symmetry is 0; in the second case it is 1. From Formulas (25.1) and (28.3) it may be readily concluded that for an isometric system of surfaces the mean cosine of normals is 0.5 with respect to any straight line. Hence it follows that the values of the mean cosine of normals, varying between 0.5 and 0, characterize the increasing lineal orientation and that values varying from 0.5 to 1.0 characterize the increasing planar orientation.

By comparing the mean cosine of normals with coefficients which characterize the degree of lineal or planar orientation (see Formulas 26.12 and 26.17) it may be seen that the latter contain the mean numbers of intersections in the direction perpendicular to the axis of symmetry of the structure (in addition to parameters, which are general for both types of orientation estimation). The mean numbers of intersection, determined

along the axis of symmetry and perpendicular to it, vary with increasing orientation in opposite directions. Therefore, the evaluation of the degree of orientation by coefficients is more "sensitive" than the evaluation by the value of the mean cosine of normals, which compensates for a certain lack of rigor in the procedure of deriving formulas which define the coefficients of the degree of orientation. It should be also noted that the experimental determination of the latter is simpler, for it requires measurements only in two directions, whereas the determination of the mean cosine of normals requires measurements in many directions and graphic integration.

The mean cosine of normals, similar to the coefficients of the degree of orientation, gives only a general notion on the orientation of boundary surface areas. For a more detailed characteristic of orientation it is necessary to evaluate the distribution of individual fractions of boundary surface area with respect to various directions of normals to them. Inasmuch as the solution of such a problem for space is connected with mathematical difficulties, A. G. Spektor considers a similar dimensional problem. "Function of relative density of normals" is introduced, which characterizes the relative length of lineal boundaries, whose normals lie within a definite range of angles. The function of density of normals is defined by the equation:

$$\psi(\alpha) = \frac{1}{L} \left( \frac{dL}{d\alpha} \right), \quad (28.4)$$

in which  $L$  is the specific length of lineal boundaries in a plane of section intersecting the axis of symmetry of the structure;  $\alpha$  and  $(\alpha = \alpha_1)$  are the angles formed with the axis of symmetry within the limits of which lie the normals to that fraction of lineal boundaries, the length of which is defined by the value of  $dL$ .

Similar to expression (28.2) we find the mean number of intersections per unit length of the secant,  $m$ , which secant has a certain direction  $n$ :

$$m = \int_L \cos(n, m) dL = L \int_{\alpha=0}^{\pi} \psi(\alpha) \cos(n, m) d\alpha. \quad (28.5)$$

From the latter equation we have to obtain the relationship between

the function of the density of normals,  $\psi(d)$  and direction expressed through the angle of  $d$ . We introduce an assumption that the angles of inclination of normals to the axis of symmetry vary continually as a multiple of a certain small angle  $d_0$ . If this angle is chosen sufficiently small, the error of this assumption will be slight. Let us consider an example of calculations, cited by A. G. Spektor, in which the angle  $d_0$  is taken equal to  $\frac{\pi}{8}$  or 22.5 degrees.

The diagram of directions chosen with respect to the axis of symmetry of the structure is shown in Figure 81. The axis of symmetry coincides with the line 8-0. From this diagram it is apparent that the mean numbers of intersections in directions 0 and 8, 1, and 7, 8 and 6, 3 and 5, coincide for each pair. Assuming that all values of cosines have a plus sign, we derive from Formula (28.5) a system of five equations, and by solving it with respect to the value of the function of density of normals we find the following working formulas:

$$\begin{aligned}\psi_0 = \psi_8 &= \frac{1}{L} (6,650 m_3 - 6,150 m_4); \\ \psi_1 = \psi_7 &= \frac{1}{L} (3,325 m_3 + 3,325 m_4); \\ \psi_2 = \psi_6 &= \frac{1}{L} (3,325 m_1 - 6,150 m_2 + 3,325 m_3); \\ \psi_3 = \psi_5 &= \frac{1}{L} (3,325 m_0 - 6,150 m_1 + 3,325 m_2); \\ \psi_4 &= \frac{1}{L} (6,650 m_1 - 6,150 m_0).\end{aligned}\quad (28.6)$$

The specific length of boundaries on the plane of polish  $L$ , found in the formula (28.6), is determined from the basic formula of the method of random secants for a plane (20.7):

$$L = \frac{\pi}{2} m = \frac{\pi}{2} \cdot \frac{m_0 + m_1 + m_2 + \dots}{\epsilon} \quad (28.7)$$

Knowing the mean numbers of intersections in five directions (0, 1, 2, 3, and 4, in the diagram shown in Figure 81) it is possible to calculate the functions of the density of normals for each direction and to plot in appropriate polar diagram, which is precisely the final characteristic of the orientation of boundary surface areas, done by the method in question.

The method described may be illustrated by an example, cited by its

author [146]. The subject of the investigation was the interfacial area of pearlite and thorite constituents in steel wire drawn from 5.5 mm down to 3.8 mm in diameter (reduction 52 %). The mean numbers of intersections, shown in Table 28, were determined on the plane of polish intersecting the axis of symmetry of this structure (which coincided with the axis of the wire).

Table 28

Direction (рис. 81)	Angle $\alpha$	Среднее число пересечений $m, \text{мм}^{-1}$	Функция плотности нормалей $\psi$
0	0	101	-0,04
1	22°,5	155	0,06
2	45°,0	227	0,24
3	67°,5	290	0,40
4	90°,0	316	1,18

*Аverage No. of Intersections  $m, \text{mm}^{-1}$*   
*Function Density of Normals  $\psi$*

In the same table are also presented the values of the function of the density of normals,  $\psi$ , calculated by us from formulas (28.6). The value of this function must be always positive, as it follows from the formula (28.4). Therefore, it should be assumed that the value of the function of the density of normals for the direction coinciding with the axis of symmetry ( $\psi_0 = -0.04$ ), is negative either because of inaccuracy of initial data or, which is more probable, due to insufficient accuracy of working formulas (28.6).

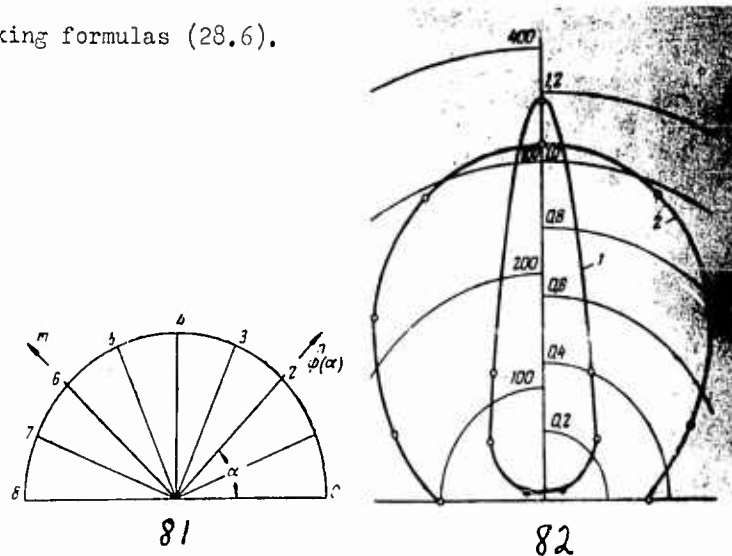


Fig. 81. For the computation of the function of the plane of the normals

Fig. 82. Diagram of the distribution of the plane of the normals

It should be noted that the mathematical tools of the method are rigorous up to Formula (23.5), inclusive. However, calculations based on this formula are approximate. Although theoretically it is possible to attain any accuracy by reducing the angle  $d_0$ , in practice it is quite difficult to attain, for the calculation in this case becomes extremely cumbersome. The value of  $d_0 = \frac{\pi}{8}$ , taken by the author of the method, is clearly too large.

The diagram of the distribution of densities of normals with respect to directions, plotted in polar coordinates (Curve 1), is given in Figure 82. It corresponds to the data found in the table. The same figure shows the rose of the number of intersections for the same system of boundary surface areas, constructed from the mean numbers of intersections,  $m$ , given in Table 28 (Curve 2). The function of the test steels normals has a maximum value in the direction which is perpendicular to the axis of symmetry. The minimum value of the function, as it should have been anticipated, coincides with the axis of symmetry. For the sake of comparison, it may be pointed out that in the case of an isometric system of surface areas, the function of density of normals is 0.318 for any direction.

When comparing the diagram of the distribution of the density of normals with the rose of the number of intersections, one cannot fail but note a number of advantages of the latter. The rose is plotted directly from experimental data, whereas when we calculate on the basis of the same data, the function of density of normals we clearly introduce additional errors. The rose of the number of intersections is more illustrative for it characterizes the density of disposition of boundary surface areas in different directions, that is it characterizes the factor which has a direct connection with the degree of anisotropy of properties. Finally, a rose may be constructed for any system of surface areas, whereas the function of the density of normals may be calculated only for a system of surface areas which have an axis of symmetry. The method considered could find applications for the fine analysis of boundary surface areas but only under the condition that a more accurate and at the same time a more simple method for calculation of the function of density of normals from Formula (23.5) would be found.

In this discourse we do not consider the evaluation of orientation by the value of diameter ratio of microparticles, for this evaluation is concerned rather with the shape of microparticles.

## Section 29. Accuracy Norms of the Method of Secants

The basic formula of the method of random secants (25.1), derived with analytical accuracy, establishes a direct proportionality between the values of the specific surface area and the mean number of intersections of surfaces per unit length of random secants. Hence it follows that the relative error in the determination of the mean number of intersections,  $m$ , predetermines the same kind of relative error in the unknown value of the specific surface area.

A number of formulas of the method of directed secants also establishes a direct proportionality between the values of the total specific surface area and its isometric and oriented fractions on one hand and mean numbers of intersections in certain definite directions on the other. These formulas are approximate and the measure of their accuracy was discussed previously. The error in determining the mean numbers of intersections in this case is algebraically superimposed on the error, and either decreases or increases it by the value proportional to the error of determination of mean numbers of intersections.

By determining the accuracy of determination of the number  $m$ , we, by doing that, also determine the accuracy of the unknown value of the specific surface area in the volume of metal directly adjacent to the plane of polish under the investigation. The question as to how accurately the obtained value characterizes the structure of the metal as a whole is not connected to the accuracy of the method of determination and is dependent upon the uniformity of this structure and the volume of metal. For this reason we can assume that the accuracy of determination of the statistical mean value of the number of intersections per 1 mm of length of secants,  $m$ , simultaneously represents the accuracy of determination of the value of the specific surface area  $\sum S$ .

A reservation should be made that this is valid in the case of correctly applied method. Thus, for example, transverse surfaces of polish of steel rods are commonly used for standard measurement of steel grain size. As it has been previously mentioned, it is more rational to substitute the measurement of the specific surface area of grains for the

measurement of the grain size. However, if the space grains are not equiaxed, which cannot be revealed on a transverse plane of polish, the application of the method of random secants will turn out to be incorrect. The greater the deviation of the grain shape from equiaxed, the greater will be the secondary error due to the application of the method of random secants to such a structure. In that case, the measurement must be made by the method of directed secants on a longitudinal plane of polish.

Ordinarily two techniques for counting the number of intersections of grain boundaries by secants on a plane of polish are used: a. with a traversing plane of polish and b. with a stationary plane of polish. Each of these methods has its own advantages, short comings, and fields of application.

In the first case an ocular with a cross hair is used. The plane of polish is continually traversed along a straight line by means of a micrometric screw of the microscope stage or by a two-coordinate specimen traverse, simultaneously counting the number of times boundary lines pass the center of the cross hair of the ocular. In this case the length of a secant is equal to the traverse of the plane of polish, recorded by the micrometric screw (in millimeters). By shifting the plane of polish or by turning it, it is possible to repeat the determination at the second secant, etc., until a reliable mean value of the number of intersections per 1 mm of secants,  $m$ , is obtained. In this technique of counting, the length of each secant is limited only by the over-all size of the plane of polish and by the traverse of the microscope stage. M T-3 apparatus, used for the microhardness determinations, is quite convenient for this purpose.

When structures are oriented and when it is necessary to use secants directed at definite angles to the axis or plane of orientation, it is expedient to use a polarized microscope of M T-2 M T-3 types, etc., equipped with opaque eliminators and rotating stages for the scale graduated in degrees, which, unfortunately, are absent in metallographic microscopes. When working with M T-3 instrument, their rotating disc with a scale graduated in degree is installed on the stage of the instrument. A small bag of the disc (see Figure 83) fits (the fit is not too

tight) a hole made in the stage. When a specimen is fixed in this manner all of its surface is available for observation. The disc is successively rotated to a definite angle and traversed by 1 micrometric screw. After that, the stage is traversed to a short distance in perpendicular direction by the second screw and again traversed by the first screw so that the line of observation passes from one edge of the specimen to another. Thus, groups of mutually parallel secants, with different directions and covering the surface subject to analysis within uniform grid, are formed on the plane of polish.

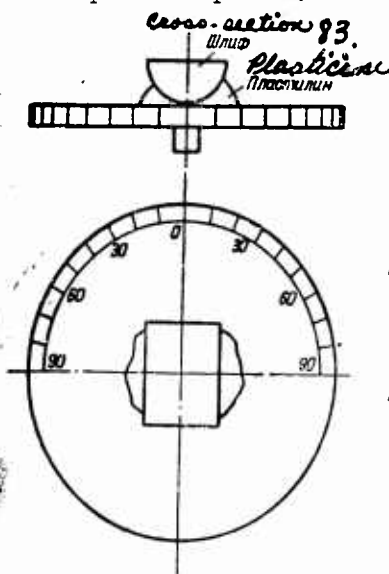


Figure 83. Device for turning the slide to a definite angle with relation to the direction of the movement of the table of the instrument PMT-3.

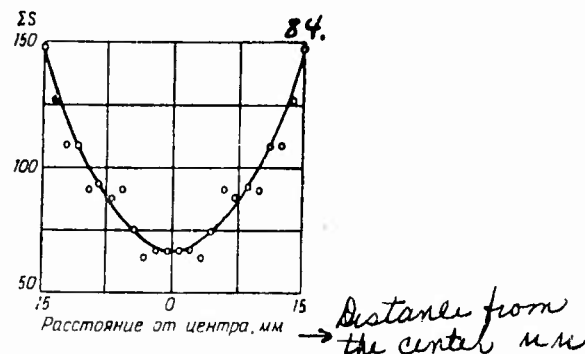


Fig. 84. Change in the magnitude of the specific surface of graphite along the cross section (diameter) of grey iron 30 mm in diameter

When working with ordinary metallographic microscopes it is expedient to set up two-coordinate specimen that traverses on their stages, which prevents traversing of the specimen into mutually perpendicular directions, recording the value of traverse on a scale with *vernier* with accuracy of 0.1 mm. It is particularly expedient to set up a specimen traverse on the stage of M IM-7 microscope, so that the traverse of the specimen could be made by left hand. In the existing design of this microscope both the traverse and focusing are made by right hand, with the left hand being free, which is quite inconvenient.

The advantage of traversing the specimen with simultaneous counting is the possibility of using maximum magnifications, which makes it possible to a more reliable recording of the fact of intersection between the grain boundary and the line of direction of the center of the cross hair. In this case, the magnification used has absolutely no effect on

the time of counting of a given number of points.

The method of traversing specimen should be preferred in all cases when it is necessary to determine the mean number of intersections of random or directed secants which characterize the entire area of the plane of polish as a whole. A differentiated determination of the size of the specific surface area from individual zones of the plane of polish requires that the numbers of intersections be counted separately for small areas of the plane of polish, usually in separate fields of vision; in these cases the method of traversing the specimen necessarily has to be replaced by the method of counting with a stationary specimen. For example, Figure 84 shows the variation of the dispersity of graphite in gray cast iron (which is estimated by the value of its specific surface area) across the section of a casting 30 mm in diameter. In such a case the count is made successively in several fields of vision arranged along the diametrical line of the transverse plane of polish separately for each field. The rule of the ocular-micrometer or the cross hair of the ocular may be used as the secant. They make it possible to count in one field of vision a large number of points into mutually perpendicular directions. When applying this method, the length of the secants, that is, the length of the projection of the ocular rule on the plane of polish or the diameter of visible field of vision are determined with the aid of object micrometer.

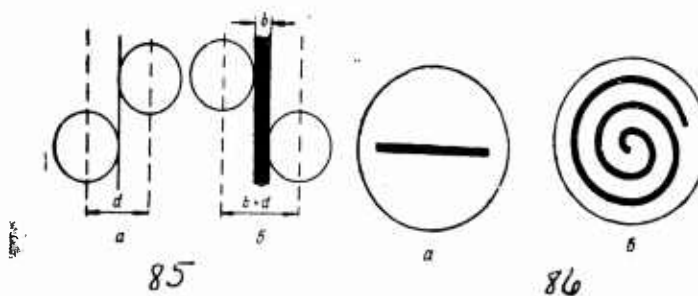


Fig. 85. Effect of the width of the sections of the line in determining the number of cross sections by the method of arbitrary secants (A. G. Spektor [104])

Fig. 86. Ocular insertions for determining the average number of cross sections by the method of arbitrary sections, these insertions being free of systematic error

The greater the number of counted points, the more accurate are the results of the determination. In view of that, when making counts with a

stationary specimen it is desirable to use low magnifications, for the number of intersections in a given field of vision is inversely proportional to the magnification. However, when using low magnifications the error increases due to difficulty of establishing the fact whether grain boundaries are intersected by the secant or pass near it. Therefore, it is necessary to apply sufficiently high amplifications (which are determined by the dispersity of the structure); the accuracy should be attained by counting in a greater number of fields of vision, which in the final analysis results in complications and slowing down of the count. For this reason, the use of the method of stationary specimen is rational only when due to conditions of investigation it is impossible to use the method of traversed specimen.

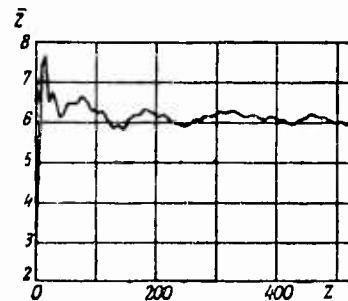


Fig. 87. Measurement of the cumulative average number of cross sections as depends on the computed over-all number of points of the cross sections in analysis by the method arbitrary sections

When making the count by the method of traversing specimen it is desirable to use an ordinary mechanical counter (Figure 16), which totals the number of times the pedal is pressed. The counting process is reduced to the traversing of the specimen and simultaneous counting of the number of intersections by the counter. The length of the traverse and the number of intersections in it are fixed only after the specimen has been completely traversed. When making counts by the method of stationary specimen, it is necessary to record the number of intersections in each field of vision, if a different shade of analysis with respect to the zones of plane of polish is made. If the number of intersections is counted for the entire plane of polish or for one of definite directions, then the number of fields of vision is fixed and the number of intersections may be counted in all fields by the counter.

Counting of the number of intersections using traversing and stationary specimens as a source of a constant error, which was noted by A. G. Spektor [104]. This error is due to the fact that the rule of the ocular micrometer or the center of the cross hair of the ocular are not geometrical lines or a point but have a definite "width" which may be measured with the aid of an object micrometer. If it is assumed that the visible diameter of sections of microparticles on a plane of polish is  $d$ , then the geometrical secant 1 mm long will intersect all spherical sections the centers of which lie within the band  $d$  wide and 1 mm long, as it may be seen in Figure 85a. If the number of circles per 1 mm square of the plane of polish is  $n$ , then the number of intersections per 1 mm of length will be equal (according to the rule of the total projection onto a plane):

$$m = 2nd. \quad (29.1)$$

However, if the secant is  $b$  wide (Figure 85b), it will intersect all circles the centers of which are within the band the width of which is  $d$  plus  $b$  and the total number of intersections per 1 mm length will be a greater value than in the preceding case:

$$m' = 2n(d + b). \quad (29.2)$$

It is obvious that the error will be the greater the more dispersed is the structure subject to observations, that is, the greater the ratio  $b/d$ , and its sine will be always positive (the calculated number of points is higher than the true one).

A. G. Spektor proposed to introduce an appropriate correction. To calculate the latter it is necessary to determine secondary parameters of the structure (the number of intersections per 1 mm<sup>2</sup> of the plane of polish), which considerably complicates the determination and is possible only when the sections of microparticles are circles. It is much more simple to reduce to zero the "width" of a secant or of a point, which may be readily accomplished in practice. The rule for counting the number of intersections, which replaces the rule of a conventional ocular micrometer, is shown in Figure 86a. The count is made from lines separating

the dark and light fields, which are geometrical lines without "width". In order to obtain a greater number of intersections in a given field of vision it is expedient to use an ocular insert with a spiral, shown in Figure 86b. The count may be made from the internal as well as external contour of a spiral. It is not difficult to measure the length of the spiral, since it is made up by semicircles. When the analysis is made by the method of traversing specimen, it is expedient to replace the ocular with a cross hair by an ocular with an insert, having a dark sector, described previously (Figure 43). The apex of the sector is the geometrical point and the need for corrections is eliminated.

These means eliminate sources of the constant error noted by A. G. Spektor and completely eliminate the need for any corrections which complicate the determination.

As a result of counts we have two figures at our disposal: the total length of secants,  $l$ , on which the count was made, and the total number of intersections of a given system of boundary lines and secants,  $Z$ . The mean number of intersections per 1 mm length of secants we find is the ratio of these two quantities:

$$m = \frac{Z}{l} \text{ mm}^{-1} . \quad (29.3)$$

As any other statistical mean value, the number  $m$  is more accurate the greater the number of separate observations or measurements, that is, in the given case the greater the number of counted intersections,  $C$ . We determined the mean number of intersections of the rule of the ocular micrometer and interfacial boundary lines of thorite and pearlite constituents in hypoeutectoid steel (0.3% C.) The count was successively made in 100 fields of vision with fixing the results for each field of vision separately. The length of the rule of the ocular micrometer in the plane of polish was 0.465 mm, with magnification 315.

Numbers of intersections 3, 12, 8, 3, 8, etc., were obtained in the course of taking measurements in the fields 1, 2, 3, 4, 5, etc. Cumulative numbers of intersections were respectively 3, 15, 23, 26, 34, etc., and cumulative means were 3.0, 7.5, 7.7, 6.5, 6.8, etc. Variations of the cumulative mean number of the intersections,  $\bar{Z}$ , with the cumulative

number of intersections,  $Z$ , are shown in Figure 87. As the latter increases, the limits of fluctuations of the cumulative mean value are becoming increasingly narrow and it becomes stabilized approximating the true value. Thus, when the number of points is greater than 500, the actual deviations from the mean value do not exceed 0.11, that is approximately 2% of the value which is being determined. At the same time, in individual fields of view, the number of intersections varies in a wide range between 2 and 14, which may be seen in combined data for all 100 fields of vision listed in Table 29. On further increase of the number of field of visions, these extreme limits may be widened even more. The common mean number of intersections for all 100 fields of vision is 5.99 for the length of 0.465 mm. The mean quadratic deviation of this number, calculated from the data in Table 29, is 2.48.

Table 29

*№. of inter-  
sections in  
one field of  
vision.  
(Distance equal-  
ling 0.465 mm)*

Число пересечений в одном поле зрения (на длине, равной 0.465 мм)	Число полей
2	2
3	16
4	12
5	20
6	13
7	11
8	8
9	12
10	—
11	2
12	3
13	1
<b>Total</b> Всего	100

*№. of fields*

As we have already stated, the error in the determination and the reliability or probability of producing precisely this error are inalienably related to each other. In order to compute the value of errors, produced with a certain probability, it is necessary to know the value of the mean quadratic deviation. In the example cited above this deviation was determined experimentally and was 2.48 intersections per singular field of vision. Therefore the absolute error of determination,  $\Delta$ , produced by examining this structure only in one field of vision, will be defined by the equation:

$$\Delta = t \sigma \{Z\} = 2.48t, \quad (29.4)$$

where  $t$  is the normalized deviation related to the validity or probability of producing an error not greater than the one defined by Formula (29.4). This relationship has been cited previously in the description of the lineal method of analysis (Section 15), and the values of normalized deviation  $t$  for different values of probability  $P$  are listed in Table 12. Using the data in this table it is possible to determine that in the example of analysis cited the probable error (when the probability  $P$  is 0.5) will be  $= 0.675 \times 2.48 = 1.67$ , that is the plus or minus deviation from the mean value of the number of intersections (5.99) will not exceed the found value of 1.67 in at least 50% of analyses (in the given case in 50% of examined fields of vision). In other words, in at least half of the number of analyses the result must satisfy the limits from  $5.99 - 1.67 = 4.32$  to  $5.99 + 1.67 = 7.66$ , or in round figures from 4 to 8 intersections in one field of vision. The examination of Table 29 shows that actually 64 fields of vision from 100 examined are found within these limits.

We cannot for each analysis carry out a series of measurements instead of only one measurement for the sole purpose of finding the mean quadratic deviation needed for the calculation of an error from Formula (29.4). At the same time the complexity of systems of grain boundaries on the plane of polish does not make it possible to calculate the geometric probability of intersection beforehand and to determine the mean quadratic deviation from it, as we had done in calculating the accuracy of the point method of analysis for A. A. Glagolev in Section 16. For this reason, we have to determine regularities which correlate the structure and the conditions of analyses with the value of the mean quadratic deviation which occurs in this case.

If the length of the secant is increased  $M$  times, the mean number of intersections of 1 secant will be increased just as many times. From the theory of probabilities it is known that when all the values of the characteristic are multiplied by one and the same number  $M$ , both its mean value and the mean quadratic deviation are increased just as many times. It is also known that the value of the mean quadratic deviation is inversely proportional to the square root of the number of observations, which in our case corresponds to the number of points counted in the course of the

analyses.

Therefore, in the final analyses, we shall have a directly proportional relationship between the mean quadratic deviation and the square root of the number of points counted during the determination. This postulate is valid, if having a single-type system of lines on a plane we shall vary the scale of the image, maintaining the length of the secant constant or, conversely, if we shall vary the length of the secant, superimposed on the one and the same system of lines. However, the coefficient of proportionality, as the study of numerous types of structures and shapes of secants has demonstrated, is not a constant value and is dependent both upon the nature of the structure (to be more exact upon the character of the system of boundary lines on the plane of polish (and upon the conditions of determination)). For the structure of lamellar graphite of gray cast iron, just examined, the relationship between the mean quadratic deviation,  $\sigma$  and the number of intersections,  $Z$ , is expressed by the formula:

$$\sigma\{Z\} = k \sqrt{Z}, \quad (29.5)$$

where coefficient  $k$  is 1.06.

Figure 88 shows the graph for a system of grain boundaries of polyhedral structure with equiaxed grains of uniform size (line 1). Here the value of the coefficient of proportionality  $k$  is 0.77. The same figure shows the relationship of the mean quadratic deviation to the number of intersections for interfacial boundaries between cementite and thorite in granular pearlite (line 2). For this case it was found that coefficient  $k$  is 1.02.

At one and the same length of secants, the same specific length of grain boundaries and, consequently, with the mean number of intersections per 1 secant being the same, the mean quadratic deviation of this number may vary. Let us consider in this connection a system of boundaries of equiaxed thorite grains shown in Figure 49. The specific lengths of grain boundaries in Figure 89 almost precisely coincides with the specific length of boundaries of equiaxed thorite grains shown in Figure 49. However, if secants of the same length are to be drawn on both figures, it can be predicted that the range of fluctuations of the number of inter-

sections per 1 secant will be considerably wider in the case of the structure shown in Figure 89 than in the case of the structure shown in Figure 49. Actually, the numbers of intersections on secants directed parallel and perpendicular to the orientation axis will differ drastically in Figure 89, whereas in Figure 49 they will be more stable, for they are not dependent upon the direction of the secant. This is valid for rectilinear secants. However, if circular secants or secants shaped as spirals are substituted for rectilinear secants, no essential scatter of intersection points would occur on individual secants even when the boundaries are oriented, for the shape of such secants assures the equal probability of the intersection angle regardless of the orientation of boundaries. In Table 30 are given the numbers of intersections for a system of boundaries, shown in Figures 49 and 89, with several secants of the same length (100 mm), but shaped either as circles or straight lines, superimposed over the former. For each of the four cases we calculate the mean numbers of intersections per 1 secant,  $\bar{Z}$ , and mean quadratic deviations of these numbers,  $Z$ , which are given in the bottom lines in Table 30. Also there are listed the values of the coefficient of proportionality,  $k$ , determined in agreement with Formula (29.5) from actually determined values.

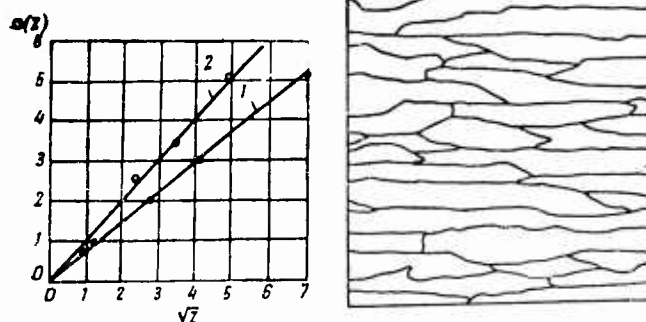


Fig. 88. Dependence of the average quadratic deviation of the number of cross sections on the over-all number of computed points of the cross sections

Fig. 89. Structure of sheet transformer steel. Plane of the slide is perpendicular to the plane of the sheet X100

The data obtained indicate that the mean numbers of intersections in all four cases differ little from each other, for the length of boundaries in Figures 49 and 89 is almost the same. In the first three cases the values of the coefficient  $k$  are also almost identical and considerably

*№. of Intersec-  
tions in 100mm  
Distance*

*Structure Accord. (Summ.)*

Table 30

Число пересечений на длине 100 мм	<i>So Fig. 49.</i> Структура по рис. 49		<i>Fig. 89</i> Структура по рис. 89		
	<i>secant</i> Секант прямая	<i>secant</i> Секант искривленная	<i>Some</i> секущая— окружность	<i>Some</i> секущая— прямая	
Число случаев					
1	—	—	—	2	
2	—	—	—	4	
3	—	—	—	5	
4	—	—	—	6	
5	—	—	—	1	
6	—	—	—	2	
7	—	—	—	7	
8	4	4	5	2	
9	8	10	6	5	
10	31	24	25	6	
11	38	32	51	2	
12	52	31	49	7	
13	39	22	35	4	
14	15	12	22	8	
15	8	4	5	11	
16	2	3	2	9	
17	—	1	—	11	
18	—	—	—	7	
19	—	—	—	1	
<i>Total</i>	<b>Всего</b>	200	146	200	100
	$Z$	11,77	11,65	11,81	11,47
	$\sigma(Z)$	1,58	1,74	1,54	1,15
	$k$	0,46	0,51	0,45	1,52

below the value found from the graph shown in Figure 88, for in that case the analysis was carried out directly on the plane of polish using many fields of vision, due to which the fact of the fluctuation of the specific length of boundaries over the plane of polish was felt. In the given case the analysis was carried out within the limits of a small area, Figures 49 and 89, corresponding to one field of vision. Just as it was anticipated, the abnormally high value of the mean quadratic deviation and of the coefficient  $k$  occur when a system of boundaries is oriented (Figure 89) and when the secant is rectilinear disposed at various angles to the orientation axis.

Let us discuss the results obtained. The value of the coefficient of proportionality  $k$  varies within a quite wide range of 0.45 to 1.52 (under different conditions it is possible that this range is wider). The value of this coefficient is first of all affected by the actual fluctuation of the specific length or the density of boundaries in individual fields of vision. Therefore, the direct analysis on the plane of polish produces the coefficient  $k$  of higher values (0.74 to 1.06) than by the analysis within the limits of a singular field of vision (0.45 to 0.51)

The uniformity of distribution of intersection points along the

secant is of great importance. Thus, under the same conditions of analysis (a singular field of vision, the same length of secants, the same specific length of boundaries), the value of the coefficient  $k$  is approximately twice as low for the isometric system of boundaries, shown in Figure 49, as compared with an oriented system, shown in Figure 89 (0.51 and 1.52, respectively). It is obvious that as the degree of orientation is increased, this ratio would be even higher. A circular secant automatically assures an equal probability of any angle of intersection with grain boundaries, regardless whether they are oriented or isometric. Therefore, circular (or spiral) secants produce a small coefficient  $k$  (0.45 to 0.46), regardless of orientation.

The nonuniformity of the density of boundaries has an essential influence on the value of coefficient  $k$  in microareas even in singular fields of vision; this nonuniformity is due to specific peculiarities of certain structures. If a secant is drawn over a polyhedral structure, similar to the one shown in Figure 49, then the points of intersections will be relatively uniformly distributed along the secant and the mean distance between two adjacent points will have a definite value. In this case, just as we have seen, the analyses on the plane of polish produces a minimum of value of the coefficient  $k = 0.74$  and the analysis in a singular field of vision produces the value of 0.46 to 0.51. In other pictures observed in structures in which intersection points of secants are distributed as if in pairs. Examples of such systems of boundaries may be boundaries of graphite in gray cast iron, boundaries of thorite or cementite in hypo- and hypereutectoid steel, if the thorite or cementite form a fine network over grain boundaries of pearlite, grain boundaries of cementite in granular pearlite, etc. In this case the drastic difference in distances between adjacent points is manifest on secant intercepts passing through the graphite and metal base of gray cast iron, through the thorite or cementite or through pearlite grains in steel, through cementite grains and thorite base of granular pearlite, etc.

If a frequency curve is plotted for distances between adjacent points of intersections on secants for a structure of the type shown in Figure

49, the curve would show one maximum. However, for types of structures enumerated above each frequency curve would exhibit two maxima. This nonuniformity of distribution of intersection points on secants predetermines their high mean quadratic deviation, obtained in these cases, and, consequently, a high coefficient of proportionality  $k$  (1.02 to 1.06 or higher).

By way of summing up, it is possible to note that in the analysis directly on the plane of polish the value of the coefficient  $k$  in Formula (29.5) on an average is 1 and more frequently is found within the limit of 0.7 and 1.2. Lower values correspond to the uniform distribution of boundaries over the plane of polish and of intersection points over the length of the secant. Higher values correspond to structures with "paired" or "doubled" boundaries, the examples of which have been presented previously and also correspond to nonuniform distribution of boundaries over the plane of polish. All of the aforesaid is applicable to isometric systems of lines on a plane of polish.

The most adverse conditions are developed in the analysis of oriented systems of boundaries using rectilinear random secants, when the values of coefficient  $k$  exceed the upper limit of above given norms. However, it should be noted that in the case of oriented structures we are using not random but directed secants and in the analysis by the method of oblique planes of polish we may employ circular or spiral secants. Therefore, in practice we have to deal with this unfavorable combination of conditions of analyses.

Further in our discourse we shall assume the coefficient  $k$  equal to unity. In connection with previously cited concrete examples in isolated cases it will be possible to introduce appropriate corrections. From Equations (29.4) and (29.5) it follows:

$$\Delta = kt \sqrt{Z}, \quad (29.6)$$

When  $\Delta$  is the absolute error in the numbers of intersection points;  $Z$  is the number of intersection points counted in the course of the analysis.

As it has been previously demonstrated, the error in the determination of the value of specific surface area is equal to the error of the determination of the mean number of intersections. The relative error

in determination of these values may be found from Formula:

$$\delta = \frac{A}{Z} 100\% = \frac{kt}{\sqrt{Z}} 100\%. \quad (29.7)$$

The latter equation finally determines the relationship between the relative error of the determination of the specific surface area by the method of secants, the validity of the determination and the number of points counted in the course of the analysis. From this formula it is possible to calculate the relative error of the carried out analysis, having specified any validity of its derivation and vice versa.

For the preliminary count of the required number of points of intersections, which assures the determination of a definite relative error with a prespecified validity, we are using Formula:

$$Z = \frac{10000 k^2 t^2}{\delta^2} \quad (29.8)$$

Let us assume that we specify the value of the relative error  $\delta = 5\%$  with the validity  $P = 0.9$  (at which the normalized deviation  $t$  has the value of 1.6449). In that case the required number of points of intersections between the secants and boundaries, which has to be calculated, may be found from the Equation (29.8) and will be equal to 1.82 (at the coefficient  $k = 1$ ).

If we shall carry out a large series of determinations (1082 points in each), then the obtained relative error will somewhat exceed the figure which we have specified, that is 5%, in not more than 10% of determinations. In other 90%, the error will be less than 5%. In other words, by carrying out a singular determination, counting 1082 points, we can assume that the validity of the obtained results is 0.9 or 90%.

In order to avoid counting in each individual case, we have compiled Table 31 which is in agreement with Formulas (29.7) and (29.8).

Specifying the permissibility of the relative error of the anticipated results of the analysis and its validity, it is possible to find directly from this table the required number of points of intersections. When calculating the data in the table the value of the coefficient  $k$  was taken as 1. Therefore, for concrete systems of boundaries the number of points of intersections derived from the table is corrected by multiplying by  $k^2$ .

Table 31

1. Standardized variation  
 2. Probability (accuracy)  
 3. Relative error  $\sigma$  %  
 4. No. of Intersection points.

1. Нормированное отклонение $t$	0.674	0.842	1.067	1.281	1.645	1.960
2. Вероятность $P$ (достоверность)	0.5 50%	0.6 60%	0.7 70%	0.8 80%	0.9 90%	0.95 95%
3. Относительная ошибка $\sigma$ , %	4. Число точек пересечений					
1	4543	7090	10754	16410	27060	38416
2	1136	1773	2689	4103	6765	9604
3	505	788	1195	1823	3007	4268
4	284	443	672	1026	1691	2401
5	182	284	430	656	1082	1537
6	126	197	299	456	752	1067
7	93	145	219	335	552	784
8	71	111	168	256	423	600
9	56	88	133	203	334	474
10	45	71	108	164	271	384
11	38	59	89	136	224	317
12	32	49	75	114	188	267
13	27	42	64	97	160	227
14	23	36	55	84	136	196
15	20	32	48	73	120	171

If the analysis has been already carried out and the total number of counted points of intersections is  $Z$ , it is possible to find the value of the relative error  $\sigma$  from Table 32. This quantity obviously will differ, depending upon its validity. Thus, if 1000 points have been counted, the relative error will be 2.1% with the validity of 0.5 (this will be "a probable error"), 2.7% with the validity of 0.6, and on to 6.2% with a validity of 0.95.

When calculations are made directly from Formulas (29.7) and (29.8) the values of normalized deviation  $t$  for different values of the probability  $P$ , which characterizes the validity of the result of the analysis, are found in Table 12.

The carried-out method of calculating the error of determination when using the analysis by the method of random secants is convenient for it does not require determination of any additional values by means of repeated analyses, etc. The total number of points of intersections, counted in a course of the analysis, is also used for the determination of the mean number of intersections,  $m$ , and for calculation of the value of the specific surface area, as well as for the calculation and determination of the error of analysis from the tables [147].

Table 32

1. Standardized variation
2. Probability (authenticity)
3. Nr. of Intersections points
4. Relative error  $\delta$ , %

1. Нормированное отклонение $t$	0,674	0,842	1,037	1,281	1,645	1,960
2. Вероятность $P$ (достоверность)	0,5 50%	0,6 60%	0,7 70%	0,8 80%	0,9 90%	0,95 95%
3. Число точек пересечений, $Z$	4. Относительная ошибка $\delta$ , %					
50	9,5	11,9	14,7	18,1	23,3	27,7
60	8,7	10,9	13,4	16,5	21,2	25,3
70	8,1	10,1	12,4	15,3	19,7	23,4
80	7,5	9,4	11,6	14,3	18,4	21,9
90	7,1	8,9	10,9	13,5	17,3	20,7
100	6,7	8,4	10,4	12,8	16,4	19,6
110	6,4	8,0	9,9	12,2	15,7	18,7
120	6,2	7,7	9,5	11,7	15,0	17,9
130	5,9	7,4	9,1	11,2	14,4	17,2
140	5,7	7,1	8,8	10,8	13,9	16,6
150	5,5	6,9	8,5	10,5	13,4	16,0
160	5,3	6,7	8,2	10,1	13,0	15,5
170	5,2	6,5	7,9	9,8	12,6	15,0
180	5,0	6,3	7,7	9,6	12,3	14,6
190	4,9	6,1	7,5	9,3	11,9	14,2
200	4,8	6,0	7,3	9,1	11,6	13,9
250	4,3	5,3	6,6	8,1	10,4	12,4
300	3,9	4,9	6,0	7,4	9,5	11,3
350	3,6	4,5	5,5	6,9	8,8	10,5
400	3,4	4,2	5,2	6,4	8,2	9,8
450	3,2	4,0	4,9	6,0	7,8	9,2
500	3,0	3,8	4,6	5,7	7,4	8,8
550	2,9	3,6	4,4	5,5	7,0	8,4
600	2,8	3,4	4,2	5,2	6,7	8,0
650	2,6	3,3	4,1	5,0	6,5	7,7
700	2,5	3,2	3,9	4,8	6,2	7,4
750	2,5	3,1	3,8	4,7	6,0	7,2
800	2,4	3,0	3,7	4,5	5,8	6,9
850	2,3	2,9	3,6	4,4	5,6	6,7
900	2,2	2,8	3,5	4,3	5,5	6,5
950	2,2	2,7	3,4	4,2	5,3	6,4
1000	2,1	2,7	3,3	4,1	5,2	6,2
1100	2,0	2,5	3,1	3,9	5,0	5,9
1200	1,9	2,4	3,0	3,7	4,7	5,7
1300	1,9	2,3	2,9	3,6	4,6	5,4
1400	1,8	2,2	2,8	3,4	4,4	5,2
1500	1,7	2,2	2,7	3,3	4,2	5,1
1600	1,7	2,1	2,6	3,2	4,1	4,9
1700	1,6	2,0	2,5	3,1	4,0	4,8
1800	1,6	2,0	2,4	3,0	3,9	4,6
1900	1,5	1,9	2,4	2,9	3,8	4,5
2000	1,5	1,9	2,3	2,9	3,7	4,4
2500	1,3	1,7	2,1	2,6	3,3	3,9
3000	1,2	1,5	1,9	2,3	3,0	3,6
3500	1,1	1,4	1,8	2,2	2,8	3,3
4000	1,1	1,3	1,6	2,0	2,6	3,1
4500	1,0	1,3	1,5	1,9	2,5	2,9
5000	1,0	1,2	1,5	1,8	2,3	2,8
6000	0,9	1,1	1,3	1,7	2,1	2,5
7000	0,8	1,0	1,2	1,5	2,0	2,3
8000	0,8	0,9	1,2	1,4	1,8	2,2
9000	0,7	0,9	1,1	1,4	1,7	2,1
10000	0,7	0,8	1,0	1,3	1,6	2,0

Section 30. Measurement of Linear Elements of the 3-Dimensional Structure of Metals and Alloys

Speaking strictly realistically no elements of spatial structure are possible having only one dimension; therefore, discussing such elements we have in mind formations whose dimensions of cross section are significantly small as compared with their linear extent.

Let us consider the spatial structure of a polycrystalline aggregate consisting of a number of crystallites of different dimensions and shapes. These crystallites are separated from each other not by just a system of boundary surfaces. Surfaces of the system, intersecting with each other, form a 3-dimensional system of lines which may be called a system of H lines of crystallites. Quantitatively a system of H lines may be estimated by the total length of all the lines per unit volume of polycrystal, measured in  $\text{mm}/\text{mm}^3$ .

By intersecting a polycrystalline aggregate by a plane, we obtain a number of traces where this plane meets with the system of lines of crystallite edges. On the microsection of a polycrystal, these traces are junction intersection points of boundary lines of the cross sections of crystallites; that is, junction points of neighboring flat grains. Extensive experience from metallographic analyses show that, as a rule, vertexes of three flat grains come together at junction points on a microsection of a single-phase polycrystal. Consequently, in space also the H lines of crystallites belong simultaneously to three adjacent crystallites. However, in some cases junction of a large<sup>r</sup>/number of grains has been found at a junction point on a microsection. Thus, for example, G. Ya. Vasil'ev measured microhardness at junction points not only of three but of four ferrite grains [148]. However, generally in such cases, when it seems to us that four grains come together at a certain junction point, additional clarification always shows that actually this is the case not of one but of two junction points located quite close to each other.

Since it is possible to draw a plane through any three points, such as three centers of crystallization the nearest to each other, let us construct in this plane the lines at which crystallites, growing

at different linear rates of spherical growth, meet. Such a structure, shown in Figure 90, indicates that the three boundary lines which separate adjacent crystallites, meet at one point. The greater the difference in the linear rate of growth of adjacent crystallites, the greater the curvature of the boundary line between them. At equal growth rate, the boundary lines happen to be straight. If the rate of growth is not spherical, the boundary lines have a more complex curvature, for instance, wavy. However, in all cases the boundary lines of three adjacent crystallites join at one point on a plane.



Fig. 90. Sketch of the formation of a joint of three grains with spherical syngony of the growth. Plane of the drawing runs through the center of the crystallization of the grain, rate of growth of which varies

In a structure containing more than one constituent, the H lines of microparticles of any one constituent may be exhibited more or less clearly, that is three phases which one of them may be joined at a smaller or greater angle. In the plane of the microsection this will correspond to sharply broken or smooth boundary lines of a given structural constituent. For example, surfaces of graphite platelets in the gray cast iron come together at very small angles forming clearly exhibited edges of platelets. For this reason in the plane of the microsection also the traces of lines of these edges are clearly manifest in a form of terminal points of cross sections of graphite platelets. Microparticles of SnS compound in babbitts are shaped as quite regular cubes and in the plane of a microsection form polygons, with number of sides ranging between three and six, whose vertexes are clearly manifest. Generally speaking, however, as compared with a single-phase structure, the traces of intersections of

edges of microparticles are less clearly exhibited on the plane of micro-section, since in the first case they are marked by junction points of three boundary lines and in the second case they are marked only by a more or less distinct rate in the boundary line.

Besides the lines of edges of microparticles, other elements of structure, in which one dimension clearly predominates over the other two, may be also of interest to us. Such elements are formations which have a special shape of rods, filaments, fibers, aciculae (should not be confused with "needles" on a plane, for example with aciculae of martensite, which in reality are shaped as platelets). Microparticles of  $\text{Cu}_6\text{Sn}_5$  compound in babbitts, which are shaped as thin cylindrical rods (see Figure 3) may be cited as an illustration of such formations.

Let us assume that a system of straight, curved, continuous or broken lines is found in space, which lines are disposed and directed in any fashion, randomly or with a geometrical regularity. The problem is set up to determine the length of lines in the system in a unit of volume, using for this purpose measurements on its planar cross section.

Let us draw a number of secant planes which intersect the volume being investigated. The planes are disposed and oriented randomly. After that, let us calculate the number of intersections formed by the planes and lines of the system as  $M$ , expressing it in  $\text{mm}^{-2}$ . The specific length of lines we shall designate as  $\sum L$ , expressing it in  $\text{mm}/\text{mm}^3$ . Let us also note that the dimensionality of both quantities is one and the same,  $\text{mm}^{-2}$ . Let us demonstrate that a unique relationship exists between the quantities  $\sum L$  and  $M$ , and that the specific length of lines and the mean number of intersections per unit area of the secant plane are directly proportional to each other. If this is so, then having readily determined the number  $M$  from the microsection, we shall also find the value of  $\sum L$ .

In order to find the relationship between quantities  $M$  and  $\sum L$ , we isolate in space a large number of thin flat platelets of disappearingly small thickness  $\Delta$ , instead of a system of secant planes. In the limit, at  $\Delta = 0$ , these platelets become secant planes. The distribution of platelets in space is statistically uniform and their orientation

random so that the number of usually parallel platelets is the same for any direction in space. Let the total area of all platelets be equal to  $F$  and the total number of intersections with the lines of the system be  $FM$ , where  $M$  is the mean number of intersections per  $1 \text{ mm}^2$  of the area of platelets. Then,  $FM$  number of intercepts of the lines of the system will be found in volume  $F\Delta$ . We shall consider the intercepts to be straight lines, since the thickness of platelets,  $\Delta$ , approaches zero. The total number of intercepts per unit volume of platelets is equal to:

$$n = \frac{FM}{F\Delta} = \frac{M}{\Delta}. \quad (30.1)$$

If the acute angles formed by intercepts and planes by which they are intersected, are designated as  $\gamma_1, \gamma_2, \gamma_3, \dots$  then the length of intercepts will be respectively:

$$\frac{\Delta}{\sin \gamma_1}, \frac{\Delta}{\sin \gamma_2}, \frac{\Delta}{\sin \gamma_3}, \dots, \frac{\Delta}{\sin \gamma_z}.$$

The total length of all intercepts per unit volume of platelets, or the same per unit volume of metal, will be:

$$\begin{aligned} \sum L &= \Delta (1/\sin \gamma_1 + 1/\sin \gamma_2 + 1/\sin \gamma_3 + \dots + 1/\sin \gamma_z) = \\ &= M \left[ \frac{1}{\Delta} \left( 1/\sin \gamma_1 + 1/\sin \gamma_2 + 1/\sin \gamma_3 + \dots + 1/\sin \gamma_z \right) \right], \end{aligned} \quad (30.2)$$

The terms found in brackets represent the reciprocal value of the sine of angle  $\gamma$ , formed by a straight line and a plane (by intercepts and platelets); furthermore, all directions of the straight lines in space with respect to the plane are equally probable and equally possible. This value has been already determined by us when deriving the basic formula of the method of random secants for space (25.1) in Section 25. It was found that it is precisely 2. For this reason:

$$\sum L = 2M \text{ mm/mm}^2, \quad (30.3)$$

i. e., the total length of lines of a system found in a unit of volume of metal, is equal to twice the number of intersections of these lines with the system of secant planes found on an average in a unit area of

the latter. The formula derived is the basic formula of the method of secant planes.

For the derivation of formula (30.3), the assumption was made that all angles at which the intersected lines meet with secant planes are equally possible and equally probable. Therefore, Formula (30.3) is valid only when this condition is satisfied. Formula (30.3) is valid in the case when at least one of the systems, mutually intersecting in space (i. e., either a system of lines the length of which is being measured, or a system of secant planes, or, finally, both of these systems simultaneously) is random and does not have any preferred direction or orientation in space. Therefore, although theoretically Formula (30.3) and the method of secant planes are applicable for any case, in practice, when the analysis is limited to a single microsection, they may be applied only for the measurement of length of isometrical systems of lines. For example, using Formula (30.3) it is possible to determine the total length of lines of crystallite edges in an isometric polyhedral structure of metal with equiaxed grains.

On the plane of the microsection, intersections between the lines of edges of volumetric grains and the plane of the microsection are junction points of boundary lines of three adjacent flat grains, as has been previously noted. Calculation of the number of junction points per unit area of microsection ( $1 \text{ mm}^2$ ) is one of the simpler techniques of quantitative microanalysis. By substituting the value of  $M$  obtained into Formula (30.3), we find directly the specific length of lines of edges in  $\text{mm}/\text{mm}^3$ .

Before commencing the analysis of systems of lines with partial linear orientation in space, let us discuss a system of completely oriented lines, which obviously must consist of straight lines (or segments) parallel to each other and parallel to the orientation axis. Filament-like nonmetallic inclusions may serve as an example of such a system of lines, in approximation. These inclusions in rolled rods or in wire are groups of approximately rectilinear fibers of different lengths, parallel to the orientation axis, i. e., to the axis of their round or wire.

Let us intersect such a wire by a number of planes perpendicular to its axis, maintaining a constant and very small distance,  $\Delta$ , between

the planes. These planes would intersect all fibers of nonmetallic inclusions into intercepts with lengths up to  $\Delta$ . Let us arbitrarily round off the length of these intercepts to  $\Delta$ , if their actual length is greater than half this value and let us disregard these intercepts if their length is less than  $0.5\Delta$ . Let us designate the number of intercepts between each pair of adjacent planes as  $M_1, M_2, M_3, \dots$ . Let us take into account that the total number of intercepts per unit volume of wire would be equal to the sum of these numbers for  $z = 1/\Delta$  planes, inasmuch as precisely this number of planes fits the length of wire equal to unity.

In that case, the total length of all intercepts of filamentary inclusions per unit volume of wire will be:

$$\begin{aligned} \sum L &= \Delta (M_1 + M_2 + M_3 + \dots + M_z) = \\ &= \frac{M_1 + M_2 + M_3 + \dots + M_z}{z} = M \text{ mm/mm}^3. \end{aligned} \quad (30.4)$$

Consequently, the specific length of a system completely oriented in space is numerically equal to the mean number of intersections between the lines and planes, perpendicular to these lines, per unit area of these planes. On transverse microsections, located along the length of a round or wire, the mean number of intersections with filamentary nonmetallic inclusions (or other elements of structure which have linear dimensions per unit area of the microsection, is a statistically constant value. Therefore, having determined the mean number of intersections of nonmetallic inclusions per  $1 \text{ mm}^2$  of microsection (or from several microsections, in the case of a more critical analyses or heterogeneous distribution of inclusions along the length), we can find from Formula (30.4) their total length in a unit volume of metal.

If a system of lines has a partial orientation, such as for example a system of lines of grain edges in a round or wire, which are elongated by rolling or drawing, we apply the same procedure for the determination of specific length of lines, just as in the case of using the method of directed secants. The length of lines in the isometric and completely oriented systems are calculated from the different formulas (30.3) and (30.4). For

this purpose it is necessary to have two microsections. The plane of the first must be parallel to the orientation axis (the symmetry axis of the structure) and the plane of the second must be perpendicular to it. The plane of the first microsection (longitudinal one) does not intersect oriented lines inasmuch as they are parallel to it, and, consequently, the number of junction points per  $1 \text{ mm}^2$  of such a microsection,  $M_{||}$ , belongs exclusively to lines of the isometric portion of the system. Therefore, the specific length of the isometric portion of lines may be found

from (30.3):

$$\sum L_{is} = 2M_{||} \text{ mm/mm}^3. \quad (30.5)$$

The plane of the second microsection (transverse one) will intersect lines disposed isometrically as well as oriented perpendicular to the plane of the microsection. Let us designate the mean number of these junction points per  $1 \text{ mm}^2$  of the transverse microsection as  $M_{\perp}$ . Inasmuch as the number of intersections with the isometrically disposed elements of lines is independent of the direction of secant plane and is equal to  $M_{||}$ , we may find the number of intersections with oriented elements of lines of the system, exclusively, from the difference:

$$M_{\perp} - M_{||} \text{ mm}^{-2}.$$

Then the specific length of the completely oriented portion of lines of the system will be found from Formula (30.4):

$$\sum L_{or} = M_{\perp} - M_{||} \text{ mm/mm}^3 \quad (30.6)$$

The total specific length of lines per unit volume of metal is equal to the sum of quantities defined by Formulas (30.5) and (30.6), i. e., equal to:

$$L_{tot} = M_{||} + M_{\perp} \text{ mm/mm}^3. \quad (30.7)$$

Using the given formulas, it is possible to calculate also the degree of orientation of lines or edges of the elongated grains or microparticles as the ratio of the specific length of oriented portion of lines to the total specific length, expressed in per cent.